CDS Complete Theory Manual

Release edition 20 September 2026

This manual explains the constitutive assumptions, governing equations and numerical limits behind CDS material, process, structural and electromagnetic studies. Start with the chapter for the physical problem, identify its required inputs and units, then compare its assumptions with the specimen or structure you intend to represent. A solved model is not by itself validated design data.

How to use this manual

Read the assumptions before choosing a model. Keep units consistent, inspect solver notices and use the recorded checks to distinguish a completed calculation from a validated result. Chapter links lead to the interactive website; exercise links open the Workbench. Account-controlled database downloads and classroom materials remain subject to their existing access rules.

Equations are editable Word mathematics. This PDF is exported from the same Word document. Historical reference chapters retain their stated scope; the current workflow and exercise chapters describe the available CDS implementation.

Contents

1 CDS Theory Manual the mechanics behind the result

Online chapter

Governing equations, model assumptions, calibration requirements and validation references. Use the User Guide for operating the software and the Training Manual to complete connected exercises. An implemented model is not automatically a validated design method.

Current Workbench, reference editions and downloads

Use the online User Guide for current controls, the released model directory for selectable models and compatibility, and the Training Manual for connected exercises. Wider theory references do not mean every formulation is enabled in Workbench.

Dated GUI captures and compiled Web r18 PDF manuals retain their stated scope; they are not a substitute for current hosted Workbench instructions. Find the overview PDF, guides and exercise databases in Your CDS library .

Workbench availability: released models, inputs and compatible study paths . The wider theory library includes reference formulations not available in every Workbench solve.

2 Eight ways to explore further

Online chapter

Current Workbench, reference editions and downloads

Use the online User Guide for current controls, the released model directory for selectable models and compatibility, and the Training Manual for connected exercises. Wider theory references do not mean every formulation is enabled in Workbench.

Dated GUI captures and compiled Web r18 PDF manuals retain their stated scope; they are not a substitute for current hosted Workbench instructions. Find the overview PDF, guides and exercise databases in Your CDS library .

Connected laminate inputs, focused analytical models, visible assumptions and editable teaching exercises.

These studies appear in Workbench → Models → Structural models and in the exercise collection. Each runs separately from coupled process or progressive analyses. Reference-state results are exploratory; analytical software checks do not establish experimentally validated design allowables.

01 Open-hole strength

Infinite-width, specially orthotropic tension screening. Point and average stress distances must be calibrated independently for this laminate. Not compression, bearing or a joint allowable.

Model tree location, inputs and result handoff

Equations, calibration and limits

$$\frac{\sigma(r)}{\sigma_\infty} = 1 + \frac{1}{2}q^2 + \frac{3}{2}q^4 - \frac{1}{2}(K_t - 3)(5q^6 - 7q^8), \quad q = \frac{a}{r}$$

For loading along x, Kt = 1 + √[2(√(Ex/Ey) − νxy) + Ex/Gxy]. The point criterion evaluates stress at a + d_0; the average criterion integrates it from a to a + a_0. Both compare with measured unnotched laminate strength. Their two characteristic lengths need independent calibration. The isotropic limit is Kt = 3.

NASA: notch-strength modelling and characteristic-distance assumptions

Exercise workflow and model layers

Two-row simulation workflow · **Open full-size map**
Linked-input preview, not solved results. Gray blocks are not configured.

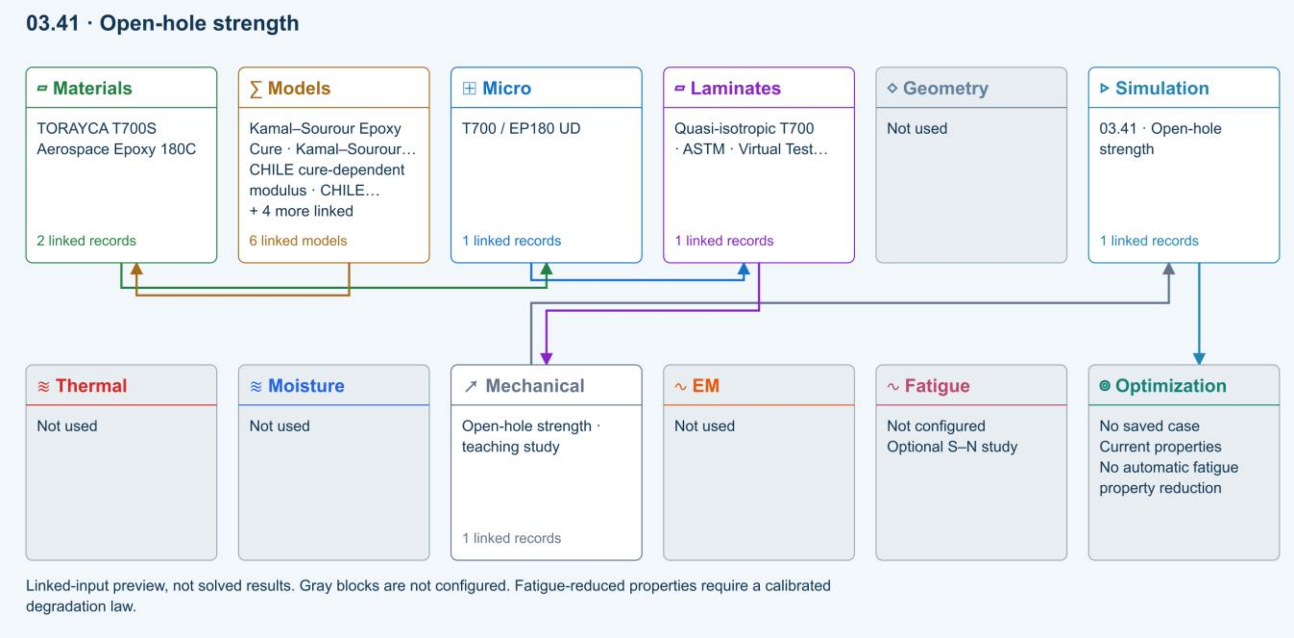

∑ Selected models & submodels

These are the exercise's linked choices, not solved results. Open a first-layer model to see its submodels and scope.

Kamal–Sourour autocatalytic · Kamal–Sourour Epoxy Cure

Reusable material model. It contributes only when assigned to a material used by this simulation; separate model records can supply independent properties.

Calibration & applicability

Illustrative model defaults — replace with characterized resin kinetics

∑ Theory & assumptions

CHILE (degree of cure) · CHILE cure-dependent modulus

Reusable material model. It contributes only when assigned to a material used by this simulation; separate model records can supply independent properties. Cure-dependent modulus does not automatically scale strength allowables.

Calibration & applicability

CHILE(α), section 2.4 of Materials 2019, 12, 259. Example parameters, not measured EP180 data. Fixed Poisson ratio; no viscoelastic relaxation or Tg softening. Incremental elastic stress integration at saved process intervals: check time-step convergence. Strength allowables are independent measured inputs, not scaled with modulus.

∑ Theory & assumptions

Temperature-dependent tabular · Temperature-dependent Thermal

Reusable material model. It contributes only when assigned to a material used by this simulation; separate model records can supply independent properties. Micro uses the 23 °C reference; Process evaluates the same table at local temperature, without extrapolation.

Calibration & applicability

Check source data, applicable environment and validity limits in the model record; saved defaults are not experimental validation.

∑ Theory & assumptions

1D Fickian diffusion · Layered Fickian Diffusion

Reusable material model. It contributes only when assigned to a material used by this simulation; separate model records can supply independent properties.

Calibration & applicability

Check source data, applicable environment and validity limits in the model record; saved defaults are not experimental validation.

∑ Theory & assumptions

Halpin–Tsai · T700 / EP180 UD

One compatible homogenization model per Micro recipe. Separate recipes compare models; their predictions are not blended.

∑ Theory & assumptions

Whitney–Nuismer open-hole tension · Open-hole strength · teaching study

Infinite-width, specially orthotropic tension screening. Point and average stress distances must be calibrated independently for this laminate. Not compression, bearing or a joint allowable.

Linked laminate reference state

Ply stiffness, thickness and orientation come from the linked laminate. Other thermal or structural analyses must be run separately.

Calibration & study controls

Teaching example

Hole radius: 3 mm

Unnotched tensile strength: 500 MPa

Measured laminate strength, not fiber strength.

Point stress distance: 1 mm

Average stress distance: 2 mm

Remote tensile stress: 100 MPa

∑ Theory & assumptions

Data travelling between blocks

Micro → Laminates
Predicted ply stiffness, strength, density and expansion properties.

Materials → Micro
Constituent stiffness, strength, density and thermal / moisture properties.

Models → Materials
Model choices and calibrated parameters.

Mechanical → Simulation
SIMULATION selects this case and its analysis model; the case owns its applicable cycle and input references.

Laminates → Mechanical
Ply angles and thicknesses, stiffness, mass and ply properties.

Simulation → Optimization
Linked inputs and current-property response for candidate evaluation.

Open teaching exercise in Workbench

02 Creep stress relaxation

Linear uniaxial response at the calibration temperature. Reference Ex is the instantaneous modulus. Three Maxwell branches; creep is solved from stress equilibrium, not the reciprocal relaxation modulus. No thermal shifting or nonlinear creep.

Model tree location, inputs and result handoff

Equations, calibration and limits

$$E(t) = E_\infty + \sum_i E_i \exp\left(-\frac{t}{\tau_i}\right), \quad E_\infty = E_0(1-\textstyle\sum_i g_i)$$

The laminate reference Ex is E_0. A held-strain experiment gives stress relaxation. For held stress, the solver evolves Maxwell branch stresses and solves equilibrium for strain; creep compliance is not 1/E(t). The calculation compares two time refinements and rejects excessive differences. Three editable branches, one calibration temperature, small uniaxial strain.

Abaqus: time-domain Prony-series viscoelasticity

Exercise workflow and model layers

Two-row simulation workflow · **Open full-size map**
Linked-input preview, not solved results. Gray blocks are not configured.

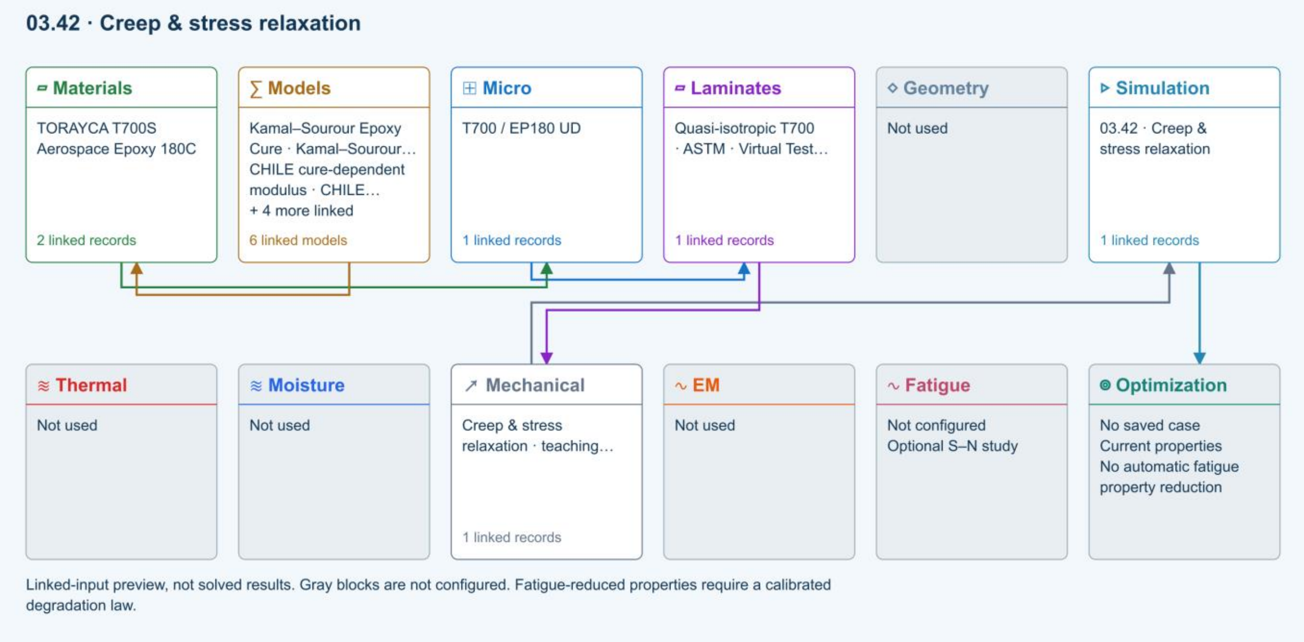

∑ Selected models & submodels

These are the exercise's linked choices, not solved results. Open a first-layer model to see its submodels and scope.

Kamal–Sourour autocatalytic · Kamal–Sourour Epoxy Cure

Reusable material model. It contributes only when assigned to a material used by this simulation; separate model records can supply independent properties.

Calibration & applicability

Illustrative model defaults — replace with characterized resin kinetics

∑ Theory & assumptions

CHILE (degree of cure) · CHILE cure-dependent modulus

Reusable material model. It contributes only when assigned to a material used by this simulation; separate model records can supply independent properties. Cure-dependent modulus does not automatically scale strength allowables.

Calibration & applicability

CHILE(α), section 2.4 of Materials 2019, 12, 259. Example parameters, not measured EP180 data. Fixed Poisson ratio; no viscoelastic relaxation or Tg softening. Incremental elastic stress integration at saved process intervals: check time-step convergence. Strength allowables are independent measured inputs, not scaled with modulus.

∑ Theory & assumptions

Temperature-dependent tabular · Temperature-dependent Thermal

Reusable material model. It contributes only when assigned to a material used by this simulation; separate model records can supply independent properties. Micro uses the 23 °C reference; Process evaluates the same table at local temperature, without extrapolation.

Calibration & applicability

Check source data, applicable environment and validity limits in the model record; saved defaults are not experimental validation.

∑ Theory & assumptions

1D Fickian diffusion · Layered Fickian Diffusion

Reusable material model. It contributes only when assigned to a material used by this simulation; separate model records can supply independent properties.

Calibration & applicability

Check source data, applicable environment and validity limits in the model record; saved defaults are not experimental validation.

∑ Theory & assumptions

Halpin–Tsai · T700 / EP180 UD

One compatible homogenization model per Micro recipe. Separate recipes compare models; their predictions are not blended.

∑ Theory & assumptions

Generalized Maxwell · axial Prony · Creep & stress relaxation · teaching study

Linear uniaxial response at the calibration temperature. Reference Ex is the instantaneous modulus. Three Maxwell branches; creep is solved from stress equilibrium, not the reciprocal relaxation modulus. No thermal shifting or nonlinear creep.

Linked laminate reference state

Ply stiffness, thickness and orientation come from the linked laminate. Other thermal or structural analyses must be run separately.

Calibration & study controls

Teaching example

Relaxation fraction 1: 0.15 —

Relaxation time 1: 10 s

Relaxation fraction 2: 0.2 —

Relaxation time 2: 100 s

Relaxation fraction 3: 0.1 —

Relaxation time 3: 1000 s

Study duration: 1000 s

Held axial stress: 10 MPa

Held axial strain: 0.001 —

Calibration temperature: 23 °C

∑ Theory & assumptions

Data travelling between blocks

Micro → Laminates
Predicted ply stiffness, strength, density and expansion properties.

Materials → Micro
Constituent stiffness, strength, density and thermal / moisture properties.

Models → Materials
Model choices and calibrated parameters.

Mechanical → Simulation
SIMULATION selects this case and its analysis model; the case owns its applicable cycle and input references.

Laminates → Mechanical
Ply angles and thicknesses, stiffness, mass and ply properties.

Simulation → Optimization
Linked inputs and current-property response for candidate evaluation.

Open teaching exercise in Workbench

03 Analytical bonded joint

Identical equivalent-elastic adherends, long free arms and a thin elastic adhesive. Compare shear-only Volkersen with eccentric single-lap shear and peel. Not a debonding, plasticity or strength calculation.

Model tree location, inputs and result handoff

Equations, calibration and limits

$$\tau(x) = \frac{F}{b} \quad \frac{\beta\cosh(\beta x)}{2\sinh(\beta L/2)}$$

β^2 = 2Ga/(ta Et) for identical adherends. The companion Goland–Reissner solution adds the eccentric-load moment factor and elastic peel distribution. The shared laminate supplies thickness and Ex, with an equivalent-isotropic beam approximation. Adhesive modulus, Poisson ratio, thickness, width and overlap remain explicit study inputs. Peak elastic stress is not a joint-strength prediction.

University of Washington: Goland–Reissner calculation equations

Exercise workflow and model layers

Two-row simulation workflow · **Open full-size map**
Linked-input preview, not solved results. Gray blocks are not configured.

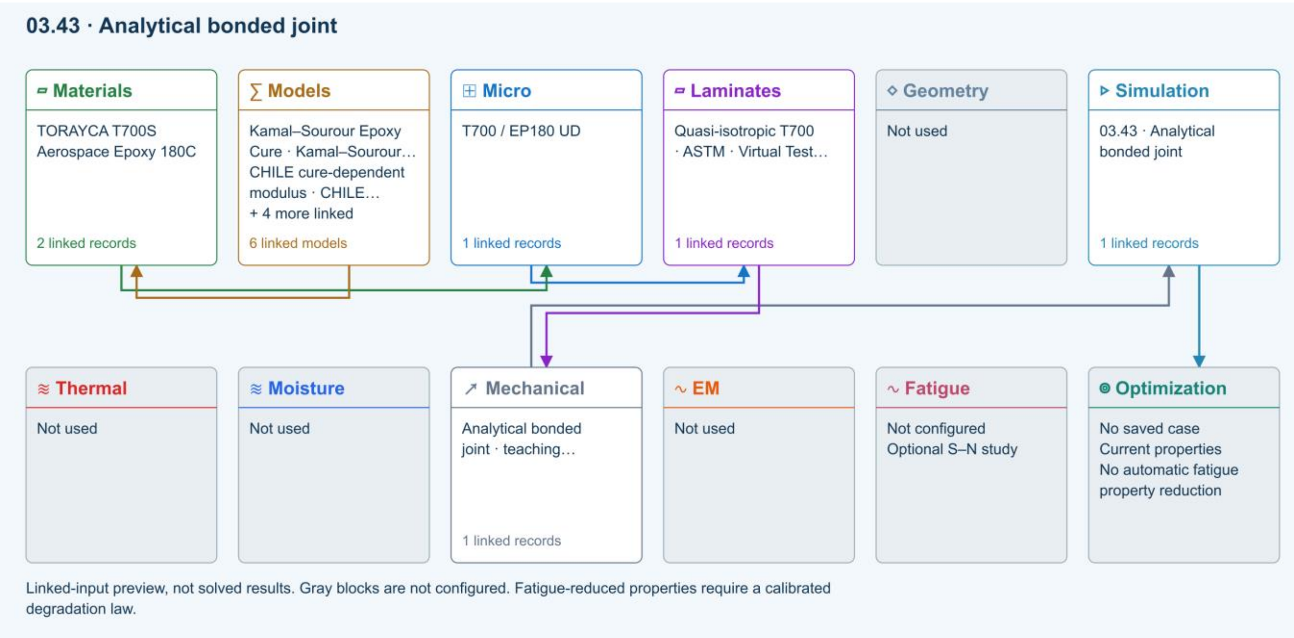

∑ Selected models & submodels

These are the exercise's linked choices, not solved results. Open a first-layer model to see its submodels and scope.

Kamal–Sourour autocatalytic · Kamal–Sourour Epoxy Cure

Reusable material model. It contributes only when assigned to a material used by this simulation; separate model records can supply independent properties.

Calibration & applicability

Illustrative model defaults — replace with characterized resin kinetics

∑ Theory & assumptions

CHILE (degree of cure) · CHILE cure-dependent modulus

Reusable material model. It contributes only when assigned to a material used by this simulation; separate model records can supply independent properties. Cure-dependent modulus does not automatically scale strength allowables.

Calibration & applicability

CHILE(α), section 2.4 of Materials 2019, 12, 259. Example parameters, not measured EP180 data. Fixed Poisson ratio; no viscoelastic relaxation or Tg softening. Incremental elastic stress integration at saved process intervals: check time-step convergence. Strength allowables are independent measured inputs, not scaled with modulus.

∑ Theory & assumptions

Temperature-dependent tabular · Temperature-dependent Thermal

Reusable material model. It contributes only when assigned to a material used by this simulation; separate model records can supply independent properties. Micro uses the 23 °C reference; Process evaluates the same table at local temperature, without extrapolation.

Calibration & applicability

Check source data, applicable environment and validity limits in the model record; saved defaults are not experimental validation.

∑ Theory & assumptions

1D Fickian diffusion · Layered Fickian Diffusion

Reusable material model. It contributes only when assigned to a material used by this simulation; separate model records can supply independent properties.

Calibration & applicability

Check source data, applicable environment and validity limits in the model record; saved defaults are not experimental validation.

∑ Theory & assumptions

Halpin–Tsai · T700 / EP180 UD

One compatible homogenization model per Micro recipe. Separate recipes compare models; their predictions are not blended.

∑ Theory & assumptions

Volkersen & Goland–Reissner joint · Analytical bonded joint · teaching study

Identical equivalent-elastic adherends, long free arms and a thin elastic adhesive. Compare shear-only Volkersen with eccentric single-lap shear and peel. Not a debonding, plasticity or strength calculation.

Linked laminate reference state

Ply stiffness, thickness and orientation come from the linked laminate. Other thermal or structural analyses must be run separately.

Calibration & study controls

Teaching example

Overlap length: 25 mm

Joint width: 25 mm

Adhesive thickness: 0.2 mm

Adhesive modulus: 2000 MPa

Adhesive Poisson ratio: 0.35 —

Joint tensile force: 1000 N

∑ Theory & assumptions

Data travelling between blocks

Micro → Laminates
Predicted ply stiffness, strength, density and expansion properties.

Materials → Micro
Constituent stiffness, strength, density and thermal / moisture properties.

Models → Materials
Model choices and calibrated parameters.

Mechanical → Simulation
SIMULATION selects this case and its analysis model; the case owns its applicable cycle and input references.

Laminates → Mechanical
Ply angles and thicknesses, stiffness, mass and ply properties.

Simulation → Optimization
Linked inputs and current-property response for candidate evaluation.

Open teaching exercise in Workbench

04 LaRC04 failure initiation

NASA LaRC04 linear-shear specialization, evaluated at both faces of every ply under membrane and bending loads. Supplied ply strengths are effective/in-situ values; no automatic thin-ply enhancement. Initiation only, not degradation or nonlinear-shear instability.

Model tree location, inputs and result handoff

Equations, calibration and limits

LaRC04 evaluates matrix tension/compression and fiber tension/kinking in their appropriate fracture and misalignment frames.

This release implements the linear-shear specialization of NASA Table 6. CLT recovers stress at both faces of each ply; the kink-frame rotation solves the linear shear equilibrium equation and the fracture-plane search is refined. Supply effective/in-situ strengths explicitly. Identical ply materials share one calibration; mixed-material calibration is rejected. This separate initiation study does not replace or silently extend the progressive-failure solver. Nonlinear-shear instability and delamination are excluded.

Pinho et al., NASA/TM-2005-213530: original LaRC04 equations

Exercise workflow and model layers

Two-row simulation workflow · **Open full-size map**
Linked-input preview, not solved results. Gray blocks are not configured.

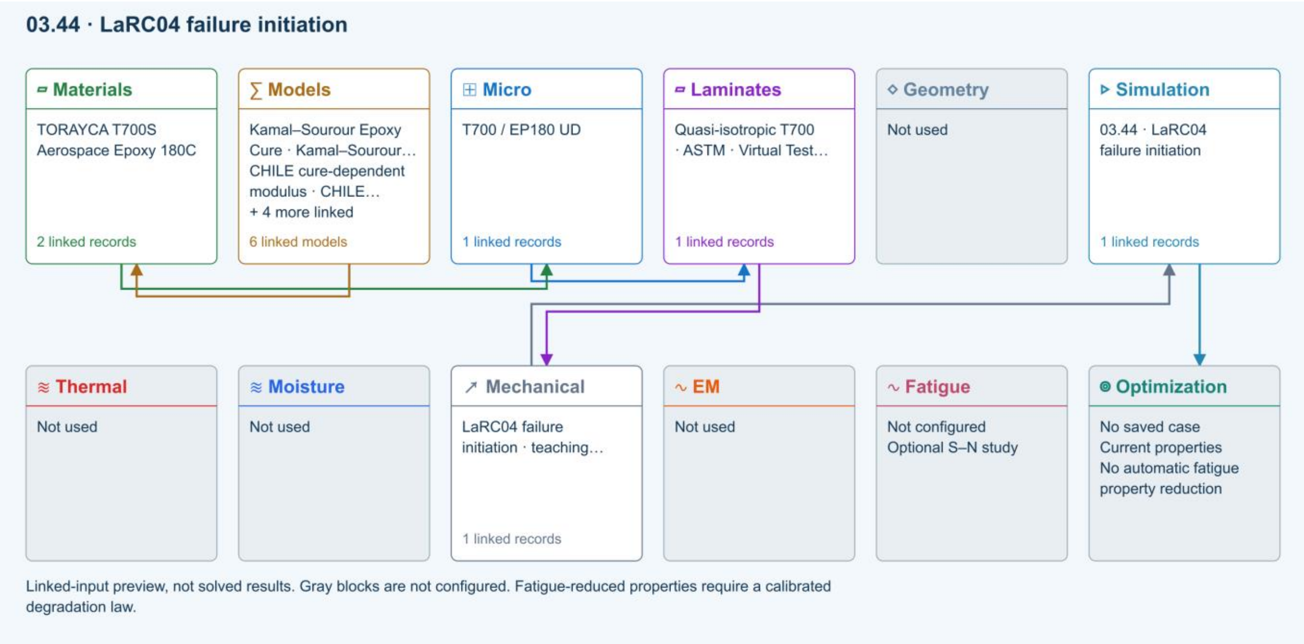

∑ Selected models & submodels

These are the exercise's linked choices, not solved results. Open a first-layer model to see its submodels and scope.

Kamal–Sourour autocatalytic · Kamal–Sourour Epoxy Cure

Reusable material model. It contributes only when assigned to a material used by this simulation; separate model records can supply independent properties.

Calibration & applicability

Illustrative model defaults — replace with characterized resin kinetics

∑ Theory & assumptions

CHILE (degree of cure) · CHILE cure-dependent modulus

Reusable material model. It contributes only when assigned to a material used by this simulation; separate model records can supply independent properties. Cure-dependent modulus does not automatically scale strength allowables.

Calibration & applicability

CHILE(α), section 2.4 of Materials 2019, 12, 259. Example parameters, not measured EP180 data. Fixed Poisson ratio; no viscoelastic relaxation or Tg softening. Incremental elastic stress integration at saved process intervals: check time-step convergence. Strength allowables are independent measured inputs, not scaled with modulus.

∑ Theory & assumptions

Temperature-dependent tabular · Temperature-dependent Thermal

Reusable material model. It contributes only when assigned to a material used by this simulation; separate model records can supply independent properties. Micro uses the 23 °C reference; Process evaluates the same table at local temperature, without extrapolation.

Calibration & applicability

Check source data, applicable environment and validity limits in the model record; saved defaults are not experimental validation.

∑ Theory & assumptions

1D Fickian diffusion · Layered Fickian Diffusion

Reusable material model. It contributes only when assigned to a material used by this simulation; separate model records can supply independent properties.

Calibration & applicability

Check source data, applicable environment and validity limits in the model record; saved defaults are not experimental validation.

∑ Theory & assumptions

Halpin–Tsai · T700 / EP180 UD

One compatible homogenization model per Micro recipe. Separate recipes compare models; their predictions are not blended.

∑ Theory & assumptions

LaRC04 · linear shear · LaRC04 failure initiation · teaching study

NASA LaRC04 linear-shear specialization, evaluated at both faces of every ply under membrane and bending loads. Supplied ply strengths are effective/in-situ values; no automatic thin-ply enhancement. Initiation only, not degradation or nonlinear-shear instability.

Linked laminate reference state

Ply stiffness, thickness and orientation come from the linked laminate. Other thermal or structural analyses must be run separately.

Calibration & study controls

Teaching example

Fiber tensile strength: 1500 MPa

Fiber compressive strength: 900 MPa

Matrix tensile strength: 50 MPa

Matrix compressive strength: 200 MPa

Longitudinal shear strength: 75 MPa

Fracture angle: 53 deg

Fracture toughness ratio: 0.35 —

∑ Theory & assumptions

Data travelling between blocks

Micro → Laminates
Predicted ply stiffness, strength, density and expansion properties.

Materials → Micro
Constituent stiffness, strength, density and thermal / moisture properties.

Models → Materials
Model choices and calibrated parameters.

Mechanical → Simulation
SIMULATION selects this case and its analysis model; the case owns its applicable cycle and input references.

Laminates → Mechanical
Ply angles and thicknesses, stiffness, mass and ply properties.

Simulation → Optimization
Linked inputs and current-property response for candidate evaluation.

Open teaching exercise in Workbench

05 Tool-release shape

Free CLT release from prescribed ply-local shrinkage/thermal eigenstrains. Corner spring-in is a separate uniform-strain estimate. Stress-free temperature and effective post-gel shrinkage need calibration. No tool friction, cure kinetics or viscoelastic restraint history.

Model tree location, inputs and result handoff

Equations, calibration and limits

$$\begin{bmatrix}\varepsilon_0 \\ \kappa\end{bmatrix} = \mathbf{ABD}^{-1}\begin{bmatrix}N^* \\ M^*\end{bmatrix}; \quad \Delta\theta = \frac{\theta(\varepsilon_{\parallel} - \varepsilon_{\text{through}})}{1 + \varepsilon_{\text{through}}}$$

The first expression computes free flat-laminate response to prescribed ply-local thermal and post-gel shrinkage strains. The second is a separate uniform-strain corner estimate; positive $\Delta\theta$ means spring-in. The plotted free sections use their center tangent as reference, not a clamp. Enter effective post-gel strains, not total resin volumetric shrinkage. Tool friction, contact and viscoelastic cure history are not resolved.

Analytical modelling of cure-induced laminate deformation

Exercise workflow and model layers

Two-row simulation workflow · **Open full-size map**
Linked-input preview, not solved results. Gray blocks are not configured.

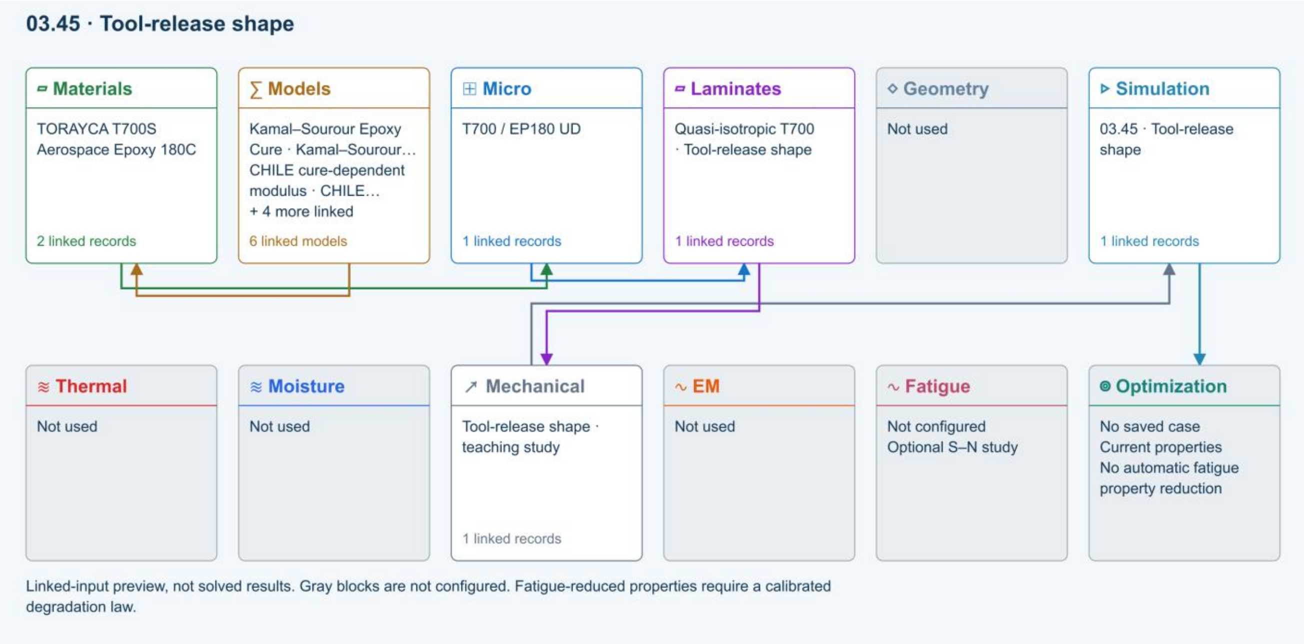

∑ Selected models & submodels

These are the exercise's linked choices, not solved results. Open a first-layer model to see its submodels and scope.

Kamal–Sourour autocatalytic · Kamal–Sourour Epoxy Cure

Reusable material model. It contributes only when assigned to a material used by this simulation; separate model records can supply independent properties.

Calibration & applicability

Illustrative model defaults — replace with characterized resin kinetics

∑ Theory & assumptions

CHILE (degree of cure) · CHILE cure-dependent modulus

Reusable material model. It contributes only when assigned to a material used by this simulation; separate model records can supply independent properties. Cure-dependent modulus does not automatically scale strength allowables.

Calibration & applicability

CHILE(α), section 2.4 of Materials 2019, 12, 259. Example parameters, not measured EP180 data. Fixed Poisson ratio; no viscoelastic relaxation or Tg softening. Incremental elastic stress integration at saved process intervals: check time-step convergence. Strength allowables are independent measured inputs, not scaled with modulus.

∑ Theory & assumptions

Temperature-dependent tabular · Temperature-dependent Thermal

Reusable material model. It contributes only when assigned to a material used by this simulation; separate model records can supply independent properties. Micro uses the 23 °C reference; Process evaluates the same table at local temperature, without extrapolation.

Calibration & applicability

Check source data, applicable environment and validity limits in the model record; saved defaults are not experimental validation.

∑ Theory & assumptions

1D Fickian diffusion · Layered Fickian Diffusion

Reusable material model. It contributes only when assigned to a material used by this simulation; separate model records can supply independent properties.

Calibration & applicability

Check source data, applicable environment and validity limits in the model record; saved defaults are not experimental validation.

∑ Theory & assumptions

Halpin–Tsai · T700 / EP180 UD

One compatible homogenization model per Micro recipe. Separate recipes compare models; their predictions are not blended.

∑ Theory & assumptions

Free-release eigenstrain & spring-in · Tool-release shape · teaching study

Free CLT release from prescribed ply-local shrinkage/thermal eigenstrains. Corner spring-in is a separate uniform-strain estimate. Stress-free temperature and effective post-gel shrinkage need calibration. No tool friction, cure kinetics or viscoelastic restraint history.

Linked laminate reference state

Ply stiffness, thickness and orientation come from the linked laminate. Other thermal or structural analyses must be run separately.

Calibration & study controls

Teaching example

Stress-free temperature: 180 °C

Release temperature: 23 °C

Axial CTE: 0 1/K

Transverse CTE: 0.00003 1/K

Through-thickness CTE: 0.00005 1/K

Axial cure shrinkage: 0 —

Signed strain: negative means contraction.

Transverse cure shrinkage: -0.002 —

Through-thickness cure shrinkage: -0.005 —

Corner angle: 90 deg

Shape length: 25 mm

∑ Theory & assumptions

Data travelling between blocks

Micro → Laminates
Predicted ply stiffness, strength, density and expansion properties.

Materials → Micro
Constituent stiffness, strength, density and thermal / moisture properties.

Models → Materials
Model choices and calibrated parameters.

Mechanical → Simulation
SIMULATION selects this case and its analysis model; the case owns its applicable cycle and input references.

Laminates → Mechanical
Ply angles and thicknesses, stiffness, mass and ply properties.

Simulation → Optimization
Linked inputs and current-property response for candidate evaluation.

Open teaching exercise in Workbench

06 Fatigue residual properties

Prescribed power-law retention fitted to constant-amplitude tests at a fixed stress ratio, amplitude and temperature. Stiffness and strength have independent coefficients. S–N life alone cannot calibrate either. Does not modify the saved laminate.

Model tree location, inputs and result handoff

Equations, calibration and limits

$$\frac{E(N)}{E_0} = 1 - a_E\left(\frac{N}{N_f}\right)^{b_E}; \quad \frac{X(N)}{X_0} = 1 - a_X\left(\frac{N}{N_f}\right)^{b_X}$$

This is a prescribed, user-fitted phenomenological retention law. Stiffness and strength use independent loss fractions and exponents. Nf, stress ratio, peak stress and temperature must describe the same constant-amplitude calibration. No extrapolation beyond Nf is allowed. Curves do not automatically modify the saved laminate, and S–N life alone cannot determine degradation coefficients. The reference illustrates why stiffness-degradation data are needed; CDS does not claim to reproduce that NASA fitted model.

NASA: measured stiffness degradation for fatigue prognosis

Exercise workflow and model layers

Two-row simulation workflow · **Open full-size map**
Linked-input preview, not solved results. Gray blocks are not configured.

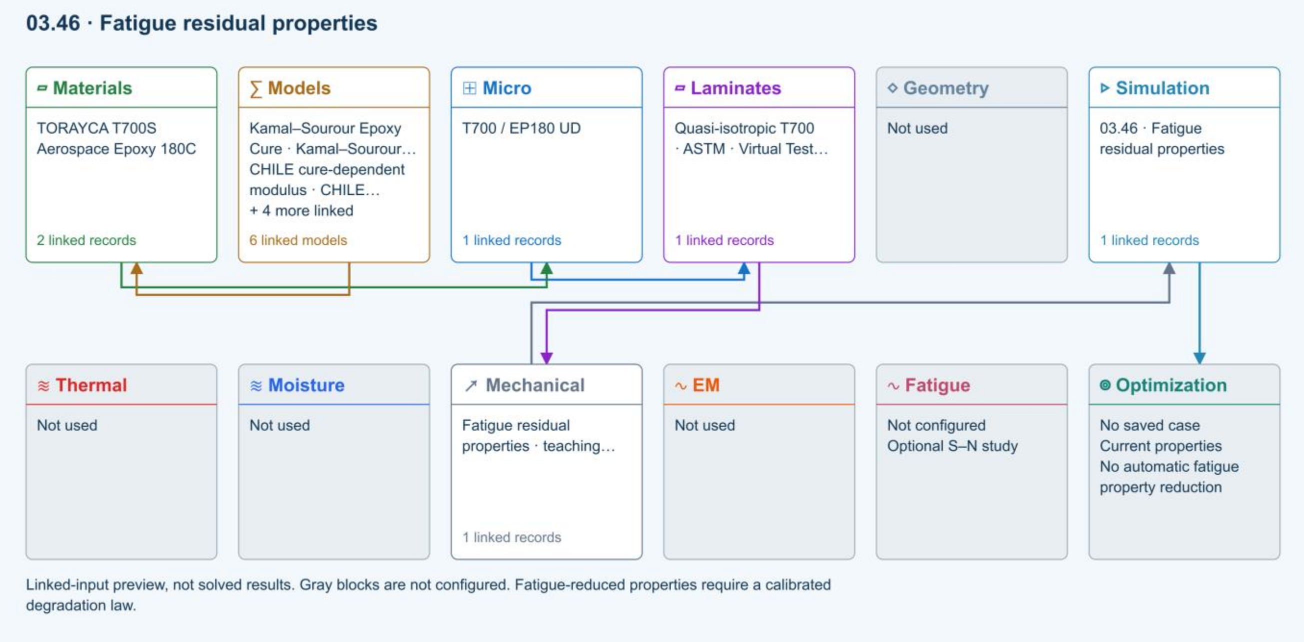

∑ Selected models & submodels

These are the exercise's linked choices, not solved results. Open a first-layer model to see its submodels and scope.

Kamal–Sourour autocatalytic · Kamal–Sourour Epoxy Cure

Reusable material model. It contributes only when assigned to a material used by this simulation; separate model records can supply independent properties.

Calibration & applicability

Illustrative model defaults — replace with characterized resin kinetics

∑ Theory & assumptions

CHILE (degree of cure) · CHILE cure-dependent modulus

Reusable material model. It contributes only when assigned to a material used by this simulation; separate model records can supply independent properties. Cure-dependent modulus does not automatically scale strength allowables.

Calibration & applicability

CHILE(α), section 2.4 of Materials 2019, 12, 259. Example parameters, not measured EP180 data. Fixed Poisson ratio; no viscoelastic relaxation or Tg softening. Incremental elastic stress integration at saved process intervals: check time-step convergence. Strength allowables are independent measured inputs, not scaled with modulus.

∑ Theory & assumptions

Temperature-dependent tabular · Temperature-dependent Thermal

Reusable material model. It contributes only when assigned to a material used by this simulation; separate model records can supply independent properties. Micro uses the 23 °C reference; Process evaluates the same table at local temperature, without extrapolation.

Calibration & applicability

Check source data, applicable environment and validity limits in the model record; saved defaults are not experimental validation.

∑ Theory & assumptions

1D Fickian diffusion · Layered Fickian Diffusion

Reusable material model. It contributes only when assigned to a material used by this simulation; separate model records can supply independent properties.

Calibration & applicability

Check source data, applicable environment and validity limits in the model record; saved defaults are not experimental validation.

∑ Theory & assumptions

Halpin–Tsai · T700 / EP180 UD

One compatible homogenization model per Micro recipe. Separate recipes compare models; their predictions are not blended.

∑ Theory & assumptions

Calibrated residual-property fatigue · Fatigue residual properties · teaching study

Prescribed power-law retention fitted to constant-amplitude tests at a fixed stress ratio, amplitude and temperature. Stiffness and strength have independent coefficients. S–N life alone cannot calibrate either. Does not modify the saved laminate.

Linked laminate reference state

Ply stiffness, thickness and orientation come from the linked laminate. Other thermal or structural analyses must be run separately.

Calibration & study controls

Teaching example

Calibrated fatigue life: 1000000 cycles

Elapsed cycles: 500000 cycles

Stiffness loss at life: 0.3 —

Stiffness exponent: 1.5 —

Strength loss at life: 0.5 —

Strength exponent: 1 —

Initial residual strength: 500 MPa

Calibration stress ratio: 0.1 —

Calibration peak stress: 200 MPa

Calibration temperature: 23 °C

∑ Theory & assumptions

Data travelling between blocks

Micro → Laminates
Predicted ply stiffness, strength, density and expansion properties.

Materials → Micro
Constituent stiffness, strength, density and thermal / moisture properties.

Models → Materials
Model choices and calibrated parameters.

Mechanical → Simulation
SIMULATION selects this case and its analysis model; the case owns its applicable cycle and input references.

Laminates → Mechanical
Ply angles and thicknesses, stiffness, mass and ply properties.

Simulation → Optimization
Linked inputs and current-property response for candidate evaluation.

Open teaching exercise in Workbench

07 Cylinder buckling

Simply supported, thin, specially orthotropic cylinder under uniform axial compression. Discrete Donnell modes; prescribed knockdown factor explores imperfection sensitivity, not a prediction from measured imperfection amplitude. No pressure, torsion, postbuckling or strength pass.

Model tree location, inputs and result handoff

Equations, calibration and limits

$$N_{x,\mathrm{cr}} = \frac{D_{11}k^4 + 2(D_{12} + 2D_{66})k^2l^2 + D_{22}l^4 + \dfrac{k^4}{R^2C}}{k^2}$$

Here k = mπ/L, l = n/R and C = a22k^4 + (2a12 + a66)k^2l^2 + a11l^4, with a = A^{-1}. The solver searches discrete axial and circumferential modes for a thin, specially orthotropic simply supported cylinder. A governing mode at the search boundary requires refinement. An explicit knockdown factor scales the ideal result; it is not an automatic prediction from measured imperfections. Pressure, torsion, postbuckling and failure interaction are excluded.

NASA: shell buckling and imperfection sensitivity

Exercise workflow and model layers

Two-row simulation workflow · **Open full-size map**
Linked-input preview, not solved results. Gray blocks are not configured.

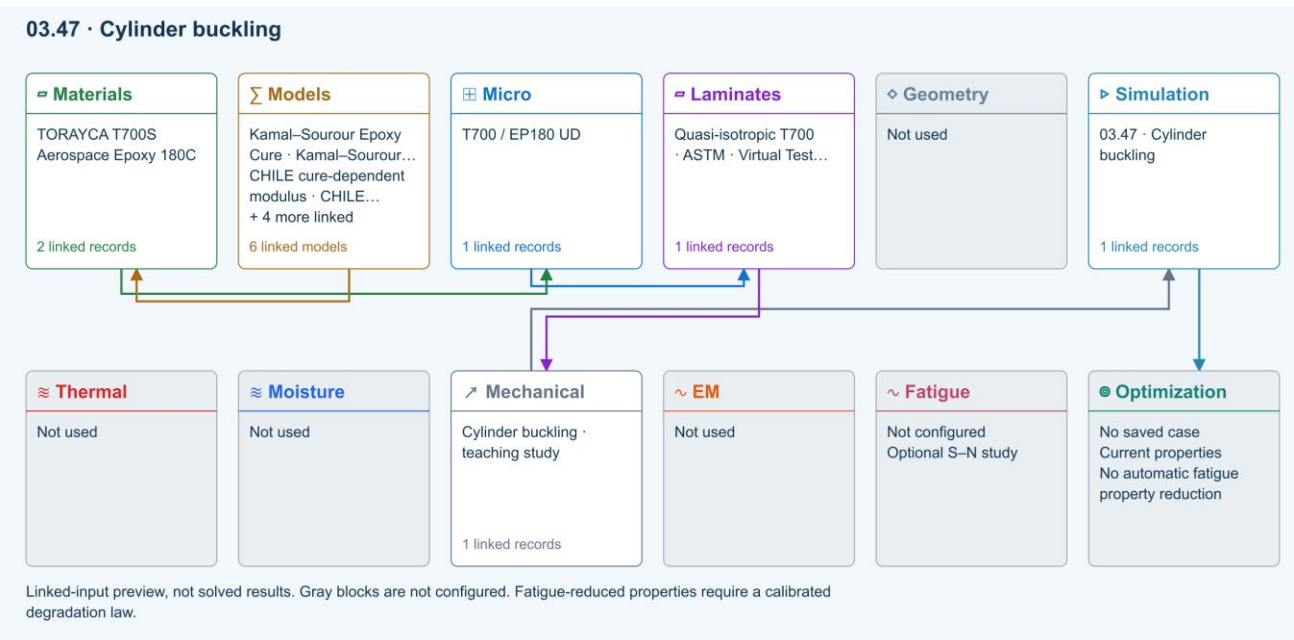

∑ Selected models & submodels

These are the exercise's linked choices, not solved results. Open a first-layer model to see its submodels and scope.

Kamal–Sourour autocatalytic · Kamal–Sourour Epoxy Cure

Reusable material model. It contributes only when assigned to a material used by this simulation; separate model records can supply independent properties.

Calibration & applicability

Illustrative model defaults — replace with characterized resin kinetics

∑ Theory & assumptions

CHILE (degree of cure) · CHILE cure-dependent modulus

Reusable material model. It contributes only when assigned to a material used by this simulation; separate model records can supply independent properties. Cure-dependent modulus does not automatically scale strength allowables.

Calibration & applicability

CHILE(α), section 2.4 of Materials 2019, 12, 259. Example parameters, not measured EP180 data. Fixed Poisson ratio; no viscoelastic relaxation or Tg softening. Incremental elastic stress integration at saved process intervals: check time-step convergence. Strength allowables are independent measured inputs, not scaled with modulus.

∑ Theory & assumptions

Temperature-dependent tabular · Temperature-dependent Thermal

Reusable material model. It contributes only when assigned to a material used by this simulation; separate model records can supply independent properties. Micro uses the 23 °C reference; Process evaluates the same table at local temperature, without extrapolation.

Calibration & applicability

Check source data, applicable environment and validity limits in the model record; saved defaults are not experimental validation.

∑ Theory & assumptions

1D Fickian diffusion · Layered Fickian Diffusion

Reusable material model. It contributes only when assigned to a material used by this simulation; separate model records can supply independent properties.

Calibration & applicability

Check source data, applicable environment and validity limits in the model record; saved defaults are not experimental validation.

∑ Theory & assumptions

Halpin–Tsai · T700 / EP180 UD

One compatible homogenization model per Micro recipe. Separate recipes compare models; their predictions are not blended.

∑ Theory & assumptions

Donnell cylinder · axial buckling · Cylinder buckling · teaching study

Simply supported, thin, specially orthotropic cylinder under uniform axial compression. Discrete Donnell modes; prescribed knockdown factor explores imperfection sensitivity, not a prediction from measured imperfection amplitude. No pressure, torsion, postbuckling or strength pass.

Linked laminate reference state

Ply stiffness, thickness and orientation come from the linked laminate. Other thermal or structural analyses must be run separately.

Calibration & study controls

Teaching example

Shell mean radius: 100 mm

Shell length: 500 mm

Axial compression resultant: 100 N/mm

Imperfection knockdown factor: 0.65 —

Mode search limit: 40 —

∑ Theory & assumptions

Data travelling between blocks

Micro → Laminates
Predicted ply stiffness, strength, density and expansion properties.

Materials → Micro
Constituent stiffness, strength, density and thermal / moisture properties.

Models → Materials
Model choices and calibrated parameters.

Mechanical → Simulation
SIMULATION selects this case and its analysis model; the case owns its applicable cycle and input references.

Laminates → Mechanical
Ply angles and thicknesses, stiffness, mass and ply properties.

Simulation → Optimization
Linked inputs and current-property response for candidate evaluation.

Open teaching exercise in Workbench

08 Uncertainty sensitivity

Seeded independent uniform sampling of shared modulus, ply-thickness and angle offsets. Recomputes laminate ABD for each sample. Bounds are assumptions, not measured distributions. Percentiles and sensitivity are exploratory, not reliability certification.

Model tree location, inputs and result handoff

Equations, calibration and limits

For each seeded sample: vary bounded inputs → rebuild ABD → solve the axial response.

Sampled independent uniform inputs are a common modulus scale, a common thickness scale and a shared ply-angle offset. The output includes strain percentiles and signed Pearson correlations. Repeating the same seed and inputs reproduces the sample set. Zero input ranges recover the deterministic result. Distributions must be justified before drawing reliability conclusions; a small correlation does not rule out nonlinear influence.

NASA: uncertainty modelling in composite analysis

Exercise workflow and model layers

Two-row simulation workflow · **Open full-size map**
Linked-input preview, not solved results. Gray blocks are not configured.

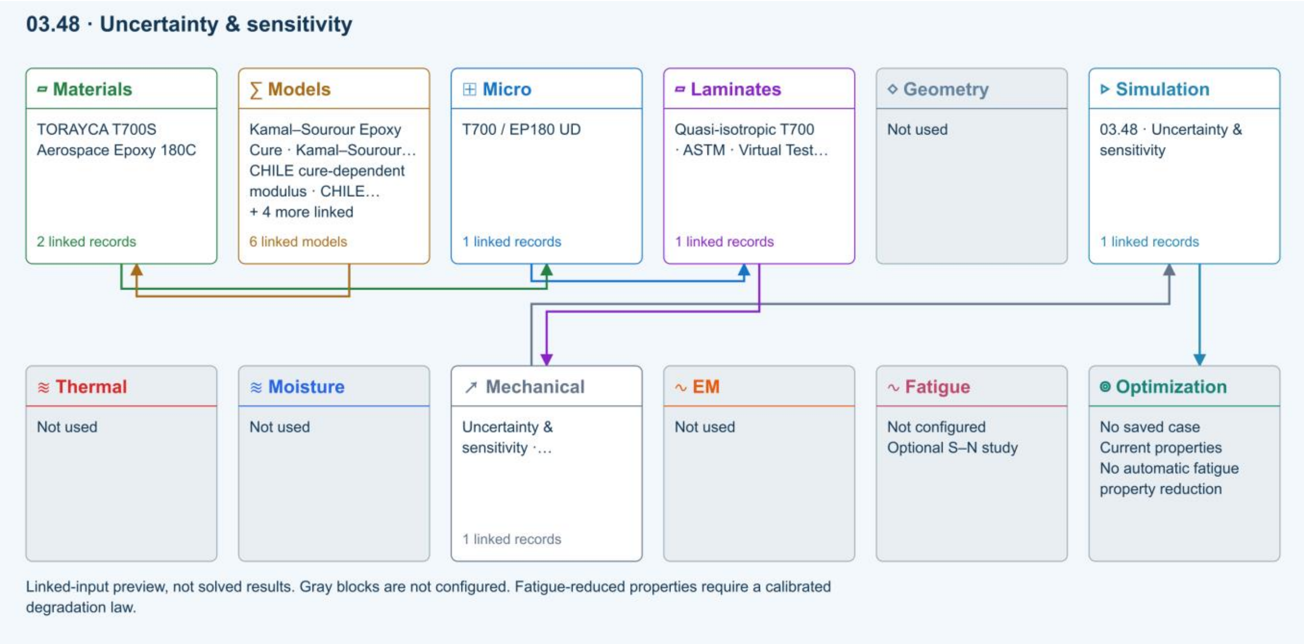

∑ Selected models & submodels

These are the exercise's linked choices, not solved results. Open a first-layer model to see its submodels and scope.

Kamal–Sourour autocatalytic · Kamal–Sourour Epoxy Cure

Reusable material model. It contributes only when assigned to a material used by this simulation; separate model records can supply independent properties.

Calibration & applicability

Illustrative model defaults — replace with characterized resin kinetics

∑ Theory & assumptions

CHILE (degree of cure) · CHILE cure-dependent modulus

Reusable material model. It contributes only when assigned to a material used by this simulation; separate model records can supply independent properties. Cure-dependent modulus does not automatically scale strength allowables.

Calibration & applicability

CHILE(α), section 2.4 of Materials 2019, 12, 259. Example parameters, not measured EP180 data. Fixed Poisson ratio; no viscoelastic relaxation or Tg softening. Incremental elastic stress integration at saved process intervals: check time-step convergence. Strength allowables are independent measured inputs, not scaled with modulus.

∑ Theory & assumptions

Temperature-dependent tabular · Temperature-dependent Thermal

Reusable material model. It contributes only when assigned to a material used by this simulation; separate model records can supply independent properties. Micro uses the 23 °C reference; Process evaluates the same table at local temperature, without extrapolation.

Calibration & applicability

Check source data, applicable environment and validity limits in the model record; saved defaults are not experimental validation.

∑ Theory & assumptions

1D Fickian diffusion · Layered Fickian Diffusion

Reusable material model. It contributes only when assigned to a material used by this simulation; separate model records can supply independent properties.

Calibration & applicability

Check source data, applicable environment and validity limits in the model record; saved defaults are not experimental validation.

∑ Theory & assumptions

Halpin–Tsai · T700 / EP180 UD

One compatible homogenization model per Micro recipe. Separate recipes compare models; their predictions are not blended.

∑ Theory & assumptions

Seeded laminate uncertainty · Uncertainty & sensitivity · teaching study

Seeded independent uniform sampling of shared modulus, ply-thickness and angle offsets. Recomputes laminate ABD for each sample. Bounds are assumptions, not measured distributions. Percentiles and sensitivity are exploratory, not reliability certification.

Linked laminate reference state

Ply stiffness, thickness and orientation come from the linked laminate. Other thermal or structural analyses must be run separately.

Calibration & study controls

Teaching example

Sample count: 200 —

Random seed: 2026 —

Modulus half-range: 0.1 —

Thickness half-range: 0.05 —

Angle half-range: 3 deg

Axial resultant: 100 N/mm

∑ Theory & assumptions

Data travelling between blocks

Micro → Laminates
Predicted ply stiffness, strength, density and expansion properties.

Materials → Micro
Constituent stiffness, strength, density and thermal / moisture properties.

Models → Materials
Model choices and calibrated parameters.

Mechanical → Simulation
SIMULATION selects this case and its analysis model; the case owns its applicable cycle and input references.

Laminates → Mechanical
Ply angles and thicknesses, stiffness, mass and ply properties.

Simulation → Optimization
Linked inputs and current-property response for candidate evaluation.

Open teaching exercise in Workbench

Verification before interpretation

Reference checks cover isotropic notch concentration, exact one-branch creep, joint load transfer, pure-load LaRC04 initiation, zero-curvature free expansion, fatigue-retention endpoints, classical isotropic shell buckling and seeded deterministic sampling. Check the scope of each model and repeat sensitivity/convergence studies for your actual inputs. A completed calculation is not an overall design pass.

Workbench availability: released models, inputs and compatible study paths . The wider theory library includes reference formulations not available in every Workbench solve.

3 RF laminate shielding and transmission

Online chapter

Follow dielectric properties into a layered-wave calculation, with explicit limits at each step.

The RF studies use passive, positive-permittivity, nonmagnetic materials. Their first purpose is to compare ideal planar laminates. They do not infer electrical properties from elastic modulus, carbon content or the T700 name. Enter measured dielectric data at the relevant frequency; the supplied values are teaching examples.

From simple to advanced

Standard includes series/parallel mixing, the Looyenga law, Maxwell–Garnett and normal-incidence laminate transmission. Advanced models use the existing Pro tier; Commercial includes them. Advanced also includes lossless 1D TLM and periodic-layer Floquet–Bloch studies; these are not arbitrary 3D full-wave solvers.

Wiener series and parallel

Standard · RF study

Positive lossless dielectric bounds; complex directional estimates.

Open the matching Workbench exercise

Looyenga / Landau Lifshitz Looyenga

Standard · RF study

One cube-root mixing law, not two independent models.

Open the matching Workbench exercise

Maxwell Garnett

Standard · RF study

Dilute subwavelength spherical inclusions in a host.

Open the matching Workbench exercise

Normal-incidence laminate TMM

Standard · RF study

Coherent isotropic nonmagnetic layers between air half-spaces.

Open the matching Workbench exercise

Bruggeman symmetric EMT

Advanced / Pro · RF study

Two positive-permittivity phases; no explicit contact network.

Open the matching Workbench exercise

EM Mori Tanaka

Advanced / Pro · RF study

Scalar principal-axis ellipsoidal field approximation.

Open the matching Workbench exercise

EM self-consistent

Advanced / Pro · RF study

Scalar principal-axis self-consistency; spherical case equals Bruggeman.

Open the matching Workbench exercise

Differential effective medium

Advanced / Pro · RF study

Incremental mixing with time-step refinement check.

Open the matching Workbench exercise

Coated sphere and interphase

Advanced / Pro · RF study

Concentric subwavelength coated spheres; no dynamic Mie scattering.

Open the matching Workbench exercise

Generalized multiphase EMT

Advanced / Pro · RF study

Spherical multiphase Bruggeman with convergence checks.

Open the matching Workbench exercise

Oblique polarized laminate TMM

Advanced / Pro · RF study

TE or TM waves; scalar isotropic layers, no polarization conversion.

Open the matching Workbench exercise

1D transmission line matrix

Advanced / Pro · RF study

Normal-incidence lossless delay-line mesh with pulse decay, energy and mesh-refinement safeguards. Explicit Run required; not a 3D solver.

Open the matching Workbench exercise

1D Floquet Bloch periodic layers

Advanced / Pro · RF study

Lossless isotropic A/B unit-cell eigenvalues, folded Bloch phase and stop-band attenuation at normal incidence. Not arbitrary-cell homogenization.

Open the matching Workbench exercise

Method references: Clemson transmission-line matrix overview and periodic bilayer characteristic matrices and Bloch dispersion . CDS implements the bounded one-dimensional cases described above.

Equations and interpretation

Passive complex permittivity

$$\varepsilon_r = \varepsilon_r' + i(\varepsilon_r' \tan\delta + \frac{\sigma}{\omega\varepsilon_0}) \tag{1}$$

Relative permittivity is dimensionless. Conductivity σ is in S/m, ω = 2πf is in rad/s and ε_0 is vacuum permittivity. The exp(−iωt) convention makes positive imaginary permittivity passive. Enter dielectric loss separately from conductivity so the same loss is not counted twice.

Maxwell Garnett mixing

$$\varepsilon_{\text{eff}} = \varepsilon_h + \frac{3v\varepsilon_h(\varepsilon_i - \varepsilon_h)}{\varepsilon_i + 2\varepsilon_h - v(\varepsilon_i - \varepsilon_h)} \tag{2}$$

Here v is inclusion volume fraction, h denotes host and i denotes inclusion. The scalar spherical approximation is appropriate for dilute, subwavelength inclusions. A numerical solution at a large fraction does not establish physical validity or account for a touching conductive network.

Power balance and shielding

$$R + T + A = 1, \quad \text{SE} = -10\log_{10}(T) \tag{3}$$

R, T and A are reflected, transmitted and absorbed power fractions. Shielding effectiveness SE is in dB. This definition includes both reflection and absorption. It is not an absorption-only measure and does not predict the performance of a finite enclosure with seams.

Material models are not interchangeable

Looyenga and Landau–Lifshitz–Looyenga name the same cube-root mixing law here. Spherical self-consistency reduces to the Bruggeman result; the Advanced principal-axis option exposes a depolarization factor. Neither method reconstructs an actual contact network. Series and parallel values are ordered Wiener bounds only for real, positive, lossless phases; lossy complex values are directional estimates.

The coated-sphere model first homogenizes the core and shell, then mixes coated particles into the host. Core fraction refers to core volume divided by coated-particle volume. The outer inclusion fraction is a separate number. Generalized multiphase EMT uses a bounded Bruggeman iteration and refuses to return an unconverged result.

Run an RF laminate study

- Start the matching EM exercise or create an EM case from Models. Run it separately from structural, thermal and moisture load cases.
- For a mixing study, enter host and inclusion dielectric properties and volume fractions. Advanced geometry factors describe a scalar principal-axis approximation, not a full anisotropic tensor.
- For transmission, enter explicit A and B layer properties, thicknesses, AB repeat count and frequency interval. Advanced TMM adds incidence angle and TE/TM polarization.
- Inspect reflection, transmission, absorption and shielding curves together. Confirm energy balance and repeat the study with a narrower frequency interval to resolve resonances.

Effective properties can currently be transferred manually into a TMM layer: enter the effective real permittivity and loss tangent, with conductivity set to zero when the effective loss already includes it. Mechanical laminate thicknesses and EM properties are not automatically coupled. Do not substitute a single directional effective property into an isotropic stack without justifying that approximation.

A result you can check

At 10 GHz, use a lossless dielectric with relative permittivity 4 and thickness 3.747405725 mm between air regions. Its refractive index is 2 and its thickness is one quarter of the wavelength inside the material. The analytic slab result is R = 0.36, T = 0.64 and A = 0. The calculated shielding is approximately 1.9382 dB. This is reflection from an ideal dielectric slab, not absorption.

Resolution and limits

The sweep samples 101 frequencies. Highly resonant stacks may require a narrower interval; a smooth curve is not proof that every resonance was resolved. The stack recursion avoids exponential growth for opaque layers. Transmission below the display floor is shown as 300 dB shielding, not as a precise experimentally measurable value. DEM compares two integration refinements, and multiphase EMT checks its residual.

All studies exclude finite edges, antennas, magnetic media, negative permittivity and thermal feedback. The 1D TLM study uses lossless delay cells, interface scattering, matched air ports and a unit impulse at normal incidence. Two resolutions must agree within two percentage points; unresolved late echoes are rejected. Inspect the reported thickness rounding error. The 1D Floquet–Bloch study solves $\lambda^2 - \mathrm{tr}(M)\lambda + 1 = 0$ for a lossless periodic A/B cell and plots folded $\mathrm{Re}(Kd)/\pi$ and stop-band $\mathrm{Im}(K)$. Evanescent decay is not absorption. These methods do not provide arbitrary-cell homogenization or 2D/3D geometry.

References

- Byrnes, Multilayer optical calculations — coherent planar layers and polarization conventions.
- COMSOL, Effective relative permittivity in effective media and mixtures — mixing-law context.
- Electromagnetic effective-medium modelling with core–shell inclusions — scope of coated-particle approximations.

Workbench availability: released models, inputs and compatible study paths . The wider theory library includes reference formulations not available in every Workbench solve.

4 Laminate Analysis

Online chapter

A unified constituent-to-process-to-laminate reference. Generate or measure the three-dimensional property definition independently for every ply, solve optional heat, moisture, cure, and crystallization histories, assemble the multi-material laminate, and progress its selected failure models under mechanical and process loading.

Workbench availability: released models, inputs and compatible study paths . The wider theory library includes reference formulations not available in every Workbench solve.

5 From elastic response to a design study

Online chapter

Equations, record connections and implementation limits for the current WB interactive calculations. The compiled backend is a separate execution path; do not infer that every backend capability is active in every WB view.

Select cases and inspect your model

Inspect the selected model in Live Sim

SIMULATE opens with Live Sim, an input-driven view of the selected cases. The four selectors remain available above the scene. Switch to Blocks to manage candidate records and trace their connections.

- Select Geometry, Laminate, a constituent or a case to inspect the inputs that are actually used. Clicking a used block heading also opens its Live Sim inspection.
- Select a ply in the stack or geometry view to inspect its source. Micro-derived and stored-property plies are identified separately. Woven sources show the fabric unit-cell preview when applicable.
- Select the Thermal or Moisture case to inspect its surface boundary schedule. Move the step slider to compare prescribed conditions. This is not a solved internal temperature or moisture field.
- Use Edit input to open the source record. The scene follows the changed inputs; rerun the simulation before trusting previous results.

Geometry, ply bands and arrows are input illustrations, not a finite-element mesh or solved deformation. Display-only thickness enlargement and any model-specific visualization assumptions are identified in the preview.

Choose the run in the SIMULATION block

SIMULATION is the control point for the run. Select a Thermal case, Moisture case, Mechanical case and EM case, or None in any slot. Each selected case shows its analysis model, laminate and applicable geometry.

- Keep candidate records in the surrounding blocks. Adding a candidate does not select it for execution.
- Select the required cases in SIMULATION and review their inputs before Run. At least one case is required.
- Use the same laminate for a supported combined run. Run standalone studies separately with the other selectors set to None.
- Run executes the selected combination. A connection or Used marker is not confirmation of a successful solve.

Selecting several cases does not add unsupported physics coupling. EM screening studies do not automatically heat the thermal case.

Review every downstream geometry dependency

A geometry record can be shared by several cases and simulations. Editing its dimensions or type affects all linked consumers, including studies that are not currently open. Unrelated records are unchanged.

- After editing geometry, open Solver messages and expand Review affected cases and simulations. Select a linked name to inspect that record.
- Check the selected model, load basis, dimensions and boundary conditions. Loads are not automatically replaced when the geometry changes.
- Resolve incompatible geometry and model combinations before running. An I-section does not turn a plate theory into a beam theory.
- Rerun affected simulations before relying on previous results. Inputs changed warnings indicate that stored results no longer match their connected inputs.

Geometry affects only dimensions consumed by the selected model. One-dimensional transport retains its through-thickness assumptions; standalone studies may own their dimensions. Under fixed total edge loads, changing plate width changes force per unit width. Under prescribed resultants, it does not.

Complete block workflow guide

1 Property and model connections

Constituent records feed the selected micromechanics model. Its effective lamina properties—or a directly selected material—feed each laminate ply. Ply angle and thickness transform and integrate those properties into the laminate stiffness. The structural case supplies loads and geometry. Thermal and moisture analyses use the linked process and boundary histories; their recovered states can supply environmental free strains when that contribution is enabled.

Saved results retain the state used by their run. Editing an upstream record changes the current model, not an earlier saved result. WB live CLT recovers current elastic response, while stored process residuals require a new solver run after relevant edits. Optimization snapshots freeze the search inputs and results for later review.

Operating guide: live sync, records and result freshness

2 Laminate stiffness and recovery

For a perfectly bonded, small-strain plane-stress laminate, each ply contributes its transformed reduced stiffness $\bar{Q}$. Using the laminate mid-plane as z = 0:

$$\mathbf{A} = \sum_k \overline{\mathbf{Q}}_k \, (z_k - z_{k-1})$$

$$\mathbf{B} = \frac{1}{2}\sum_k \overline{\mathbf{Q}}_k \, (z_k^2 - z_{k-1}^2)$$

$$\mathbf{D} = \frac{1}{3}\sum_k \overline{\mathbf{Q}}_k \, (z_k^3 - z_{k-1}^3)$$

$$\begin{bmatrix} \mathbf{N} \\ \mathbf{M} \end{bmatrix} = \begin{bmatrix} \mathbf{A} & \mathbf{B} \\ \mathbf{B} & \mathbf{D} \end{bmatrix} \begin{bmatrix} \boldsymbol{\varepsilon}^0 \\ \boldsymbol{\kappa} \end{bmatrix} - \begin{bmatrix} \mathbf{N}^* \\ \mathbf{M}^* \end{bmatrix}$$

$$\boldsymbol{\sigma}_k(z) = \overline{\mathbf{Q}}_k [\boldsymbol{\varepsilon}^0 + z\boldsymbol{\kappa} - \boldsymbol{\varepsilon}_k^*(z)]$$

N is membrane force per width, M is moment per width, ε^0 is mid-plane engineering strain, κ is curvature and ε* is the enabled free strain. With $\bar{Q}$ in MPa and z in mm, A is N/mm, B is N and D is N·mm.

Keep this consistent with the input load units. Local stresses require the ply-axis transformation, including the engineering shear convention.

The six-by-six inverse ABD gives compliance. Effective $E_x = 1/(a_{11} h)$, $E_y = 1/(a_{22} h)$, $G_{xy} = 1/(a_{66} h)$ and $\nu_{xy} = -a_{12}/a_{11}$ for the corresponding force-controlled compliance definition. An unsymmetric laminate can couple extension and curvature; these values are not the same as artificially imposing zero curvature.

Full CLT and environmental coupling reference

3 Implemented WB first-ply criteria

WB implements Maximum stress, Maximum strain, Tsai–Hill, Tsai–Wu and plane-stress Hashin screening. Puck is not implemented. LaRC04 linear-shear initiation is available as a separate reference-state study; it is not an envelope or progressive-degradation option. Positive tensile/compressive strengths, shear allowable and elastic moduli are required.

- Maximum stress compares the absolute local normal stresses with sign-appropriate strengths and shear with S12.
- Maximum strain compares local strains with explicit strain limits when available; otherwise limits are derived from strength/modulus. That derivation is an assumption, not measured strain-to-failure data.
- Tsai–Hill uses sign-dependent X and Y and the implemented interaction $\sigma_1^2/X^2 - \sigma_1\sigma_2/X^2 + \sigma_2^2/Y^2 + \tau_{12}^2/S_{12}^2$.
- Tsai–Wu combines linear tension/compression terms with quadratic interaction. The normalized interaction F_{12}^* defaults to −0.5; it must be strictly between −1 and 1. Calibrate it when validation data is available.
- Hashin separates tensile/compressive fiber and matrix interactions. WB's r17-derived shear-dominant attribution maps the governing interaction to shear damage; it is not a separate experimental failure-mode identification.

For proportional elastic loading with no fixed residual offset, each active criterion can be written $qR^2 + lR = 1$. The positive root gives a reserve factor; a linear criterion gives $R = 1/l$. The minimum across sampled ply locations and modes controls first failure. A general failure index is not always the reciprocal of reserve factor.

Failure criterion definitions and assumptions

4 Envelopes and progressive damage are different analyses

An envelope samples directions in a two-component load plane and searches for the first-failure point along each ray under the specified background state. The joined points are a numerical approximation. If a residual load/free-strain state is present, the response is affine rather than purely proportional: evaluate the fixed state plus the ramped increment. Do not blindly scale the complete combined response.

Progressive failure updates the selected mode stiffness after activation, recomputes equilibrium and continues to the selected terminal condition or search limit. First activation, terminal load, retained stiffness and last-ply metrics are not interchangeable. Increment size, same-load iterations, degradation factors, criterion and stopping rule affect the outcome.

Through-thickness sampling can reveal variation in a recovered field but cannot validate missing transverse, cohesive, fatigue or nonlinear physics. The WB interactive plane-stress workflow is narrower than the complete compiled solver theory library.

Progressive update reference · Envelope operating procedure

5 Carpet plots fixed-stack elastic sweeps

Two distinct absolute-angle families are selected from the current visible stack. Their magnitudes are swept independently over 0–90°, using 2–21 samples each. Existing negative signs, other angle families, material properties, ply thicknesses and ordering are retained. Each grid point is a fresh elastic laminate-property calculation.

The α lines are solid and the β lines dashed. Their color gradients identify the swept angles. The current stack is a reference point; the live laminate preview displays the hovered candidate. Balance is checked from matched positive/negative angle contributions with compatible elastic properties and thickness. A family originally at 0° has no implicit negative partner, so sweeping it can create an unbalanced candidate.

These curves describe elastic design sensitivity—not failure probability, a feasible strength region, or manufacturing approval. Select a candidate and evaluate all relevant load, stability and process constraints separately.

6 Discrete laminate optimization

The current WB search uses one material, uniform ply thickness, elastic CLT and a mechanical resultant vector. It rejects reused process free strains after redesign. For each candidate it calculates the selected first-failure reserve factor λ, areal mass mA = Σρk tk and the selected absolute mid-plane strain at first failure.

$$\text{Mass objective:} \quad min m_A \quad \text{subject to } \lambda \geq \lambda_{\text{required}}$$

$$\text{Strength objective:} \quad max \lambda \quad \text{at fixed ply count}$$

$$\text{Strain objective:} \quad max |\varepsilon^0_{\text{component}}(\lambda)| \quad \text{at fixed ply count}$$

The strain objective uses εx, εy or γxy in microstrain at first failure—not displacement, service-load strain or a guaranteed ductility measure. Under pure bending, a mid-plane component can be zero. Load factors from different cases are relative to different reference vectors and must not be compared without their context.

Allowed angles are discrete. Symmetry mirrors the half-stack; balanced-pair construction uses adjacent ±θ pairs, with repeated 0°/90° blocks. Both options together constrain counts to multiples of four. This is a restricted construction space, not every possible balanced laminate.

Small spaces are enumerated completely. Larger spaces use a seeded multi-start elitist mutation search with random exploration and a bounded candidate budget. Report “best found,” the budget, seed, feasible count and objective. A flat curve or exhausted budget does not establish a global optimum.

Constraints on contiguity, disorientation, buckling, fatigue, joints, defects, delamination and coupled environmental response are not implicitly enforced. Apply the candidate or create a separate laminate, then rerun the complete engineering assessment.

7 Validation data and reproducibility

An optimization snapshot stores the study, source ply properties, load vector, configuration, baseline, candidates and convergence. It is an immutable record of that search—not an automatic update to a simulation or a solver certification. Keep its downloaded CDS_DB together with the complete simulation dependency package.

Document which execution path produced each result: WB live elastic preview, interactive WB failure/optimization, saved coupled solver run, or compiled solver/Runtime release. Preserve model identity, units, calibration sources and unavailable-contribution warnings. Existing compiled acceptance validation data applies only to its tested release and cases.

Step-by-step failure and optimization guide · Laminate assumptions and limitations

Workbench availability: released models, inputs and compatible study paths . The wider theory library includes reference formulations not available in every Workbench solve.

6 Web access and module entitlements

Online chapter

Understand account verification, demo access, licensed models, group seats and payment activation.

Accounts demo and your library

Workspace modules are open for browsing. Standard, Pro and Commercial package templates distinguish the complexity of models inside them: thin-wall cylinder and CLT are Standard; thick-wall elasticity and FSDT are Pro; coupled delamination and specialist calibrated studies are Commercial. Structural Advanced is a specialist commercial-model bundle. Research prescriptions remain customizable. Existing licenses and paid package snapshots keep their issued permissions; the model badge in Workbench reports your actual access, not just your edition name.

Workbench requires a registered, verified CDS account, including the 30-day demo. The demo has a limited feature set; it is not the full commercial package. After its term ends, an active license is required to continue. A feature reminder links back to the CDS website.

Your CDS library brings together the overview PDF, current manuals, theory and exercises. Database downloads require active license access; opening a database does not grant permission to run every model it contains. The editable overview PowerPoint is restricted to the CDS owner.

Trust boundary

CDS stores account, organization, project, role, plan, module, and expiration information in protected server-side records. The browser never receives signing material or backend service credentials.

Compiled deployment boundary. The production integration requires authorization before a Recipe enters the execution queue. A configured Python worker assembles the structured Web r18 request only for an entitled project and stores validation data against that immutable Recipe. This describes the compiled-service deployment requirements; the native WB live/service calculations are a separate execution path.

Authorization sequence

- Authenticate the verified CDS account and its active session.
- Resolve the effective personal or group license, including an assigned educator or commercial team seat.
- Check license status, expiration, seat policy, modules and selected model permissions.
- Apply the same permissions to Workbench workflows and server-side run requests; a visible selector or imported database is not authorization.
- Validate the requested analysis and its connected inputs before execution.
- Review the completed result with its input context and diagnostics. Compiled-service queuing follows the separate deployment requirements described above.

Module and audience policies

- **Educator–student:** the Standard teaching package defaults to a 180-day semester. Verified students on an active educator roster inherit that group's permitted modules, model selections, and expiration; student status does not unlock every module.
- **Commercial:** a monthly or annual package with its configured modules, model selections, seat count, and expiration. An assigned team seat uses the active group license.
- **Research or institutional:** a custom selection of modules and models, with administrator review available. Standard subscriptions default to one month unless the package specifies another term.
- **Expandable catalog:** administrators may add stable keys without redesigning the entitlement schema; existing explicit plans do not silently gain a new module.

Payment fulfillment

A configured Stripe price maps to a CDS package, billing term, modules, and model permissions. Only verified payment events are eligible for paid fulfillment. CDS checks the webhook signature and avoids granting the same payment twice. The package's approval policy determines whether eligible payment activates access automatically or creates a request for administrator review. Subscription invoice periods determine the paid access term; a checkout return page alone does not grant a license.

Suspension and revocation

Suspension, expiration, seat changes, or revocation take effect at the next authenticated request. Existing engineering results remain preserved and traceable, while new edits and solver runs are blocked according to policy.

Workbench availability: released models, inputs and compatible study paths . The wider theory library includes reference formulations not available in every Workbench solve.

7 Trusted material data from the source

Online chapter

Current Workbench, reference editions and downloads

Use the online User Guide for current controls, the released model directory for selectable models and compatibility, and the Training Manual for connected exercises. Wider theory references do not mean every formulation is enabled in Workbench.

Dated GUI captures and compiled Web r18 PDF manuals retain their stated scope; they are not a substitute for current hosted Workbench instructions. Find the overview PDF, guides and exercise databases in Your CDS library .

Prepare traceable engineering records, calibrated thermoset cure kinetics, and semicrystalline thermoplastic crystallization models before the data enters micromechanics, processing, laminate, or structural analyses.

Workbench availability: released models, inputs and compatible study paths . The wider theory library includes reference formulations not available in every Workbench solve.

8 AI Import

Online chapter

Research with ChatGPT. Review sources, units and conditions in Workbench before creating new material records.

Read the step-by-step material import guide

Open Material → Find / Import with AI in Workbench to copy a research prompt, load research JSON, attach local datasheets for comparison, and selectively import reviewed properties. Existing records are not overwritten.

Web search and automatic PDF extraction are not connected inside CDS in this version. Unknown values remain absent; estimates require explicit approval. Save the resulting workspace as CDS_DB and retain original source files separately.

9 PEEK/PEKK crystallization pipeline

Online chapter

Current Workbench, reference editions and downloads

Use the online User Guide for current controls, the released model directory for selectable models and compatibility, and the Training Manual for connected exercises. Wider theory references do not mean every formulation is enabled in Workbench.

Dated GUI captures and compiled Web r18 PDF manuals retain their stated scope; they are not a substitute for current hosted Workbench instructions. Find the overview PDF, guides and exercise databases in Your CDS library .

Represent calibrated semicrystalline thermoplastic evolution with single- or double-branch Nakamura/Avrami-style kinetics, latent heat, and anisotropic crystallization shrinkage. Expand any equation for its physical meaning, variables, units, model connection, and theory source.

State normalization and temperature window

Select thermoplastic crystallization for a semicrystalline polymer. Crystallinity X is bounded between its initial value and the user-supplied maximum X_{max}. Kinetics are active only when the current nodal temperature lies strictly between the calibrated glass-transition and melting temperatures.

Eq. 05.1.3-01 **Normalized crystallinity**

$$\xi = X/X_{\max}, 0 \leq \xi \leq 1$$

Expresses current absolute crystallinity as a fraction of the maximum crystallinity available to the selected thermoplastic grade.

Variables

ξ *normalized crystallinity* dimensionless, 0–1

X *current absolute crystallinity* dimensionless mass or volume fraction

X_{max} *calibrated maximum crystallinity* dimensionless mass or volume fraction

Model connection The normalized state is used by both Nakamura branches and the bounded integration rule; the crystallinity history retains the absolute crystallinity X.

Theory basis Nakamura nonisothermal crystallization

Eq. 05.1.3-02 **Temperature and undercooling factor**

$$K_j(T) = K_{0j}\exp\left[-E_{\mathrm{xj}}/(RT)\right]\left[(T_m - T)/\left(T_m - T_g\right)\right]^p$$

Combines Arrhenius temperature dependence with a calibrated undercooling function that vanishes at the melting temperature and is evaluated only inside the Tg–Tm process window.

Variables

K_j *crystallization rate coefficient for branch j* s^{-1}

K_{0j} *branch pre-exponential coefficient* s^{-1}

$\mathbf{E}_{xj}$ *branch activation energy* J/mol

$\mathbf{T}_g$, $\mathbf{T}_m$ *glass-transition and melting temperatures* K

p *undercooling exponent* dimensionless

R, T *gas constant and local absolute temperature* J/(mol·K), K

Model connection Evaluated at every active thermoplastic transport node using the current thermal iterate. Outside Tg<T<Tm, R15 sets the crystallization rate to zero.

Theory basis PEEK dual-mechanism crystallization model

Nakamura/Avrami evolution

Eq. 05.1.3-03 **Single-branch normalized crystallization rate**

$$\dot{\xi}_j = n_j K_j(T)(1-\xi)[-\ln(1-\xi)]^{(n_j-1)/n_j}$$

Differentiates the Nakamura form of Avrami crystallization to obtain an instantaneous nonisothermal rate in the normalized state. Numerical floors protect the logarithm near ξ=0 and ξ=1.

Variables

$\dot{\boldsymbol{\xi}}_j$ *normalized crystallization rate of branch j* s^{-1}

$\mathbf{n}_j$ *Avrami exponent for branch j* dimensionless

$\mathbf{K}_j\mathbf{(T)}$ *temperature-dependent branch coefficient* s^{-1}

ξ *normalized crystallinity* dimensionless

Model connection The single-branch crystallization law uses its calibrated rate directly. The rate is then advanced using the irreversible bounded update.

Theory basis Nakamura rate formulation

Eq. 05.1.3-04 **Double-branch crystallization rate**

$$\dot{\xi} = w\dot{\xi}_1 + (1-w)\dot{\xi}_2$$

Blends two independently calibrated Nakamura branches to represent two-stage crystallization with one bounded weighting factor.

Variables

$\dot{\boldsymbol{\xi}}$ *combined normalized crystallization rate* s^{-1}

$\dot{\boldsymbol{\xi}}_1$, $\dot{\boldsymbol{\xi}}_2$ *normalized rates of branches 1 and 2* s^{-1}

w *branch-1 weight* dimensionless, 0–1

Model connection The dual-branch crystallization law. The same combined rate controls crystallinity growth, latent heat release, and the subsequent shrinkage state.

Theory basis Velisaris–Seferis dual-mechanism PEEK model

Eq. 05.1.3-05 **Bounded irreversible crystallinity update**

$$r_\xi = 1 - \xi^n$$

$$\xi^{n+1} = \min\left[1, \max\left(\xi^n, \xi^n + r_\xi\left\{1 - \exp\left(-\dot{\xi}^n \Delta t / r_\xi\right)\right\}\right)\right], X^{n+1} = X_{\max}\xi^{n+1}$$

Integrates the normalized rate over the process step without consuming more than the remaining crystallizable fraction, then maps the state back to absolute crystallinity.

Variables

ξ^n, ξ^{n+1} *old and new normalized crystallinity* dimensionless

r_ξ *remaining crystallizable fraction, 1–ξ^n* dimensionless

$\dot{\xi}^n$ *selected single- or double-branch rate* s^{-1}

Δt *transport time increment* s

X^{n+1} *new absolute crystallinity* dimensionless fraction

Model connection Applied independently at every active thermoplastic node. The crystallization-rate history reports $(X^{n+1}–X^n)/\Delta t$ rather than the normalized branch rate.

Theory basis Nonisothermal Nakamura state evolution

Latent heat and crystallization shrinkage

Eq. 05.1.3-06 **Crystallization heat source**

$$q_x = \rho H_x \dot{X}$$

Converts absolute crystallinity growth and the calibrated heat of crystallization into a volumetric heat source.

Variables

q_x *volumetric crystallization heat generation* W/m^3

ρ *local effective ply density* kg/m^3

H_x *heat of crystallization per unit mass* J/kg

$\dot{X}$ *absolute crystallinity rate* s^{-1}

Model connection Included in the heat equation only when the crystallization-exotherm option is enabled and reported as crystallization heat generation.

Theory basis PEEK crystallization calorimetry basis

Eq. 05.1.3-07 **Local crystallization-shrinkage free strain**

$$\varepsilon_k^x = -s_k^x (X - X_0)/X_{\max}$$

Maps crystallinity gained after the initial state into an anisotropic contraction in each ply material direction.

Variables

ε^x_k *crystallization free strain in local direction k* strain

s^x_k *full-crystallization shrinkage magnitude* strain

X_0 *initial absolute crystallinity* dimensionless fraction

$\mathbf{X}_{max}$ *maximum absolute crystallinity* dimensionless fraction

k *local ply direction 1, 2, or 3* index

Model connection Stored in the process-shrinkage history, fitted through each ply, and optionally added to the laminate process resultants and local failure-stress recovery.

Theory basis Process-shrinkage residual-stress framework

Material-grade calibration is required. PEEK and PEKK grade, molecular architecture, cooling history, prior melt state, reinforcement, and measurement method change the fitted kinetics. The pipeline is a model family, not a generic property card.

Required validation data

- DSC-derived crystallization rate and heat over relevant cooling/heating histories.
- T_g, T_m, and maximum crystallinity for the selected grade.
- Dilatometry or dimensional data for local crystallization shrinkage.
- Verification against nonisothermal process cycles before residual-stress use.

Theory references

- Nakamura et al., “Some aspects of nonisothermal crystallization of polymers. I,” Journal of Applied Polymer Science 16 (1972) 1077–1091.
- Velisaris and Seferis, “Crystallization kinetics of polyetheretherketone (PEEK) matrices,” Polymer Engineering & Science 26 (1986) 1574–1581.
- NASA composite process modeling reference for coupled heat generation, shrinkage, and residual response.

Workbench availability: released models, inputs and compatible study paths . The wider theory library includes reference formulations not available in every Workbench solve.

10 Thermoset cure kinetics

Online chapter

Current Workbench, reference editions and downloads

Use the online User Guide for current controls, the released model directory for selectable models and compatibility, and the Training Manual for connected exercises. Wider theory references do not mean every formulation is enabled in Workbench.

Dated GUI captures and compiled Web r18 PDF manuals retain their stated scope; they are not a substitute for current hosted Workbench instructions. Find the overview PDF, guides and exercise databases in Your CDS library .

Define calibrated epoxy cure, heat release, and irreversible process shrinkage at the material/ply level before solving the laminate process history. Expand any equation for its physical meaning, variables, units, model connection, and theory source.

State variable and model routing

Degree of cure α is the reacted fraction of the available thermoset chemistry. R15 bounds α to [0,1], prevents reverse reaction, and evaluates kinetics independently at every transport node. Each ply selects its own polymer family and kinetics model in the process definition. Select thermoset cure for a reacting resin or an inert material for a nonreacting layer.

Eq. 05.1.2-01 **Arrhenius rate constant**

$$k_i(T) = A_i \exp[-E_i/(RT)]$$

Converts each calibrated kinetic prefactor and activation energy into a temperature-dependent reaction-rate constant. Absolute temperature must be used.

Variables

k_i *rate constant for reaction branch i* s^{-1}

A_i *pre-exponential factor for branch i* s^{-1}

E_i *activation energy for branch i* J/mol

R *universal gas constant* 8.314462618 J/(mol·K)

T *local nodal absolute temperature* K

Model connection Evaluated from the current thermal iterate before the selected cure law is advanced; it therefore couples cure rate to the transient temperature field.

Theory basis Sourour–Kamal cure kinetics

Selectable reaction laws

The model ID chooses one of four rate laws. These laws describe chemistry only after their coefficients have been fit to DSC or equivalent measurements for the actual resin formulation.

Eq. 05.1.2-02 **Nth-order cure**

$$\dot{\alpha} = k_1(T)(1-\alpha)^n$$

Represents a non-autocatalytic reaction whose rate decreases as the unreacted fraction is consumed.

Variables

α *degree of cure* dimensionless, 0–1

$\dot{\alpha}$ *instantaneous cure rate* s^{-1}

k_1 *Arrhenius rate constant from Eq. 05.1.2-01* s^{-1}

n *reaction-order exponent* dimensionless

Model connection The nth-order cure law. The returned nonnegative rate is passed to the bounded irreversible state update.

Theory basis Thermoset kinetic model basis

Eq. 05.1.2-03 **Kamal–Sourour autocatalytic cure**

$$\dot{\alpha} = [k_1(T)+k_2(T)\alpha^m](1-\alpha)^n$$

Adds an autocatalytic branch that grows with degree of cure to the nth-order branch, allowing an isothermal rate peak after the reaction begins.

Variables

k_1, k_2 *non-autocatalytic and autocatalytic Arrhenius rate constants* s^{-1}

α *degree of cure* dimensionless, 0–1

m *autocatalytic exponent* dimensionless

n *unreacted-fraction exponent* dimensionless

$\dot{\alpha}$ *instantaneous cure rate* s^{-1}

Model connection The Kamal–Sourour cure law, also used as the base reaction law before vitrification limitation is applied.

Theory basis Sourour–Kamal autocatalytic model

Eq. 05.1.2-04 **Prout–Tompkins cure**

$$\dot{\alpha} = k_1(T)\alpha^m(1-\alpha)^n$$

Uses a single autocatalytic rate constant with reacted- and unreacted-fraction powers. A small positive numerical floor on α prevents a zero-to-a-negative-power singularity.

Variables

k_1 *Arrhenius rate constant* s^{-1}

α *degree of cure* dimensionless, 0–1

m, n *autocatalytic and reaction-order exponents* dimensionless

$\dot{\alpha}$ *instantaneous cure rate* s^{-1}

Model connection The Prout–Tompkins cure law. It shares the same bounded state update, heat source, and shrinkage mapping as the other cure laws.

Theory basis NASA composite cure-process formulation

Eq. 05.1.2-05 **Diffusion-limited Kamal multiplier**

$$f_d = \{1 + \exp[s_v(\alpha - \alpha_v)]\}^{-1}, \dot{\alpha}_{\text{limited}} = f_d \dot{\alpha}_{\text{Kamal}}$$

Suppresses the chemical Kamal–Sourour rate as cure passes a calibrated vitrification threshold. It is an empirical mobility correction, not an independently predicted glass-transition model.

Variables

f_d *diffusion or vitrification rate multiplier* dimensionless, 0–1

s_v *logistic vitrification slope* dimensionless

α_v *degree of cure at the logistic midpoint* dimensionless

$\dot{\alpha}_{\text{Kamal}}$ *unlimited rate from Eq. 05.1.2-03* s^{-1}

$\dot{\alpha}_{\text{limited}}$ *mobility-limited cure rate* s^{-1}

Model connection The diffusion-limited cure law. The limited rate, rather than the raw chemical rate, advances α and produces reaction heat.

Theory basis Cure-process modeling and vitrification context

Irreversible state integration

Eq. 05.1.2-06 **Bounded exponential cure update**

$$r_\alpha = 1 - \alpha^n, \alpha^{n+1} = \min[1, \max(\alpha^n, \alpha^n + r_\alpha\{1 - \exp(-r^n \Delta t / r_\alpha)\})]$$

Advances cure over one transport step without consuming more than the remaining unreacted fraction. The outer bounds enforce irreversibility and α≤1.

Variables

α^n, α^{n+1} *degree of cure at the old and new process times* dimensionless

r^n *selected raw or diffusion-limited kinetic rate* s^{-1}

Δt *transport time increment* s

r_α *available unreacted fraction, $1-\alpha^n$* dimensionless

Model connection Applied independently at every active thermoset node inside each staggered thermal/kinetic iteration. The reported rate is $(\alpha^{n+1}-\alpha^n)/\Delta t$.

Theory basis Numerical cure-process integration context

Reaction heat and chemical shrinkage

Eq. 05.1.2-07 **Volumetric cure heat source**

$$q_c = \rho H_c \dot{\alpha}$$

Converts cure progress and mass-specific total heat of reaction into a volumetric source for the one-dimensional heat equation.

Variables

q_c *volumetric cure heat generation* W/m^3

ρ *local effective ply density* kg/m^3

H_c *total heat of cure per unit mass* J/kg

$\dot{\alpha}$ *bounded cure rate over the current step* s^{-1}

Model connection Included in the thermal right-hand side only when the cure-exotherm option is enabled and reported separately as cure heat generation.

Theory basis NASA composite cure-process heat balance

Eq. 05.1.2-08 **Local cure-shrinkage free strain**

$$\varepsilon_k^c = -s_k^c(\alpha - \alpha_0)$$

Maps the increase in degree of cure into an anisotropic contraction in the ply material axes. Positive calibrated shrinkage magnitudes therefore produce negative free strain.

Variables

ε^c_k *cure-shrinkage free strain in material direction k* strain

s^c_k *full-cure shrinkage magnitude in direction k* strain

α_0 *initial degree of cure* dimensionless

k *local ply direction 1, 2, or 3* index

Model connection Stored at each process node, fitted across each ply, transformed to laminate axes, and optionally included in the process force and moment resultants.

Theory basis NASA cure-induced residual-stress study

Calibration boundary. Pre-exponential factors, activation energies, exponents, total reaction heat, vitrification controls, and shrinkage are resin-system data. R15 defaults to an inert row and does not represent a universal epoxy.

Material inputs and outputs

Input family	Purpose	Primary output
A_1, E_1, A_2, E_2, m, n	Temperature-dependent reaction rate	Cure-rate history
H_c	Total heat of cure per unit mass	Cure-heat history
$s^c_{1,2,3}$	Full-process local shrinkage magnitudes	Process-shrinkage history
α_0, α_v, s_v	Initial state and optional mobility limitation	Degree-of-cure history

Theory references

- Sourour and Kamal, “Differential scanning calorimetry of epoxy cure: isothermal cure kinetics,” Thermochimica Acta 14 (1976) 41–59.
- NASA, Composite Cure Process Modeling and Simulations using Finite Element Analysis (2016).
- NASA/TM–20205009287, residual stresses induced during matrix cure.

Workbench availability: released models, inputs and compatible study paths . The wider theory library includes reference formulations not available in every Workbench solve.

11 Micromechanics of Composites

Online chapter

This theory library includes wider research formulations. Check the released model directory for selectable models, required inputs, limits and exercises. The event-driven RVE branch is not enabled in hosted Workbench.

The complete CDS theory chain: continuous and discontinuous fibers, mean-field homogenization, Chou orientation factors, textile architectures, fillers and voids, thermophysics, damage and failure, constituent-limit recovery, and the per-ply handoff into progressive laminate analysis.

Workbench availability: released models, inputs and compatible study paths . The wider theory library includes reference formulations not available in every Workbench solve.

12 Semi-analytical aligned discontinuous-composite theory

Online chapter

This theory library includes wider research formulations. Check the released model directory for selectable models, required inputs, limits and exercises. The event-driven RVE branch is not enabled in hosted Workbench.

Reference formulation — not enabled in hosted Workbench.

This Revision 8 chapter documents a separate research / compiled-solver branch. Its event-driven breaks, nonlinear shear, RVE series coupling and stochastic failure are not selectable in hosted Workbench. Cox shear-lag elastic homogenization is available, not this failure model. Released models and connections

1 Theory basis and role in CDS

Henry and Pimenta model aligned short-fiber material across specimen, RVE, fiber, neighboring-fiber interaction, and interaction-segment scales. Random fiber ends create nonuniform overlaps, matrix shear transfers load, fiber strength is stochastic, and final failure occurs when a local cluster becomes unstable.

The reference implementation associates this formulation with aligned-discontinuous material type 1 / criterion 6; this is not a selectable hosted Workbench path. Its specimen response supplies longitudinal ply stiffness and tensile strength to the common orthotropic ply property definition. Laminate ABD assembly and laminate-scale progressive degradation remain separate downstream operations.

2 Paper-to-CDS traceability

Henry–Pimenta mechanism	Revision 8 status	CDS implementation
Random longitudinal fiber-end locations	Implemented	Each RVE draws one end location per fiber over the selected fiber length.
Square n × n aligned-fiber RVE	Implemented	The user controls fibers per row and the number of independent RVEs.
Four-nearest-neighbor topology	Implemented	Horizontal and vertical interactions are rebuilt from fiber ends and inserted breaks.
Generic nonlinear matrix constitutive law	Implemented	An optional piecewise-linear $\tau(\gamma)$ table is accepted; otherwise CDS builds an elastic-yield-friction law.

Henry–Pimenta mechanism	Revision 8 status	CDS implementation
Broken and shear-lag interaction segments	Implemented	Same-fiber endpoints create broken segments; different-fiber endpoints create nonlinear shear-lag segments.
Length- and field-scaled Weibull strength	Implemented	Ordered thresholds use fiber/reference length, Weibull scale and shape, and stress-field correction.
Event-driven break insertion and rebuilding	Implemented	The governing break coordinate is inserted, its interaction is deactivated, and the network is rebuilt at the same strain.
Debonding and frictional pull-out toughness	Implemented	Resistance is integrated over realized overlaps from mode-II toughness and residual friction.
Dugdale critical-cluster instability	Implemented	Square clusters are screened with the nonlinear energy-release expression and physical cluster radius.
Specimen curve from RVEs in series	Implemented	RVE strains are interpolated at common stress and averaged; the first RVE cutoff governs.

3 Interaction-segment mechanics

3 1 Discontinuity reconstruction

For each horizontal and vertical neighbor pair, CDS sorts both fiber ends and all inserted break coordinates. Consecutive discontinuities define the current interaction segments. If both endpoints belong to the same fiber, the segment is broken; if they belong to different fibers, load crosses the matrix through shear lag.

Eq. ADF-01$\sigma_{\mathrm{Br}}^{I} = \frac{E_f}{2}\varepsilon_{\mathrm{Br}}^{I}$

$$\sigma_{\mathrm{Br}}^{I} = \left(E_f/2\right)\varepsilon_{\mathrm{Br}}^{I}$$

Relates interaction stress to strain in a segment bounded by discontinuities on the same fiber.

Variables

σBrI *Broken-segment interaction stress* Pa

Ef *Fiber Young’s modulus* Pa

εBrI *Broken-segment interaction strain* dimensionless

Model connection Supplies the broken-segment response used in the length-weighted interaction strain.

Theory basis Henry and Pimenta (2017), reference formulation

3 2 Nonlinear shear lag

With fiber half-thickness T = $\varphi_f/4$ and effective matrix gap t_m, the fiber stress difference follows:

Eq. ADF-02 $\frac{d^2\Delta\sigma}{dx^2} = \pm\lambda^2\Delta\sigma, \quad \lambda = \left[\frac{2|G_m|}{T t_m E_f}\right]^{1/2}$

$$d^2\Delta\sigma/\mathrm{dx}^2 = \pm\lambda^2\Delta\sigma, \lambda = [2|G_m|/(T t_m E_f)]^{1/2}$$

Describes how the stress difference between neighboring fibers varies along an interaction segment. The active matrix-law branch determines the sign and stiffness used.

Variables

Δσ *Stress difference between neighboring fibers* Pa

x *Position along the fiber* m

λ *Shear-transfer parameter* 1/m

Gm *Matrix shear modulus for the active constitutive branch* Pa

T *Fiber half-thickness, equal to one quarter of the fiber diameter* m

tm *Effective matrix gap between fibers* m

Ef *Fiber Young's modulus* Pa

Model connection Provides the nonlinear shear-lag segment response before segments are combined in series.

Theory basis Henry and Pimenta (2017), reference formulation

The active secant/tangent behavior comes from the selected piecewise-linear matrix law. The interaction stress is common to its segments, and their strain contributions are length-weighted in series. The weakest segment limits the interaction.

Eq. ADF-03 $\varepsilon_{\mathrm{RVE}}(\sigma^I) = \frac{1}{l_f}\sum_s \Delta\, l_s \varepsilon_s^I(\sigma^I)$

$$\varepsilon_{\mathrm{RVE}}(\sigma^I) = (1/l_f)\Sigma_s \Delta l_s \varepsilon_s^I(\sigma^I)$$

Averages segment strains by their lengths at a common interaction stress.

Variables

εRVE *Representative-volume strain* dimensionless

σI *Common interaction stress* Pa

lf *Fiber length* m

Δls *Length of segment s* m

εsI *Strain of segment s at the common interaction stress* dimensionless

s *Segment index* dimensionless

Model connection Connects individual broken and shear-lag segments to the representative-volume response.

Theory basis Henry and Pimenta (2017), reference formulation

4 Progressive fiber-break events

Each fiber receives ordered Weibull thresholds. Length and stress-field scaling follow:

Eq. ADF-04 $F(\sigma_f) = 1 - \exp\left[\; -C_l C_\sigma \left(\frac{\sigma_f}{\sigma_0}\right)^m \right], \quad C_l = \frac{l_f}{4 l_r}$

$$F(\sigma_f) = 1 - \exp\left[-C_l C_\sigma (\sigma_f/\sigma_0)^m\right], C_l = l_f/(4 l_r)$$

Expresses the probability of fiber failure with corrections for fiber length and the nonuniform stress field.

Variables

F *Cumulative probability of fiber failure* dimensionless

σf *Fiber stress* Pa

σ0 *Weibull reference strength scale* Pa

m *Weibull shape parameter* dimensionless

Cl *Fiber-length scaling factor* dimensionless

Cσ *Stress-field scaling factor* dimensionless

lf *Fiber length* m

lr *Weibull reference length* m

Model connection Generates the ordered fiber-strength thresholds that trigger break insertion and network rebuilding.

Theory basis Henry and Pimenta (2017), reference formulation

Four adjacent interactions generate the fiber peak. When that peak exceeds the current threshold, CDS inserts a break at the governing neighboring discontinuity at the end of the longest segment, advances the ordered threshold, deactivates the responsible interaction, and rebuilds the network without advancing applied strain. Events repeat until stable.

5 RVE specimen and cluster failure

Eq. ADF-05 $\sigma_{\mathrm{RVE}} = V_f \frac{\Sigma \sigma_V^I + \Sigma \sigma_H^I}{2n(n-1)} + V_m \sigma_m$

$$\sigma_{\mathrm{RVE}} = V_f (\Sigma \sigma_V^I + \Sigma \sigma_H^I)/[2n(n-1)] + V_m \sigma_m$$

Combines the horizontal and vertical interaction stresses with the matrix contribution to obtain the representative-volume stress.

Variables

σRVE *Representative-volume average axial stress* Pa

Vf *Fiber volume fraction* dimensionless

Vm *Matrix volume fraction* dimensionless

σVI *Vertical-neighbor interaction stress* Pa

σHI *Horizontal-neighbor interaction stress* Pa

n *Fibers per row in the square array* count

σm *Matrix axial stress* Pa

Model connection Produces each representative volume's stress–strain curve for specimen assembly.

Theory basis Henry and Pimenta (2017), reference formulation

Independent RVEs are placed in series. At a common stress, their interpolated strains are averaged; the earliest RVE cutoff limits the specimen.

Eq. ADF-06 $\varepsilon_{\text{spec}}(\sigma) = \frac{1}{N_{\text{RVE}}} \sum_r \varepsilon_r(\sigma)$

$$\varepsilon_{\text{spec}}(\sigma) = (1/N_{\text{RVE}}) \Sigma_r \varepsilon_r(\sigma)$$

Averages representative-volume strains evaluated at the same axial stress.

Variables

εspec *Specimen axial strain* dimensionless

σ *Common axial stress* Pa

NRVE *Number of representative volumes* count

εr *Axial strain in representative volume r* dimensionless

r *Representative-volume index* dimensionless

Model connection Builds the specimen response from volumes in series; the earliest volume cutoff limits the specimen.

Theory basis Henry and Pimenta (2017), reference formulation

Cluster termination uses the nonlinear Dugdale energy release rate and the paper's cluster-radius scaling:

Eq. ADF-07 $J_{\text{NL}} = \frac{32}{\pi^3} \frac{X_g^2}{E_g} a \ln\left[\sec\left(\frac{\pi\sigma}{2X_g}\right)\right], \quad a = \frac{n_a \varphi_f}{\sqrt{2V_f}}$

$$J_{\text{NL}} = (32/\pi^3)\left(X_g{}^2/E_g\right) a \ln\left[\sec\left(\pi\sigma/\left(2X_g\right)\right)\right], a = n_a \varphi_f / \sqrt{}\left(2V_f\right)$$

Evaluates nonlinear energy release for a damaged cluster and relates its physical radius to the fiber array.

Variables

JNL *Nonlinear energy release rate* J/m^2

Xg *Strength parameter of the cluster model* Pa

Eg *Elastic modulus used in the cluster model* Pa

a *Physical cluster radius* m

σ *Applied axial stress* Pa

na *Cluster-size parameter* dimensionless

φf *Fiber diameter* m

Vf *Fiber volume fraction* dimensionless

Model connection The cluster energy release is compared with calibrated fracture resistance to determine instability.

Theory basis Henry and Pimenta (2017), reference formulation

Eq. ADF-08 $g_{\text{deb}} = \frac{2V_f}{\varphi_f} G_{\text{IIc}} \Delta l, \quad g_{\text{po}} = \frac{V_f}{\varphi_f} \tau_\mu \Delta l^2$

$$g_{\text{deb}} = (2V_f/\varphi_f)G_{\text{IIc}}\Delta l, g_{\text{po}} = (V_f/\varphi_f)\tau_\mu \Delta l^2$$

Evaluates the debonding and frictional pull-out contributions for a realized overlap length.

Variables

gdeb *Debonding resistance per unit area* $\mathrm{J/m^2}$

gpo *Frictional pull-out resistance per unit area* $\mathrm{J/m^2}$

Vf *Fiber volume fraction* dimensionless

φf *Fiber diameter* m

GIIc *Mode-II interfacial fracture toughness* $\mathrm{J/m^2}$

Δl *Realized overlap length* m

τμ *Residual frictional shear stress* Pa

Model connection These resistance contributions enter the critical-cluster instability assessment.

Theory basis Henry and Pimenta (2017), reference formulation

6 Connected workflow

- **Constituents** Fiber elastic/Weibull data and matrix elastic, strength, toughness, friction, and optional τ(γ) data
- **Stochastic geometry** Fiber length/diameter, volume fraction, n × n RVE, independent realizations, and seed
- **Interaction network** Ends + breaks → broken/shear-lag segments → nonlinear segment series response
- **Fiber events** Local peaks → ordered Weibull threshold → break insertion → network rebuild at the same strain
- **RVE and specimen** Interaction average → complete RVE curves → common-stress series coupling
- **Cluster and ply property connection** Dugdale cutoff → E_1/X_t → 3D ply properties → laminate and structural analysis

7 What to supply and what to examine

Study quantity	Physical meaning
Fiber variability and interactions	Specify fiber-strength statistics, representative-volume size, flaw assumptions and calibrated fracture resistance.
Matrix shear behavior	Supply measured shear strain and shear stress in Pa. Strain values must be nonnegative and strictly increasing.
Specimen response	Series-coupled specimen curves.
RVE response	RVE curves, break counts, active-interaction counts, and cutoff state.
Fiber-break events	Every progressive fiber-break event and governing interaction.
Critical clusters	Critical cluster location, size, J_{NL}, and resistance.
Matrix shear law	Resolved matrix shear-law points and piecewise tangent.

8 Calibration and validation boundary

- Calibrate the matrix shear law, Weibull scale/shape/reference length, stress-field correction, interface limit, mode-II toughness, and friction stress to the intended material state.
- RVE row count, RVE count, strain resolution, cluster limit, and flaw opportunities require convergence studies.
- Static and analytical release checks do not replace a complete model run or coupon validation.
- Use measured ply overrides when a qualified dataset should supersede a predicted property.

9 Primary reference

Henry, J., and Pimenta, S. (2017). “Semi-analytical simulation of aligned discontinuous composites.” *Composites Science and Technology*, 144, 230–244. https://doi.org/10.1016/j.compscitech.2017.01.027

13 Connect moisture transport to stress response

Online chapter

Current Workbench, reference editions and downloads

Use the online User Guide for current controls, the released model directory for selectable models and compatibility, and the Training Manual for connected exercises. Wider theory references do not mean every formulation is enabled in Workbench.

Dated GUI captures and compiled Web r18 PDF manuals retain their stated scope; they are not a substitute for current hosted Workbench instructions. Find the overview PDF, guides and exercise databases in Your CDS library .

Generate concentration histories, recover moisture expansion, assemble environmental resultants, and carry the coupled response into progressive laminate assessment.

Workbench availability: released models, inputs and compatible study paths . The wider theory library includes reference formulations not available in every Workbench solve.

14 Resolve the thermal history before structural loading

Online chapter

Current Workbench, reference editions and downloads

Use the online User Guide for current controls, the released model directory for selectable models and compatibility, and the Training Manual for connected exercises. Wider theory references do not mean every formulation is enabled in Workbench.

Dated GUI captures and compiled Web r18 PDF manuals retain their stated scope; they are not a substitute for current hosted Workbench instructions. Find the overview PDF, guides and exercise databases in Your CDS library .

Create independent thermal surface schedules, solve heterogeneous heat transport, evolve polymer state, and map temperature fields into laminate residual stress.

Workbench availability: released models, inputs and compatible study paths . The wider theory library includes reference formulations not available in every Workbench solve.

15 Heterogeneous moisture diffusion

Online chapter

Current Workbench, reference editions and downloads

Use the online User Guide for current controls, the released model directory for selectable models and compatibility, and the Training Manual for connected exercises. Wider theory references do not mean every formulation is enabled in Workbench.

Dated GUI captures and compiled Web r18 PDF manuals retain their stated scope; they are not a substitute for current hosted Workbench instructions. Find the overview PDF, guides and exercise databases in Your CDS library .

Predict water uptake or release through a multi-material laminate using per-ply diffusivity, saturation, independent moisture boundaries, and the same interpolated process time grid used by heat transfer. Expand any equation for its physical meaning, variables, units, model connection, and theory source.

Fickian continuum model

Eq. 05.5.1-01 **One-dimensional moisture balance**

$$\partial C/\partial t = \partial/\partial z[D(T,z)\partial C/\partial z]$$

Applies Fick's second law through the laminate thickness. The divergence form permits temperature- and ply-dependent diffusivity while preserving concentration flux at material interfaces.

Variables

C(z,t) *local moisture concentration stored by the laminate model* percentage points

D(T,z) *local through-thickness diffusivity* m^2/s

z *through-thickness coordinate* m

t *process or exposure time* s

Model connection Solved on the same cell-centered mesh and time grid as heat transfer. The current temperature field updates D before the moisture equation is advanced.

Theory basis NASA moisture diffusion in composites

Eq. 05.5.1-02 **Arrhenius diffusivity**

$$D(T,z) = D_0(z)\exp[-E_D(z)/(RT)]$$

Adjusts each ply's reference diffusivity for the current absolute temperature using a calibrated activation energy.

Variables

D(T,z) *temperature-dependent ply diffusivity* m^2/s

D_0(z) *ply diffusivity prefactor* m^2/s

E_D(z) *diffusion activation energy* J/mol

R *universal gas constant* 8.314462618 J/(mol·K)

T *local nodal absolute temperature* K

Model connection Evaluated after the thermal solve in each staggered process iteration; different plies may use different D0 and ED values.

Theory basis Temperature-dependent environmental diffusion

Heterogeneous finite-volume form

Eq. 05.5.1-03 **Harmonic moisture face conductance**

$$H_{i+1/2} = [\Delta z_i/(2D_i) + \Delta z_{i+1}/(2D_{i+1})]^{-1}$$

Adds the adjacent half-cell diffusion resistances in series, conserving interfacial moisture flux across dissimilar ply materials.

Variables

$H_{i+1/2}$ *moisture conductance across a shared cell face* m/s

D_i, D_{i+1} *diffusivities in adjacent cells* m^2/s

Δz_i, Δz_{i+1} *adjacent cell thicknesses* m

Model connection Populates the moisture transport operator. A zero diffusivity on either side closes that interface in the current reduced-order model.

Theory basis Layered-composite diffusion treatment

Eq. 05.5.1-04 **Semidiscrete moisture balance**

$$\Delta z_i \mathrm{dC}_i/\mathrm{dt} = H_{i+1/2}(C_{i+1} - C_i) - H_{i-1/2}(C_i - C_{i-1})$$

Balances concentration storage in a cell with the moisture flux entering and leaving through its two faces.

Variables

C_i *cell-center concentration* percentage points

Δz_i *cell storage thickness per unit area* m

$H_{i\pm1/2}$ *left and right moisture face conductances* m/s

Model connection Assembled into the same theta-family integrator as the thermal equation, but with cell thickness rather than heat capacity as the storage matrix.

Theory basis Fickian layered finite-difference/volume balance

Independent moisture boundaries

Eq. 05.5.1-05 **Moisture surface boundary operators**

$$\text{Prescribed: } H_s = 2D/\Delta z, S_{C,s} = H_s C_s$$

$$\text{Insulated: } H_s = 0, S_{C,s} = 0$$

$$\text{Film: } H_s = [\Delta z/(2D) + 1/h_m]^{-1}, S_{C,s} = H_s C_s$$

$$\text{Custom inward flux: } H_s = 0, S_{C,s} = J_{\mathrm{in}}$$

Writes prescribed concentration, insulated, film-transfer, and custom inward-flux conditions as a conductance and source on the surface control volume.

Variables

$\mathbf{H}_s$ *effective surface moisture conductance* m/s

$\mathbf{S}_{C,s}$ *surface concentration-flux source* percentage-point·m/s

$\mathbf{C}_s$ *scheduled surface or environmental moisture* percentage points

$\mathbf{h}_m$ *moisture film-transfer coefficient* m/s

$\mathbf{J}_{in}$ *user-defined signed inward concentration flux* percentage-point·m/s

D, Δz *surface-cell diffusivity and thickness* m^2/s, m

Model connection Top and bottom selections are independent and are interpolated from columns 3, 5, and 7 of their respective surface tables.

Theory basis Composite environmental-exposure boundary modeling

Eq. 05.5.1-06 **Theta moisture integration**

$$[S/\Delta t + \theta_C K_C^{n+1}]C^{n+1} = [S/\Delta t - (1-\theta_C)K_C^{n}]C^{n} + J^{n+\theta}$$

Advances the heterogeneous diffusion system while allowing fully implicit or Crank–Nicolson weighting of the old and new operators and boundary sources.

Variables

S *diagonal moisture storage matrix of cell thicknesses* m

$\mathbf{K}_C^n$, $\mathbf{K}_C^{n+1}$ *old and new diffusion-plus-boundary matrices* m/s

$\mathbf{C}^n$, $\mathbf{C}^{n+1}$ *old and new concentration vectors* percentage points

$\mathbf{J}^{n+\theta}$ *theta-weighted boundary source vector* percentage-point·m/s

$\boldsymbol{\theta}_C$ *moisture time-integration parameter* dimensionless, 0–1

Δt *transport time step* s

Model connection Executed only when the moisture-diffusion flag is active. The solved field is clipped to nonnegative values and, where supplied, each node's ply saturation limit.

Theory basis Transient Fickian diffusion solution

Eq. 05.5.1-07 **Physical concentration bounds**

$$C_i^{n+1} = \min\left[C_{\mathrm{sat},i}, \max(0, C_i^*)\right]$$

Prevents negative concentration and limits each node to its calibrated saturation concentration when a positive saturation value is supplied.

Variables

$\mathbf{C}_i^*$ *unbounded concentration returned by the linear solve* percentage points

$\mathbf{C}_{sat,i}$ *saturation concentration of the node's ply material* percentage points

$\mathbf{C}_i^{n+1}$ *accepted bounded concentration* percentage points

Model connection Applied node-by-node after each moisture solve. When Csat is zero or omitted, only the nonnegative lower bound is imposed.

Theory basis Equilibrium moisture-content context

Hygroscopic strain coupling

Concentration is stored in percentage points to match the coefficient of moisture expansion used by the laminate model. Every ply may carry its own β_1, β_2, and β_3.

Eq. 05.5.1-08 **Local moisture free strain**

$$\varepsilon_k^M(z,t) = \beta_k \Delta C_k(z,t)$$

Maps moisture change relative to the ply reference state into unconstrained hygroscopic strain in each local material direction.

Variables

$\boldsymbol{\varepsilon}^M_k$ *moisture free strain in local direction k* strain

$\boldsymbol{\beta}_k$ *coefficient of moisture expansion* strain per percentage point

$\boldsymbol{\Delta C}_k$ *local moisture change from the reference state* percentage points

k *local ply material direction 1, 2, or 3* index

Model connection The nodal field is fitted across each ply and optionally included in process resultants, local/global field recovery, and ply failure checks.

Theory basis NASA hygrothermal laminate mechanics

Scope boundary. The model is one-dimensional and Fickian. Edge drying, damage-assisted transport, two-stage sorption, concentration-dependent diffusivity, imperfect ply-interface partitioning, and stress-assisted diffusion require extension or calibrated effective parameters.

Theory references

- NASA composite moisture-diffusion formulation and environmental response reference.
- NASA, Prediction of moisture and temperature changes in composites during atmospheric exposure.
- Nettles, Basic Mechanics of Laminated Composite Plates, NASA RP-1351, including hygrothermal effects.

Workbench availability: released models, inputs and compatible study paths . The wider theory library includes reference formulations not available in every Workbench solve.

16 Heterogeneous 1D transient heat

Online chapter

Current Workbench, reference editions and downloads

Use the online User Guide for current controls, the released model directory for selectable models and compatibility, and the Training Manual for connected exercises. Wider theory references do not mean every formulation is enabled in Workbench.

Dated GUI captures and compiled Web r18 PDF manuals retain their stated scope; they are not a substitute for current hosted Workbench instructions. Find the overview PDF, guides and exercise databases in Your CDS library .

Solve the laminate temperature history first using effective through-thickness ply properties, user-selected nodes per ply, independent surface schedules, and optional cure or crystallization heat. Expand any equation for its physical meaning, variables, units, model connection, and theory source.

Continuum energy balance

Eq. 05.4.1-01 **Heterogeneous transient heat equation**

$$\rho(z)c_p(z)\partial T/\partial t = \partial/\partial z[k_z(z)\partial T/\partial z] + q_c + q_x$$

Balances local sensible-energy storage with through-thickness conduction and volumetric heat released by thermoset cure and thermoplastic crystallization. Material coefficients may change abruptly at ply interfaces.

Variables

ρ(z) *effective ply density at through-thickness coordinate z* kg/m^3

c_p(z) *effective specific heat capacity* J/(kg·K)

T(z,t) *temperature field* K

k_z(z) *effective through-thickness thermal conductivity* W/(m·K)

q_c, q_x *cure and crystallization volumetric heat sources* W/m^3

z, t *through-thickness coordinate and process time* m, s

Model connection The micromechanics stage supplies ρ, cp, and k3 for every ply; the material kinetics pages supply qc and qx. The resulting T(z,t) feeds thermal strain and temperature-dependent diffusion.

Theory basis NASA composite cure-process heat model

Cell-centered finite-volume form

Every active ply is divided into a user-selected number of cell-centered control volumes. Each cell belongs to exactly one physical ply, so its storage and conductivity are taken from that ply. Flux continuity is enforced at every shared face.

Eq. 05.4.1-02 **Areal heat capacity of a transport cell**

$$C_i = \rho_i c_{p,i} \Delta z_i$$

Collapses volumetric heat capacity across the thickness of one unit-area finite volume, producing the storage coefficient used in the semidiscrete equations.

Variables

C_i *areal heat capacity of cell i* J/(m²·K)

ρ_i *effective density assigned to cell i* kg/m³

$c_{p,i}$ *effective specific heat assigned to cell i* J/(kg·K)

Δz_i *cell thickness* m

Model connection Forms the diagonal capacity matrix C used by the theta time integrator. Refining nodes per ply reduces Δzi while conserving total areal heat capacity.

Theory basis Conservative finite-volume heat discretization

Eq. 05.4.1-03 **Harmonic face conductance**

$$G_{i+1/2} = [\Delta z_i/(2k_i) + \Delta z_{i+1}/(2k_{i+1})]^{-1}$$

Adds the two half-cell thermal resistances in series. This is essential when adjacent plies have different conductivities because an arithmetic average does not preserve the correct interface heat flux.

Variables

$G_{i+1/2}$ *conductance per unit area across the shared face* W/(m²·K)

k_i, k_{i+1} *through-thickness conductivity in the adjacent cells* W/(m·K)

Δz_i, Δz_{i+1} *thicknesses of the adjacent cells* m

Model connection Populates the tridiagonal conduction operator. The same resistance construction is reused for the heterogeneous moisture-diffusion operator.

Theory basis Finite-volume interface-flux treatment

Eq. 05.4.1-04 **Semidiscrete cell energy balance**

$$C_i \mathrm{dT}_i/\mathrm{dt} = G_{i+1/2}(T_{i+1} - T_i) - G_{i-1/2}(T_i - T_{i-1}) + q_i \Delta z_i$$

States that heat stored in a cell equals net conductive inflow plus the local volumetric reaction source integrated through the cell thickness.

Variables

T_i *cell-center temperature* K

C_i *cell areal heat capacity* J/(m²·K)

$G_{i\pm1/2}$ *left and right face conductances* W/(m²·K)

q_i *combined local volumetric cure/crystallization heat* W/m³

Δz_i *cell thickness* m

Model connection Assembled for every transport cell into C dT/dt + K T = Q before application of surface boundary terms.

Theory basis Conservative cell energy balance

Independent top and bottom boundary histories

Top and bottom use separate seven-column tables. Continuous temperature, moisture, and coefficient/flux fields are linearly interpolated to the transport time grid; integer boundary IDs are held piecewise constant. A five-row schedule can therefore drive a thousand-step solve without changing the intended boundary mode between schedule breakpoints.

Eq. 05.4.1-05 **Schedule interpolation and boundary-ID hold**

$$y(t) = y_r + (y_{r+1} - y_r)(t - t_r)/(t_{r+1} - t_r)$$

$$b(t) = b_r, t_r \leq t < t_{r+1}$$

Linearly interpolates continuous boundary data while selecting the last declared discrete boundary type until the next table time is reached.

Variables

y(t) *interpolated continuous surface value* field-dependent

y_r, y_{r+1} *values in adjacent boundary-table rows* field-dependent

t_r, t_{r+1} *adjacent schedule times* s

b(t) *discrete boundary-condition ID* integer ID

Model connection Applied separately to both surfaces. Temperature, moisture, and coefficients/fluxes use y(t); thermal and moisture type columns use b(t).

Theory basis Process-cycle boundary-history context

Eq. 05.4.1-06 **Thermal surface boundary operators**

$$\text{Prescribed: } G_s = 2k/\Delta z, S_s = G_s T_s$$

$$\text{Adiabatic: } G_s = 0, S_s = 0$$

$$\text{Convection: } G_s = [\Delta z/(2k) + 1/h]^{-1}, S_s = G_s T_s$$

$$\text{Custom inward flux: } G_s = 0, S_s = q_{\text{in}}$$

Expresses prescribed temperature, adiabatic, convection, and custom inward heat-flux conditions in the same linear source form used by the finite-volume matrix.

Variables

G_s *effective surface conductance* W/(m²·K)

S_s *surface source added to the cell balance* W/m²

T_s *scheduled surface or ambient temperature* K

h *convective heat-transfer coefficient* W/(m²·K)

q_{in} *user-defined signed inward heat flux* W/m²

k, Δz *surface-cell conductivity and thickness* W/(m·K), m

Model connection The selected pair (Gs,Ss) modifies only the first or last transport equation. Top and bottom types, temperatures, and coefficients remain independent.

Theory basis Finite-volume Dirichlet, Neumann, and Robin boundaries

Column	Surface-table field	Interpolation
1–3	Time, surface temperature, surface moisture	Continuous fields linear in time
4	Thermal ID: prescribed, adiabatic, convection, custom inward heat flux	Previous-value hold
5	Moisture ID: prescribed, insulated, film, custom inward concentration flux	Previous-value hold
6–7	Thermal and moisture coefficient or signed custom flux	Linear in time

Theta time integration and coupling

Current Workbench implementation. The general theta equation below describes the theory family, not a selectable theta control in WB. The current transient Workbench solver uses backward Euler with a full-step/two-half-step error estimate. It stops at schedule changes and requested outputs; output spacing is not the integration accuracy target. Rejected trials do not commit temperature or reaction state. If the computation budget or supported schedule size is exceeded, the run fails explicitly rather than accepting a coarser result. Through-thickness mesh convergence, calibration and experimental validation must still be checked separately.

Linked thermal tables use the same property convention in Micro and Process: Micro reports the 23 °C reference, while Process evaluates the table at local temperature without extrapolation. Constituent-based through-thickness closure uses transverse fiber conductivity and matrix conductivity; a stored homogenized ply retains its own through-thickness conductivity.

Eq. 05.4.1-07 **Theta time integration**

$$[C/\Delta t + \theta K^{n+1}]T^{n+1} = [C/\Delta t - (1-\theta)K^n]T^n + Q^{n+\theta}$$

Advances the matrix heat balance between old and new time levels. θ=1 is backward Euler; θ=0.5 is Crank–Nicolson. The source includes both interpolated boundaries and enabled reaction heat.

Variables

C *diagonal areal heat-capacity matrix* J/(m²·K)

$\mathbf{K}^n$, $\mathbf{K}^{n+1}$ *old and new conduction-plus-boundary matrices* W/(m²·K)

$\mathbf{T}^n$, $\mathbf{T}^{n+1}$ *old and new nodal temperature vectors* K

$\mathbf{Q}^{n+\theta}$ *theta-weighted surface and reaction source vector* W/m²

θ *time-integration parameter* dimensionless, 0–1

Δt *transport time step* s

Model connection Solved repeatedly within each process step while kinetics and heat sources are updated. Convergence is checked using the largest normalized temperature or moisture change.

Theory basis Implicit theta-method discretization

Solver modes. Bypassing transport uses the prescribed temperature for each ply. A process-only study calculates the temperature field. A coupled study also maps the field into structural residual stress and progressive failure. Temperature inputs may be entered in kelvin or Celsius, but the internal kinetics evaluation always uses kelvin.

Theory references

- NASA, Composite Cure Process Modeling and Simulations using Finite Element Analysis (2016).
- NASA composite cure-process heat-transfer formulation and material-state coupling.
- CDS micromechanics theory: effective thermal conductivity, density, and heat capacity supplied to the ply transport cells.

Workbench availability: released models, inputs and compatible study paths . The wider theory library includes reference formulations not available in every Workbench solve.

17 Move from laminate mechanics to structural decisions

Online chapter

Current Workbench, reference editions and downloads

Use the online User Guide for current controls, the released model directory for selectable models and compatibility, and the Training Manual for connected exercises. Wider theory references do not mean every formulation is enabled in Workbench.

Dated GUI captures and compiled Web r18 PDF manuals retain their stated scope; they are not a substitute for current hosted Workbench instructions. Find the overview PDF, guides and exercise databases in Your CDS library .

Connect idealization, mechanical and process loading, residual stress, recovered fields, independent ply failure, damage progression, structural outputs, and verification.

Workbench availability: released models, inputs and compatible study paths . The wider theory library includes reference formulations not available in every Workbench solve.

18 Hyer thick laminated cylinder

Online chapter

Current Workbench, reference editions and downloads

Use the online User Guide for current controls, the released model directory for selectable models and compatibility, and the Training Manual for connected exercises. Wider theory references do not mean every formulation is enabled in Workbench.

Dated GUI captures and compiled Web r18 PDF manuals retain their stated scope; they are not a substitute for current hosted Workbench instructions. Find the overview PDF, guides and exercise databases in Your CDS library .

Resolve the radial coordinate explicitly through every ply so pressure tractions, interlaminar stress, and displacement continuity are retained across a thick laminated wall.

Methodology

The Hyer route follows the generalized-plane-deformation treatment for long laminated cylinders. Each concentric orthotropic ply is transformed into the axial–hoop–radial coordinate system. The solver constructs a layer solution, enforces radial equilibrium inside each ply, applies displacement and traction continuity at every interface, and closes the system with inner and outer pressure boundary conditions.

H-01 **Axisymmetric strain field**

$$\varepsilon_x = \overline{\varepsilon}_x$$

$$\varepsilon_\theta = u_r(r)/r$$

$$\varepsilon_r = \mathrm{d}u_r(r)/\mathrm{d}r$$

Defines the axial, hoop, and radial strains for an axisymmetric cylinder with generalized uniform axial extension and layerwise radial displacement.

Variables

ε_x *Uniform generalized axial strain* m/m

u_r *Layerwise radial displacement* m

r *Current radial coordinate in the reference wall* m

ε_θ *Hoop strain* m/m

ε_r *Radial strain* m/m

Model connection These kinematic fields are evaluated separately in each ply while sharing interface displacement constraints.

Theory basis Hyer (1988), stress analysis of thick laminated cylinders

H-02 **Layer constitutive equation**

$$\sigma^{(k)} = \overline{C}^{(k)} \left[\varepsilon^{(k)} - \overline{\alpha}^{(k)} \Delta T^{(k)} - \overline{\beta}^{(k)} \Delta C^{(k)} \right]$$

Relates the three-dimensional stress state in each transformed orthotropic ply to mechanical strain after thermal and moisture free strains are removed.

Variables

$\boldsymbol{\sigma}^{(k)}$ *Stress vector in ply k* Pa

$\bar{\mathbf{C}}^{(k)}$ *Transformed 3D ply stiffness* Pa

$\bar{\boldsymbol{\alpha}}^{(k)}$ *Transformed ply CTE vector* 1/K

$\bar{\boldsymbol{\beta}}^{(k)}$ *Transformed moisture-expansion vector* 1 or concentration basis

Model connection The pristine or damaged per-ply property source is resolved upstream and passed unchanged into this layerwise cylinder branch.

Theory basis CDS independent per-ply material routing

H-03 **Radial equilibrium**

$$d\sigma_r/\mathrm{dr} + (\sigma_r - \sigma_\theta)/r = 0$$

$$d\tau_{\mathrm{rx}}/\mathrm{dr} + \tau_{\mathrm{rx}}/r = 0$$

Enforces axisymmetric equilibrium through the wall so radial and hoop stress are mechanically compatible in every ply.

Variables

$\boldsymbol{\sigma}_r$ *Radial normal stress* Pa

$\boldsymbol{\sigma}_\theta$ *Hoop normal stress* Pa

$\boldsymbol{\tau}_{rx}$ *Radial–axial shear stress* Pa

Model connection The resulting ordinary differential system determines each layer's radial solution coefficients.

Theory basis Hyer (1988), radial equilibrium formulation

H-04 **Interface and pressure boundary conditions**

$$u_r^{(k)} = u_r^{(k+1)}, \sigma_r^{(k)} = \sigma_r^{(k+1)}, \tau_{\mathrm{rx}}^{(k)} = \tau_{\mathrm{rx}}^{(k+1)}$$

$$\sigma_r(r_i) = -p_i, \sigma_r(r_o) = -p_o$$

Closes the multilayer system by preserving radial displacement and traction at ply interfaces and applying pressure tractions at the inner and outer radii.

Variables

$\mathbf{r}_i$ *Cylinder inner radius* m

$\mathbf{r}_o$ *Cylinder outer radius* m

$\mathbf{p}_i$ *Internal pressure* Pa

$\mathbf{p}_o$ *External pressure* Pa

Model connection CDS assembles these equations and conditions into one linear coefficient system for the active laminate wall.

Theory basis Hyer (1988), layer and surface conditions

Recovered results

The model recovers radial displacement and the axial, hoop, radial, and interlaminar shear stresses at requested through-wall positions. Named results provide the load and resultant histories plus the final radial-coordinate and stress-recovery table.

Selection guidance

Use shell cylinder when	Use Hyer cylinder when
Rapid sizing, membrane dominance, and large radius-to-thickness ratio	Thick walls, strong radial gradients, or interface tractions matter
Hoop/axial resultants are the primary design quantities	Layerwise radial displacement and interlaminar stress are required

Verification basis. Check single-layer isotropic limits, traction continuity, pressure boundary recovery, equilibrium, and convergence of through-wall sampling before using the layerwise solution in design decisions.

Workbench availability: released models, inputs and compatible study paths . The wider theory library includes reference formulations not available in every Workbench solve.

19 Constant-section shell cylinder

Online chapter

Current Workbench, reference editions and downloads

Use the online User Guide for current controls, the released model directory for selectable models and compatibility, and the Training Manual for connected exercises. Wider theory references do not mean every formulation is enabled in Workbench.

Dated GUI captures and compiled Web r18 PDF manuals retain their stated scope; they are not a substitute for current hosted Workbench instructions. Find the overview PDF, guides and exercise databases in Your CDS library .

Resolve pressure, axial force, and torque through a laminate membrane-shell idealization with a constant circular section and the shared CDS laminate property definition.

Scope and coordinates

Current Workbench pressure summary. The thin-wall pressure strain summary uses the complete inverse laminate extensional stiffness, including Poisson and extension–shear coupling: $\varepsilon^0 = A^{-1}N$ with curvature constrained to zero. Its x direction is axial and y is hoop. Open ends omit the pressure end-cap force, but axial Poisson contraction remains. This summary is not the general free-curvature ABD shell solution shown below, and it does not resolve radial stress or local end effects. Keep the separate layerwise thick-wall profile and supported ply-failure calculations distinct.

The shell route uses axial **x**, circumferential arc-length $\mathbf{y} = \mathbf{r}_m\boldsymbol{\theta}$, and outward radial **z** coordinates. It is intended for thin-to-moderately-thick cylinders where a membrane-dominant sizing solution is appropriate. The laminate ABD matrix, environmental resultants, damage state, and density come from the same upstream solver used by the plate and beam branches.

S-01 **Net pressure and pressure resultants**

$$\Delta p = p_i - p_o$$

$$N_{y,p} = \Delta p r_m$$

$$N_{x,p} = \Delta p r_m / 2$$

Converts the pressure difference across a closed-end cylinder into hoop and axial membrane force per unit length.

Variables

$\boldsymbol{\Delta p}$ *Internal minus external pressure* Pa

$\mathbf{r}_m$ *Cylinder mean radius* m

$\mathbf{N}_{y,p}$ *Pressure-generated hoop resultant* N/m

$\mathbf{N}_{x,p}$ *Pressure-generated axial resultant for closed ends* N/m

Model connection These pressure terms enter the common laminate resultant vector before constitutive recovery.

Theory basis CDS online structural theory, structural geometry module

S-02 **Applied force and torque resultants**

$$N_x = N_{x,p} + F_x/(2\pi r_m)$$

$$N_{xy} = T/(2\pi r_m^2)$$

Superimposes user-applied axial force and torque on the pressure-generated membrane actions.

Variables

F_x *Applied axial force* N

T *Applied torque* N·m

N_x *Total axial membrane resultant* N/m

N_{xy} *In-plane shear resultant* N/m

Model connection The load-scaler inputs remain independent of geometry and are transformed into the shell resultant basis here.

Theory basis CDS online structural theory, cylinder loading

S-03 **Laminate constitutive recovery**

$$[N; M] = [AB; BD][\varepsilon^0; \kappa] - [N^{\text{env}}; M^{\text{env}}]$$

Uses the active laminate ABD matrix to recover mid-surface strain and curvature after mechanical and environmental resultants are combined.

Variables

A *Extensional stiffness matrix* N/m

B *Extension–bending coupling matrix* N

D *Bending stiffness matrix* N·m

ε^0 *Mid-surface strain vector* m/m

κ *Curvature vector* 1/m

Model connection Recovered ply strains and stresses feed the selected failure and progressive-damage models.

Theory basis CDS hygrothermal CLT and ABD theory

Radial response and outputs

For the membrane shell path, the mean radial displacement is recovered from the hoop strain as $\mathbf{w} \approx \mathbf{r}_m \boldsymbol{\varepsilon}_y$. Named results provide the cylinder summary, pressure, force, torque and resultant histories, plus the final radial-coordinate and recovered-stress table.

Assumptions and limits

- Axisymmetric constant circular section with small strains and small displacement.

- Membrane-dominant response; local end effects, ovalization, openings, and geometric imperfections require higher-fidelity analysis.
- Closed-end axial pressure force is included only when the selected end condition requires it.
- Use the Hyer route when through-wall radial stress and layer-interface traction continuity are important.

Workbench availability: released models, inputs and compatible study paths . The wider theory library includes reference formulations not available in every Workbench solve.

20 Fatigue S-N assessment

Online chapter

Current Workbench, reference editions and downloads

Use the online User Guide for current controls, the released model directory for selectable models and compatibility, and the Training Manual for connected exercises. Wider theory references do not mean every formulation is enabled in Workbench.

Dated GUI captures and compiled Web r18 PDF manuals retain their stated scope; they are not a substitute for current hosted Workbench instructions. Find the overview PDF, guides and exercise databases in Your CDS library .

Fatigue S N assessment

Five calibrated stress–life models alongside the existing progressive-failure assessment.

Trace the selected input path

Ply property source

Include thermal analysis

Include moisture analysis

Include optional fatigue assessment

Stored ply properties bypass Micro. Mixed stacks keep both paths. Gray blocks are not selected. Geometry, process schedules and other model records are omitted here for clarity; a real run must include all required references.

Fatigue uses intact CLT endpoint stresses and measured S–N calibration. It is evaluated separately from Run and progressive failure. The dashed handoff is not active: optimization still uses current properties until a degradation law is supplied.

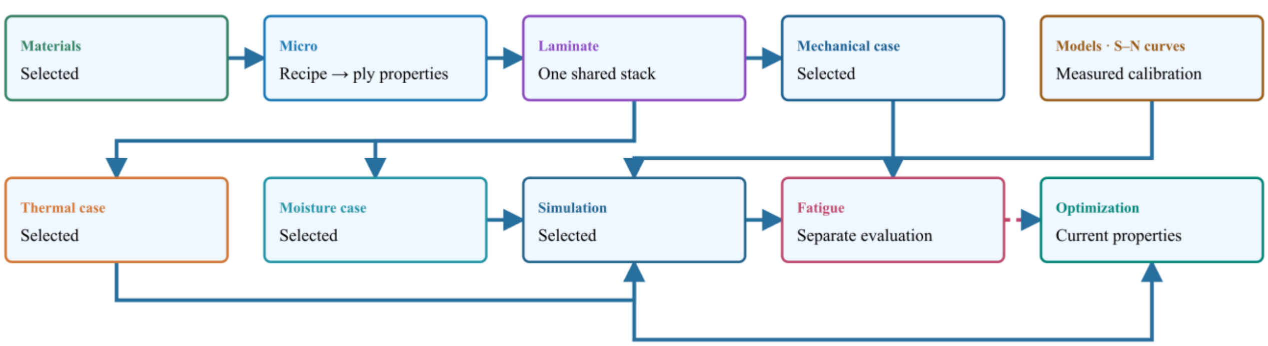

Dashed pink arrow: residual-fatigue study is separate—not an automatic property transfer.

Materials → Micro → Laminate.

Where to find it

In the CLT structural response workspace, open Response → Failure → Fatigue. Run the populated connected simulation first. Supply measured effective-ply fatigue calibration for every active source and stress channel. Fatigue is evaluated separately; the ordinary simulation Run does not evaluate cyclic life automatically.

Upstream coupling

Stored material plies and solved Micro plies use their existing elastic properties, angles and individual thicknesses. The laminate recovers bottom, middle and top ply stresses at two mechanical endpoints. The full six-component Load vector is used at one endpoint and Rload times that vector at the other. Progressive-ramp checkboxes are not fatigue amplitude selectors.

Selected saved thermal, cure and moisture histories contribute fixed residual strain at both endpoints. Available cure-conditioned stiffness is reused through the existing process-state pathway. Changed inputs require a new connected run. The fatigue calibration must independently cover the effective composition, orientation, process state, environment and cycling frequency; elastic homogenization does not create fatigue coefficients.

Model conventions

All stresses are in MPa and N is cycles, not reversals. U is a calibrated curve intercept, not an automatically inferred fiber strength. For peak-based curves, S is the dominant signed endpoint magnitude. Compression-dominated channels reverse sign before forming local R; calibrate with that same convention. Basquin uses half the stress range. No automatic Goodman or other mean-stress correction is applied.

Kim–Zhang

Implemented relation

$$N = N_0 + U^{-\beta}\left[(S/U)^{1-\beta} - 1\right]/[\alpha(\beta-1)]$$

Inputs

U, $\alpha > 0$, $\beta > 1$, $N_0 > 0$

Sendeckyj

Implemented relation

$$S = U[1 + C(N-1)]^{-s}$$

Inputs

U, $C > 0$, $s > 0$; controls use α=C and β=s

Weibull S–N

Implemented relation

$$S = L + (U-L)\exp\left[-\alpha(\log_{10} N)^{\beta}\right]$$

Inputs

U, 0 ≤ L < U, α > 0, β > 0

Kohout–Vechet

Implemented relation

$$S = U[(1 + N/B)/(1 + N/C)]^b$$

Inputs

U, 0 < B < C, b < 0

Basquin

Implemented relation

$$S_a = AN^b$$

Inputs

A > 0, b < 0. Convert reversal-based coefficients before entry.

The Kim–Zhang stress curve is obtained by algebraically inverting the stated life equation with $N - N_0$, preserving S=U at $N=N_0$. Weibull uses log base 10 explicitly: coefficients fitted with natural logarithms must be converted. The Weibull S–N curve is not a probability distribution and supplies no reliability percentile.

Calibration and persistence

- Select the effective ply source, σ1, σ2 or τ12 channel, and dominant sign.
- Select a model and enter its coefficients, published/test source, local stress-ratio bounds and tested cycle range. No material-specific coefficients are prefilled.
- Check that the calibration covers the current composition, process, temperature, moisture and frequency. Confirm applicability; changing inputs resets confirmation.
- Use Store fatigue inputs in CASES, then save the database. The setup follows that case record. Re-run the simulation after storing inputs, then Evaluate fatigue.

Reading results without a false pass

The table reports local endpoint stresses and R, estimated cycles when inside the calibrated domain, and requested cycles divided by estimated life. Missing calibration, zero-amplitude creep-only channels or an endpoint that fails the static ply check are not evaluated. Stresses above the fitted range and lives beyond it are reported separately, with no invented numeric life. Completed does not mean passed; no overall pass is issued, even when requested cycles are below estimated life.

Scope and verification

This is intact, in-plane CLT constant-amplitude screening. It does not update progressive fatigue damage or evolve temperature/cure during cycling. It does not assess delamination growth, adhesive/core fatigue, out-of-plane/FSDT shear, multiaxial fatigue interaction, variable-amplitude accumulation, creep or self-heating. The FSDT, sandwich, joint and layerwise solvers are not replaced by this panel. Frequency is a recorded calibration condition, not a numerical life correction.

Implementation checks cover forward/inverse equations, cycle conventions, monotonicity, numerical stability, thickness/load scaling, fixed residual stresses, missing data, static failure guards and saved-input round trips. These checks are not experimental benchmark validation. No existing teaching material is marked fatigue-qualified by adding this module.

Sources

- Burhan & Kim (2018), S–N Curve Models for Composite Materials Characterisation : equations 8, 11 and 22; model conventions and comparison.
- Sendeckyj (1981), Fitting Models to Composite Materials Fatigue Data : equivalent static strength and fitted fatigue data.
- Kohout & Věchet (2001), A new function for fatigue curves characterization and its multiple merits : full-range curve.
- A generalization of the fatigue Kohout–Věchet model : equivalent parameterizations.
- Kim & Zhang (2001), Fatigue Damage and Life Prediction of Glass/Vinyl Ester Composites : original model study.
- Weibull (1961), Fatigue Testing and Analysis of Results : original fatigue-curve reference.

∑ CLT and residual-strain recovery · ∑ Monotonic progressive failure · ∑ Process coupling

Workbench availability: released models, inputs and compatible study paths . The wider theory library includes reference formulations not available in every Workbench solve.

21 Shear-deformable laminated plates

Online chapter

Current Workbench, reference editions and downloads

Use the online User Guide for current controls, the released model directory for selectable models and compatibility, and the Training Manual for connected exercises. Wider theory references do not mean every formulation is enabled in Workbench.

Dated GUI captures and compiled Web r18 PDF manuals retain their stated scope; they are not a substitute for current hosted Workbench instructions. Find the overview PDF, guides and exercise databases in Your CDS library .

One laminate definition. Shared CLT stiffness. An integrated FSDT structural formulation.

Two-row simulation workflow · **Open full-size map**
Linked-input preview, not solved results. Gray blocks are not configured.

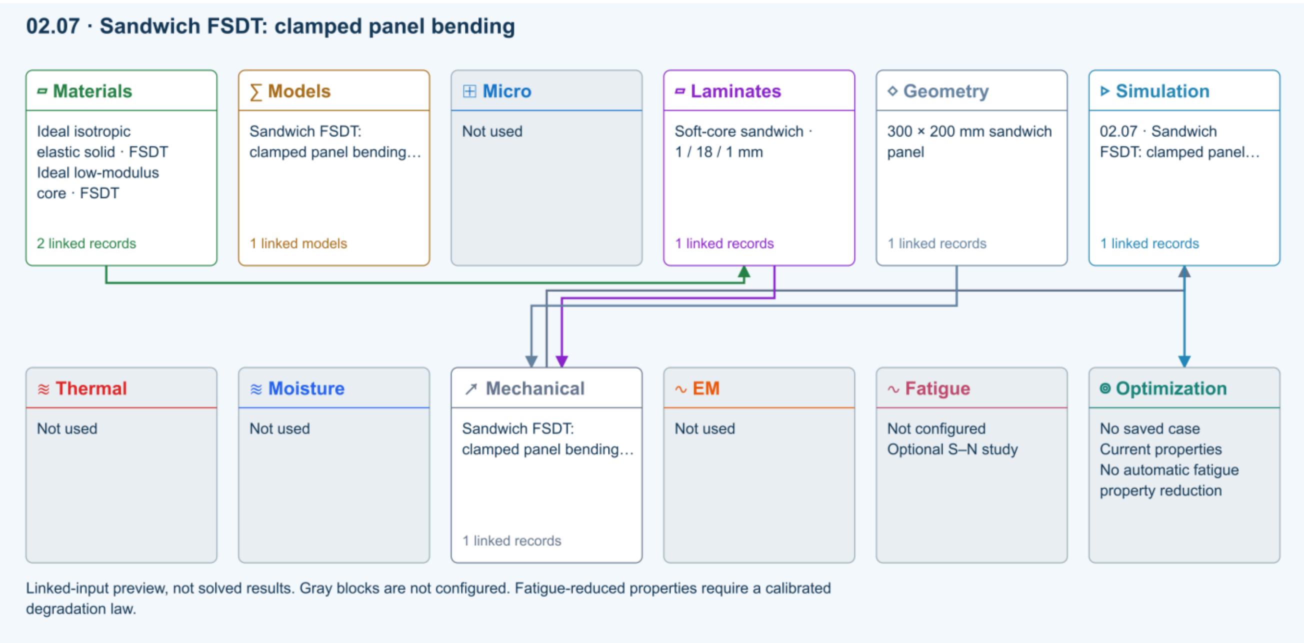

∑ Selected models & submodels

These are the exercise's linked choices, not solved results. Open a first-layer model to see its submodels and scope.

Automatic · Finite plate · Sandwich FSDT: clamped panel bending · load

Automatic selects FSDT for sandwich architecture and CLT otherwise. Static bending requires FSDT. Finite-plate studies do not consume process links or run progressive failure/fatigue.

Study · Static bending

Reference-elastic plate study; progressive failure and fatigue are not evaluated here.

Numerical settings

Ritz order: 6. Shear correction (FSDT only): Energy equivalent. Increase resolution to check convergence.

∑ Theory & assumptions

Data travelling between blocks

Materials → Laminates
Stored ply stiffness, strength, density and expansion properties.

Mechanical → Simulation
SIMULATION selects this case and its analysis model; the case owns its applicable cycle and input references.

Laminates → Mechanical
Ply angles and thicknesses, stiffness, mass and ply properties.

Geometry → Mechanical
Part shape and dimensions, thickness or section definition, and model-specific geometric inputs. Each selected case consumes only the dimensions its model supports.

Simulation → Optimization
Linked inputs and current-property response for candidate evaluation.

Where FSDT fits

Classical laminate theory supplies membrane, extension–bending and bending stiffness: A, B and D. First-order shear deformation theory (FSDT, or Reissner–Mindlin plate theory) retains those matrices and adds transverse shear flexibility. It does not generate a second set of constituent properties or replace the Micro model.

Sandwich plate default: new finite-plate analyses use Automatic theory. When the linked laminate Architecture is Sandwich Structures, Automatic resolves to FSDT; other architectures resolve to CLT. The choice is reevaluated when the linked laminate changes. Explicit CLT and FSDT selections are retained for comparisons. Use the default Energy equivalent shear correction for compatible sandwich plates. Missing shear properties or unsupported symmetry/geometry stop the run, rather than silently substituting CLT.

The three-point-bend sandwich beam example retains its separate shear-flexible beam and skin/core/bond screening model. Its concentrated load and failure checks are not replaced by the current uniform-pressure FSDT plate solver. FSDT completion does not establish a sandwich failure pass.

Stage	Inputs and responsibility
Materials / Micro	Each ply supplies E_1, E_2, ν_{12}, G_{12}, G_{13}, G_{23} and density. Stored materials and solved Micro plies can share the laminate.

Stage	Inputs and responsibility
Laminate	Angles and unequal ply thicknesses generate the common A/B/D matrices, transverse shear matrix As and thickness-integrated mass.
Geometry	Finite rectangular plate length and width. Thickness remains owned by the laminate.
CASES / SIMULATE	Select CLT or FSDT, study, edge restraints, pressure or reference membrane loads. One Run executes the chosen formulation.

Kinematics and stiffness

$$u(x,y,z) = u_0(x,y) + z\theta_x(x,y)$$

$$v(x,y,z) = v_0(x,y) + z\theta_y(x,y)$$

$$w(x,y,z) = w_0(x,y)$$

$$\gamma_{xz} = \theta_x + \frac{\partial w}{\partial x}, \quad \gamma_{yz} = \theta_y + \frac{\partial w}{\partial y}$$

$$\begin{bmatrix} \mathbf{N} \\ \mathbf{M} \end{bmatrix} = \begin{bmatrix} \mathbf{A} & \mathbf{B} \\ \mathbf{B} & \mathbf{D} \end{bmatrix} \begin{bmatrix} \boldsymbol{\varepsilon}_0 \\ \boldsymbol{\kappa} \end{bmatrix}$$

$$\begin{bmatrix} Q_x \\ Q_y \end{bmatrix} = \mathbf{A}_s \begin{bmatrix} \gamma_{xz} \\ \gamma_{yz} \end{bmatrix}$$

Rotations are independent of the displacement slope. The thin-plate limit drives transverse shear strain toward zero. The current CDS plate release solves w, θx and θy for symmetric reference-elastic laminates; it rejects non-negligible B coupling rather than discard in-plane/bending coupling. A/B/D are calculated by the same laminate implementation used by CLT.

Transverse shear properties

FSDT requires positive G13 and G23 for every ply. An isotropic stored material may derive them from its isotropic shear modulus; orthotropic records need directional data. Missing values cannot be replaced silently by G12.

- **Energy equivalent:** the default directional pure-bending approximation integrates equilibrium shear profiles through all plies, matches their shear strain energy and inverts the resulting 2×2 flexibility. It requires symmetric, specially orthotropic bending stiffness (D16 and D26 negligible). It recovers 5/6 Gh for a homogeneous section while accounting for a soft core.
- **Uniform 5/6:** explicitly applies 5/6 to the integrated rotated shear stiffness. This is a homogeneous-reference approximation, not a universal correction for sandwich or strongly heterogeneous laminates.

Directional energy approximation:

$$q_i(z) = -\frac{\int_{\text{bottom}}^{z} \overline{Q}_{ii}\,(s)s \quad ds}{D_{ii}}$$

$$C_{s,ij} = \sum_{\text{layers}} \int\, q_i(z)[\overline{\mathbf{G}}_s(z)^{-1}]_{ij} q_j(z) \quad dz$$

$$\mathbf{A}_s = \mathbf{C}_s^{-1}$$

Uniform approximation:

$$\mathbf{A}_s = \frac{5}{6} \sum_{k \in \text{layers}} \overline{\mathbf{G}}_{s,k}\, t_k$$

The directional approximation is not a complete 3D stress recovery or a universal anisotropic warping solution. Its limits remain visible in results. As is reported in N/mm; Qx and Qy are integrated shear force per unit width, not interface stress.

Studies and boundary conditions

- **Static bending:** FSDT with uniform Plate pressure in MPa (= N/mm^2). Clear Nx, Ny and Nxy. Outputs include physical w in mm, rotations in radians, Qx/Qy in N/mm, cursor sections, sampled peak |w| and the shear share of elastic energy.
- **Modal:** unprestressed, undamped frequencies. Through-thickness density integration includes rotary inertia I2 = $\int \rho z^2$ dz. Explicit positive density and symmetric mass distribution are required.
- **Buckling:** elastic bifurcation under uniform proportional Nx, Ny and Nxy. Negative normal resultants mean compression. The multiplier scales that load vector; it is not a strength or postbuckling limit.

Edge	FSDT restraint
Simply supported	w = 0 and tangential rotation = 0; normal bending moment is natural. This is the hard simply supported convention.
Clamped	w = θx = θy = 0.
Free	Natural moment and transverse shear conditions; no essential displacement restraint.

Numerical method and applicability

CDS uses a polynomial Rayleigh–Ritz formulation with independent displacement/rotation fields, enriched rotation spaces and exact-enough Gaussian integration for the polynomial products. Ritz order 4–8 controls spatial approximation. Refinement is essential, particularly for clamped edges, thin plates, soft cores and higher modes. A small algebraic residual does not establish spatial convergence.

The FSDT release accepts thickness / shorter side up to 0.2 as an implementation guard, not a universal accuracy guarantee. It excludes holes, thickness stretch, geometric nonlinearity, process residual preload, damping, contact, unsymmetric extension–bending coupling and mass coupling. Buckling and modal runs do not consume transverse-pressure preload. Extremely thin plates may be better conditioned with CLT.

No false failure pass. FSDT improves global response but does not establish interface peel stress, bond strength, delamination growth, core crushing or ply failure. Those require separately supported constitutive and interface models. The current FSDT release cannot be combined silently with the layerwise progressive-damage or delamination solver.

Try the dedicated exercises

These six examples are part of the shared default database and the searchable curriculum. They use idealized teaching properties, not qualified material allowables.

- Thick isotropic plate — static bending and thickness sensitivity
- Cross-ply plate — CLT/FSDT buckling and frequency comparison
- Soft-core plate — transverse shear and correction sensitivity
- Sandwich panel — clamped uniform-pressure bending
- Sandwich panel — biaxial compression buckling
- Sandwich panel — directional-core natural frequencies

Find these examples by searching FSDT or selecting the FSDT model →

Sandwich exercise sequence

Find these four studies under **07 · Sandwich FSDT** in the default database simulation tree, or filter the exercise manual by FSDT and sandwich application. All use symmetric 1 / 18 / 1 mm skin–core–skin stacks, explicit shear properties and Automatic → FSDT. The unchanged teaching materials are shared; duplicate a record before making an independent variant.

Exercise	Baseline setup	What to inspect
fsdt-03 · Shear-dominated bending	200 × 200 mm; simply supported; 0.001 MPa uniform pressure	Physical deflection and shear-energy fraction; compare shear corrections.
fsdt-04 · Clamped panel bending	300 × 200 mm; all edges clamped; 0.001 MPa uniform pressure	w, rotations and Qx/Qy cursor sections; compare simply supported edges and pressure scaling.
fsdt-05 · Biaxial buckling	300 × 200 mm; simply supported; Nx = −1000 N/m, Ny = −500 N/m; pressure zero	First positive multiplier and proportional critical load pair; compare uniaxial compression and CLT.
fsdt-06 · Directional-core modes	300 × 200 mm; simply supported; all applied loads zero; core G13 = 0.025 GPa, G23 = 0.0125 GPa	First three frequencies and normalized mode shapes, including rotary inertia; exchange core shear directions.

For every study, refine Ritz order from 6 to 8 and record convergence before interpreting trends. These are idealized elastic teaching problems, not strength allowables or experimentally validated sandwich designs. Biaxial buckling is not a wrinkling, bond or core failure criterion; natural-frequency mode amplitudes are not physical vibration displacements.

Verification and validation

Automated module checks compare homogeneous shear stiffness with 5/6 Gh, simply supported static displacement with an independent double Fourier series, buckling with the shear-flexible Navier solution, and frequency with a rotary-inertia eigenvalue reference. Tests also check convergence toward CLT, clamped-edge refinement, required-property errors and the production data definition. These are analytical software verification, not experimental validation or validation of every exercise variation. Dedicated example results are not automatically given a full-model benchmark badge.

Primary references

- FEniCS-Shells: laminate ABD and Reissner–Mindlin shear stiffness — the separation between common laminate stiffness and transverse shear stiffness.
- FEniCS-Shells: clamped Reissner–Mindlin plate — independent rotations, shear energy and the need to control shear locking. CDS uses Ritz approximation, not this finite-element implementation.
- Abaqus theory: transverse shear stiffness in composite shells — energy-equivalent shear concepts and layered-section limitations. CDS's directional approximation is not identical to Abaqus's formulation.

Workbench availability: released models, inputs and compatible study paths . The wider theory library includes reference formulations not available in every Workbench solve.

22 Plate cylinder and beam models

Online chapter

Current Workbench, reference editions and downloads

Use the online User Guide for current controls, the released model directory for selectable models and compatibility, and the Training Manual for connected exercises. Wider theory references do not mean every formulation is enabled in Workbench.

Dated GUI captures and compiled Web r18 PDF manuals retain their stated scope; they are not a substitute for current hosted Workbench instructions. Find the overview PDF, guides and exercise databases in Your CDS library .

Change the structural idealization without changing the shared material, micromechanics, laminate, process, or damage definition.

Choose the structure

Geometry ID	Idealization	Primary results
1	Rectangular laminate plate	Deflection, moments, buckling factor, natural frequency
2	Circular laminate cylinder	Radial/hoop/axial response using shell or Hyer formulation
3	Composite beam section	Centroid, I2/I3, EI, strain energy, deflection, buckling, frequency

Plate boundaries

For the current Workbench plate module, choose Plate theory = CLT or FSDT in CASES. FSDT adds transverse shear and rotary inertia using shared laminate properties. Read the FSDT formulation, current scope and dedicated examples →

Geometry entries 8–11 assign the x0, x1, y0, and y1 edges independently: 1 simply supported, 2 fixed, or 3 free. Plate stiffness comes from the active laminate D matrix; mass and frequency use the calculated effective laminate density.

Cylinder formulations

Cylinder coordinates are axial x, hoop arc-length y, and radial z. Geometry entry 4 selects 1 for the engineering shell solution or 2 for the Hyer formulation. Pressure, axial force, and torque remain in the load-scaler group.

Model 1 Constant-section shell cylinder theory → Model 2 Hyer thick laminated cylinder theory →

Beam sections

Geometry entry 12 selects rectangle, I section, circular tube, rectangular tube, or solid circle. The section dimensions occupy entries 14–21; end conditions occupy 22–23. The solver reports both geometric moments of inertia and laminate-effective EI.

Output interface

- The **structural summary** contains cylinder, plate, and beam section, response, energy, buckling, and frequency results.
- The **cylinder load history** contains pressure, force, torque, resultants, and radial traction.
- The **cylinder stress-recovery table** contains final radial coordinates and recovered stresses.

Engineering scope. These are reduced-order plate, cylinder, and beam calculations for sizing, comparison, and workflow integration. Validate boundary assumptions and model fidelity before certification or safety-critical use.

Workbench availability: released models, inputs and compatible study paths . The wider theory library includes reference formulations not available in every Workbench solve.

23 Process fields in progressive laminate failure

Online chapter

Current Workbench, reference editions and downloads

Use the online User Guide for current controls, the released model directory for selectable models and compatibility, and the Training Manual for connected exercises. Wider theory references do not mean every formulation is enabled in Workbench.

Dated GUI captures and compiled Web r18 PDF manuals retain their stated scope; they are not a substitute for current hosted Workbench instructions. Find the overview PDF, guides and exercise databases in Your CDS library .

Map temperature, moisture, cure shrinkage, and crystallization shrinkage into each ply, form their laminate resultants, and superimpose them with static or progressive mechanical loading. Expand any equation for its physical meaning, variables, units, model connection, and theory source.

Enabled local free strains

Eq. 05.6.4-01 **Flag-controlled local free strain**

$$\varepsilon_k^{\text{free}} = \lambda_T \alpha_k \Delta T_k + \lambda_M \beta_k \Delta C_k + \lambda_c \varepsilon_k^c + \lambda_x \varepsilon_k^x$$

Adds the unconstrained strain caused by temperature change, moisture change, thermoset chemical shrinkage, and thermoplastic crystallization shrinkage. Independent binary switches let each contribution enter or leave the structural solve without changing the process solution.

Variables

$\boldsymbol{\varepsilon}^{\text{free}}_{\text{k}}$ *total enabled free strain in local ply direction k* strain

$\boldsymbol{\lambda}_{\text{T}}$**,** $\boldsymbol{\lambda}_{\text{M}}$**,** $\boldsymbol{\lambda}_{\text{c}}$**,** $\boldsymbol{\lambda}_{\text{x}}$ *thermal, moisture, cure, and crystallization inclusion flags* 0 or 1

$\boldsymbol{\alpha}_{\text{k}}$ *local coefficient of thermal expansion* 1/K

$\boldsymbol{\beta}_{\text{k}}$ *local coefficient of moisture expansion* strain per percentage point

$\mathbf{\Delta T}_{\text{k}}$**,** $\mathbf{\Delta C}_{\text{k}}$ *temperature and moisture changes from each ply reference state* K, percentage points

$\boldsymbol{\varepsilon}^{\text{c}}_{\text{k}}$**,** $\boldsymbol{\varepsilon}^{\text{x}}_{\text{k}}$ *cure and crystallization shrinkage strains* strain

Model connection Evaluated at mapped bottom, middle, and top structural recovery points for every ply. These are the same free strains subtracted during stress recovery and failure evaluation.

Theory basis NASA hygrothermal laminate mechanics

Eq. 05.6.4-02 **Local-to-global free-strain transformation**

$$\varepsilon_{\text{xy},k}^{\text{free}}(z) = T_\varepsilon(\theta_k)\varepsilon_{12,k}^{\text{free}}(z)$$

Rotates each local engineering free-strain vector from material axes 1–2 into laminate axes x–y using the ply orientation.

Variables

$\boldsymbol{\varepsilon}^{\text{free}}_{\text{xy,k}}$ *global in-plane free-strain vector [εx, εy, γxy]^T* strain

$\boldsymbol{\varepsilon}^{free}_{12,k}$ *local in-plane free-strain vector [ε1, ε2, γ12]^T* strain

$\mathbf{T}_\varepsilon(\boldsymbol{\theta}_k)$ *engineering-strain transformation matrix* dimensionless

$\boldsymbol{\theta}_k$ *orientation of ply k* degrees or radians consistently

Model connection The transformed field is multiplied by the ply's damaged transformed stiffness Q̄d when process force and moment resultants are integrated.

Theory basis Classical lamina transformation relations

Mapping the process mesh to three structural nodes per ply

The transport mesh may contain any user-selected number of cells per ply, whereas structural visualization and field output retain exactly three recovery nodes per ply. R15 least-squares fits each process field to a linear function within its owning physical ply, then evaluates that fit at the bottom, middle, and top coordinates.

Eq. 05.6.4-03 **Per-ply linear process-field fit**

$$[a_k, b_k]^T = (Z_k^T Z_k)^{-1} Z_k^T f_k$$

$$\hat{f}_k(z) = a_k + b_k z$$

Finds the best constant and gradient for temperature, moisture, cure shrinkage, and crystallization shrinkage within one ply from all transport cells belonging to that ply.

Variables

$\mathbf{f}_{k,j}$ *process quantity at transport node j of ply k* field-dependent

$\mathbf{a}_k$, $\mathbf{b}_k$ *least-squares intercept and through-thickness gradient* field unit, field unit/m

$\mathbf{Z}_k$ *design matrix with rows [1, zj]* mixed

$\mathbf{z}_{k,j}$ *transport-node coordinate* m

$\hat{\mathbf{f}}_k(\mathbf{z})$ *linear field reconstructed at a structural coordinate* field-dependent

Model connection Preserves both the ply-average process state and its first through-thickness gradient while keeping the stress/strain field histories and animation mesh fixed at three structural nodes per ply.

Theory basis Reduced-order process-to-structure mapping

Damaged laminate stiffness and process resultants

Eq. 05.6.4-04 **Damaged ABD stiffness integrals**

$$A^d = \Sigma_k \int_{z_{k-1}}^{z_k} \overline{Q}_k^d \, \mathrm{dz}$$

$$B^d = \Sigma_k \int_{z_{k-1}}^{z_k} z\,\overline{Q}_k^d \mathrm{dz}, D^d = \Sigma_k \int_{z_{k-1}}^{z_k} z^2\,\overline{Q}_k^d \mathrm{dz}$$

Integrates the current transformed stiffness of every ply through the laminate thickness. Progressive failure changes Q̄d and therefore rebuilds A, B, and D.

Variables

A^d, B^d, D^d *damaged extensional, coupling, and bending stiffness matrices* N/m, N, N·m

$\bar{Q}^d_k$ *damaged transformed reduced stiffness of ply k* Pa

z_{k-1}, z_k *bottom and top coordinates of ply k* m

Model connection The same damaged stiffness used for mechanical equilibrium also weights the process resultants, so a new ply failure changes load redistribution and residual-stress restraint at the same accepted load.

Theory basis NASA classical laminate ABD formulation

Eq. 05.6.4-05 **Process force and moment resultants**

$$N^p = \Sigma_k \int \overline{Q}_k^d \varepsilon_k^{\text{free}}(z)\text{dz}$$

$$M^p = \Sigma_k \int z\overline{Q}_k^d \varepsilon_k^{\text{free}}(z)\text{dz}$$

Converts an otherwise free process strain into equivalent in-plane forces and moments representing the restraint imposed by the bonded laminate. A gradient contributes directly to process bending moment.

Variables

N^p, M^p *process-induced membrane force and bending moment resultants* N/m, N

$\bar{Q}^d_k$ *current damaged transformed ply stiffness* Pa

$\varepsilon^{free}_k(z)$ *enabled global free-strain field in ply k* strain

z *coordinate measured from the laminate reference plane* m

Model connection Recomputed after any new damage state before same-load re-equilibration. The process-resultant history reports each component over the structural increments.

Theory basis Hygrothermal force and moment resultants

Combined generalized equilibrium

Eq. 05.6.4-06 **Damaged mechanical–process equilibrium**

$$[A^d B^d; B^d D^d]\{\varepsilon^0, \kappa\}^T = \{N^{\text{mech}} + N^p, M^{\text{mech}} + M^p\}^T$$

Solves simultaneously for mid-plane strains and curvatures under the sum of enabled mechanical and process-equivalent resultants. This is the governing superposition step, not a postprocessed stress offset.

Variables

ε^0 *laminate mid-plane strain vector* strain

κ *laminate curvature/twist vector* 1/m

N^{mech}, M^{mech} *applied mechanical membrane and moment resultants* N/m, N

N^p, M^p *enabled process force and moment resultants* N/m, N

A^d, B^d, D^d *current damaged laminate stiffness blocks* N/m, N, N·m

Model connection Used for a static mechanical state or at every progressive load increment. The mechanical-load flag may remove Nmech and Mmech while retaining process-only residual response.

Theory basis NASA generalized laminate equilibrium

Eq. 05.6.4-07 **Through-thickness strain and stress recovery**

$$\varepsilon(z) = \varepsilon^0 + z\kappa$$

$$\sigma_k(z) = \overline{Q}_k^d\left[\varepsilon(z) - \varepsilon_k^{\text{free}}(z)\right]$$

Recovers the compatible global strain at any z and subtracts the enabled free strain before applying the current damaged stiffness. The result is the actual constrained ply stress used by failure criteria.

Variables

ε(z) *total compatible global in-plane strain* strain

ε^0, κ *mid-plane strain and curvature from generalized equilibrium* strain, 1/m

σ_k(z) *global stress in ply k* Pa

$\bar{Q}^d_k$ *damaged transformed ply stiffness* Pa

ε^{free}_k(z) *enabled global free strain* strain

Model connection Evaluated at the bottom, middle, and top of every ply and then transformed to local 1–2 axes. Top and bottom surface states govern the progressive failure check.

Theory basis Classical laminate stress recovery with hygrothermal strain

Eq. 05.6.4-08 **Auditable contribution decomposition**

$$y^{\text{tot}} = y^{\text{mech}} + y^T + y^M + y^c + y^x$$

Reports total fields together with separately evaluated mechanical, thermal, moisture, cure-shrinkage, and crystallization-shrinkage contributions at the same increment and damaged material state.

Variables

y^{tot} *reported total stress or strain field* Pa or strain

y^{mech} *mechanical contribution* Pa or strain

y^T, y^M *thermal and moisture contributions* Pa or strain

y^c, y^x *cure- and crystallization-shrinkage contributions* Pa or strain

Model connection Supports the global, local, principal, and process-only field histories so CDS can display each contribution without reconstructing it outside the solver.

Theory basis Process-induced residual-response decomposition

Progressive same-load update

At each accepted increment the solver recovers all three structural nodes per ply; checks both surfaces; evaluates the independent criterion assigned to that ply; degrades only newly activated stiffness families; rebuilds damaged ABD and process resultants; and re-equilibrates at the same combined mechanical–process load until no new event occurs.

Coupling boundary. The process solver is one-way with respect to structural damage in r15: process fields create structural strains and stresses, while ply damage changes the stiffness that restrains those fields. Damage does not yet change k_3, c_p, diffusivity, cure kinetics, or crystallization kinetics.

Auditable outputs

- **Stress and strain histories:** total, mechanical, thermal, and moisture contributions.
- **Transport histories:** mesh, fields, state, rates, heat, shrinkage, and surface interpolation.
- **Structural process mapping:** mapped states and active physical components.
- **Process-only fields:** global and local stress and strain.
- **Process resultants:** force and moment components at every structural increment.

Theory references

- Nettles, Basic Mechanics of Laminated Composite Plates, NASA RP-1351, including ABD and hygrothermal effects.
- NASA, Composite Cure Process Modeling and Simulations using Finite Element Analysis (2016).
- NASA/TM–20205009287, cure-induced residual stress development.

Workbench availability: released models, inputs and compatible study paths . The wider theory library includes reference formulations not available in every Workbench solve.

24 Connect process history to structural response

Online chapter

Current Workbench, reference editions and downloads

Use the online User Guide for current controls, the released model directory for selectable models and compatibility, and the Training Manual for connected exercises. Wider theory references do not mean every formulation is enabled in Workbench.

Dated GUI captures and compiled Web r18 PDF manuals retain their stated scope; they are not a substitute for current hosted Workbench instructions. Find the overview PDF, guides and exercise databases in Your CDS library .

A laminate remembers how it was processed and the environment it experienced. Define those conditions before interpreting its loaded response.

Read time and travel distance

Boundary peak: 120 °C

Pull speed: 10 mm/min

Time cursor: 30 min

Show length instead of time

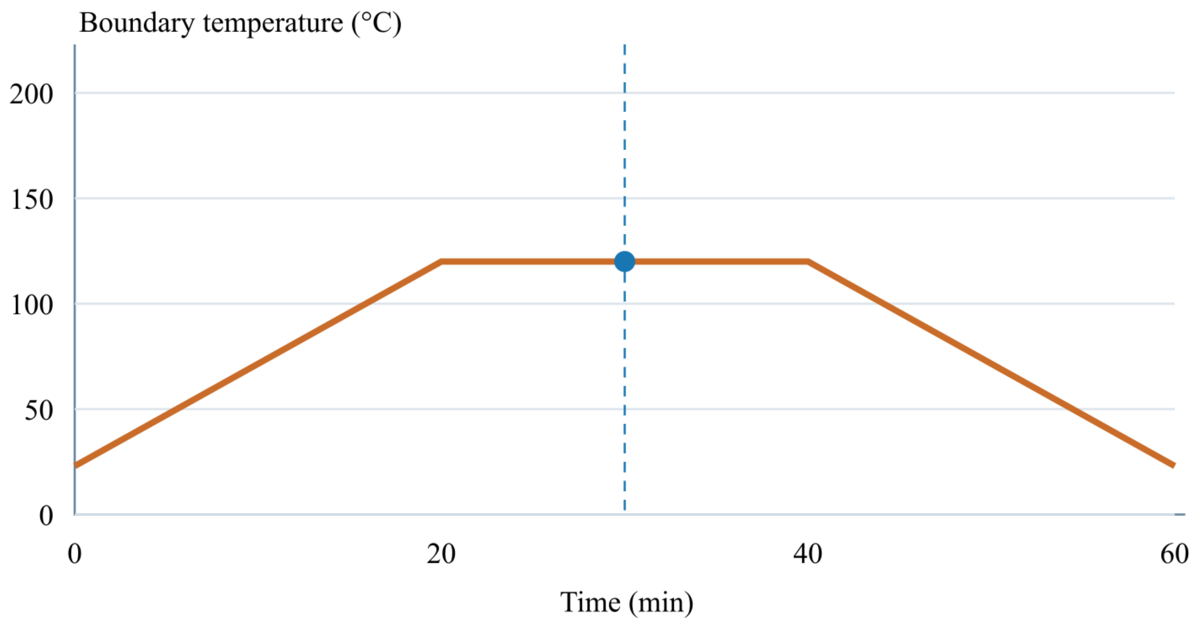

Cursor: 30 min · 300 mm · 120.0 °C

What the study needs

Choice	Why it matters
Material and layup	Elastic properties and fiber directions determine stiffness; strengths and fracture data are needed for the selected failure models.
Geometry and support	Shape, dimensions and boundary conditions determine how a component deforms and carries load.
Mechanical loads	Specify the forces and moments, including which components increase during progressive failure.
Process and environment	Temperature, moisture and material state can produce expansion, shrinkage and residual stresses.

Define the surfaces and the material state

- Give the upper and lower surfaces independent histories when their surroundings differ.
- Choose prescribed temperature, convection or another supported thermal boundary condition.
- Define moisture exposure and the corresponding diffusion properties when studying uptake or drying.
- Provide calibrated cure or crystallization kinetics for reacting materials; use an inert material when no reaction is intended.
- A recorded pressure history is not, by itself, proof that pressure has been mechanically coupled. Check the selected structural loads.

Named response and traceability outputs

Named result group	Contents
Transport histories	Transport metadata, time, temperature, and moisture
Material-state histories	Cure/crystallinity states, rates, heat sources, and shrinkage
Surface and ply summaries	Interpolated surfaces and final per-ply process summary
Process-to-structure results	Structural mapping, process-only field contributions, and process resultants
Double-Double recommendation	Compatibility, recommended angles, stiffness error, and selected ply angles
Structural summary	Cylinder summary plus plate/beam section, response, energy, buckling, and frequency results
Cylinder load history	Cylinder loads and resultants

Named result group	Contents
Cylinder stress recovery	Final radial-coordinate and recovered-stress table

Interpret before comparing. Check the final material state and residual stresses, then compare the loaded response. Missing transport or strength data must not be treated as a validated pass. Try the coupled exercise →

Workbench availability: released models, inputs and compatible study paths . The wider theory library includes reference formulations not available in every Workbench solve.

25 Trace temperature from properties to structural response

Online chapter

Current Workbench, reference editions and downloads

Use the online User Guide for current controls, the released model directory for selectable models and compatibility, and the Training Manual for connected exercises. Wider theory references do not mean every formulation is enabled in Workbench.

Dated GUI captures and compiled Web r18 PDF manuals retain their stated scope; they are not a substitute for current hosted Workbench instructions. Find the overview PDF, guides and exercise databases in Your CDS library .

Connect constituent conductivity, heat capacity, expansion, boundary histories, temperature fields, laminate resultants, and recovered thermomechanical response.

Workbench availability: released models, inputs and compatible study paths . The wider theory library includes reference formulations not available in every Workbench solve.

26 Explore a test Understand its limits

Online chapter

Ten connected analytical and measured-data studies, organized by familiar composite test families.

Find these in Workbench → Models → Structural models → ASTM · Virtual Test Lab, or filter exercises by ASTM. Each opens a separate connected SIMULATE study. Review the laminate, edit the test inputs, then Run or use live refresh where available.

Test-inspired, not ASTM certification. Defaults are hypothetical teaching values. The standards define physical test procedures; these bounded calculations do not reproduce every fixture, correction or validity requirement. Always consult the applicable current standard.

D6641 Compression coupon

Uniform small-strain compression using linked laminate Ex and thickness. Measured compressive strength supplies a screening ratio; fixture, tabs, buckling and failure evolution are not simulated.

Equations, inputs and interpretation

$\sigma = P/(wt)$, $\varepsilon = \sigma/E_x$, $\delta = \varepsilon L$.

Ex and total thickness come from the connected laminate. Stress, strain and force are positive compression magnitudes. The curve is elastic specimen shortening, not crosshead travel. Measured compressive strength is an independent input; the solver does not predict it from Ex. The small-strain limit is 2%.

- Specimen width (mm)
- Gauge length (mm)
- Applied force (N)
- Measured compressive strength (MPa)

ASTM composite standards catalog

Connected workflow

Two-row simulation workflow · **Open full-size map**
Linked-input preview, not solved results. Gray blocks are not configured.

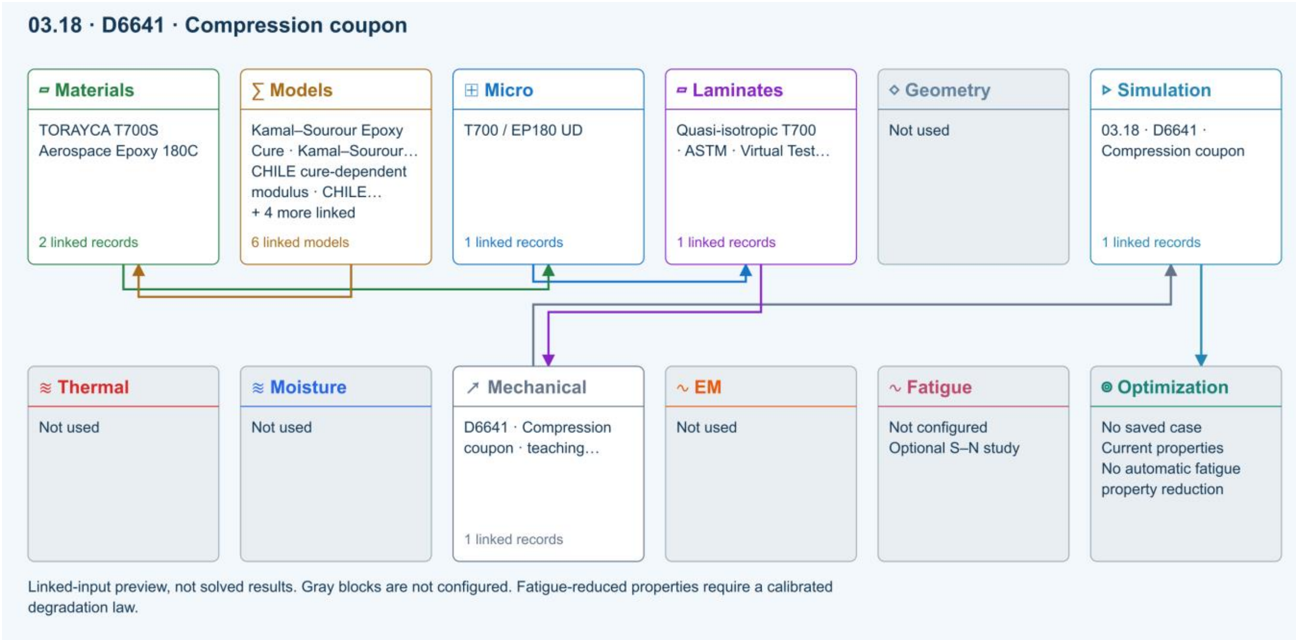

∑ Selected models & submodels

These are the exercise's linked choices, not solved results. Open a first-layer model to see its submodels and scope.

Kamal–Sourour autocatalytic · Kamal–Sourour Epoxy Cure

Reusable material model. It contributes only when assigned to a material used by this simulation; separate model records can supply independent properties.

Calibration & applicability

Illustrative model defaults — replace with characterized resin kinetics

∑ Theory & assumptions

CHILE (degree of cure) · CHILE cure-dependent modulus

Reusable material model. It contributes only when assigned to a material used by this simulation; separate model records can supply independent properties. Cure-dependent modulus does not automatically scale strength allowables.

Calibration & applicability

CHILE(α), section 2.4 of Materials 2019, 12, 259. Example parameters, not measured EP180 data. Fixed Poisson ratio; no viscoelastic relaxation or Tg softening. Incremental elastic stress integration at saved process intervals: check time-step convergence. Strength allowables are independent measured inputs, not scaled with modulus.

∑ Theory & assumptions

Temperature-dependent tabular · Temperature-dependent Thermal

Reusable material model. It contributes only when assigned to a material used by this simulation; separate model records can supply independent properties. Micro uses the 23 °C reference; Process evaluates the same table at local temperature, without extrapolation.

Calibration & applicability

Check source data, applicable environment and validity limits in the model record; saved defaults are not experimental validation.

∑ Theory & assumptions

1D Fickian diffusion · Layered Fickian Diffusion

Reusable material model. It contributes only when assigned to a material used by this simulation; separate model records can supply independent properties.

Calibration & applicability

Check source data, applicable environment and validity limits in the model record; saved defaults are not experimental validation.

∑ Theory & assumptions

Halpin–Tsai · T700 / EP180 UD

One compatible homogenization model per Micro recipe. Separate recipes compare models; their predictions are not blended.

∑ Theory & assumptions

Virtual test · compression coupon · D6641 · Compression coupon · teaching study

Uniform small-strain compression using linked laminate Ex and thickness. Measured compressive strength supplies a screening ratio; fixture, tabs, buckling and failure evolution are not simulated.

Linked laminate reference state

Ply stiffness, thickness and orientation come from the linked laminate. Other thermal or structural analyses must be run separately.

Calibration & study controls

Teaching example

Specimen width: 25 mm

Gauge length: 25 mm

Applied force: 1000 N

Positive magnitude. Compression is reported as a magnitude.

Measured compressive strength: 400 MPa

∑ Theory & assumptions

Data travelling between blocks

Micro → Laminates
Predicted ply stiffness, strength, density and expansion properties.

Materials → Micro
Constituent stiffness, strength, density and thermal / moisture properties.

Models → Materials
Model choices and calibrated parameters.

Mechanical → Simulation
SIMULATION selects this case and its analysis model; the case owns its applicable cycle and input references.

Laminates → Mechanical
Ply angles and thicknesses, stiffness, mass and ply properties.

Simulation → Optimization
Linked inputs and current-property response for candidate evaluation.

Open this exercise in SIMULATE · Model inputs and outputs

D5379 / D7078 Shear coupon

Uniform nominal shear between notches using linked laminate Gxy and thickness. Not a notch/fixture stress field or nonlinear shear solution. Gauge length is the effective shear deformation length, not crosshead travel.

Equations, inputs and interpretation

$\tau = P/(b_{net}\, t)$, $\gamma = \tau/G_{xy}$, $\delta = \gamma L_g$.

Gxy and thickness come from the connected laminate. This uniform nominal-field approximation does not resolve the V-notch or grip stresses. Lg is an effective shear gauge length, not fixture travel. Supply measured shear strength separately. Both D5379 and D7078 are represented only at this nominal-response level.

- Net section width (mm)
- Shear gauge length (mm)
- Applied force (N)
- Measured shear strength (MPa)

ASTM composite standards catalog

Connected workflow

Two-row simulation workflow · **Open full-size map**
Linked-input preview, not solved results. Gray blocks are not configured.

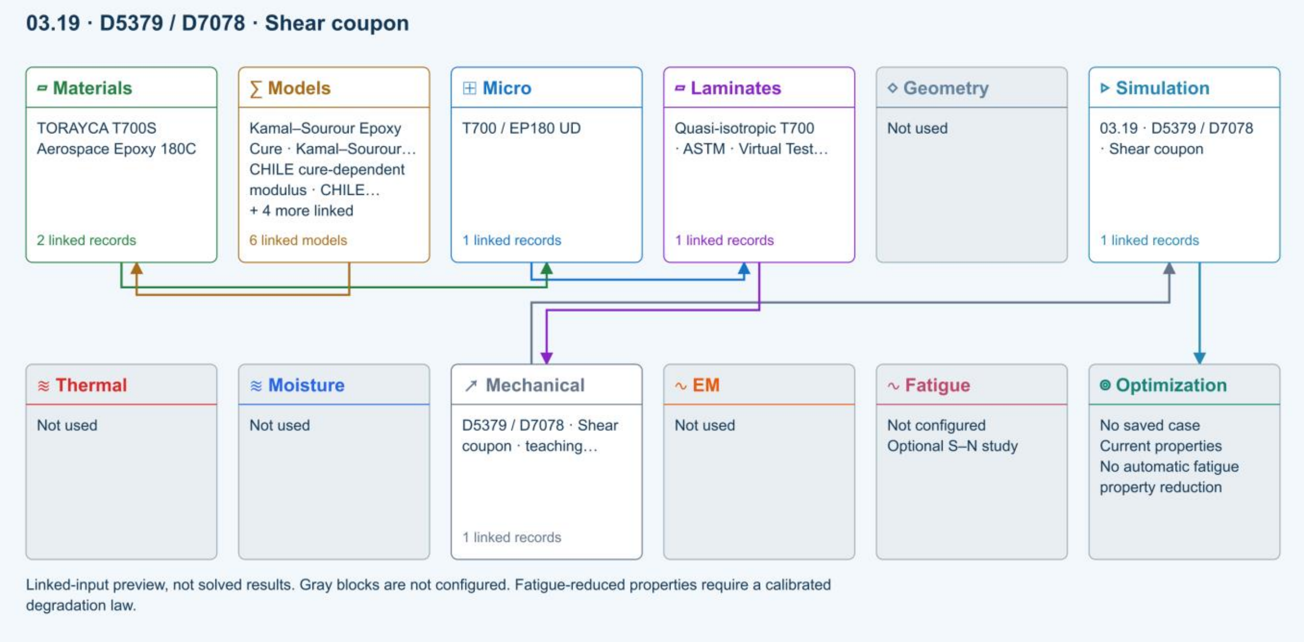

∑ Selected models & submodels

These are the exercise's linked choices, not solved results. Open a first-layer model to see its submodels and scope.

Kamal–Sourour autocatalytic · Kamal–Sourour Epoxy Cure

Reusable material model. It contributes only when assigned to a material used by this simulation; separate model records can supply independent properties.

Calibration & applicability

Illustrative model defaults — replace with characterized resin kinetics

∑ Theory & assumptions

CHILE (degree of cure) · CHILE cure-dependent modulus

Reusable material model. It contributes only when assigned to a material used by this simulation; separate model records can supply independent properties. Cure-dependent modulus does not automatically scale strength allowables.

Calibration & applicability

CHILE(α), section 2.4 of Materials 2019, 12, 259. Example parameters, not measured EP180 data. Fixed Poisson ratio; no viscoelastic relaxation or Tg softening. Incremental elastic stress integration at saved process intervals: check time-step convergence. Strength allowables are independent measured inputs, not scaled with modulus.

∑ Theory & assumptions

Temperature-dependent tabular · Temperature-dependent Thermal

Reusable material model. It contributes only when assigned to a material used by this simulation; separate model records can supply independent properties. Micro uses the 23 °C reference; Process evaluates the same table at local temperature, without extrapolation.

Calibration & applicability

Check source data, applicable environment and validity limits in the model record; saved defaults are not experimental validation.

∑ Theory & assumptions

1D Fickian diffusion · Layered Fickian Diffusion

Reusable material model. It contributes only when assigned to a material used by this simulation; separate model records can supply independent properties.

Calibration & applicability

Check source data, applicable environment and validity limits in the model record; saved defaults are not experimental validation.

∑ Theory & assumptions

Halpin–Tsai · T700 / EP180 UD

One compatible homogenization model per Micro recipe. Separate recipes compare models; their predictions are not blended.

∑ Theory & assumptions

Virtual test · nominal shear coupon · D5379 / D7078 · Shear coupon · teaching study

Uniform nominal shear between notches using linked laminate Gxy and thickness. Not a notch/fixture stress field or nonlinear shear solution. Gauge length is the effective shear deformation length, not crosshead travel.

Linked laminate reference state

Ply stiffness, thickness and orientation come from the linked laminate. Other thermal or structural analyses must be run separately.

Calibration & study controls

Teaching example

Net section width: 12 mm

Shear gauge length: 10 mm

Applied force: 500 N

Measured shear strength: 80 MPa

∑ Theory & assumptions

Data travelling between blocks

Micro → Laminates
Predicted ply stiffness, strength, density and expansion properties.

Materials → Micro
Constituent stiffness, strength, density and thermal / moisture properties.

Models → Materials
Model choices and calibrated parameters.

Mechanical → Simulation
SIMULATION selects this case and its analysis model; the case owns its applicable cycle and input references.

Laminates → Mechanical
Ply angles and thicknesses, stiffness, mass and ply properties.

Simulation → Optimization
Linked inputs and current-property response for candidate evaluation.

Open this exercise in SIMULATE · Model inputs and outputs

D5528 DCB opening

Ideal Euler–Bernoulli DCB with equal homogeneous 0° arms, each half the linked laminate thickness. No root rotation, shear, large displacement or cohesive growth. Critical load is an initiation estimate from supplied GIc.

Equations, inputs and interpretation

$$C = 8a^3/(Ebh^3),\ GI = 12P^2a^2/(Eb^2h^3),\ Pc = \sqrt{[GIc\ Eb^2h^3/(12a^2)]}.$$

Each identical homogeneous 0° arm has thickness $h = t/2$. P is the force on each arm and $\delta = CP$ is relative opening. The linked ply E1 supplies the ideal beam modulus. Crack length stays fixed; Pc estimates initiation only. Root rotation, shear deformation, large deflection and compliance corrections required in experimental interpretation are absent. Use $a/h \geq 10$.

- Specimen width (mm)
- Crack length (mm)
- Applied force (N)
- Critical fracture energy (N/mm)

ASTM composite standards catalog

Connected workflow

Two-row simulation workflow · **Open full-size map**
Linked-input preview, not solved results. Gray blocks are not configured.

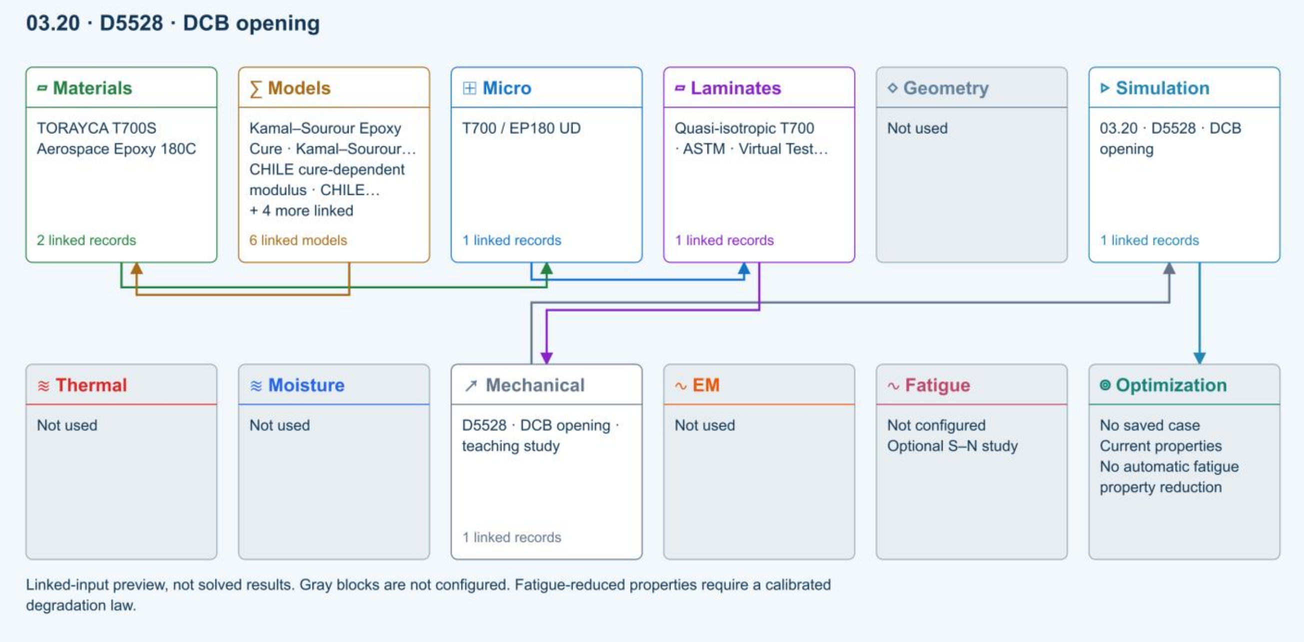

∑ Selected models & submodels

These are the exercise's linked choices, not solved results. Open a first-layer model to see its submodels and scope.

Kamal–Sourour autocatalytic · Kamal–Sourour Epoxy Cure

Reusable material model. It contributes only when assigned to a material used by this simulation; separate model records can supply independent properties.

Calibration & applicability

Illustrative model defaults — replace with characterized resin kinetics

∑ Theory & assumptions

CHILE (degree of cure) · CHILE cure-dependent modulus

Reusable material model. It contributes only when assigned to a material used by this simulation; separate model records can supply independent properties. Cure-dependent modulus does not automatically scale strength allowables.

Calibration & applicability

CHILE(α), section 2.4 of Materials 2019, 12, 259. Example parameters, not measured EP180 data. Fixed Poisson ratio; no viscoelastic relaxation or Tg softening. Incremental elastic stress integration at saved process intervals: check time-step convergence. Strength allowables are independent measured inputs, not scaled with modulus.

∑ Theory & assumptions

Temperature-dependent tabular · Temperature-dependent Thermal

Reusable material model. It contributes only when assigned to a material used by this simulation; separate model records can supply independent properties. Micro uses the 23 °C reference; Process evaluates the same table at local temperature, without extrapolation.

Calibration & applicability

Check source data, applicable environment and validity limits in the model record; saved defaults are not experimental validation.

∑ Theory & assumptions

1D Fickian diffusion · Layered Fickian Diffusion

Reusable material model. It contributes only when assigned to a material used by this simulation; separate model records can supply independent properties.

Calibration & applicability

Check source data, applicable environment and validity limits in the model record; saved defaults are not experimental validation.

∑ Theory & assumptions

Halpin–Tsai · T700 / EP180 UD

One compatible homogenization model per Micro recipe. Separate recipes compare models; their predictions are not blended.

∑ Theory & assumptions

Virtual test · DCB beam compliance · D5528 · DCB opening · teaching study

Ideal Euler–Bernoulli DCB with equal homogeneous 0° arms, each half the linked laminate thickness. No root rotation, shear, large displacement or cohesive growth. Critical load is an initiation estimate from supplied GIc.

Linked laminate reference state

Ply stiffness, thickness and orientation come from the linked laminate. Other thermal or structural analyses must be run separately.

Calibration & study controls

Teaching example

Specimen width: 25 mm

Crack length: 30 mm

Applied force: 5 N

Critical fracture energy: 0.3 N/mm

Measured fracture energy; default is hypothetical.

∑ Theory & assumptions

Data travelling between blocks

Micro → Laminates
Predicted ply stiffness, strength, density and expansion properties.

Materials → Micro
Constituent stiffness, strength, density and thermal / moisture properties.

Models → Materials
Model choices and calibrated parameters.

Mechanical → Simulation
SIMULATION selects this case and its analysis model; the case owns its applicable cycle and input references.

Laminates → Mechanical
Ply angles and thicknesses, stiffness, mass and ply properties.

Simulation → Optimization
Linked inputs and current-property response for candidate evaluation.

Open this exercise in SIMULATE · Model inputs and outputs

D7905 ENF sliding

Ideal equal-arm, homogeneous 0° ENF beam; support span is twice the half-span. Crack must be shorter than the half-span. No shear/root correction or unstable crack growth. GIIc is supplied, not fitted automatically.

Equations, inputs and interpretation

$$C = (2L^3 + 3a^3)/(8Ebh^3),\ GII = 9P^2a^2/(16Eb^2h^3).$$

L is the support HALF-span; each identical 0° arm has thickness $h = t/2$. The crack must satisfy $a < L$. At fixed crack length, $\delta = CP$ and the supplied GIIc determines the ideal initiation load. This is not an unstable crack-propagation simulation or a complete standard test reduction. Use slender beams.

- Specimen width (mm)
- Crack length (mm)
- Applied force (N)
- Critical fracture energy (N/mm)
- Support half-span (mm)

ASTM composite standards catalog

Connected workflow

Two-row simulation workflow · **Open full-size map**
Linked-input preview, not solved results. Gray blocks are not configured.

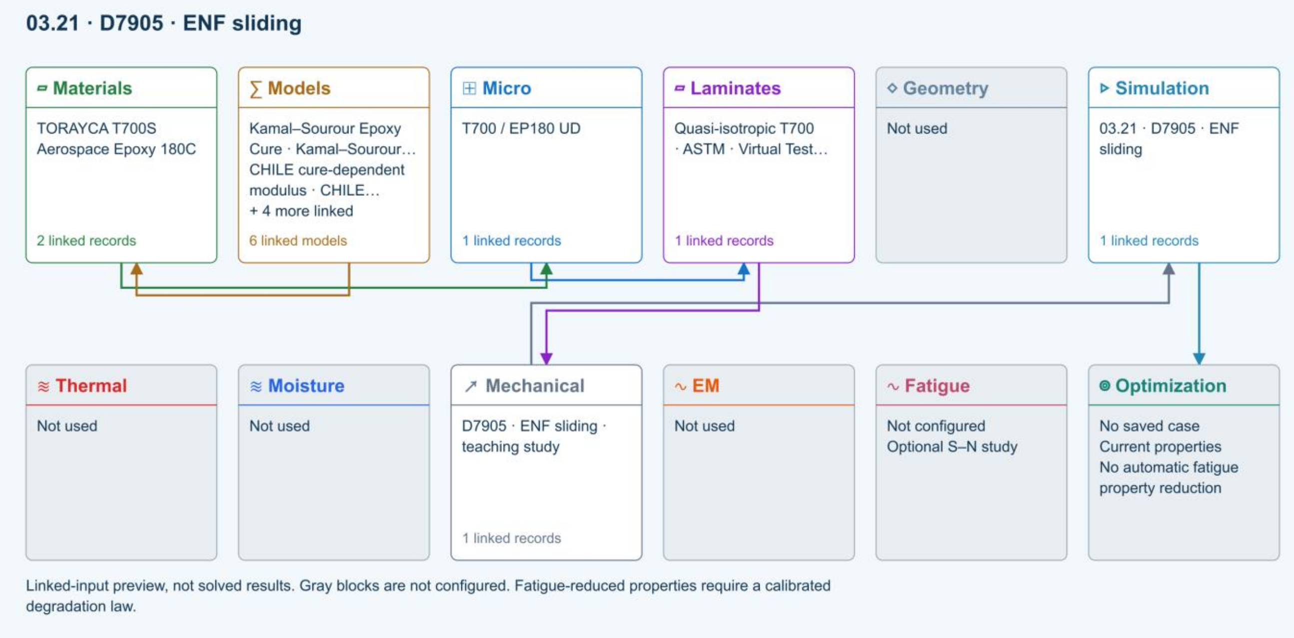

∑ Selected models & submodels

These are the exercise's linked choices, not solved results. Open a first-layer model to see its submodels and scope.

Kamal–Sourour autocatalytic · Kamal–Sourour Epoxy Cure

Reusable material model. It contributes only when assigned to a material used by this simulation; separate model records can supply independent properties.

Calibration & applicability

Illustrative model defaults — replace with characterized resin kinetics

∑ Theory & assumptions

CHILE (degree of cure) · CHILE cure-dependent modulus

Reusable material model. It contributes only when assigned to a material used by this simulation; separate model records can supply independent properties. Cure-dependent modulus does not automatically scale strength allowables.

Calibration & applicability

CHILE(α), section 2.4 of Materials 2019, 12, 259. Example parameters, not measured EP180 data. Fixed Poisson ratio; no viscoelastic relaxation or Tg softening. Incremental elastic stress integration at saved process intervals: check time-step convergence. Strength allowables are independent measured inputs, not scaled with modulus.

∑ Theory & assumptions

Temperature-dependent tabular · Temperature-dependent Thermal

Reusable material model. It contributes only when assigned to a material used by this simulation; separate model records can supply independent properties. Micro uses the 23 °C reference; Process evaluates the same table at local temperature, without extrapolation.

Calibration & applicability

Check source data, applicable environment and validity limits in the model record; saved defaults are not experimental validation.

∑ Theory & assumptions

1D Fickian diffusion · Layered Fickian Diffusion

Reusable material model. It contributes only when assigned to a material used by this simulation; separate model records can supply independent properties.

Calibration & applicability

Check source data, applicable environment and validity limits in the model record; saved defaults are not experimental validation.

∑ Theory & assumptions

Halpin–Tsai · T700 / EP180 UD

One compatible homogenization model per Micro recipe. Separate recipes compare models; their predictions are not blended.

∑ Theory & assumptions

Virtual test · ENF beam compliance · D7905 · ENF sliding · teaching study

Ideal equal-arm, homogeneous 0° ENF beam; support span is twice the half-span. Crack must be shorter than the half-span. No shear/root correction or unstable crack growth. GIIc is supplied, not fitted automatically.

Linked laminate reference state

Ply stiffness, thickness and orientation come from the linked laminate. Other thermal or structural analyses must be run separately.

Calibration & study controls

Teaching example

Specimen width: 25 mm

Crack length: 30 mm

Applied force: 5 N

Critical fracture energy: 0.3 N/mm

Measured fracture energy; default is hypothetical.

Support half-span: 50 mm

∑ Theory & assumptions

Data travelling between blocks

Micro → Laminates
Predicted ply stiffness, strength, density and expansion properties.

Materials → Micro
Constituent stiffness, strength, density and thermal / moisture properties.

Models → Materials
Model choices and calibrated parameters.

Mechanical → Simulation
SIMULATION selects this case and its analysis model; the case owns its applicable cycle and input references.

Laminates → Mechanical
Ply angles and thicknesses, stiffness, mass and ply properties.

Simulation → Optimization
Linked inputs and current-property response for candidate evaluation.

Open this exercise in SIMULATE · Model inputs and outputs

D6671 Mixed-mode fracture envelope

Benzeggagh–Kenane envelope from calibrated GIc, GIIc and exponent. Supplied GI/GII are energy-release rates from a separate test reduction or analysis. This does not resolve the MMB lever fixture or propagate a crack.

Equations, inputs and interpretation

$G_c = G_{Ic} + (G_{IIc} - G_{Ic}) [G_{II}/(G_I + G_{II})]^\eta$.

The BK envelope interpolates between measured pure-mode toughnesses using a calibrated exponent. The supplied GI and GII must come from an independent test reduction or compatible analysis. No lever-arm geometry or MMB fixture is solved. The laminate link keeps study provenance; laminate stiffness is not used to infer these energy-release rates.

- Mode I toughness (N/mm)
- Mode II toughness (N/mm)
- BK exponent (—)
- Applied GI (N/mm)
- Applied GII (N/mm)

ASTM composite standards catalog

Connected workflow

Two-row simulation workflow · **Open full-size map**
Linked-input preview, not solved results. Gray blocks are not configured.

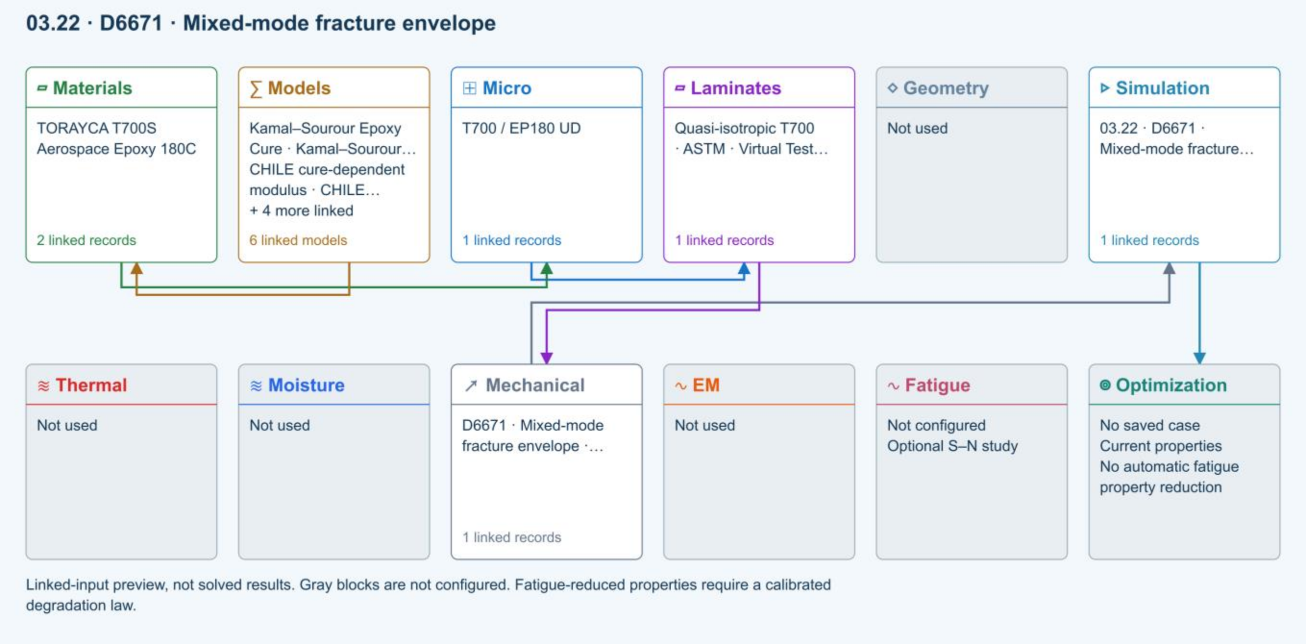

∑ Selected models & submodels

These are the exercise's linked choices, not solved results. Open a first-layer model to see its submodels and scope.

Kamal–Sourour autocatalytic · Kamal–Sourour Epoxy Cure

Reusable material model. It contributes only when assigned to a material used by this simulation; separate model records can supply independent properties.

Calibration & applicability

Illustrative model defaults — replace with characterized resin kinetics

∑ Theory & assumptions

CHILE (degree of cure) · CHILE cure-dependent modulus

Reusable material model. It contributes only when assigned to a material used by this simulation; separate model records can supply independent properties. Cure-dependent modulus does not automatically scale strength allowables.

Calibration & applicability

CHILE(α), section 2.4 of Materials 2019, 12, 259. Example parameters, not measured EP180 data. Fixed Poisson ratio; no viscoelastic relaxation or Tg softening. Incremental elastic stress integration at saved process intervals: check time-step convergence. Strength allowables are independent measured inputs, not scaled with modulus.

∑ Theory & assumptions

Temperature-dependent tabular · Temperature-dependent Thermal

Reusable material model. It contributes only when assigned to a material used by this simulation; separate model records can supply independent properties. Micro uses the 23 °C reference; Process evaluates the same table at local temperature, without extrapolation.

Calibration & applicability

Check source data, applicable environment and validity limits in the model record; saved defaults are not experimental validation.

∑ Theory & assumptions

1D Fickian diffusion · Layered Fickian Diffusion

Reusable material model. It contributes only when assigned to a material used by this simulation; separate model records can supply independent properties.

Calibration & applicability

Check source data, applicable environment and validity limits in the model record; saved defaults are not experimental validation.

∑ Theory & assumptions

Halpin–Tsai · T700 / EP180 UD

One compatible homogenization model per Micro recipe. Separate recipes compare models; their predictions are not blended.

∑ Theory & assumptions

Virtual test · BK mixed-mode envelope · D6671 · Mixed-mode fracture envelope · teaching study

Benzeggagh–Kenane envelope from calibrated GIc, GIIc and exponent. Supplied GI/GII are energy-release rates from a separate test reduction or analysis. This does not resolve the MMB lever fixture or propagate a crack.

Linked laminate reference state

Ply stiffness, thickness and orientation come from the linked laminate. Other thermal or structural analyses must be run separately.

Calibration & study controls

Teaching example

Mode I toughness: 0.3 N/mm

Mode II toughness: 0.9 N/mm

BK exponent: 1.6 —

Applied GI: 0.1 N/mm

Applied GII: 0.2 N/mm

∑ Theory & assumptions

Data travelling between blocks

Micro → Laminates
Predicted ply stiffness, strength, density and expansion properties.

Materials → Micro
Constituent stiffness, strength, density and thermal / moisture properties.

Models → Materials
Model choices and calibrated parameters.

Mechanical → Simulation
SIMULATION selects this case and its analysis model; the case owns its applicable cycle and input references.

Laminates → Mechanical
Ply angles and thicknesses, stiffness, mass and ply properties.

Simulation → Optimization
Linked inputs and current-property response for candidate evaluation.

Open this exercise in SIMULATE · Model inputs and outputs

D5229 Moisture uptake calibration

Homogeneous slab, initially dry, both faces held at equilibrium moisture. Fits diffusivity from two early uptake measurements (both ≤50% saturation) using the square-root-time approximation. Edge ingress and temperature dependence are excluded. Does not overwrite material properties.

Equations, inputs and interpretation

$$D = \pi\,[t \times \text{slope}/(4M_\infty)]^2;\ M(T)/M_\infty = 1 - (8/\pi^2)\,\Sigma \exp[-(2j+1)^2\pi^2 DT/t^2]/(2j+1)^2.$$

Here t is total slab thickness and T is elapsed time. Two increasing early mass-gain points define slope = $\Delta M/\Delta\sqrt{T}$. Both must remain at or below 50% of equilibrium; an inconsistent dry intercept is rejected. The model assumes an initially dry homogeneous slab with both faces held at equilibrium, no edge ingress and constant diffusivity. D is reported in mm^2/s. Copy it into a material only after independent validation; no saved material is changed. No temperature shifting or hot-wet strength degradation is inferred.

- Equilibrium mass gain (percent)
- Measurement time 1 (h)
- Mass gain 1 (percent)
- Measurement time 2 (h)
- Mass gain 2 (percent)
- Conditioning duration (h)

ASTM composite standards catalog

Connected workflow

Two-row simulation workflow · **Open full-size map**
Linked-input preview, not solved results. Gray blocks are not configured.

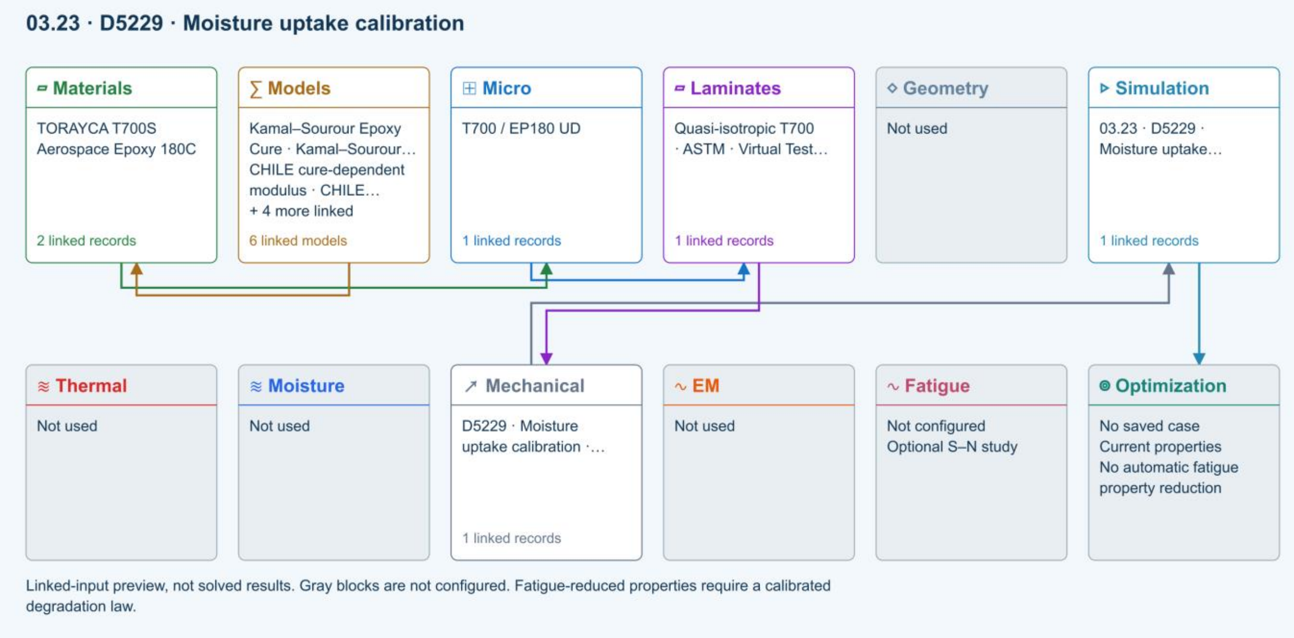

∑ Selected models & submodels

These are the exercise's linked choices, not solved results. Open a first-layer model to see its submodels and scope.

Kamal–Sourour autocatalytic · Kamal–Sourour Epoxy Cure

Reusable material model. It contributes only when assigned to a material used by this simulation; separate model records can supply independent properties.

Calibration & applicability

Illustrative model defaults — replace with characterized resin kinetics

∑ Theory & assumptions

CHILE (degree of cure) · CHILE cure-dependent modulus

Reusable material model. It contributes only when assigned to a material used by this simulation; separate model records can supply independent properties. Cure-dependent modulus does not automatically scale strength allowables.

Calibration & applicability

CHILE(α), section 2.4 of Materials 2019, 12, 259. Example parameters, not measured EP180 data. Fixed Poisson ratio; no viscoelastic relaxation or Tg softening. Incremental elastic stress integration at saved process intervals: check time-step convergence. Strength allowables are independent measured inputs, not scaled with modulus.

∑ Theory & assumptions

Temperature-dependent tabular · Temperature-dependent Thermal

Reusable material model. It contributes only when assigned to a material used by this simulation; separate model records can supply independent properties. Micro uses the 23 °C reference; Process evaluates the same table at local temperature, without extrapolation.

Calibration & applicability

Check source data, applicable environment and validity limits in the model record; saved defaults are not experimental validation.

∑ Theory & assumptions

1D Fickian diffusion · Layered Fickian Diffusion

Reusable material model. It contributes only when assigned to a material used by this simulation; separate model records can supply independent properties.

Calibration & applicability

Check source data, applicable environment and validity limits in the model record; saved defaults are not experimental validation.

∑ Theory & assumptions

Halpin–Tsai · T700 / EP180 UD

One compatible homogenization model per Micro recipe. Separate recipes compare models; their predictions are not blended.

∑ Theory & assumptions

Virtual test · Fickian uptake calibration · D5229 · Moisture uptake calibration · teaching study

Homogeneous slab, initially dry, both faces held at equilibrium moisture. Fits diffusivity from two early uptake measurements (both ≤50% saturation) using the square-root-time approximation. Edge ingress and temperature dependence are excluded. Does not overwrite material properties.

Linked laminate reference state

Ply stiffness, thickness and orientation come from the linked laminate. Other thermal or structural analyses must be run separately.

Calibration & study controls

Teaching example

Equilibrium mass gain: 1 percent

Measurement time 1: 1 h

Mass gain 1: 0.05 percent

Measurement time 2: 4 h

Mass gain 2: 0.1 percent

Conditioning duration: 100 h

∑ Theory & assumptions

Data travelling between blocks

Micro → Laminates
Predicted ply stiffness, strength, density and expansion properties.

Materials → Micro
Constituent stiffness, strength, density and thermal / moisture properties.

Models → Materials
Model choices and calibrated parameters.

Mechanical → Simulation
SIMULATION selects this case and its analysis model; the case owns its applicable cycle and input references.

Laminates → Mechanical
Ply angles and thicknesses, stiffness, mass and ply properties.

Simulation → Optimization
Linked inputs and current-property response for candidate evaluation.

Open this exercise in SIMULATE · Model inputs and outputs

D5961 Bearing / bypass screening

Single-pin nominal bearing, net-section and shear-out checks with independent measured allowables. Bypass tension is added to net-section load only. No contact, bolt preload, load redistribution or validated bearing–bypass interaction envelope.

Equations, inputs and interpretation

$\sigma_{bearing} = P/(dt)$; $\sigma_{net} = (P + P_{bypass})/[(w - d)t]$; $\tau_{out} = P/[2(e - d/2)t]$.

e is the hole-center distance to the loaded free edge. Each nominal stress is compared with its own measured allowable. Bypass tension contributes to the net-section load. These independent ratios are not a validated bearing–bypass interaction surface. Bolt preload, contact, friction, multi-fastener load sharing and progressive damage require further modeling.

- Specimen width (mm)
- Hole diameter (mm)
- Edge distance (mm)
- Pin force (N)
- Bypass tensile force (N)
- Bearing allowable (MPa)
- Net tensile allowable (MPa)
- Shear-out allowable (MPa)

ASTM composite standards catalog

Connected workflow

Two-row simulation workflow · **Open full-size map**
Linked-input preview, not solved results. Gray blocks are not configured.

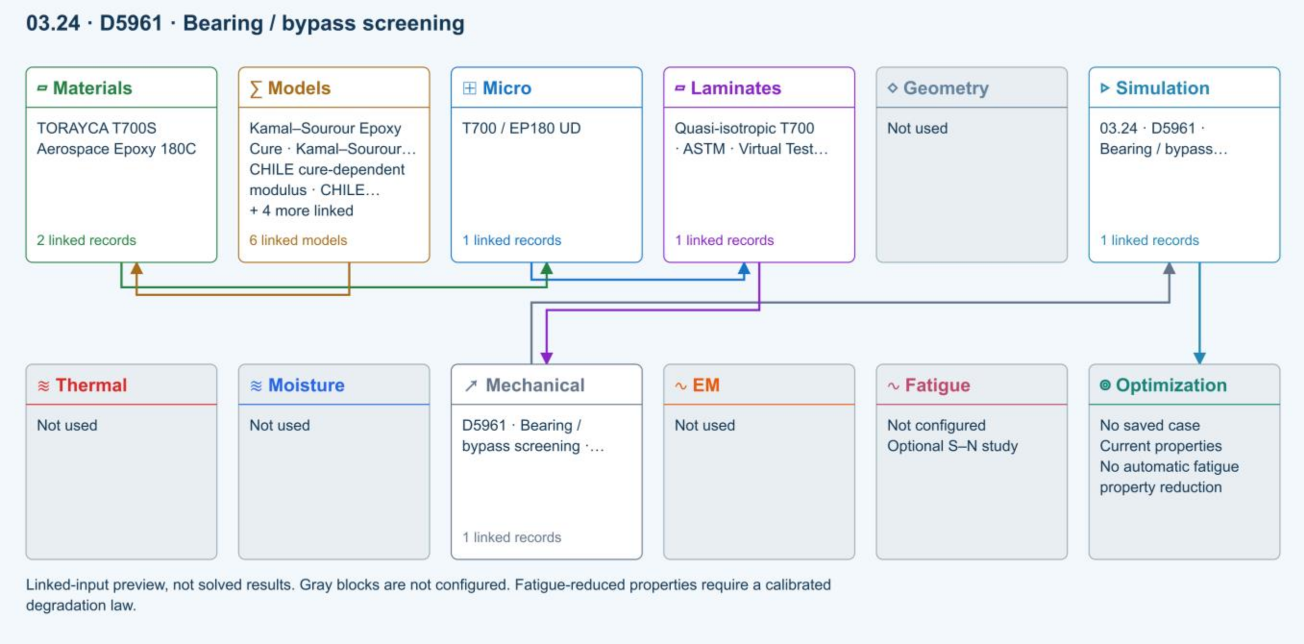

∑ Selected models & submodels

These are the exercise's linked choices, not solved results. Open a first-layer model to see its submodels and scope.

Kamal–Sourour autocatalytic · Kamal–Sourour Epoxy Cure

Reusable material model. It contributes only when assigned to a material used by this simulation; separate model records can supply independent properties.

Calibration & applicability

Illustrative model defaults — replace with characterized resin kinetics

∑ Theory & assumptions

CHILE (degree of cure) · CHILE cure-dependent modulus

Reusable material model. It contributes only when assigned to a material used by this simulation; separate model records can supply independent properties. Cure-dependent modulus does not automatically scale strength allowables.

Calibration & applicability

CHILE(α), section 2.4 of Materials 2019, 12, 259. Example parameters, not measured EP180 data. Fixed Poisson ratio; no viscoelastic relaxation or Tg softening. Incremental elastic stress integration at saved process intervals: check time-step convergence. Strength allowables are independent measured inputs, not scaled with modulus.

∑ Theory & assumptions

Temperature-dependent tabular · Temperature-dependent Thermal

Reusable material model. It contributes only when assigned to a material used by this simulation; separate model records can supply independent properties. Micro uses the 23 °C reference; Process evaluates the same table at local temperature, without extrapolation.

Calibration & applicability

Check source data, applicable environment and validity limits in the model record; saved defaults are not experimental validation.

∑ Theory & assumptions

1D Fickian diffusion · Layered Fickian Diffusion

Reusable material model. It contributes only when assigned to a material used by this simulation; separate model records can supply independent properties.

Calibration & applicability

Check source data, applicable environment and validity limits in the model record; saved defaults are not experimental validation.

∑ Theory & assumptions

Halpin–Tsai · T700 / EP180 UD

One compatible homogenization model per Micro recipe. Separate recipes compare models; their predictions are not blended.

∑ Theory & assumptions

Virtual test · bearing bypass screening · D5961 · Bearing / bypass screening · teaching study

Single-pin nominal bearing, net-section and shear-out checks with independent measured allowables. Bypass tension is added to net-section load only. No contact, bolt preload, load redistribution or validated bearing–bypass interaction envelope.

Linked laminate reference state

Ply stiffness, thickness and orientation come from the linked laminate. Other thermal or structural analyses must be run separately.

Calibration & study controls

Teaching example

Specimen width: 36 mm

Hole diameter: 6 mm

Edge distance: 18 mm

Hole center to loaded free edge.

Pin force: 1000 N

Bypass tensile force: 500 N

Bearing allowable: 300 MPa

Net tensile allowable: 400 MPa

Shear-out allowable: 80 MPa

∑ Theory & assumptions

Data travelling between blocks

Micro → Laminates
Predicted ply stiffness, strength, density and expansion properties.

Materials → Micro
Constituent stiffness, strength, density and thermal / moisture properties.

Models → Materials
Model choices and calibrated parameters.

Mechanical → Simulation
SIMULATION selects this case and its analysis model; the case owns its applicable cycle and input references.

Laminates → Mechanical
Ply angles and thicknesses, stiffness, mass and ply properties.

Simulation → Optimization
Linked inputs and current-property response for candidate evaluation.

Open this exercise in SIMULATE · Model inputs and outputs

D6484 Open-hole compression

Nominal gross/net stress and demand relative to measured open-hole compressive strength for this geometry and layup. This is test-data screening, not an uncalibrated notch-strength prediction. No local buckling or kink-band simulation.

Equations, inputs and interpretation

$\sigma_{gross} = P/(wt)$; $\sigma_{net} = P/[(w - d)t]$; demand = σ_{gross}/X_{OHC}.

X_{OHC} is the measured gross-section compressive strength for this layup and hole geometry. Do not compare net stress with a gross-section allowable. This assessment does not reuse the Whitney–Nuismer tension model or predict compressive notch strength.

- Specimen width (mm)
- Hole diameter (mm)
- Applied force (N)
- Measured open-hole compressive strength (MPa)

ASTM composite standards catalog

Connected workflow

Two-row simulation workflow · **Open full-size map**
Linked-input preview, not solved results. Gray blocks are not configured.

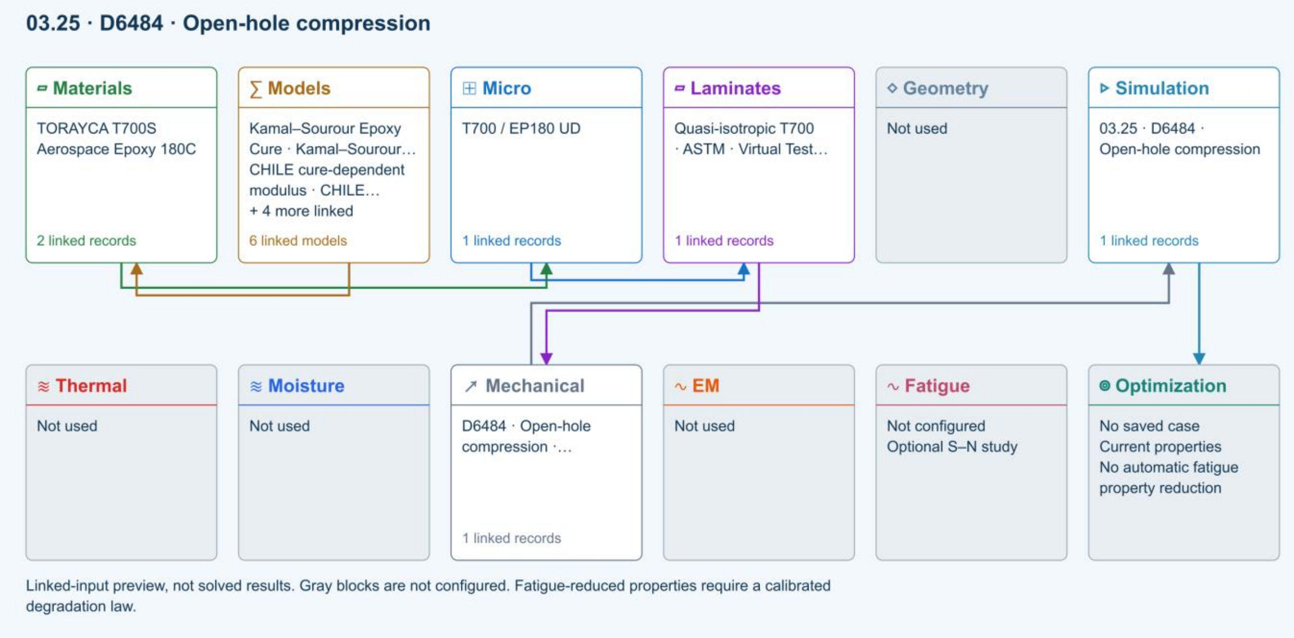

∑ Selected models & submodels

These are the exercise's linked choices, not solved results. Open a first-layer model to see its submodels and scope.

Kamal–Sourour autocatalytic · Kamal–Sourour Epoxy Cure

Reusable material model. It contributes only when assigned to a material used by this simulation; separate model records can supply independent properties.

Calibration & applicability

Illustrative model defaults — replace with characterized resin kinetics

∑ Theory & assumptions

CHILE (degree of cure) · CHILE cure-dependent modulus

Reusable material model. It contributes only when assigned to a material used by this simulation; separate model records can supply independent properties. Cure-dependent modulus does not automatically scale strength allowables.

Calibration & applicability

CHILE(α), section 2.4 of Materials 2019, 12, 259. Example parameters, not measured EP180 data. Fixed Poisson ratio; no viscoelastic relaxation or Tg softening. Incremental elastic stress integration at saved process intervals: check time-step convergence. Strength allowables are independent measured inputs, not scaled with modulus.

∑ Theory & assumptions

Temperature-dependent tabular · Temperature-dependent Thermal

Reusable material model. It contributes only when assigned to a material used by this simulation; separate model records can supply independent properties. Micro uses the 23 °C reference; Process evaluates the same table at local temperature, without extrapolation.

Calibration & applicability

Check source data, applicable environment and validity limits in the model record; saved defaults are not experimental validation.

∑ Theory & assumptions

1D Fickian diffusion · Layered Fickian Diffusion

Reusable material model. It contributes only when assigned to a material used by this simulation; separate model records can supply independent properties.

Calibration & applicability

Check source data, applicable environment and validity limits in the model record; saved defaults are not experimental validation.

∑ Theory & assumptions

Halpin–Tsai · T700 / EP180 UD

One compatible homogenization model per Micro recipe. Separate recipes compare models; their predictions are not blended.

∑ Theory & assumptions

Virtual test · measured open-hole compression · D6484 · Open-hole compression · teaching study

Nominal gross/net stress and demand relative to measured open-hole compressive strength for this geometry and layup. This is test-data screening, not an uncalibrated notch-strength prediction. No local buckling or kink-band simulation.

Linked laminate reference state

Ply stiffness, thickness and orientation come from the linked laminate. Other thermal or structural analyses must be run separately.

Calibration & study controls

Teaching example

Specimen width: 36 mm

Hole diameter: 6 mm

Applied force: 1000 N

Measured open-hole compressive strength: 250 MPa

∑ Theory & assumptions

Data travelling between blocks

Micro → Laminates
Predicted ply stiffness, strength, density and expansion properties.

Materials → Micro
Constituent stiffness, strength, density and thermal / moisture properties.

Models → Materials
Model choices and calibrated parameters.

Mechanical → Simulation
SIMULATION selects this case and its analysis model; the case owns its applicable cycle and input references.

Laminates → Mechanical
Ply angles and thicknesses, stiffness, mass and ply properties.

Simulation → Optimization
Linked inputs and current-property response for candidate evaluation.

Open this exercise in SIMULATE · Model inputs and outputs

D6742 Filled-hole comparison

Compares user-measured open- and filled-hole compressive strengths using gross-section stress. Use matched layup, hole, environment and fastener condition. Filling a hole does not automatically recover strength; no fastener contact/preload model is applied.

Equations, inputs and interpretation

Demandopen = σgross/XOHC; Demandfilled = σgross/XFHC.

Compare matched measured open- and filled-hole compressive strengths. Pin fit, preload, environment and geometry must match the calibration basis. Filling the hole is not assumed to restore strength, and the curves show nominal demand scaling rather than predicted damage or load–deflection.

- Specimen width (mm)
- Hole diameter (mm)
- Applied force (N)
- Measured open-hole compressive strength (MPa)
- Measured filled-hole compressive strength (MPa)

ASTM composite standards catalog

Connected workflow

Two-row simulation workflow · **Open full-size map**
Linked-input preview, not solved results. Gray blocks are not configured.

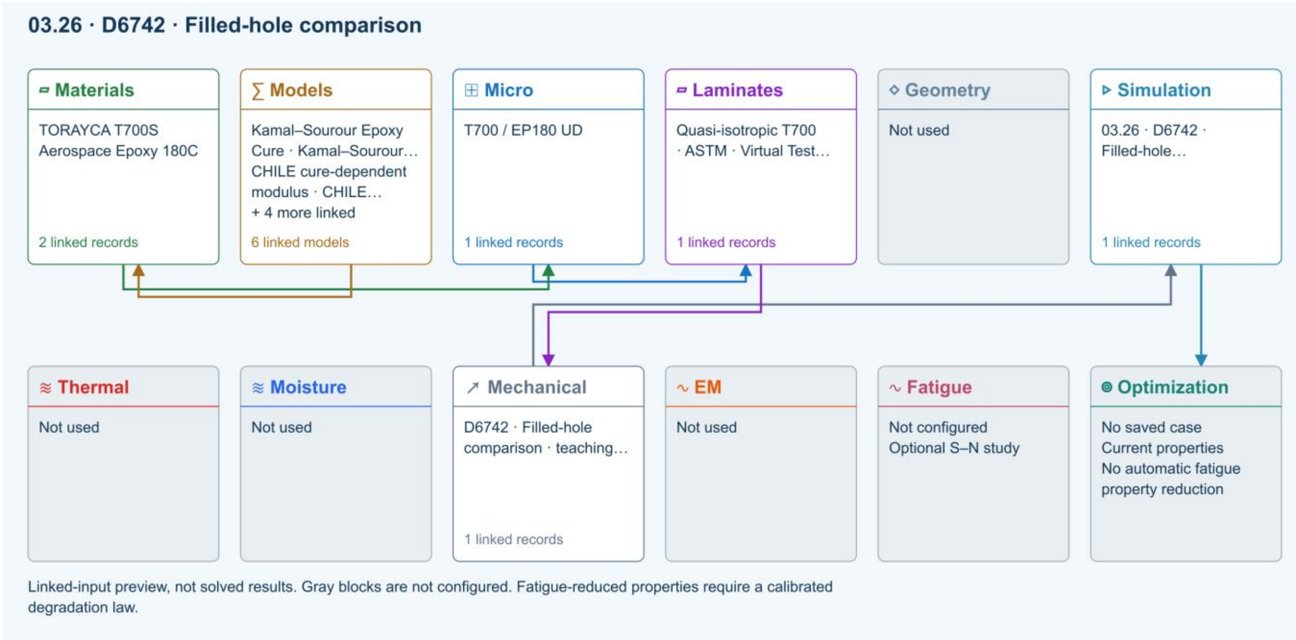

∑ Selected models & submodels

These are the exercise's linked choices, not solved results. Open a first-layer model to see its submodels and scope.

Kamal–Sourour autocatalytic · Kamal–Sourour Epoxy Cure

Reusable material model. It contributes only when assigned to a material used by this simulation; separate model records can supply independent properties.

Calibration & applicability

Illustrative model defaults — replace with characterized resin kinetics

∑ Theory & assumptions

CHILE (degree of cure) · CHILE cure-dependent modulus

Reusable material model. It contributes only when assigned to a material used by this simulation; separate model records can supply independent properties. Cure-dependent modulus does not automatically scale strength allowables.

Calibration & applicability

CHILE(α), section 2.4 of Materials 2019, 12, 259. Example parameters, not measured EP180 data. Fixed Poisson ratio; no viscoelastic relaxation or Tg softening. Incremental elastic stress integration at saved process intervals: check time-step convergence. Strength allowables are independent measured inputs, not scaled with modulus.

∑ Theory & assumptions

Temperature-dependent tabular · Temperature-dependent Thermal

Reusable material model. It contributes only when assigned to a material used by this simulation; separate model records can supply independent properties. Micro uses the 23 °C reference; Process evaluates the same table at local temperature, without extrapolation.

Calibration & applicability

Check source data, applicable environment and validity limits in the model record; saved defaults are not experimental validation.

∑ Theory & assumptions

1D Fickian diffusion · Layered Fickian Diffusion

Reusable material model. It contributes only when assigned to a material used by this simulation; separate model records can supply independent properties.

Calibration & applicability

Check source data, applicable environment and validity limits in the model record; saved defaults are not experimental validation.

∑ Theory & assumptions

Halpin–Tsai · T700 / EP180 UD

One compatible homogenization model per Micro recipe. Separate recipes compare models; their predictions are not blended.

∑ Theory & assumptions

Virtual test · measured filled-hole comparison · D6742 · Filled-hole comparison · teaching study

Compares user-measured open- and filled-hole compressive strengths using gross-section stress. Use matched layup, hole, environment and fastener condition. Filling a hole does not automatically recover strength; no fastener contact/preload model is applied.

Linked laminate reference state

Ply stiffness, thickness and orientation come from the linked laminate. Other thermal or structural analyses must be run separately.

Calibration & study controls

Teaching example

Specimen width: 36 mm

Hole diameter: 6 mm

Applied force: 1000 N

Measured open-hole compressive strength: 250 MPa

Measured filled-hole compressive strength: 300 MPa

∑ Theory & assumptions

Data travelling between blocks

Micro → Laminates
Predicted ply stiffness, strength, density and expansion properties.

Materials → Micro
Constituent stiffness, strength, density and thermal / moisture properties.

Models → Materials
Model choices and calibrated parameters.

Mechanical → Simulation
SIMULATION selects this case and its analysis model; the case owns its applicable cycle and input references.

Laminates → Mechanical
Ply angles and thicknesses, stiffness, mass and ply properties.

Simulation → Optimization
Linked inputs and current-property response for candidate evaluation.

Open this exercise in SIMULATE · Model inputs and outputs

D7136 / D7137 Impact CAI assessment

Incident energy from measured impact velocity; residual compressive strength from measured peak CAI force. Rebound energy estimates energy not returned to the striker, NOT damage energy. No impact/contact solver, damage-area prediction or energy-to-strength extrapolation.

Equations, inputs and interpretation

Eincident = $mv^2/2$; Erebound = $mvr^2/2$; XCAI = Ppeak/(wt).

Enter measured impact and rebound velocities, measured CAI peak force and pristine compressive strength. Energy not returned to the striker includes mechanisms other than damage. The strength-retention ratio is a measured comparison, not an energy-to-strength prediction. No synthetic impact pulse, damage footprint or full-wave impact solution is generated.

- Impactor mass (kg)
- Impact speed (m/s)
- Rebound speed (m/s)
- Specimen width (mm)
- Measured CAI peak force (N)
- Measured pristine compressive strength (MPa)

ASTM composite standards catalog

Connected workflow

Two-row simulation workflow · **Open full-size map**
Linked-input preview, not solved results. Gray blocks are not configured.

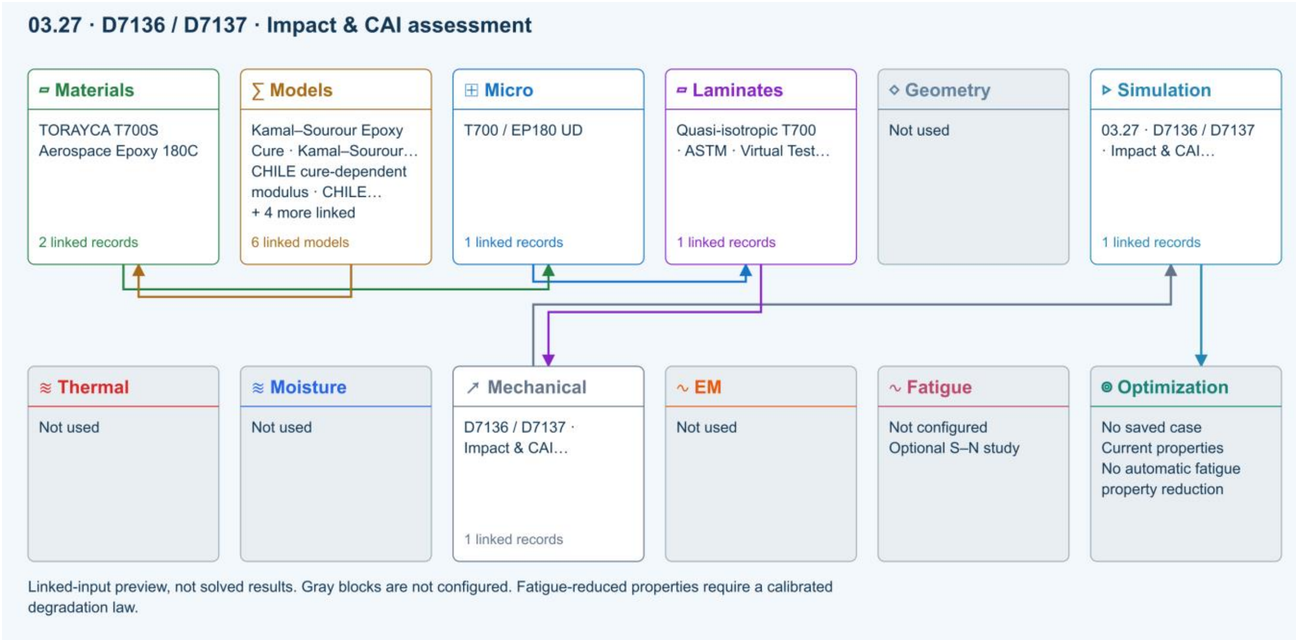

∑ Selected models & submodels

These are the exercise's linked choices, not solved results. Open a first-layer model to see its submodels and scope.

Kamal–Sourour autocatalytic · Kamal–Sourour Epoxy Cure

Reusable material model. It contributes only when assigned to a material used by this simulation; separate model records can supply independent properties.

Calibration & applicability

Illustrative model defaults — replace with characterized resin kinetics

∑ Theory & assumptions

CHILE (degree of cure) · CHILE cure-dependent modulus

Reusable material model. It contributes only when assigned to a material used by this simulation; separate model records can supply independent properties. Cure-dependent modulus does not automatically scale strength allowables.

Calibration & applicability

CHILE(α), section 2.4 of Materials 2019, 12, 259. Example parameters, not measured EP180 data. Fixed Poisson ratio; no viscoelastic relaxation or Tg softening. Incremental elastic stress integration at saved process intervals: check time-step convergence. Strength allowables are independent measured inputs, not scaled with modulus.

∑ Theory & assumptions

Temperature-dependent tabular · Temperature-dependent Thermal

Reusable material model. It contributes only when assigned to a material used by this simulation; separate model records can supply independent properties. Micro uses the 23 °C reference; Process evaluates the same table at local temperature, without extrapolation.

Calibration & applicability

Check source data, applicable environment and validity limits in the model record; saved defaults are not experimental validation.

∑ Theory & assumptions

1D Fickian diffusion · Layered Fickian Diffusion

Reusable material model. It contributes only when assigned to a material used by this simulation; separate model records can supply independent properties.

Calibration & applicability

Check source data, applicable environment and validity limits in the model record; saved defaults are not experimental validation.

∑ Theory & assumptions

Halpin–Tsai · T700 / EP180 UD

One compatible homogenization model per Micro recipe. Separate recipes compare models; their predictions are not blended.

∑ Theory & assumptions

Virtual test · measured impact and CAI · D7136 / D7137 · Impact & CAI assessment · teaching study

Incident energy from measured impact velocity; residual compressive strength from measured peak CAI force. Rebound energy estimates energy not returned to the striker, NOT damage energy. No impact/contact solver, damage-area prediction or energy-to-strength extrapolation.

Linked laminate reference state

Ply stiffness, thickness and orientation come from the linked laminate. Other thermal or structural analyses must be run separately.

Calibration & study controls

Teaching example

Impactor mass: 5 kg

Impact speed: 2 m/s

Rebound speed: 0.5 m/s

Specimen width: 100 mm

Measured CAI peak force: 30000 N

Measured pristine compressive strength: 400 MPa

∑ Theory & assumptions

Data travelling between blocks

Micro → Laminates
Predicted ply stiffness, strength, density and expansion properties.

Materials → Micro
Constituent stiffness, strength, density and thermal / moisture properties.

Models → Materials
Model choices and calibrated parameters.

Mechanical → Simulation
SIMULATION selects this case and its analysis model; the case owns its applicable cycle and input references.

Laminates → Mechanical
Ply angles and thicknesses, stiffness, mass and ply properties.

Simulation → Optimization
Linked inputs and current-property response for candidate evaluation.

Open this exercise in SIMULATE · Model inputs and outputs

What comes next

Full impact/contact/damage prediction, fixture-resolved compression and shear, experimental compliance corrections, crack-growth validation and bearing–bypass interaction calibration remain separate development and validation work. This release does not claim those capabilities.

Workbench availability: released models, inputs and compatible study paths . The wider theory library includes reference formulations not available in every Workbench solve.

27 Elastic Micromechanics Theory

Online chapter

Table of Contents

1 Preface

2 Abstract

A compact elastic micromechanics framework is described for predicting the effective orthotropic stiffness of continuous fiber, discontinuous fiber, woven, filler-reinforced, and general multiphase composite materials. The model permits selection among four main homogenization branches: rule of mixtures, Halpin–Tsai, Mori–Tanaka engineering approximation, and a self-consistent engineering approximation. Constituent properties are supplied through Workbench vector inputs, while microstructure descriptors are supplied through scalar flags and scalar parameters. Fiber architecture effects are represented using fiber volume fraction, aspect ratio, and Tsu-Wei Chou axial and planar architecture parameters, denoted F_a and F_p. The model outputs effective Young's moduli, shear moduli, Poisson ratios, and related quantities for use in subsequent laminate and structural studies.

3 Nomenclature

Symbol	Definition	Units
E_1, E_2, E_3	Effective orthotropic Young's moduli	Pa
G_{12}, G_{13}, G_{23}	Effective orthotropic shear moduli	Pa
$\nu_{12}, \nu_{13}, \nu_{23}$	Effective major Poisson ratios	–
V_f, V_m, V_p, V_v	Fiber, matrix, particle/filler, and void volume fractions	–
E_f, E_m, E_p	Fiber, matrix, and particle moduli	Pa
G_f, G_m, G_p	Fiber, matrix, and particle shear moduli	Pa
AR	Fiber or inclusion aspect ratio, usually l/d	–
η_L	Fiber length efficiency factor	–
η_O	Orientation efficiency factor	–
F_a	Chou axial architecture factor	–

Symbol	Definition	Units
F_p	Chou planar/random architecture factor	–
ξ	Halpin–Tsai shape parameter	–
η	Halpin–Tsai contrast parameter	–
$\mathbf{C}$	Stiffness matrix or fourth-order stiffness tensor	Pa
$\mathbf{S}$	Compliance matrix or Eshelby tensor depending on context	Pa^{-1} or –
$\mathbf{A}$	Strain concentration tensor or matrix	–
$\overline{\boldsymbol{\sigma}}$	Macroscopic stress	Pa
$\overline{\boldsymbol{\varepsilon}}$	Macroscopic strain	–
θ	Global material orientation angle	deg

4 1 Model Scope

The solver model predicts effective properties of composite materials from constituent properties and architecture descriptors. The main elastic outputs are the orthotropic engineering constants

$$\{E_1, E_2, E_3, G_{12}, G_{13}, G_{23}, \nu_{12}, \nu_{13}, \nu_{23}\}.$$

These properties are used to generate Abaqus material definitions. Choose from the following stiffness models:

Model branch
Rule of mixtures
Halpin–Tsai
Mori–Tanaka engineering approximation
Self-consistent engineering approximation

Choose the material architecture independently of the stiffness model:

Architecture branch
Continuous unidirectional fiber composite
Discontinuous fiber composite

Architecture branch
Woven fabric composite
General multiphase composite

This separation allows, for example, a discontinuous-fiber material to be evaluated using a simple rule-of-mixtures approximation or a more interaction-aware self-consistent approximation.

5 2 Constituent Property Inputs

Specify the properties of each constituent. The fiber property vector contains anisotropic stiffnesses, strengths, density, and thermophysical values. In Volume I only the elastic terms are required:

$$\mathbf{x}_f = \left[E_{f1}, E_{f2}, E_{f3}, G_{f12}, G_{f13}, G_{f23}, \nu_{f12}, \nu_{f13}, \nu_{f23}, \rho_f, \ldots\right]^T.$$

The matrix vector contains isotropic elastic properties,

$$\mathbf{x}_m = [E_m, \nu_m, \rho_m, \ldots]^T,$$

and the filler vector contains particle properties,

$$\mathbf{x}_p = \left[E_p, \nu_p, \rho_p, AR_p, \ldots\right]^T.$$

The matrix shear modulus is computed from isotropic elasticity:

$$G_m = \frac{E_m}{2(1+\nu_m)}.$$

Similarly, for an isotropic particle phase,

$$G_p = \frac{E_p}{2\left(1+\nu_p\right)}.$$

6 3 Constituent Stiffness and Compliance

$$\boldsymbol{\sigma}^{(r)} = \mathbf{C}^{(r)}\boldsymbol{\varepsilon}^{(r)},$$

where r denotes the phase. For an isotropic phase, the stiffness tensor is

$$C_{ijkl} = \lambda\delta_{ij}\delta_{kl} + \mu\left(\delta_{ik}\delta_{jl}+\delta_{il}\delta_{jk}\right),$$

with

$$\mu = \frac{E}{2(1+\nu)}, \qquad \lambda = \frac{E\nu}{(1+\nu)(1-2\nu)}.$$

For an orthotropic fiber, the compliance matrix in material coordinates is conventionally written as

$$\mathbf{S}_f = \begin{bmatrix} 1/E_{f1} & -\nu_{f12}/E_{f1} & -\nu_{f13}/E_{f1} & 0 & 0 & 0 \\ -\nu_{f21}/E_{f2} & 1/E_{f2} & -\nu_{f23}/E_{f2} & 0 & 0 & 0 \\ -\nu_{f31}/E_{f3} & -\nu_{f32}/E_{f3} & 1/E_{f3} & 0 & 0 & 0 \\ 0 & 0 & 0 & 1/G_{f23} & 0 & 0 \\ 0 & 0 & 0 & 0 & 1/G_{f13} & 0 \\ 0 & 0 & 0 & 0 & 0 & 1/G_{f12} \end{bmatrix}.$$

The reciprocal Poisson ratios satisfy

$$\frac{\nu_{ij}}{E_i} = \frac{\nu_{ji}}{E_j}.$$

The stiffness matrix is obtained by inversion:

$$\mathbf{C}_f = \mathbf{S}_f^{-1}.$$

7 4 Volume Fractions and Phase Normalization

The model normalizes phase volume fractions so that

$$V_f + V_m + V_p + V_v = 1,$$

where V_v is the optional void volume fraction. If the filler is treated implicitly, the matrix is first modified and the explicit particle phase is set to zero. If the filler is treated explicitly, the global particle fraction is estimated from the filler fraction inside the resin phase:

$$V_p = V_{p|resin}\left(1 - V_f - V_v\right).$$

The remaining matrix fraction is then

$$V_m = 1 - V_f - V_p - V_v.$$

This normalization is important because all mixture and mean-field equations assume that the phase fractions sum to unity.

8 5 Implicit Filled Matrix Model

Before fiber/matrix homogenization, a filler can be used to modify the matrix modulus. The current script uses a Halpin–Tsai style spherical-particle correction. The effective filled matrix modulus is

$$E_m^* = E_m \frac{1 + 2\eta_E V_{p|resin}}{1 - \eta_E V_{p|resin}},$$

where

$$\eta_E = \frac{E_p/E_m - 1}{E_p/E_m + 2}.$$

The filled matrix shear modulus is

$$G_m^* = G_m \frac{1 + 2\eta_G V_{p|resin}}{1 - \eta_G V_{p|resin}},$$

with

$$\eta_G = \frac{G_p/G_m - 1}{G_p/G_m + 2}.$$

A consistent effective Poisson ratio is recovered by

$$\nu_m^* = \frac{E_m^*}{2G_m^*} - 1.$$

This option is computationally efficient and appropriate when filler is treated as a matrix modifier rather than as a separate interacting phase.

9 6 Rule of Mixtures

The rule-of-mixtures model is the simplest model and is retained as a bounding and verification option. In the fiber direction, the iso-strain assumption gives

$$\varepsilon_f = \varepsilon_m = \overline{\varepsilon}.$$

The phase-averaged stress is

$$\overline{\sigma} = V_f \sigma_f + V_m \sigma_m.$$

Substituting phase constitutive laws yields the Voigt axial modulus

$$E_1 = V_f E_{f1} + (1 - V_f) E_m.$$

For transverse loading, the inverse or Reuss estimate is used:

$$\frac{1}{E_2} = \frac{V_f}{E_{f2}} + \frac{1 - V_f}{E_m}.$$

Similarly,

$$\frac{1}{E_3} = \frac{V_f}{E_{f3}} + \frac{1 - V_f}{E_m}.$$

The shear moduli are estimated using inverse mixtures:

$$\frac{1}{G_{12}} = \frac{V_f}{G_{f12}} + \frac{1 - V_f}{G_m},$$

$$\frac{1}{G_{13}} = \frac{V_f}{G_{f13}} + \frac{1 - V_f}{G_m},$$

and

$$\frac{1}{G_{23}} = \frac{V_f}{G_{f23}} + \frac{1 - V_f}{G_m}.$$

The major Poisson ratios are computed by direct mixture:

$$\nu_{12} = V_f \nu_{f12} + (1 - V_f) \nu_m.$$

The same form is used for ν_{13} and ν_{23}. The rule-of-mixtures option is not intended to capture inclusion interaction, but it provides a transparent reference case and useful numerical sanity check.

10 7 Halpin Tsai Model

The Halpin–Tsai model provides a semi-empirical correction for reinforcement geometry and phase contrast. For a generic engineering modulus M, the Halpin–Tsai form is

$$M = M_m \frac{1 + \xi \eta V_f}{1 - \eta V_f},$$

where

$$\eta = \frac{M_f/M_m - 1}{M_f/M_m + \xi}.$$

For transverse Young's modulus, the code uses the common circular-fiber estimate

$$\xi_E \approx 2,$$

so that

$$E_2 = E_m \frac{1 + \xi_E \eta_{E2} V_f}{1 - \eta_{E2} V_f},$$

with

$$\eta_{E2} = \frac{E_{f2}/E_m - 1}{E_{f2}/E_m + \xi_E}.$$

The third-direction modulus is treated analogously:

$$E_3 = E_m \frac{1 + \xi_E \eta_{E3} V_f}{1 - \eta_{E3} V_f}.$$

The shear moduli are estimated using

$$G_{12} = G_m \frac{1 + \xi_G \eta_{G12} V_f}{1 - \eta_{G12} V_f},$$

where

$$\eta_{G12} = \frac{G_{f12}/G_m - 1}{G_{f12}/G_m + \xi_G}.$$

The code uses $\xi_G \approx 1$ as a default engineering estimate. The same equation form is applied to G_{13} and G_{23}. Halpin–Tsai is more physically representative than rule of mixtures for transverse and shear properties, but the parameter ξ is empirical and should be calibrated when reliable data are available.

11 8 Mori Tanaka Mean-Field Theory

The classical Mori–Tanaka method is based on an inclusion phase embedded in a matrix reference medium. In compact tensor notation, the inclusion strain concentration tensor is

$$\mathbf{A}_f = \left[\mathbf{I} + \mathbf{S}: \mathbf{C}_m^{-1}: \left(\mathbf{C}_f - \mathbf{C}_m\right)\right]^{-1},$$

where **S** is the Eshelby tensor. The Mori–Tanaka stiffness is commonly written as

$$\mathbf{C}^{MT} = \mathbf{C}_m + V_f\left(\mathbf{C}_f - \mathbf{C}_m\right)\mathbf{A}_f\left[V_m \mathbf{I} + V_f \mathbf{A}_f\right]^{-1}.$$

For multiple inclusion phases, a normalized mean-field form may be written as

$$\mathbf{C}^{MT} = \left(\sum_r V_r\, \mathbf{C}_r \mathbf{A}_r\right)\left(\sum_r V_r\, \mathbf{A}_r\right)^{-1}.$$

$$E_1^{MT} = E_m + \eta_L \eta_O V_f \left(E_{f1} - E_m\right) \Phi_{MT},$$

where Φ_{MT} is an interaction factor depending on V_f and stiffness contrast. The implemented form is an engineering approximation to the interaction behavior of a mean-field model:

$$\Phi_{MT} = \frac{1}{1 + 0.15 V_f \left(E_{f1}/E_m\right)^{0.25}}.$$

The transverse and shear terms are based on Halpin–Tsai values with a small aspect-ratio-dependent correction. The aspect ratio factor is

$$\chi_{AR} = \frac{AR}{AR + 5}.$$

A representative transverse correction is

$$E_2^{MT} = E_2^{HT}\left(1 + 0.05 \chi_{AR} V_f\right).$$

The Mori–Tanaka option should therefore be interpreted as a computationally robust engineering approximation to mean-field behavior rather than a complete fourth-order tensor Mori–Tanaka implementation.

12 9 Self-Consistent Field Theory and Implemented Approximation

In the full self-consistent theory, each phase is embedded in the unknown effective medium instead of in the matrix. The governing consistency equation is

$$\sum_{r=1}^{N_p} V_r \left(\mathbf{C}_r - \mathbf{C}^{SC}\right) : \mathbf{A}_r = \mathbf{0}.$$

The phase concentration tensor is

$$\mathbf{A}_r = \left[\mathbf{I} + \mathbf{S}_r : \left(\mathbf{C}^{SC}\right)^{-1} : \left(\mathbf{C}_r - \mathbf{C}^{SC}\right)\right]^{-1}.$$

A fixed-point update form is

$$\mathbf{C}^{SC} = \left(\sum_r V_r\, \mathbf{C}_r \mathbf{A}_r\right)\left(\sum_r V_r\, \mathbf{A}_r\right)^{-1}.$$

$$E_1^{SC} = E_m + \eta_L \eta_O V_f \left(E_{f1} - E_m\right) \Phi_{SC},$$

with

$$\Phi_{SC} = \frac{1}{1 + 0.08 V_f \left(E_{f1}/E_m\right)^{0.20}}.$$

The transverse moduli are blended from Halpin–Tsai and a stiffness-interaction term:

$$E_2^{SC} = \frac{1}{2}\left(E_2^{HT} + 0.18\sqrt{E_2^{HT} E_1^{SC}}\right),$$

$$E_3^{SC} = \frac{1}{2}\left(E_3^{HT} + 0.18\sqrt{E_3^{HT} E_1^{SC}}\right).$$

The shear moduli use analogous blended expressions:

$$G_{12}^{SC} = \frac{1}{2}\left(G_{12}^{HT} + 0.09\sqrt{G_{12}^{HT} E_1^{SC}}\right),$$

and similarly for G_{13}^{SC}. This form is designed to remain stable in Workbench while providing a stronger interaction correction than the pure Halpin–Tsai model.

13 10 Continuous Fiber Composite Model

For continuous fibers, the length efficiency is set to unity:

$$\eta_L = 1.$$

The axial orientation factor is forced close to the aligned limit:

$$\eta_O \approx 1.$$

For continuous aligned fibers, the axial modulus approaches the Voigt expression

$$E_1 \rightarrow V_f E_{f1} + (1 - V_f) E_m.$$

However, the transverse and shear properties are still computed from the selected micromechanics branch. This distinction is important: even when the axial response is mixture-like, the transverse stiffness and shear stiffness remain controlled by matrix constraint, fiber packing, and phase interaction. The continuous fiber branch is appropriate for unidirectional prepreg laminae, pultruded rods, filament-wound laminae, and tow-level properties in woven fabrics.

14 11 Discontinuous Fiber Composite Model

Web r17 implementation note. This section describes the compact elastic architecture-efficiency path. The unified solver's criterion-6 tensile branch implements the complete Henry and Pimenta (2017) event-driven workflow: reconstructed broken/shear-lag interaction segments, a generic nonlinear matrix shear law, ordered Weibull breaks, same-strain network rebuilding, RVE series coupling, pull-out resistance, and nonlinear critical-cluster termination. See the aligned discontinuous-fiber theory and traceability page .

In short-fiber composites, a fiber does not generally reach the full far-field axial stress because stress must build up through matrix-to-fiber shear transfer. The model uses a compact length efficiency factor

$$\eta_L = \frac{AR}{AR + 2},$$

where

$$AR = \frac{l}{d}.$$

This expression has the correct limits:

$$\eta_L \to 0 \quad \text{as} \quad AR \to 0,$$

and

$$\eta_L \to 1 \quad \text{as} \quad AR \to \infty.$$

The axial contribution of short fibers is then reduced by length and orientation factors:

$$E_1 = E_m + \eta_L \eta_O V_f \left(E_{f1} - E_m\right).$$

The implemented code uses the Chou axial factor F_a as the default orientation efficiency:

$$\eta_O = F_a.$$

The transverse moduli are modified by a planar/random architecture correction. A representative engineering correction is

$$E_2^{short} = E_2\left(1 - 0.25F_a + 0.25F_p\right),$$

with a similar expression for E_3. This correction reduces directional stiffness when fibers are less aligned and redistributes stiffness into planar directions as the random component increases.

15 12 Tsu-Wei Chou Architecture Factors

The model uses compact Chou-style architecture parameters to describe orientation effects without requiring the Workbench user to enter a full orientation tensor. The axial parameter F_a represents the fourth-order projection of fiber direction onto the primary material axis:

$$F_a = \langle cos^4\theta \rangle.$$

The planar or random contribution is represented as

$$F_p = 1 - F_a,$$

or as an independently supplied parameter when calibrated from data. The axial stiffness contribution is governed primarily by F_a:

$$\Delta E_1 \propto F_a V_f \left(E_f - E_m\right).$$

A compact architecture-modified stiffness expression is

$$E_1^{arch} = E_m + \eta_L F_a V_f \left(E_{f1} - E_m\right).$$

For a perfectly aligned material,

$$F_a = 1, \qquad F_p = 0.$$

For planar random orientation, F_a is smaller and F_p is larger. For three-dimensional random orientation, the axial fourth-order projection is lower still. The F_a, F_p representation is less general than a full second- and fourth-order orientation tensor, but it is much more compact and well suited for Workbench front-panel entry.

16 13 Orthotropic Engineering Constant Extraction

After the selected micromechanics branch and architecture corrections are applied, the model assembles effective engineering constants. The major Poisson ratios are estimated by direct mixture:

$$\nu_{12} = V_f \nu_{f12} + (1 - V_f)\nu_m,$$

$$\nu_{13} = V_f \nu_{f13} + (1 - V_f)\nu_m,$$

$$\nu_{23} = V_f \nu_{f23} + (1 - V_f)\nu_m.$$

The effective compliance matrix is then assembled as

$$\mathbf{S}^{eff} = \begin{bmatrix} 1/E_1 & -\nu_{12}/E_1 & -\nu_{13}/E_1 & 0 & 0 & 0 \\ -\nu_{12}/E_1 & 1/E_2 & -\nu_{23}/E_2 & 0 & 0 & 0 \\ -\nu_{13}/E_1 & -\nu_{23}/E_2 & 1/E_3 & 0 & 0 & 0 \\ 0 & 0 & 0 & 1/G_{23} & 0 & 0 \\ 0 & 0 & 0 & 0 & 1/G_{13} & 0 \\ 0 & 0 & 0 & 0 & 0 & 1/G_{12} \end{bmatrix}.$$

The stiffness matrix used for anisotropic Abaqus export is

$$\mathbf{C}^{eff} = \left(\mathbf{S}^{eff}\right)^{-1}.$$

When the positive-definite projection flag is enabled, the model applies lower bounds to moduli and regularizes ill-conditioned matrices to prevent nonphysical Abaqus material definitions.

17 14 Workflow Summary

- Parse material and architecture flags.
- Construct matrix, fiber, filler, and void phase properties.
- Apply implicit filled-matrix correction if required.
- Normalize all phase volume fractions.
- Choose the micromechanics model.
- Choose the material architecture.
- Compute baseline elastic constants.
- Apply discontinuous-fiber, Chou, or woven architecture corrections.
- Compute Poisson ratios and assemble the compliance matrix.
- Pass the dense property state through the thermophysical, void, damage, and failure branches documented in Volumes II and III.
- Apply the global constituent-limit recovery check to the final property state.
- Rebuild compliance, stiffness, finite-element properties, and material exports from the recovered state.
- Store results in Workbench scalar, vector, matrix, and selected-string outputs.

18 15 Constituent-Limit Recovery

Every homogenization branch is required to recover the exact active constituent at a pure-phase endpoint. This is an implementation verification condition as well as a physical consistency condition. If phase r is dominant within the selected tolerance, the final mechanical and thermophysical property vector is replaced by that phase vector:

$$\mathbf{P}^{final} = \mathbf{P}^{(r)} \quad \text{when} \quad V_r \geq 1 - \varepsilon.$$

The recovered vector includes the elastic constants, density, specific heat, directional conductivity, and directional CTE. Thus $V_f \to 1$ returns the fiber properties exactly; matrix- and filler-dominated limits recover their corresponding phase definitions. The void endpoint uses the defined void state.

Recovery is deliberately applied after homogenization, architecture, thermophysical, void, and damage/failure operations. Every dependent quantity is then regenerated: orthotropic and anisotropic stiffness and compliance matrices, effective properties, scalar diagnostics, Workbench FE matrices, and the selected material export. This ordering prevents a later correction from overwriting the endpoint state or an export from retaining stale pre-recovery values.

19 16 Applicability and Limitations

The current implementation is most appropriate for preliminary design, material screening, embedded Workbench workflows, and automated Abaqus material-card generation. It is not intended to replace detailed finite-element RVE homogenization when exact tow geometry, interphase behavior, nonlinear matrix response, or progressive damage evolution must be resolved explicitly.

20 References

Advani, S. G., and Tucker, C. L. III (1987). The use of tensors to describe and predict fiber orientation in short fiber composites. *Journal of Rheology*, 31, 751–784.

Benveniste, Y. (1987). A new approach to the application of Mori–Tanaka's theory in composite materials. *Mechanics of Materials*, 6, 147–157.

Budiansky, B. (1965). On the elastic moduli of some heterogeneous materials. *Journal of the Mechanics and Physics of Solids*, 13, 223–227.

Chou, T.-W., Nomura, S., and Taya, M. (1980). A self-consistent approach to the elastic stiffness of short-fiber composites. *Journal of Composite Materials*, 14, 178–188.

Christensen, R. M. (1979). *Mechanics of Composite Materials*. Wiley.

Cox, H. L. (1952). The elasticity and strength of paper and other fibrous materials. *British Journal of Applied Physics*, 3, 72–79.

Henry, J., and Pimenta, S. (2017). Semi-analytical simulation of aligned discontinuous composites. *Composites Science and Technology*, 144, 230–244. doi:10.1016/j.compscitech.2017.01.027 .

Eshelby, J. D. (1957). The determination of the elastic field of an ellipsoidal inclusion, and related problems. *Proceedings of the Royal Society of London A*, 241, 376–396.

Folgar, F., and Tucker, C. L. III (1984). Orientation behavior of fibers in concentrated suspensions. *Journal of Reinforced Plastics and Composites*, 3, 98–119.

Halpin, J. C., and Kardos, J. L. (1976). The Halpin–Tsai equations: A review. *Polymer Engineering and Science*, 16, 344–352.

Hill, R. (1965). A self-consistent mechanics of composite materials. *Journal of the Mechanics and Physics of Solids*, 13, 213–222.

Jones, R. M. (1999). *Mechanics of Composite Materials*, 2nd ed. Taylor & Francis.

Mori, T., and Tanaka, K. (1973). Average stress in matrix and average elastic energy of materials with misfitting inclusions. *Acta Metallurgica*, 21, 571–574.

Mura, T. (1987). *Micromechanics of Defects in Solids*, 2nd ed. Martinus Nijhoff.

Nemat-Nasser, S., and Hori, M. (1999). *Micromechanics: Overall Properties of Heterogeneous Materials*, 2nd ed. Elsevier.

Tandon, G. P., and Weng, G. J. (1984). The effect of aspect ratio of inclusions on the elastic properties of unidirectionally aligned composites. *Polymer Composites*, 5, 327–333.

28 Section 1 - Textile and Thermophysical Framework

Online chapter

Section 1 Textile and Thermophysical Framework

Volume II Textile and Thermophysical Micromechanics

Section 1 Introduction and Multiscale Framework

1 1 Purpose and Scope

Volume II documents the textile, hybrid, and thermophysical extensions of the Workbench micromechanics solver model. Volume I established the elastic micromechanics foundation for continuous and discontinuous fiber composites. The present volume extends that foundation to woven, braided, stitched, and non-crimp fabric architectures, and to the effective thermophysical properties needed for coupled thermal and structural finite-element simulations.

The model treats the composite as a hierarchy of homogenization problems. Constituent fibers, polymer matrix, particulate filler, and void phases are first assembled into local material descriptions. These local descriptions are then homogenized into tow properties, textile representative volume element properties, and finally orthotropic lamina properties suitable for Abaqus material-card export.

The Volume II model branches predict the following quantities:

- effective orthotropic elastic constants influenced by fabric architecture;
- effective density;
- effective specific heat capacity;
- effective thermal conductivity in the material directions;
- effective coefficients of thermal expansion in the material directions;
- architecture factors for weave, braid, non-crimp, and stitched reinforcement systems;
- effective properties and Abaqus thermophysical material-card entries.

The goal is not to replace detailed finite-element textile unit-cell analysis. Instead, the intent is to provide a robust, deterministic, Workbench-safe engineering model that captures the dominant effects of tow homogenization, warp–weft balance, crimp, interlacing, fillers, voids, and orthotropic thermal response.

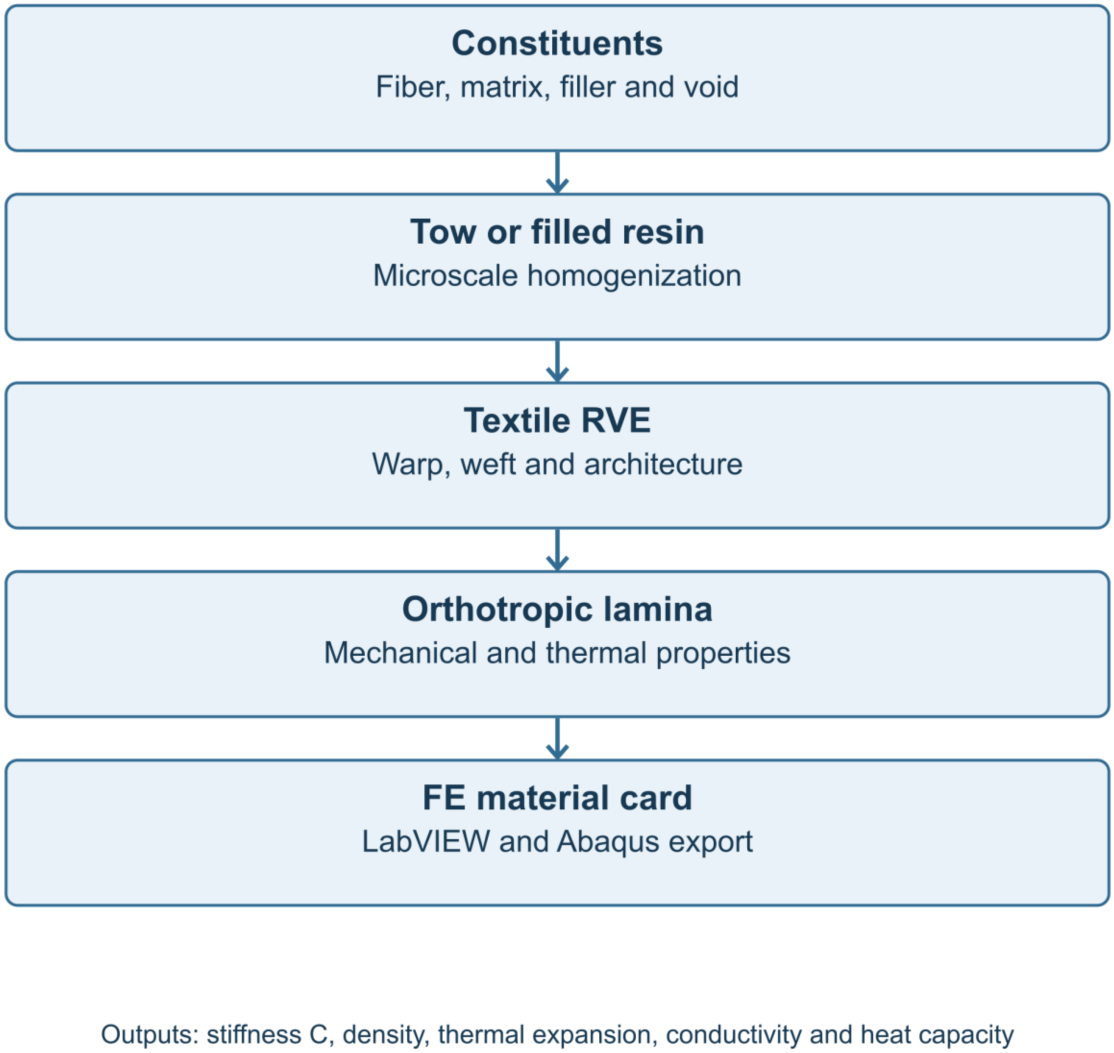

Figure V-II-S1-1. Multiscale textile and thermophysical homogenization workflow.

1 2 Multiscale Material Hierarchy

The model is organized around the assumption that each length scale may be represented by an effective property vector. The general homogenization mapping is written as

$$\mathbf{P}^{eff} = \mathcal{H}\left(\mathbf{P}^{(1)}, \mathbf{P}^{(2)}, \dots, \mathbf{P}^{(N)}, V_1, V_2, \dots, V_N, \boldsymbol{\chi}\right),$$

where $\mathbf{P}^{(r)}$ is the property vector for phase r, V_r is its volume fraction, N is the number of active phases, and $\boldsymbol{\chi}$ denotes geometry or architecture descriptors such as weave type, crimp amplitude, warp/weft balance, stitch knockdown, binder fraction, or braid angle.

For the textile and thermophysical model, the phase-property vector is defined as

$$\mathbf{P}^{(r)} = \left\{\mathbf{C}^{(r)}, \rho^{(r)}, \boldsymbol{\alpha}^{(r)}, \mathbf{k}^{(r)}, C_p^{(r)}, \mathbf{S}^{(r)}\right\},$$

where $\mathbf{C}$ is the stiffness tensor, ρ is density, $\boldsymbol{\alpha}$ is the coefficient of thermal expansion tensor, $\mathbf{k}$ is the thermal conductivity tensor, C_p is specific heat capacity, and $\mathbf{S}$ represents strength allowables when damage and failure calculations are enabled.

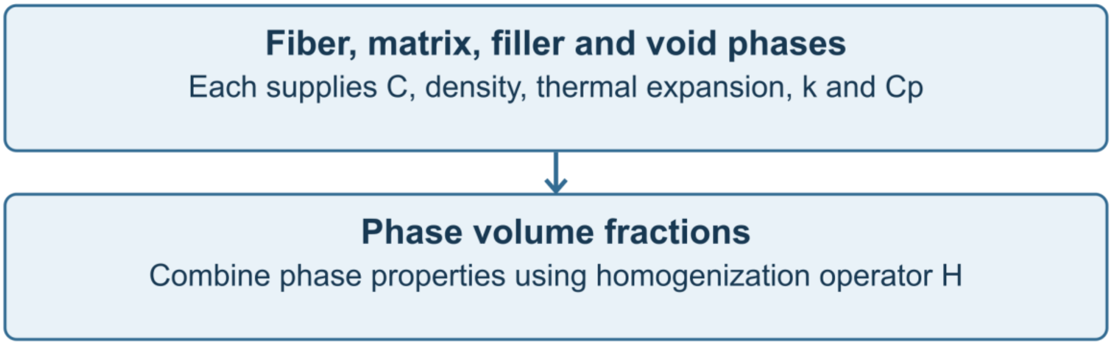

Figure V-II-S1-2. Phase-property representation used by the textile and thermophysical model.

1 3 Phase Volume Fractions

The phase fractions satisfy the conservation constraint

$$\sum_{r=1}^{N} V_r = 1.$$

For the fiber–matrix–filler–void representation used in the solver implementation,

$$V_f + V_m + V_p + V_v = 1,$$

where V_f is fiber volume fraction, V_m is matrix volume fraction, V_p is particulate filler volume fraction, and V_v is void volume fraction.

When filler is treated as an implicit modifier of the resin phase, the model first constructs a filled-matrix property set and then performs fiber/tow/fabric homogenization using that modified matrix. When filler is treated explicitly, the filler remains a distinct phase in the phase list used for the homogenization calculation.

1 4 Textile Architecture as a Reduced-Order Descriptor

A detailed textile unit cell may require tow cross-section shape, nesting, local waviness, inter-tow resin pockets, contact surfaces, and through-thickness binder geometry. The implemented Workbench model reduces this complexity to a set of architecture descriptors that can be specified through scalar inputs:

$$\boldsymbol{\chi}_{fabric} = \{I_{fabric}, F_{warp}, F_{weft}, k_c, k_i, k_s, k_{stitch}, V_b, \theta_b\},$$

where I_{fabric} is the fabric architecture identifier, F_{warp} and F_{weft} are warp and weft weighting fractions, k_c is a crimp factor, k_i is an interlacing factor, k_s is an in-plane shear factor, k_{stitch} is a stitching knockdown factor, V_b is binder or through-thickness reinforcement fraction, and θ_b is a bias or braid angle.

The architecture library in the current solver implementation includes plain weave, 2 by 2 twill, four-harness satin, five-harness satin, eight-harness satin, basket weave, leno weave, non-crimp biaxial stitched fabric, and triaxial braid. These options are implemented as engineering corrections rather than as a finite-element textile meshing scheme.

1 5 General Textile Homogenization Operator

The textile-level homogenization problem may be written in the compact form

$$\mathbf{C}_{fabric} = \mathcal{H}_{textile}(\mathbf{C}_{tow}, \mathbf{C}_m, F_{warp}, F_{weft}, \boldsymbol{\chi}_{fabric}).$$

In the engineering implementation, this relationship is evaluated through warp–weft weighted tow properties modified by architecture factors. The same conceptual form is also used for conductivity and thermal expansion,

$$\mathbf{k}_{fabric} = \mathcal{H}^{k}_{textile}(\mathbf{k}_{tow}, \mathbf{k}_m, \boldsymbol{\chi}_{fabric}),$$

and

$$\boldsymbol{\alpha}_{fabric} = \mathcal{H}^{\alpha}_{textile}(\boldsymbol{\alpha}_{tow}, \boldsymbol{\alpha}_m, \boldsymbol{\chi}_{fabric}).$$

This unified notation is useful because all material properties ultimately feed the same finite-element material description.

1 7 Volume II Output Philosophy

The final orthotropic property vector assembled by the Volume II branches is

$$\mathbf{P}^{ortho} = \left[E_1, E_2, E_3, G_{12}, G_{13}, G_{23}, \nu_{12}, \nu_{13}, \nu_{23}, \rho, \alpha_1, \alpha_2, \alpha_3, k_1, k_2, k_3, C_p\right]^T.$$

The effective thermophysical properties are exported to Abaqus using the material-card blocks

*DENSITY, *EXPANSION, *CONDUCTIVITY, *SPECIFIC HEAT

1 8 Assumptions and Limitations

The Volume II formulation is a reduced-order engineering homogenization model. The principal assumptions are:

- tow properties can be represented by homogenized orthotropic engineering constants;
- textile architecture can be represented using warp/weft weights and architecture correction factors;
- crimp and interlacing are treated as stiffness and shear knockdown factors rather than explicit curved tow finite elements;
- filler and void phases are represented through effective phase-volume terms;
- thermophysical properties are homogenized through volume averaging, series/parallel conductivity estimates, and architecture corrections;
- all outputs are deterministic scalar, vector, matrix, or string quantities suitable for Workbench and Abaqus export.

These assumptions make the method much faster than detailed textile finite-element unit-cell analysis, but they also limit its ability to capture local tow contact, resin pocket stress concentration, inter-tow delamination, nesting effects, local permeability, and nonlinear compaction.

1 9 Section Summary

Section 1 defines the multiscale and software framework for Volume II. The following sections document the individual textile and thermophysical model components: textile representative volume elements, fabric architecture factors, warp–weft averaging, crimp correction, filled matrix micromechanics, void effects, density, specific heat, thermal conductivity, thermal expansion, and final orthotropic property assembly.

References

Advani, S. G., and Tucker, C. L. III (1987). The use of tensors to describe and predict fiber orientation in short fiber composites. *Journal of Rheology*, 31, 751–784.

Chou, T.-W. (1992). *Microstructural Design of Fiber Composites*. Cambridge University Press.

Dvorak, G. J. (2013). *Micromechanics of Composite Materials*. Springer.

Ishikawa, T., and Chou, T.-W. (1982). Stiffness and strength behavior of woven fabric composites. *Journal of Materials Science*, 17, 3211–3220.

Jones, R. M. (1999). *Mechanics of Composite Materials*, 2nd ed. Taylor & Francis.

Mura, T. (1987). *Micromechanics of Defects in Solids*, 2nd ed. Martinus Nijhoff.

Naik, N. K. (1994). *Woven Fabric Composites*. Technomic.

Whitcomb, J. D. (2001). Three-dimensional stress analysis of plain weave composites. *Composite Materials: Fatigue and Fracture*, ASTM STP.

29 Section 2 - Fabric Micromechanics Theory

Online chapter

Section 2 Fabric Micromechanics Theory

2 Fabric Micromechanics Theory

2 1 Scope and purpose

This section documents the fabric micromechanics branch of the Workbench solver composite-material model. The fabric branch extends the elastic micromechanics framework of Volume I from unidirectional and discontinuous reinforcement to textile architectures. The current implementation supports common woven, stitched, non-crimp, and braided fabrics using a reduced-order representative-volume-element (RVE) framework. The goal is not to resolve every tow cross-section with a mesoscopic finite-element mesh. Instead, the model provides a fast engineering homogenization suitable for material screening, Workbench embedding, and automatic finite-element material-card generation.

For a woven or textile composite, choose the fabric family that represents the reinforcement. Architecture-specific factors then modify tow-dominated stiffness, in-plane shear response, thermophysical properties, and through-thickness reinforcement contributions. This section describes the theory behind those factors and explains how the model maps textile architecture into final orthotropic engineering constants.

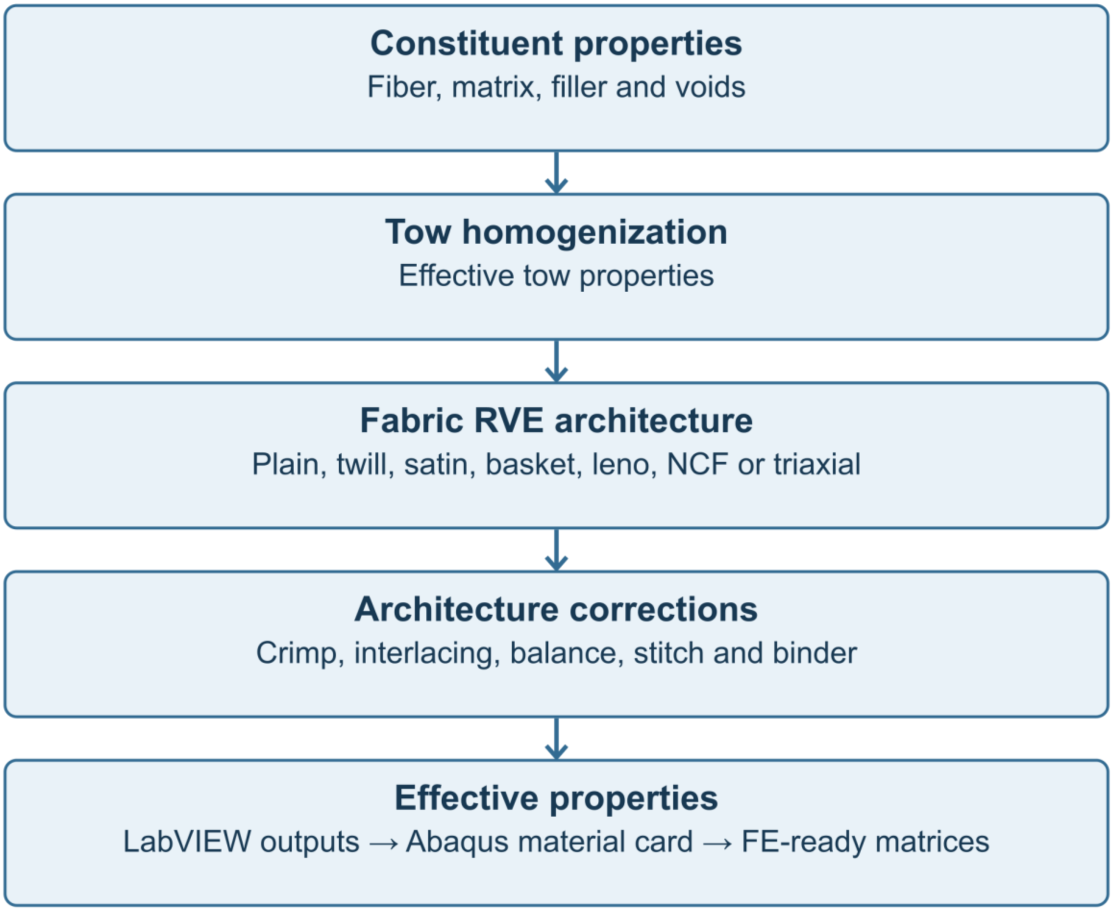

Figure V-II-S2-1. Fabric micromechanics workflow implemented in the Workbench solver model.

2 2 Textile composite scale hierarchy

The fabric formulation assumes three nested scales. At the constituent scale, fiber, matrix, filler, and void properties are specified independently. At the tow scale, fibers and matrix are homogenized into an equivalent orthotropic tow. At the textile scale, warp, weft, bias, stitch, and binder contributions are assembled into an effective fabric lamina.

The homogenization chain is represented as

$$\{\mathbf{P}_f, \mathbf{P}_m, \mathbf{P}_p, V_f, V_m, V_p, V_v\} \overset{\mathcal{H}_{tow}}{\rightarrow} \mathbf{P}_{tow} \overset{\mathcal{H}_{fabric}}{\rightarrow} \mathbf{P}_{fabric}$$

where $\mathbf{P}_f$, $\mathbf{P}_m$, and $\mathbf{P}_p$ are the fiber, matrix, and particle property sets, respectively; V_f, V_m, V_p, and V_v are fiber, matrix, particle, and void volume fractions; $\mathcal{H}_{tow}$ is the selected tow homogenization model; and $\mathcal{H}_{fabric}$ is the textile-level homogenization operator.

The final fabric property vector is

$$\mathbf{P}_{fabric} = \{E_1, E_2, E_3, G_{12}, G_{13}, G_{23}, \nu_{12}, \nu_{13}, \nu_{23}, \rho, \alpha_1, \alpha_2, \alpha_3, k_1, k_2, k_3, C_p\}.$$

2 3 Representative volume element definition

A textile RVE is the smallest repeating domain that preserves the relevant fabric architecture. The RVE contains a warp tow family, a weft tow family, matrix-rich pockets, and optional binder or stitching reinforcement. For non-crimp fabrics and triaxial braids, the RVE additionally contains bias tow families.

The phase volume-fraction constraint is

$$V_f + V_m + V_p + V_v = 1.$$

At the fabric level, the tow fractions satisfy

$$w_{warp} + w_{weft} + w_{bias} + w_{binder} + w_{matrix} = 1.$$

For a two-family woven fabric without explicit bias or binder phases,

$$w_{warp} + w_{weft} = 1.$$

Balanced woven fabrics use

$$w_{warp} = w_{weft} = \frac{1}{2},$$

whereas unbalanced fabrics use architecture- or user-specified values. In the solver implementation, this weighting is controlled by fabric_warp_bias_fraction, woven_warp_volume_fraction, and woven_weft_volume_fraction.

2 4 Supported fabric architecture library

The following fabric architectures are supported.

Architecture	Primary modeling effect
User-defined textile	User-defined correction factors
Plain weave	High interlacing, high crimp, stable balanced response
2×2 twill	Moderate interlacing, moderate crimp, improved drape
4-harness satin	Low interlacing, lower crimp
5-harness satin	Lower interlacing than 4HS
8-harness satin	Low interlacing, high tow straightness
Basket weave	Grouped tows, reduced interlacing density
Leno weave	Locked yarns, high geometric stability, stronger yarn distortion
Non-crimp biaxial stitched fabric	Low tow crimp, stitch knockdown included
Triaxial braid	Axial and bias tow families with angle-dependent contribution

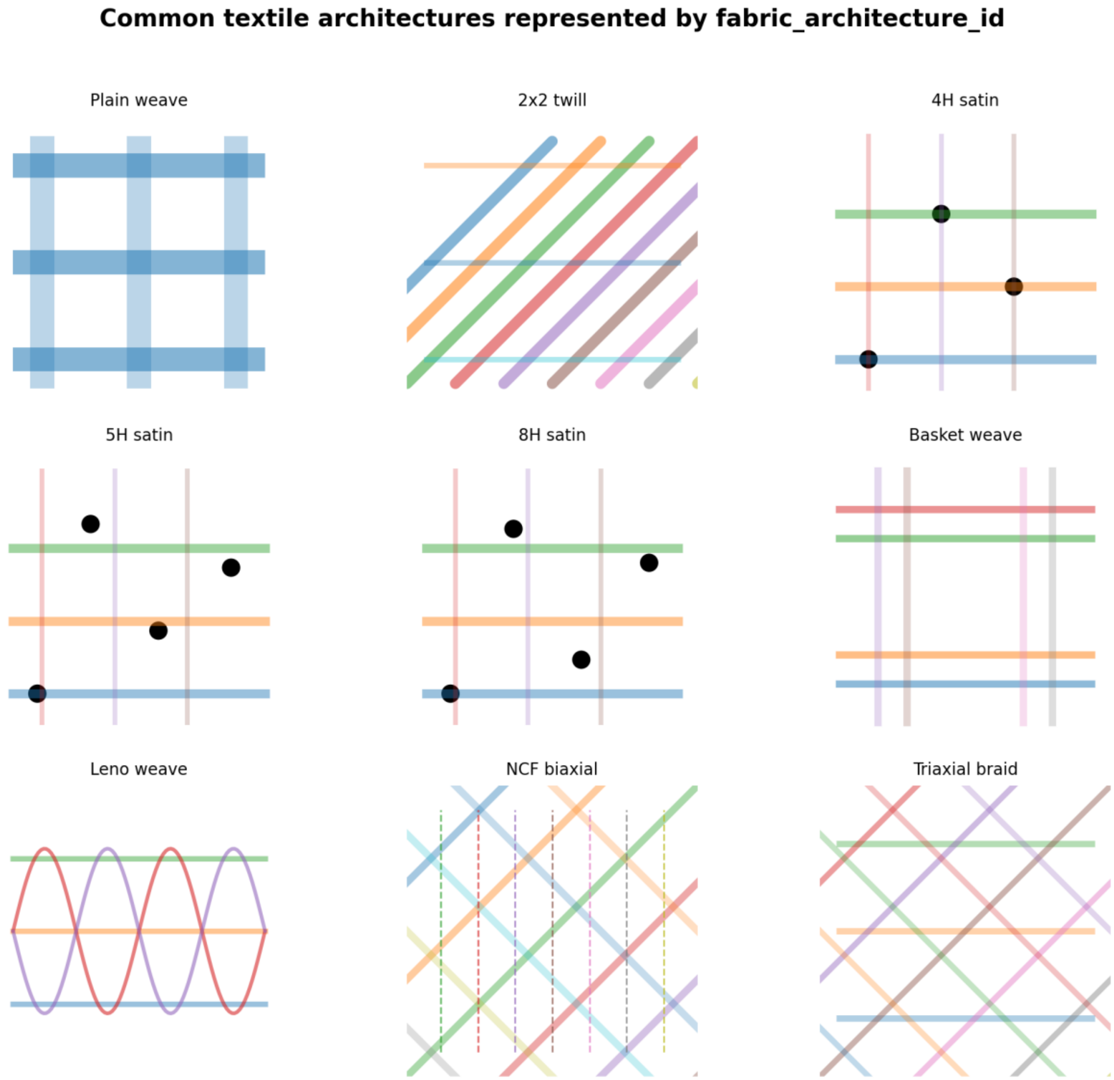

Figure V-II-S2-2. Common textile architectures represented in the fabric branch.

2 5 Tow homogenization

The tow is treated as a unidirectional composite sub-material. The selected constituent-level micromechanics model produces tow properties from the fiber and matrix properties. In high-level operator form,

$$\mathbf{C}_{tow} = \mathcal{H}_{tow}\left(\mathbf{C}_{fiber}, \mathbf{C}_{matrix}, V_{f,tow}\right),$$

where $V_{f,tow}$ is the fiber volume fraction inside the tow.

The axial tow modulus used in the implemented engineering approximation is

$$E_{tow,1} = V_{f,tow}E_{f,1} + \left(1 - V_{f,tow}\right)E_m.$$

A transverse tow modulus may be estimated using a Halpin-Tsai-like expression,

$$E_{tow,2} = E_m \frac{1 + 2\eta_E V_{f,tow}}{1 - \eta_E V_{f,tow}},$$

with

$$\eta_E = \frac{E_{f,2}/E_m - 1}{E_{f,2}/E_m + 2}.$$

The same tow-level concept is applied to shear properties,

$$G_{tow,12} = \mathcal{H}_{tow}\left(G_{f,12}, G_m, V_{f,tow}\right).$$

These tow-level properties become the input to the fabric-level homogenization step.

2 6 Warp-weft stiffness assembly

The fabric stiffness is assembled from warp and weft tow contributions. For a balanced woven architecture, the warp and weft fractions are equal. For an unbalanced fabric, the weighting is user-defined or architecture-derived.

The normalized tow-family fractions are

$$\widehat{w}_{warp} = \frac{w_{warp}}{w_{warp} + w_{weft}}, \qquad \widehat{w}_{weft} = \frac{w_{weft}}{w_{warp} + w_{weft}}.$$

The implemented in-plane Young's moduli are represented by

$$E_1 = f_c f_b\left(\widehat{w}_{warp} E_{tow,1} + \widehat{w}_{weft} E_{tow,2}\right),$$

$$E_2 = f_c f_b\left(\widehat{w}_{warp} E_{tow,2} + \widehat{w}_{weft} E_{tow,1}\right),$$

where f_c is the architecture-adjusted crimp factor and f_b is the balance factor. The through-thickness modulus is treated as a tow-transverse-dominated quantity modified by interlacing and optional binder reinforcement,

$$E_3 = f_c f_i E_{tow,2},$$

where f_i is the interlacing penalty factor.

2 7 Crimp interlacing balance and shear correction factors

Fabric architecture influences stiffness through geometric tow waviness and the number of over-under interlacings. The model uses reduced-order scalar correction factors rather than explicit meso-scale finite-element tow geometry.

The crimp factor is modeled as a decreasing function of the tow waviness amplitude ratio,

$$f_c = \frac{1}{1 + a_c (A_c/L_c)^2},$$

where A_c is tow waviness amplitude, L_c is crimp wavelength, and a_c is an architecture-dependent constant. Plain weaves use a larger effective a_c because they interlace more frequently, while satin weaves use smaller values because they have longer floats and lower interlacing density.

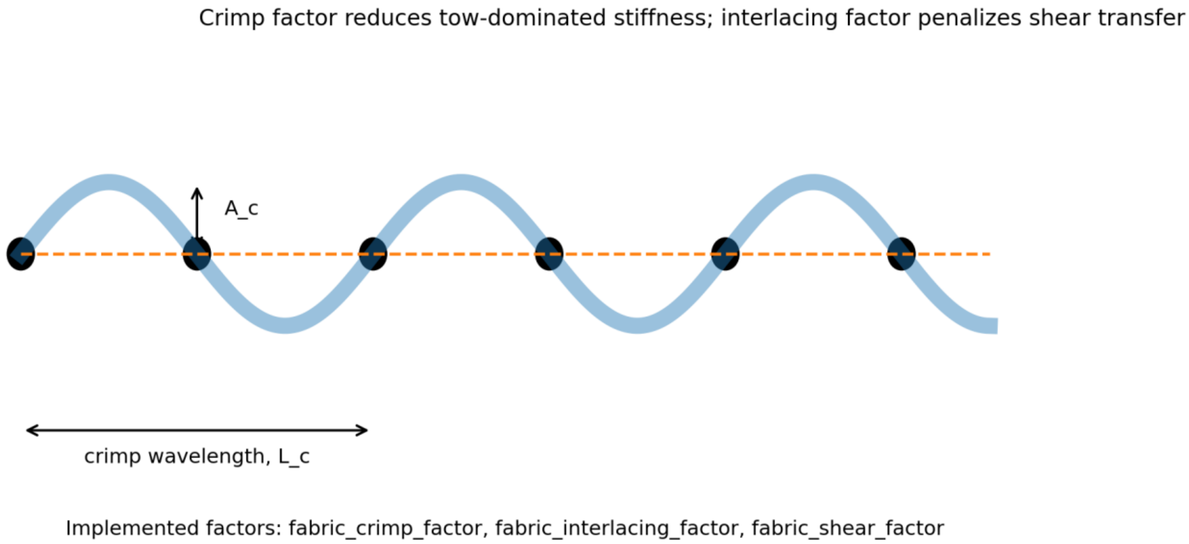

Figure V-II-S2-3. Crimp and interlacing correction concept used by the fabric branch.

The balance factor is defined from warp and weft fractions,

$$f_b = 1 - \left|\widehat{w}_{warp} - \widehat{w}_{weft}\right|.$$

This factor approaches unity for balanced fabrics and decreases as the architecture becomes strongly warp- or weft-dominated.

The interlacing penalty is represented by

$$f_i = max\left(f_{i,min}, \quad 1 - b_i I_a\right),$$

where I_a is the architecture interlacing factor and b_i is a calibration constant. The in-plane shear correction is expressed as

$$G_{12} = f_c f_s f_i \overline{G}_{12,tow},$$

where f_s is the architecture shear factor and $\overline{G}_{12,tow}$ is the averaged tow-level shear modulus.

2 8 Architecture-specific interpretation

Plain weave has the highest interlacing density among the common balanced fabrics. It therefore receives the largest crimp and interlacing penalties. Twill fabrics reduce the interlacing frequency and improve drape, so the stiffness knockdown is less severe. Satin fabrics introduce longer tow floats, which reduce crimp and preserve tow axial stiffness but may reduce fabric stability during handling. Basket weaves group tows and reduce crossing density; leno weaves lock yarns together and improve dimensional stability but increase local yarn distortion. Non-crimp fabrics preserve tow straightness and therefore use very low crimp penalties, but stitching effects are included through a stitch knockdown factor. Triaxial braids include a bias-angle contribution that redistributes stiffness and increases in-plane shear coupling.

The architecture-dependent stiffness correction can be summarized as

$$\mathbf{C}_{fabric} = \mathcal{F}_{arch}(f_c, f_i, f_s, f_b, f_{stitch}, V_{binder}, \theta_b) : \mathbf{C}_{tow},$$

where $\mathcal{F}_{arch}$ denotes the reduced-order architecture operator.

2 9 Non-crimp fabrics and triaxial braids

For non-crimp stitched fabrics, the tow path remains comparatively straight, and the crimp correction is weak. The stiffness is primarily reduced by the stitching knockdown factor,

$$E_{NCF} = f_{stitch} E_{straight \quad tow}.$$

For triaxial braids, a bias angle θ_b introduces additional axial-to-shear coupling. The implemented high-level bias contribution is represented by

$$f_{bias} = sin^2(\theta_b).$$

The in-plane shear modulus is then increased by a bias contribution,

$$G_{12}^{braid} = G_{12}^{base}(1+c_b f_{bias}),$$

where c_b is an engineering calibration coefficient.

2 10 Through-thickness binder and stitching effects

Through-thickness binder yarns or stitches can contribute to E_3, G_{13}, and G_{23}. The model represents this contribution by a scalar binder volume fraction V_b:

$$E_3^{eff} = (1-V_b)E_3^{base} + V_b E_{b,1},$$

$$G_{13}^{eff} = (1-V_b)G_{13}^{base} + V_b G_{b,13},$$

$$G_{23}^{eff} = (1-V_b)G_{23}^{base} + V_b G_{b,23}.$$

In the current solver model, the binder stiffness is approximated using the fiber axial and shear properties, and V_b is supplied by fabric_z_binder_volume_fraction.

2 11 Thermophysical extension for fabric architectures

The same architecture concept is applied to thermal conductivity and coefficient of thermal expansion. The warp- and weft-weighted conductivity components are

$$k_1 = f_c\left(\hat{w}_{warp} k_{tow,1} + \hat{w}_{weft} k_{tow,2}\right),$$

$$k_2 = f_c\left(\hat{w}_{warp} k_{tow,2} + \hat{w}_{weft} k_{tow,1}\right),$$

and

$$k_3 = max\left(f_c k_{tow,3}, k_{min}\right).$$

The in-plane coefficients of thermal expansion are assembled as

$$\alpha_1 = \hat{w}_{warp} \alpha_{tow,1} + \hat{w}_{weft} \alpha_{tow,2},$$

$$\alpha_2 = \hat{w}_{warp} \alpha_{tow,2} + \hat{w}_{weft} \alpha_{tow,1}.$$

The scalar density and specific heat are not strongly dependent on fabric interlacing and are instead determined by phase volume fractions as described in Section 5 of this volume.

2 13 Assumptions and limitations

The fabric model is an engineering homogenization model. It does not solve local meso-scale tow contact, resin-pocket stress concentrations, yarn compaction, cure-dependent tow nesting, or finite-strain shear locking. The architecture factors provide a compact way to represent first-order fabric effects within a Workbench-safe micromechanics script. Detailed textile unit-cell finite-element analysis may be required for local damage initiation, matrix pocket cracking, tow debonding, and compaction modeling.

Despite these limitations, the model is appropriate for rapid architecture screening, laminate-level finite-element material definition, preliminary material design, and parametric comparison of common fabric types.

2 14 References

- Ishikawa, T., and Chou, T.-W. Stiffness and strength behavior of woven fabric composites. *Journal of Materials Science*, 1982.
- Ishikawa, T., and Chou, T.-W. One-dimensional micromechanical analysis of woven fabric composites. *AIAA Journal*, 1983.
- Chou, T.-W. *Microstructural Design of Fiber Composites*. Cambridge University Press, 1992.
- Naik, N. K. *Woven Fabric Composites*. Technomic Publishing, 1994.
- Whitcomb, J. D. Three-dimensional stress analysis of plain weave composites. *Composite Materials: Testing and Design*, ASTM STP series.
- Cox, B. N., and Flanagan, G. *Handbook of Analytical Methods for Textile Composites*. NASA Contractor Report, 1997.
- Lomov, S. V., Ivanov, D. S., Verpoest, I., et al. Meso-FE modelling of textile composites: Road map, data flow and algorithms. *Composites Science and Technology*, 2007.
- Advani, S. G., and Tucker, C. L. III. The use of tensors to describe and predict fiber orientation in short fiber composites. *Journal of Rheology*, 1987.
- Jones, R. M. *Mechanics of Composite Materials*. Taylor & Francis, 1999.
- Daniel, I. M., and Ishai, O. *Engineering Mechanics of Composite Materials*. Oxford University Press, 2006.

30 Section 3 - Warp-Weft Averaging and Crimp Correction

Online chapter

Section 3 Warp Weft Averaging and Crimp Correction

Volume II - Section 3

Warp-Weft Averaging and Crimp Correction in Fabric Micromechanics

3 1 Purpose and Scope

This section documents the fabric-level homogenization step used in the Workbench solver micromechanics model. Volume I defines the constituent and tow-level elastic micromechanics. Volume II Section 2 defines the textile architecture library. The present section describes how the homogenized tow properties are combined into effective fabric properties using warp-weft weighting, crimp correction, interlacing correction, shear correction, and optional through-thickness binder contributions.

This model applies to woven or textile composites. Select the fabric architecture that represents the reinforcement.

The fabric architecture options are listed in Table 3.1.

Fabric architecture	Primary correction features
User-defined	User-specified crimp/interlacing factors
Plain weave	High interlacing, high crimp
2 x 2 twill	Moderate interlacing, moderate crimp
4-harness satin	Low interlacing, low crimp
5-harness satin	Lower interlacing, lower crimp
8-harness satin	Very low interlacing, very low crimp
Basket weave	Grouped-tow behavior, moderate locking
Leno weave	High yarn locking and distortion
Non-crimp biaxial stitched fabric	Low crimp with stitch knockdown
Triaxial braid	Bias reinforcement contribution

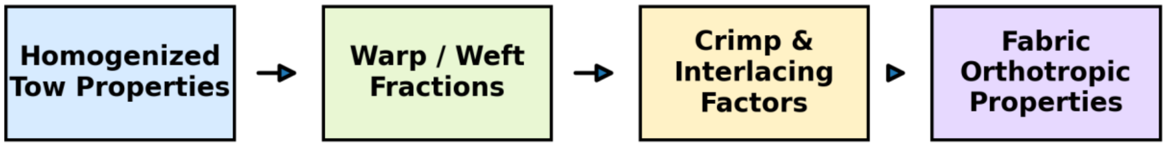

Figure V-II-S3-1: Warp-weft averaging and crimp-correction workflow

Figure V-II-S3-1. Warp-weft averaging and crimp-correction workflow.

3 2 Tow Properties Passed from Constituent Micromechanics

Each fabric architecture begins with an equivalent homogenized tow. The tow may be obtained from any micromechanics branch described in Volume I, including rule of mixtures, Halpin-Tsai, Mori-Tanaka approximation, or the self-consistent engineering approximation. The homogenized tow property vector is represented by

$$\mathbf{P}_{tow} = \{E_1^{tow}, E_2^{tow}, E_3^{tow}, G_{12}^{tow}, G_{13}^{tow}, G_{23}^{tow}, \nu_{12}^{tow}, \nu_{13}^{tow}, \nu_{23}^{tow}\}.$$

The tow homogenization operator can be written abstractly as

$$\mathbf{P}_{tow} = \mathcal{H}_{micro}\left(\mathbf{P}_f, \mathbf{P}_m, V_f^{tow}\right),$$

The two input vectors contain the fiber and matrix properties. The tow fiber volume fraction specifies the fraction of the tow occupied by fiber. These constituent data supply the tow homogenization operator shown above.

The simplified tow axial modulus used in the woven branch is

$$E_1^{tow} = V_f^{tow} E_1^f + \left(1 - V_f^{tow}\right) E_m^*,$$

The matrix term represents either the neat matrix or the filled matrix. The transverse tow modulus uses the same Halpin-type interaction relation as the other micromechanics branches.

$$E_2^{tow} = E_m^* \frac{1 + 2\eta_E V_f^{tow}}{1 - \eta_E V_f^{tow}},$$

with

$$\eta_E = \frac{E_2^f / E_m^* - 1}{E_2^f / E_m^* + 2}.$$

These expressions are engineering approximations used to keep the Workbench implementation robust. They are consistent with the classical tow-property hierarchy used in textile composite micromechanics.

3 3 Warp and Weft Coordinate Systems

The fabric is modeled as two interacting orthotropic tow families. Warp tows are aligned nominally with the material 1-direction, while weft tows are aligned nominally with the material 2-direction. The effective fabric response is assembled from the contributions of both families.

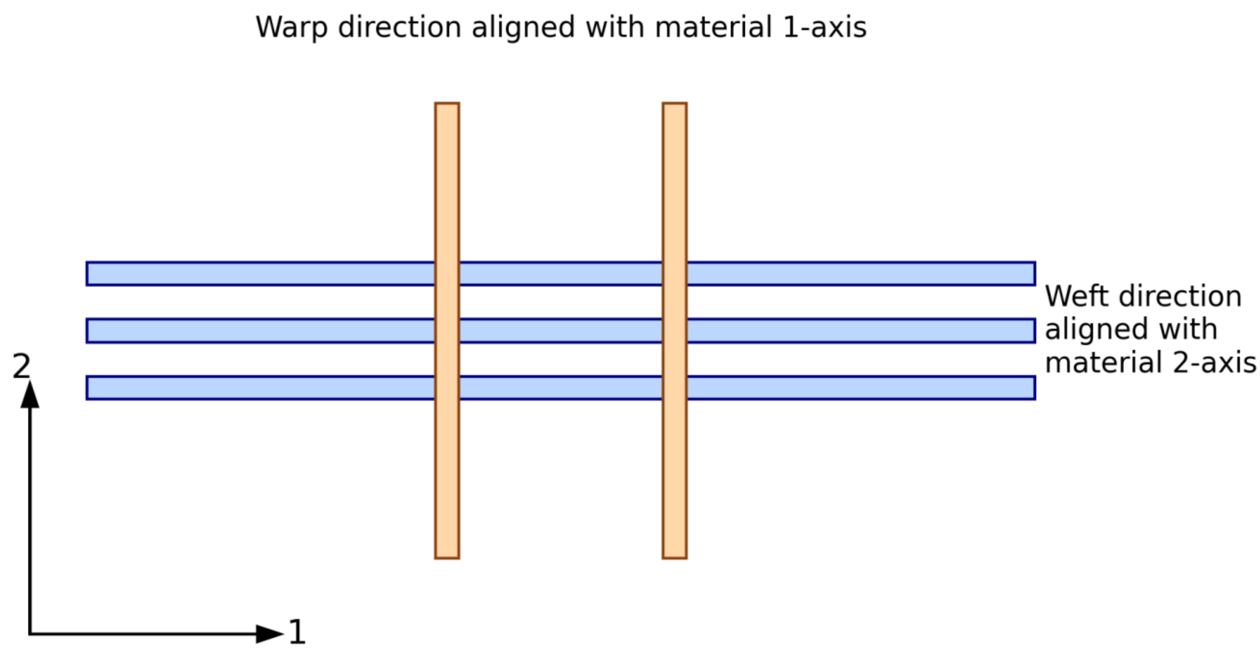

Figure V-II-S3-2: Material, warp, and weft coordinate systems

Figure V-II-S3-2. Material, warp, and weft coordinate systems.

The normalized warp and weft weights are

$$w_{warp} = \frac{V_{warp}}{V_{warp} + V_{weft}},$$

$$w_{weft} = \frac{V_{weft}}{V_{warp} + V_{weft}},$$

with

$$w_{warp} + w_{weft} = 1.$$

In the code these quantities are initialized using woven_warp_volume_fraction and woven_weft_volume_fraction, then optionally overwritten by fabric_warp_bias_fraction. A balanced fabric has

$$w_{warp} = w_{weft} = \frac{1}{2}.$$

An unbalanced fabric is represented by

$$w_{warp} \neq w_{weft}.$$

3 4 Warp-Weft Stiffness Averaging

The effective axial moduli are computed by assigning the tow axial stiffness to the direction in which a tow family runs and assigning the transverse tow stiffness to the orthogonal direction. The high-level uncorrected averaging model is

$$\hat{E}_1 = w_{warp}E_1^{tow} + w_{weft}E_2^{tow},$$

$$\hat{E}_2 = w_{warp}E_2^{tow} + w_{weft}E_1^{tow},$$

$$\hat{E}_3 = E_2^{tow}.$$

This captures the first-order architecture effect: increasing the warp fraction increases the longitudinal modulus, while increasing the weft fraction increases the transverse in-plane modulus. For balanced fabrics, the in-plane moduli become nearly equal if the warp and weft tow properties are equivalent.

The in-plane shear modulus is represented by

$$\hat{G}_{12} = \frac{1}{2}\left(G_{12}^{tow} + G_{12}^{base}\right),$$

where the baseline in-plane shear modulus is the selected matrix/tow interaction shear estimate from the micromechanics branch. The through-thickness shear moduli are represented by the corresponding matrix-constrained terms,

$$\hat{G}_{13} = G_{13}^{base}, \qquad \hat{G}_{23} = G_{23}^{base}.$$

3 5 Tow Crimp Geometry

Tow crimp describes the waviness of a tow centerline relative to a straight reference direction. A sinusoidal representation provides a compact engineering measure of waviness,

$$y(x) = A sin\left(\frac{2\pi x}{L_c}\right),$$

Here A is the crimp amplitude and the subscript c identifies the crimp wavelength.

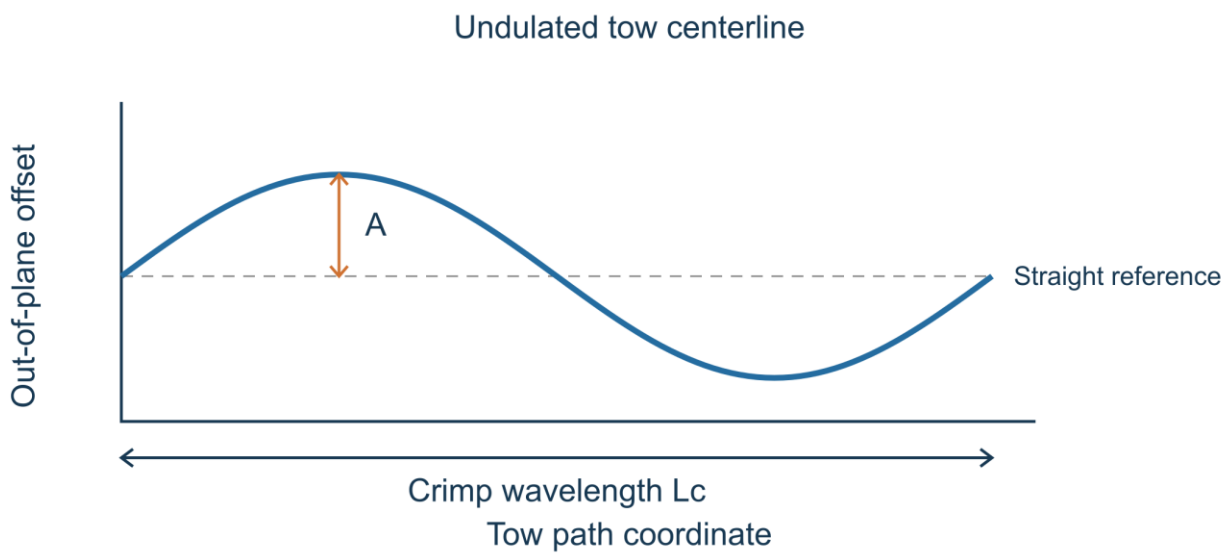

Figure V-II-S3-3. Tow crimp amplitude and wavelength definition.

The nondimensional crimp amplitude ratio used by the model is

$$\gamma_c = \frac{A}{L_c}.$$

A crimp knockdown factor is then introduced as

$$f_c = \frac{1}{1 + \beta_c \gamma_c^2},$$

The crimp penalty coefficient depends on the architecture. This expression has the following limiting behavior.

$$\lim_{\gamma_c \to 0} f_c = 1,$$

and

$$f_c < 1 \quad \text{for} \quad \gamma_c > 0.$$

The code uses architecture-specific values of the crimp penalty coefficient. Plain weave and leno weave use stronger crimp penalties. Satin and non-crimp architectures use smaller penalties because the tows are straighter.

3 6 Architecture-Specific Correction Factors

The solver model applies four primary architecture correction factors:

$$f_c = \text{crimp factor},$$

$$f_i = \text{interlacing factor},$$

$$f_s = \text{shear factor},$$

$$f_b = \text{balance factor}.$$

The balance factor is computed from the warp/weft fraction difference,

$$f_b = 1 - |w_{warp} - w_{weft}|.$$

The architecture factors provide an engineering reduction of the textile unit-cell mechanics into scalar modifiers. The corrected in-plane moduli are

$$E_1^{fabric} = f_c(1+0.06f_b)\hat{E}_1,$$

$$E_2^{fabric} = f_c(1+0.06f_b)\hat{E}_2,$$

and the through-thickness modulus is

$$E_3^{fabric} = f_c f_i^* \hat{E}_3,$$

where the interlacing penalty used in the code is

$$f_i^* = max(0.50, \quad 1 - 0.08f_i).$$

The corrected shear moduli are

$$G_{12}^{fabric} = f_c f_s f_i^* \hat{G}_{12},$$

$$G_{13}^{fabric} = f_c f_i^* \hat{G}_{13},$$

$$G_{23}^{fabric} = f_c f_i^* \hat{G}_{23}.$$

Figure V-II-S3-4 summarizes representative relative values used for common fabric families.

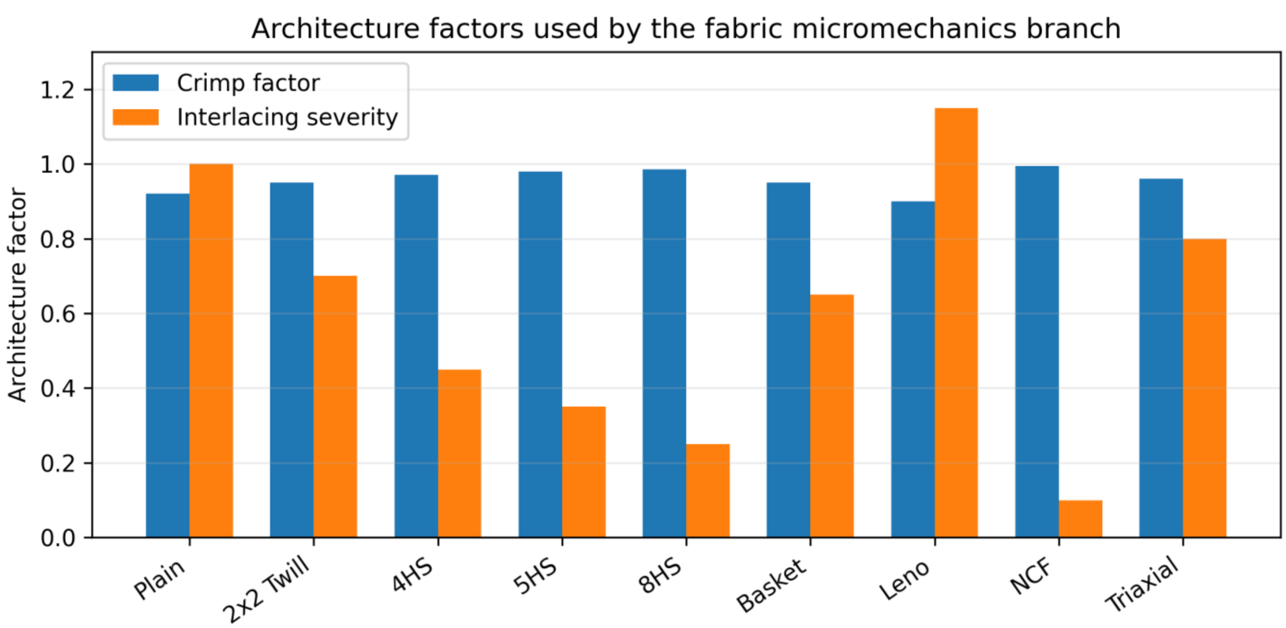

Figure V-II-S3-4: Representative relative fabric architecture factors

Figure V-II-S3-4. Representative relative fabric architecture factors.

3 7 Common Architecture Behavior

The architecture factors are selected to reproduce expected trends among common textile composites:

- Plain weave has high interlacing, higher tow crimp, and lower in-plane shear mobility.
- Twill weave has lower interlacing than plain weave and therefore a smaller crimp penalty.
- Satin weaves reduce interlacing further, increasing axial tow efficiency.
- Basket weave behaves like a grouped-tow plain weave with reduced interlacing density.
- Leno weave has strong tow locking and higher local yarn distortion.
- Non-crimp stitched fabric has low crimp but includes a stitch knockdown factor.
- Triaxial braid includes a bias-fiber contribution that increases in-plane coupling and shear response.

For triaxial braid architectures, the bias contribution is represented by

$$f_{bias} = sin^2\theta_b,$$

The braid bias angle determines the bias factor. The following relation increases the in-plane shear modulus using that factor.

$$G_{12}^{braid} = G_{12}^{fabric}(1+0.40 f_{bias}).$$

For non-crimp fabric architectures, the stitch knockdown factor modifies the tow-dominated response as follows.

$$E_i^{NCF} = f_{st} E_i^{fabric}, \qquad i = 1,2.$$

3 8 Through-Thickness Binder and Stitch Contribution

An optional binder or stitch phase can increase through-thickness stiffness and shear stiffness. The following relations use its volume fraction to blend the fabric and binder contributions.

$$E_3^{fabric,b} = (1-V_b)E_3^{fabric} + V_b E_1^f,$$

$$G_{13}^{fabric,b} = (1-V_b)G_{13}^{fabric} + V_b G_{13}^f,$$

$$G_{23}^{fabric,b} = (1-V_b)G_{23}^{fabric} + V_b G_{23}^f.$$

This is not a full three-dimensional woven unit-cell model, but it provides a useful engineering correction for stitched, 3D woven, and binder-stabilized textile preforms.

3 9 Thermophysical Warp-Weft Averaging

Thermal conductivity is treated using the same architecture logic. Before fabric correction, the longitudinal and transverse conductivity estimates are

$$\hat{k}_1 = w_{warp} k_1^{tow} + w_{weft} k_2^{tow},$$

$$\hat{k}_2 = w_{warp} k_2^{tow} + w_{weft} k_1^{tow}.$$

The corrected in-plane conductivities are

$$k_1^{fabric} = f_c \hat{k}_1,$$

$$k_2^{fabric} = f_c \hat{k}_2,$$

with the through-thickness value reduced by the crimp-dominated transverse transfer factor,

$$k_3^{fabric} = max(f_c, 0.5) k_3^{tow}.$$

The coefficients of thermal expansion are averaged as

$$\alpha_1^{fabric} = w_{warp}\alpha_1^{tow} + w_{weft}\alpha_2^{tow},$$

$$\alpha_2^{fabric} = w_{warp}\alpha_2^{tow} + w_{weft}\alpha_1^{tow}.$$

3 11 Recommended Use

The fabric model is intended for engineering material-property generation, early design, sensitivity studies, and Workbench-driven material screening. It is appropriate when the user needs fast predictions across fabric families without constructing detailed textile finite-element RVEs. For final allowables, the model should be calibrated to coupon data and validated against the specific textile architecture, resin system, compaction state, and cure process.

References

- Ishikawa, T., and Chou, T.-W. "Stiffness and strength behaviour of woven fabric composites." *Journal of Materials Science*, 1982.
- Ishikawa, T., and Chou, T.-W. "One-dimensional micromechanical analysis of woven fabric composites." *AIAA Journal*, 1983.
- Chou, T.-W. *Microstructural Design of Fiber Composites*. Cambridge University Press, 1992.
- Naik, N. K. *Woven Fabric Composites*. Technomic, 1994.
- Whitcomb, J. D. "Three-dimensional stress analysis of plain weave composites." *Composite Materials: Testing and Design*, ASTM STP, 1990s.
- Bogdanovich, A. E., and Pastore, C. M. *Mechanics of Textile and Laminated Composites*. Chapman & Hall, 1996.
- Advani, S. G., and Tucker, C. L. "The use of tensors to describe and predict fiber orientation in short fiber composites." *Journal of Rheology*, 1987.
- Cox, H. L. "The elasticity and strength of paper and other fibrous materials." *British Journal of Applied Physics*, 1952.
- Jones, R. M. *Mechanics of Composite Materials*. Taylor & Francis, 1999.
- Daniel, I. M., and Ishai, O. *Engineering Mechanics of Composite Materials*. Oxford University Press, 2006.

31 Section 4 - Filled Matrix Hybrid and Void Micromechanics

Online chapter

Section 4 Filled Matrix Hybrid and Void Micromechanics

Volume II Section 4

Filled-Matrix Hybrid Reinforcement and Void Micromechanics

4 1 Purpose and Scope

The section covers four related capabilities:

- implicit filler modification of the polymer matrix;
- explicit treatment of filler as a separate phase;
- hybrid fiber or hybrid tow property assembly; and
- void effects on stiffness, density, conductivity, and heat capacity.

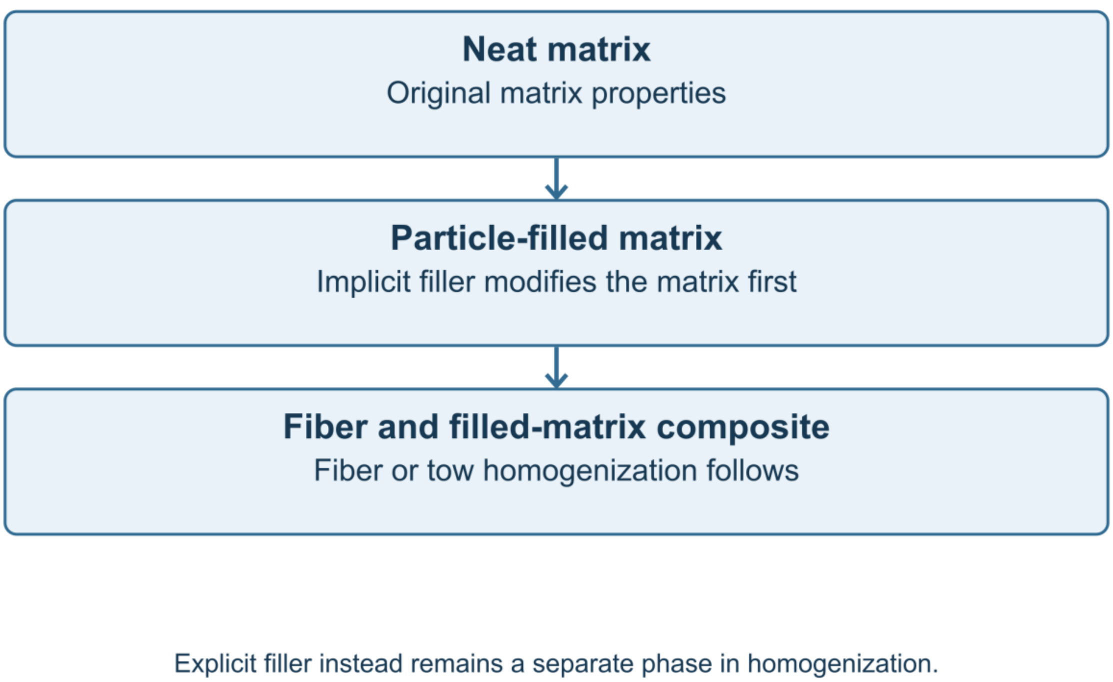

Figure V-II-S4-1. Filled-matrix homogenization workflow. The implicit branch modifies the resin before tow or fabric homogenization; the explicit branch retains filler as an independent phase.

4 2 Phase Definitions and Volume Conservation

The current material system is represented by fiber, matrix, filler, and void phases. The normalized phase fractions satisfy

$$V_f + V_m + V_p + V_v = 1,$$

where V_f is fiber volume fraction, V_m is polymer matrix volume fraction, V_p is particulate filler volume fraction, and V_v is void volume fraction. In the solver implementation, a filler fraction may be specified as a fraction of the resin phase and then mapped into the global composite volume.

For a resin-relative filler input $V_{p|r}$, the global filler fraction is approximated as

$$V_p = V_{p|r}\left(1 - V_f - V_v\right),$$

and the remaining matrix fraction becomes

$$V_m = 1 - V_f - V_p - V_v.$$

This convention prevents double-counting filler volume when the filler is introduced through the resin phase rather than directly through the total composite volume.

4 3 Implicit Filled-Matrix Model

In the implicit approach, the filler modifies the matrix before the fiber/tow/fabric homogenization step. The effective filled-matrix modulus is represented by a Halpin–Tsai / Kerner-style particle relation,

$$E_m^* = E_m \frac{1 + 2\eta_E V_{p|r}}{1 - \eta_E V_{p|r}},$$

where

$$\eta_E = \frac{E_p/E_m - 1}{E_p/E_m + 2}.$$

The corresponding shear modulus update is

$$G_m^* = G_m \frac{1 + 2\eta_G V_{p|r}}{1 - \eta_G V_{p|r}},$$

with

$$\eta_G = \frac{G_p/G_m - 1}{G_p/G_m + 2}.$$

The modified Poisson ratio is recovered from elastic consistency,

$$\nu_m^* = \frac{E_m^*}{2G_m^*} - 1.$$

This branch is computationally efficient and is appropriate when particles are small, well dispersed, and primarily act by stiffening the resin-rich phase. It also preserves the two-level textile workflow: first generate a filled matrix, then homogenize the tow or fabric.

4 4 Explicit Filler Phase Model

In the explicit approach, the filler is retained as a distinct phase in the global homogenization list. The effective property vector is written generally as

$$\mathbf{P}^{eff} = \mathcal{H}\left(V_f, V_m, V_p, V_v, \mathbf{P}_f, \mathbf{P}_m, \mathbf{P}_p, \mathbf{P}_v\right),$$

where $\mathcal{H}$ denotes the selected homogenization operator. This form is more general than the implicit filled-matrix relation because it allows filler stiffness, density, thermal conductivity, CTE, and specific heat to enter independently.

For a stiffness-like property in a simple upper-bound estimate,

$$\mathbf{C}^{eff} \approx V_f \mathbf{C}_f + V_m \mathbf{C}_m + V_p \mathbf{C}_p + V_v \mathbf{C}_v.$$

For matrix-dominated or transverse properties, the model may instead use inverse or interaction-corrected estimates to avoid overpredicting reinforcement from disconnected phases.

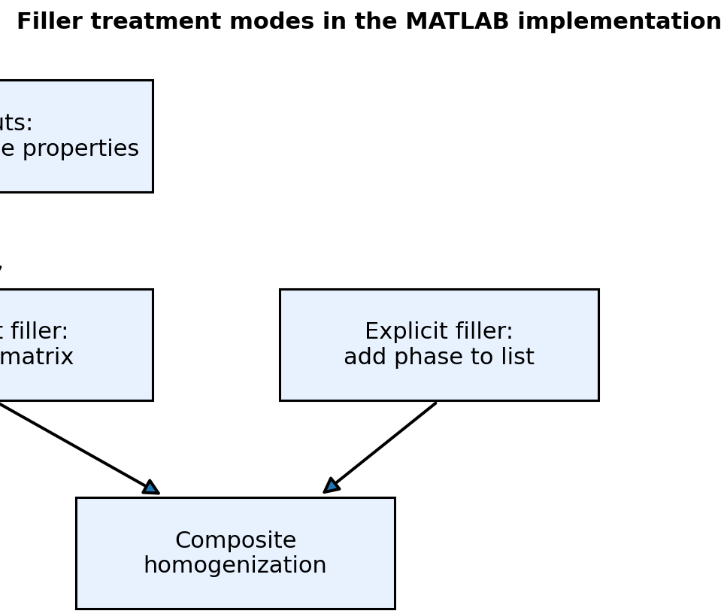

Figure V-II-S4-4. Implicit and explicit filler treatment modes. The implicit branch modifies the resin properties; the explicit branch adds filler as a separate homogenized phase.

4 5 Hybrid Fiber and Hybrid Tow Formulation

Hybrid composites contain two or more reinforcement families. Examples include carbon/glass hybrids, carbon/aramid hybrids, woven/braided hybrids, and fabrics containing binder or stitching yarns. The high-level hybrid stiffness relation can be written as

$$\mathbf{C}^{hyb} = \sum_{a=1}^{N_h} V_a \, \mathbf{T}_a : \mathbf{C}_a : \mathbf{T}_a^T + V_m \mathbf{C}_m,$$

where N_h is the number of reinforcement families, V_a is the volume fraction of family a, $\mathbf{C}_a$ is its homogenized stiffness, and $\mathbf{T}_a$ is the transformation operator associated with its orientation or textile path.

For a two-family hybrid tow in an aligned limit,

$$E_1^{hyb} \approx V_A E_{1A} + V_B E_{1B} + V_m E_m,$$

with

$$V_A + V_B + V_m = 1.$$

The same concept is used in textile systems by treating warp, weft, bias, binder, or stitched reinforcements as separate reinforcement families with architecture-dependent weighting.

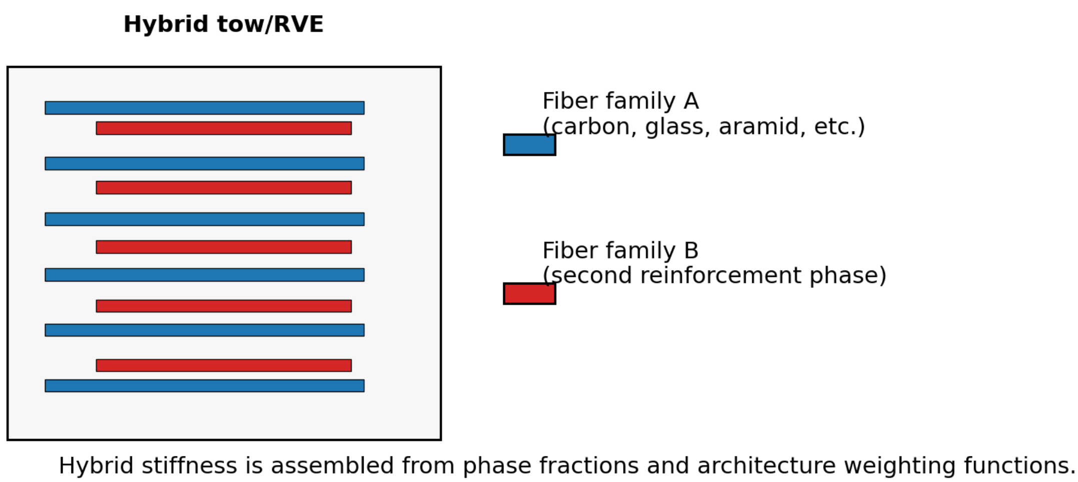

Figure V-II-S4-2. Hybrid fiber/tow representative volume element. Different reinforcement families are assembled using phase fractions and architecture-dependent weighting.

4 6 Void Phase Approximation

Voids are treated as a near-zero-stiffness phase or through property knockdown factors. The explicit void stiffness is represented by

$$\mathbf{C}_v \approx \epsilon_v \mathbf{I}, \qquad \epsilon_v \ll E_m,$$

which avoids singular numerical operations while preserving the strong softening effect of porosity. A first-order stiffness reduction can be written as

$$\mathbf{C}_v^{eff} \approx (1 - \chi_v V_v) \mathbf{C}_0^{eff},$$

where $\mathbf{C}_0^{eff}$ is the void-free effective stiffness and χ_v is a void sensitivity factor. In engineering use, χ_v is larger for transverse and shear properties than for longitudinal fiber-dominated properties.

For density, the void contribution is negligible,

$$\rho_{eff} = V_f \rho_f + V_m \rho_m + V_p \rho_p + V_v \rho_v, \qquad \rho_v \approx 0.$$

Voids also reduce thermal conductivity by interrupting heat-transfer paths,

$$k_i^{eff} \approx \left(1 - \psi_{k,i} V_v\right) k_{i,0}^{eff},$$

where $\psi_{k,i}$ is direction dependent.

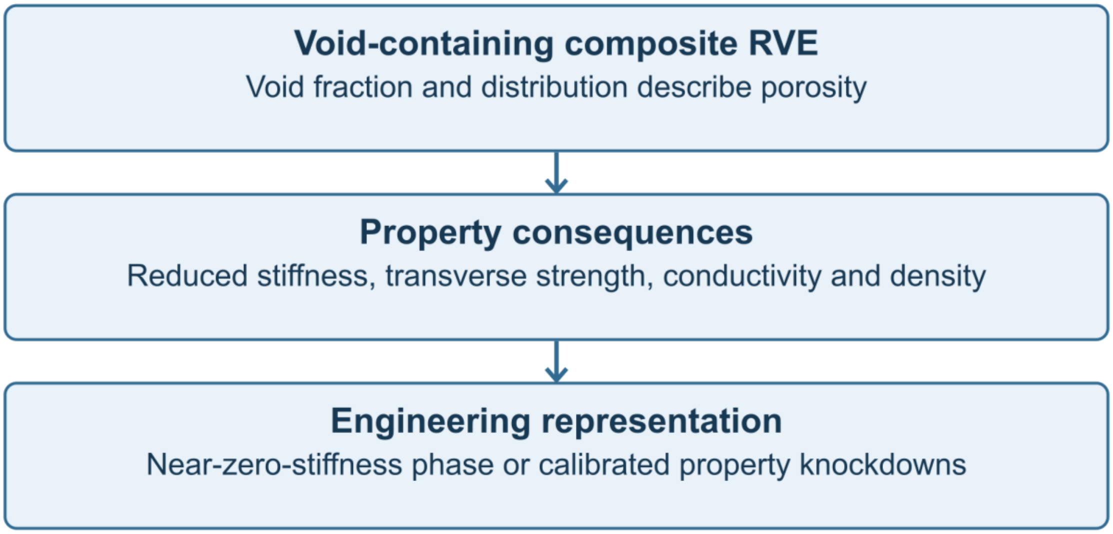

Figure V-II-S4-3. Void-containing composite RVE. Voids reduce stiffness, density, transverse strength, and effective conductivity.

4 7 Filled Matrix Density Heat Capacity and Conductivity

The filled matrix density follows direct volume averaging,

$$\rho_m^* = (1 - V_{p|r})\rho_m + V_{p|r}\rho_p.$$

The filled matrix specific heat is computed from volumetric heat capacity,

$$C_{p,m}^* = \frac{(1 - V_{p|r})\rho_m C_{p,m} + V_{p|r}\rho_p C_{p,p}}{\rho_m^*}.$$

For approximately spherical filler particles, the filled-matrix thermal conductivity is estimated as

$$k_m^* = k_m \frac{1 + 2\eta_k V_{p|r}}{1 - \eta_k V_{p|r}},$$

where

$$\eta_k = \frac{k_p/k_m - 1}{k_p/k_m + 2}.$$

These equations are consistent with the mechanical filled-matrix treatment and provide an efficient way to introduce filler effects into coupled thermomechanical analysis.

4 8 Effective Phase List Used by the solver Model

$$\mathbf{P}_{m,like} = \{E_m^*, G_m^*, \nu_m^*, \rho_m^*, \alpha_m^*, k_m^*, C_{p,m}^*\}.$$

When filler is explicit, the matrix-like properties are built from matrix, filler, and void fractions only for engineering approximation of matrix-dominated behavior:

$$P_{like} = \frac{V_m P_m + V_p P_p + V_v P_v}{V_m + V_p + V_v}.$$

This keeps the Workbench data path compact while retaining the ability to account for particle and void effects.

4 10 Directional Dilute-Porosity Correction

The preferred void model separates dense-solid homogenization from porosity degradation. Fiber, matrix, and filler fractions are first normalized over the solid fraction $V_{solid} = 1 - V_v$. The fully dense composite is calculated first, avoiding the excessive sensitivity produced when a near-zero-stiffness void is inserted directly into a transverse Reuss-type relation.

Each property group then receives its own calibrated degradation factor:

$$f_j = max(f_{min}, 1 - k_j V_v), \quad P_j^{por} = f_j P_j^{dense}.$$

Property group	Default coefficient	Effect at 1% void
Longitudinal modulus, E1	1.0	approximately 1% reduction
Transverse moduli, E2/E3	3.0	approximately 3% reduction
Shear moduli, G12/G13/G23	3.5	approximately 3.5% reduction
Longitudinal strengths, Xt/Xc	2.0	approximately 2% reduction
Transverse strengths	6.0	approximately 6% reduction
Shear strengths	5.0	approximately 5% reduction
Thermal conductivity	1.5	approximately 1.5% reduction

Longitudinal stiffness is therefore less sensitive than transverse and shear stiffness, while effective strengths receive their own directional factors before failure evaluation and material export. A legacy explicit near-zero-stiffness void phase remains available for comparison. Setting void_phase_enabled_flag to zero forces the global void fraction to zero. The applied factors are returned as diagnostics for calibration and verification.

After porosity correction, the model continues to constituent-limit recovery , then rebuilds the dependent stiffness, compliance and output properties. The general porosity and multiphase bounds are supported by References [1]–[6] below.

4 11 Applicability and Limitations

The filled-matrix and hybrid phase models are intended for engineering screening, Workbench deployment, and finite-element material-card generation. The implicit filler model is most appropriate for fine particles at moderate loading, while the explicit phase model is preferred for high filler fraction, large property contrast, non-spherical filler, or systems where filler affects transport properties strongly.

Void modeling is intentionally conservative and should be calibrated against measured porosity/property data when used for qualification or acceptance. The current formulation does not resolve local stress concentrations around individual voids and does not replace a full finite-element RVE when local failure initiation near pores is of interest.

References

[1] R. M. Christensen, *Mechanics of Composite Materials*, Wiley, 1979.
[2] T. Mura, *Micromechanics of Defects in Solids*, 2nd ed., Martinus Nijhoff, 1987.
[3] G. J. Dvorak, *Micromechanics of Composite Materials*, Springer, 2013.
[4] S. Torquato, *Random Heterogeneous Materials: Microstructure and Macroscopic Properties*, Springer, 2002.
[5] J. C. Halpin and J. L. Kardos, "The Halpin–Tsai equations: A review," *Polymer Engineering and Science*, 16, 344–352, 1976.
[6] Z. Hashin and S. Shtrikman, "A variational approach to the theory of the elastic behaviour of multiphase materials," *Journal of the Mechanics and Physics of Solids*, 11, 127–140, 1963.
[7] G. P. Tandon and G. J. Weng, "The effect of aspect ratio of inclusions on the elastic properties of unidirectionally aligned composites," *Polymer Composites*, 5, 327–333, 1984.
[8] R. M. Jones, *Mechanics of Composite Materials*, 2nd ed., Taylor & Francis, 1999.

32 Section 5 - Effective Density and Specific Heat

Online chapter

Section 5 Effective Density and Specific Heat

Volume II Section 5 Effective Density and Specific Heat Capacity

5 1 Purpose and Scope

This section documents the high-level theory used in the solver micromechanics model to predict effective density and effective specific heat capacity for continuous, discontinuous, woven, hybrid, filler-reinforced, and void-containing composite materials. These quantities are thermophysical properties rather than stiffness properties; therefore, the governing equations are based primarily on conservation of mass and conservation of thermal energy rather than strain-concentration tensors. The model treats density and heat capacity as phase-averaged quantities that are evaluated after the phase volume fractions have been normalized.

Figure V-II-S5-1. Phase-volume averaging for effective density

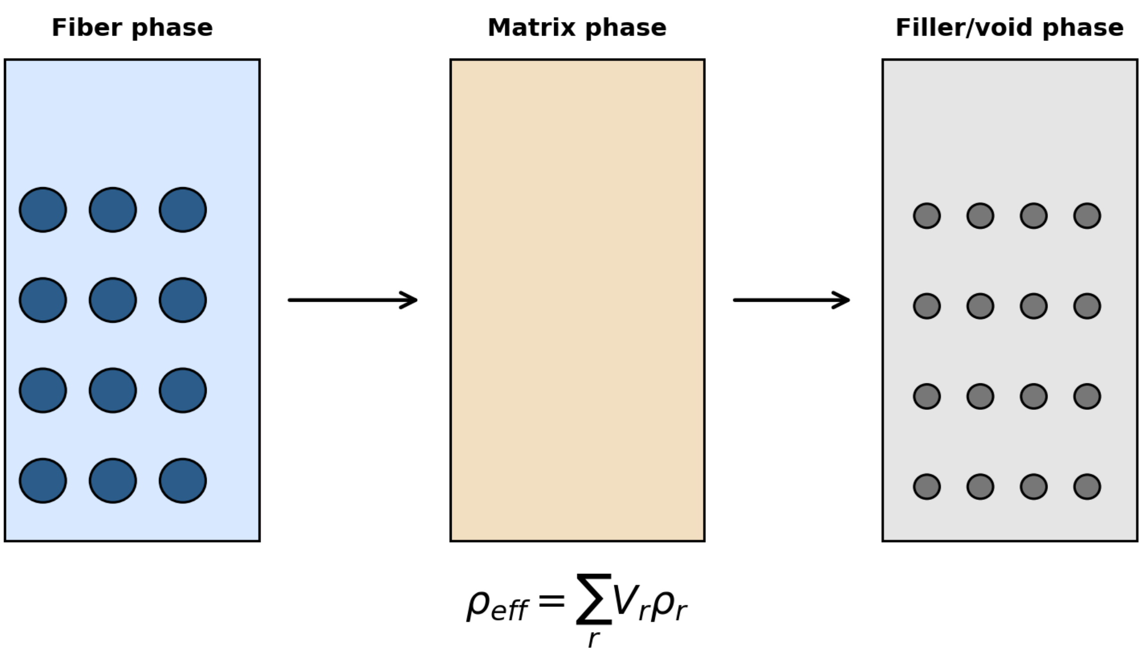

Figure V-II-S5-1. Phase-volume averaging for effective density.

5 2 Phase Definitions and Volume Constraint

The model considers up to four phase classes: fiber, matrix, filler, and void. The phase set is denoted by

$$P = \{f, m, p, v\},$$

where the subscripts represent fiber, matrix, particle/filler, and void, respectively. The normalized phase volume fractions satisfy

$$V_f + V_m + V_p + V_v = 1.$$

For the current Workbench, the filler volume may be treated either explicitly as a separate phase or implicitly as a modification to the matrix. When filler is treated explicitly, the global filler volume fraction is computed from the filler fraction inside the resin-rich phase. When filler is treated implicitly, the matrix density and matrix heat capacity are first modified and then used as effective matrix values in the remaining calculations.

5 3 Effective Density

Density is mass per unit volume. The total mass of the representative volume element is the sum of the phase masses:

$$M = \sum_{r \in P} M_r.$$

For a phase volume $V_r V$ and density ρ_r, the phase mass is

$$M_r = \rho_r V_r V.$$

The effective density is therefore

$$\rho_{eff} = \frac{M}{V} = \sum_{r \in P} V_r \, \rho_r.$$

For the fiber–matrix–filler–void system used by the solver model,

$$\rho_{eff} = V_f \rho_f + V_m \rho_m + V_p \rho_p + V_v \rho_v.$$

The void density is taken to be a very small positive value in the implementation to avoid numerical singularities. For most engineering applications, the void contribution to density is negligible and Eq. (5.6) reduces to the weighted average of the solid phases.

5 4 Explicit and Implicit Filler Treatments

For explicit filler treatment, the filler phase appears directly in Eq. (5.6). The model uses the global phase fractions

$$\{V_f, V_m, V_p, V_v\}$$

and the corresponding densities

$$\{\rho_f, \rho_m, \rho_p, \rho_v\}.$$

For implicit filler treatment, the filled matrix density is computed first:

$$\rho_m^* = (1 - V_{p|m})\rho_m + V_{p|m}\rho_p,$$

where $V_{p|m}$ is the filler volume fraction within the resin phase. The effective density then becomes

$$\rho_{eff} = V_f \rho_f + (1 - V_f - V_v)\rho_m^* + V_v \rho_v.$$

This distinction is important because the same physical filler can be represented either as a separate phase in the homogenization list or as a modified matrix property.

Figure V-II-S5-2. Volumetric heat-capacity averaging

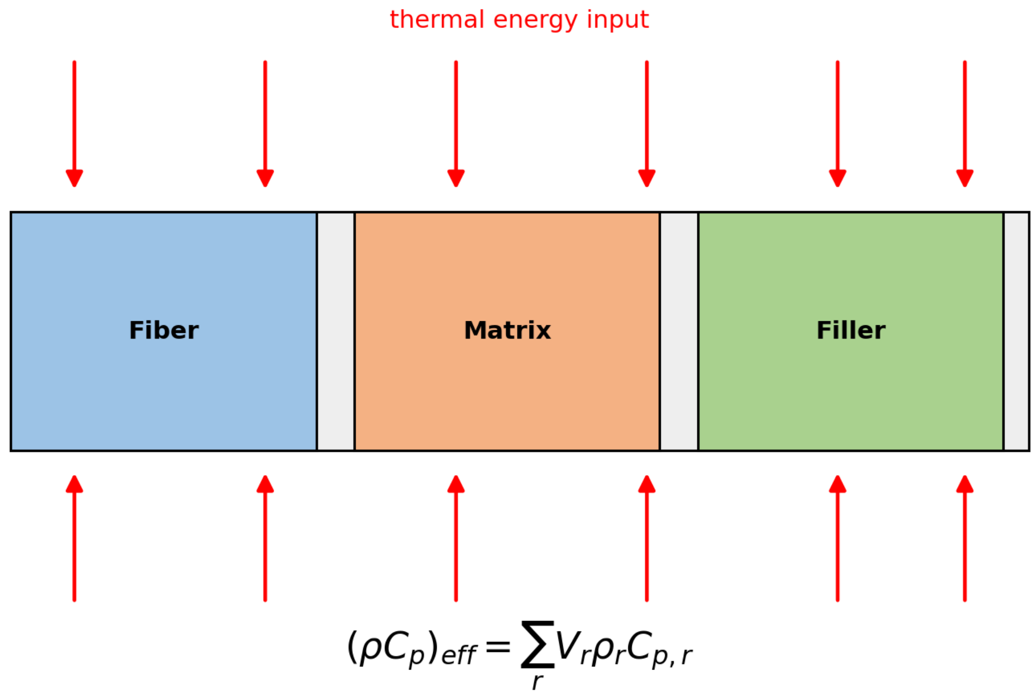

Figure V-II-S5-2. Volumetric heat-capacity averaging.

5 5 Effective Volumetric Heat Capacity

Specific heat capacity is defined per unit mass, while heat storage in a composite representative volume element is naturally additive per unit volume. For a uniform temperature change ΔT, the heat stored in phase r is

$$Q_r = \rho_r C_{p,r} V_r V \Delta T.$$

The total heat stored in the RVE is

$$Q = \sum_{r \in P} Q_r.$$

The effective volumetric heat capacity is therefore

$$\left(\rho C_p\right)_{eff} = \sum_{r \in P} V_r \, \rho_r C_{p,r}.$$

The effective mass-specific heat capacity is obtained by dividing by the effective density:

$$C_{p,eff} = \frac{\sum_{r \in P} V_r \, \rho_r C_{p,r}}{\rho_{eff}}.$$

For fiber, matrix, filler, and void phases,

$$C_{p,eff} = \frac{V_f \rho_f C_{p,f} + V_m \rho_m C_{p,m} + V_p \rho_p C_{p,p} + V_v \rho_v C_{p,v}}{\rho_{eff}}.$$

In most composite analyses the void term is negligible; however, it is retained in the code for consistency with the general multiphase framework.

5 6 Filled-Matrix Heat Capacity

For implicit filler treatment, the filled-matrix volumetric heat capacity is

$$\left(\rho C_p\right)_m^* = \left(1 - V_{p|m}\right) \rho_m C_{p,m} + V_{p|m} \rho_p C_{p,p}.$$

The filled-matrix specific heat is then

$$C_{p,m}^* = \frac{\left(1 - V_{p|m}\right) \rho_m C_{p,m} + V_{p|m} \rho_p C_{p,p}}{\rho_m^*}.$$

This is the form used when the filler is not included as an explicit phase in the global phase list.

5 7 Textile and Fabric Composite Considerations

For woven and stitched fabric composites, density and specific heat are not strongly affected by tow crimp or interlacing in the same way as stiffness. The primary dependence is through the phase volume fractions. However, the fabric architecture affects the final phase fractions because warp, weft, stitch, binder, and matrix-rich regions occupy different portions of the unit cell. A textile RVE may be represented by

$$V_{cell} = V_{warp} + V_{weft} + V_{binder} + V_{matrix} + V_{filler} + V_{void}.$$

The corresponding effective density is

$$\rho_{fabric} = \frac{\rho_{warp} V_{warp} + \rho_{weft} V_{weft} + \rho_{binder} V_{binder} + \rho_m V_m + \rho_p V_p + \rho_v V_v}{V_{cell}}.$$

If the warp and weft tows are made from the same constituent materials and use the same tow fiber volume fraction, the textile density reduces to the phase-averaged expression of Eq. (5.6). If different tow systems are used, Eq. (5.19) provides the appropriate hybrid-fabric form.

5 10 Verification Checks

The density and heat-capacity modules are verified using limiting and conservation checks. If all phases have the same density, then

$$\rho_{eff} = \rho_f = \rho_m = \rho_p.$$

If the fiber volume fraction vanishes and the filler is disabled, then

$$\rho_{eff} \to \rho_m, \qquad C_{p,eff} \to C_{p,m}.$$

If the composite contains only fiber, then

$$\rho_{eff} \to \rho_f, \qquad C_{p,eff} \to C_{p,f}.$$

These limiting checks are useful because density and heat capacity should be exact under phase averaging and should not depend on stiffness-model selection.

5 11 References

- R. M. Jones, *Mechanics of Composite Materials*, 2nd ed., Taylor & Francis, 1999.
- T. Mura, *Micromechanics of Defects in Solids*, 2nd ed., Martinus Nijhoff, 1987.
- G. J. Dvorak, *Micromechanics of Composite Materials*, Springer, 2013.
- C. C. Chamis, "Simplified composite micromechanics equations for hygral, thermal and mechanical properties," *SAMPE Quarterly*, 15, 14–23, 1983.
- R. M. Christensen, *Mechanics of Composite Materials*, Wiley, 1979.
- S. Torquato, *Random Heterogeneous Materials: Microstructure and Macroscopic Properties*, Springer, 2002.
- N. K. Naik, *Woven Fabric Composites*, Technomic, 1994.
- D. Hull and T. W. Clyne, *An Introduction to Composite Materials*, Cambridge University Press, 1996.

33 Section 6 - Thermal Conductivity Micromechanics

Online chapter

Section 6 Thermal Conductivity Micromechanics

Volume II - Section 6 Thermal Conductivity Micromechanics

6 1 Purpose and Scope

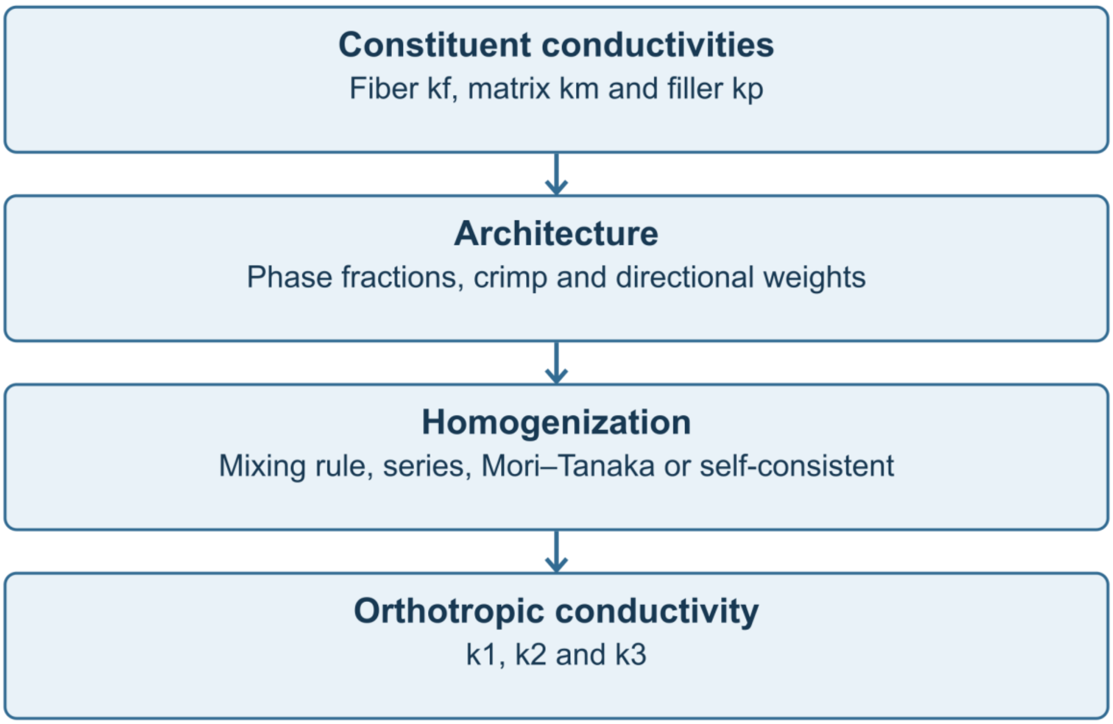

Figure V-II-S6-1. Thermal-conductivity homogenization workflow used by the Workbench micromechanics implementation.

6 2 Local Heat-Conduction Law

The local thermal field is assumed to satisfy Fourier's law in each phase,

$$q_i^{(r)} = -k_{ij}^{(r)} \frac{\partial T^{(r)}}{\partial x_j}$$

where $q_i^{(r)}$ is the phase heat flux vector, $k_{ij}^{(r)}$ is the phase thermal conductivity tensor, and $T^{(r)}$ is the local temperature field. For an effective homogeneous composite, the corresponding macroscopic relation is

$$\overline{q}_i = -k_{ij}^{eff} \frac{\partial \overline{T}}{\partial x_j}.$$

For an orthotropic material aligned with the material principal axes, the conductivity tensor is diagonal,

$$\mathbf{k}^{eff} = \begin{bmatrix} k_1 & 0 & 0 \\ 0 & k_2 & 0 \\ 0 & 0 & k_3 \end{bmatrix}.$$

The solver implementation outputs the three principal components k_1, k_2, and k_3 because these are the values required by Abaqus for an orthotropic conductivity card.

6 3 Rule-of-Mixtures Conductivity Limits

For heat flow parallel to continuous fibers or aligned high-conductivity inclusions, the Voigt-type expression is used,

$$k_{parallel} = \sum_{r=1}^{N_p} V_r\, k_r.$$

For heat flow normal to layered or fiber-like phase paths, the Reuss-type series expression is

$$\frac{1}{k_{series}} = \sum_{r=1}^{N_p} \frac{V_r}{k_r}.$$

For a fiber-matrix-filler-void system, the implemented parallel idealization is

$$k_1 = V_f k_{f1} + V_m k_m + V_p k_p + V_v k_v.$$

The transverse or through-thickness conductivity may be estimated as

$$\frac{1}{k_2} = \frac{V_f}{k_{f2}} + \frac{V_m}{k_m} + \frac{V_p}{k_p} + \frac{V_v}{k_v}$$

and

$$\frac{1}{k_3} = \frac{V_f}{k_{f3}} + \frac{V_m}{k_m} + \frac{V_p}{k_p} + \frac{V_v}{k_v}.$$

In the numerical implementation, the void conductivity k_v is assigned a small positive value rather than zero so that division by zero is avoided.

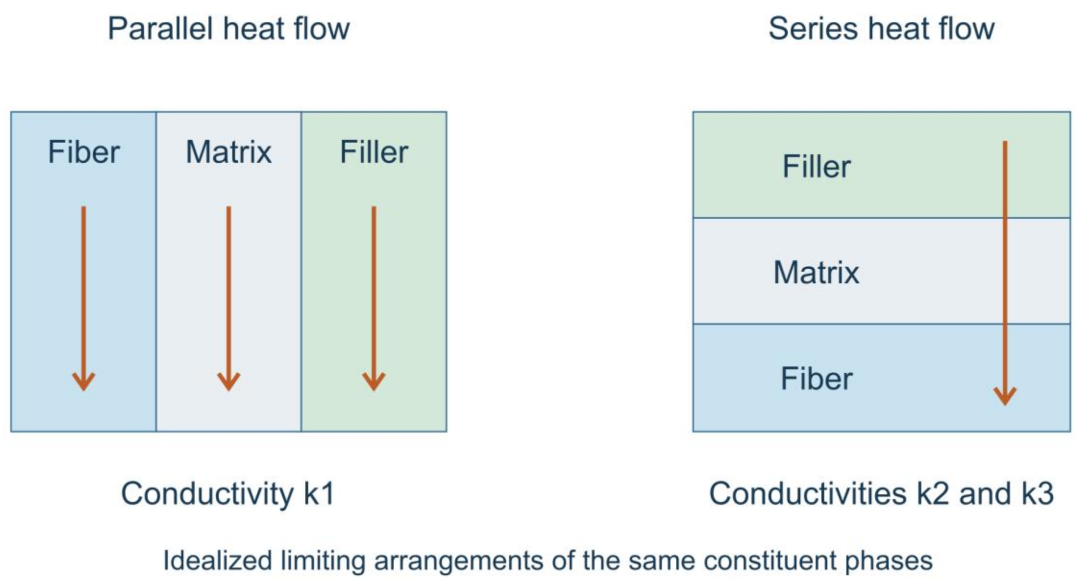

Figure V-II-S6-2. Parallel and series conductivity idealizations used as upper and lower engineering estimates.

6 4 Filler-Modified Matrix Conductivity

If filler is treated implicitly as a matrix modifier, the filled matrix conductivity is estimated using a Maxwell-type expression for dispersed particles,

$$\eta_k = \frac{k_p/k_m - 1}{k_p/k_m + 2},$$

$$k_m^* = k_m \frac{1 + 2\eta_k V_p}{1 - \eta_k V_p}.$$

Here k_m^* is the effective conductivity of the filled resin, k_m is the neat matrix conductivity, k_p is the particulate filler conductivity, and V_p is the filler volume fraction within the resin phase. This expression is consistent with the dilute spherical-inclusion limit and provides a stable engineering model for filled polymer matrices.

If filler is treated explicitly, the filler enters the multiphase conductivity equations through its own global volume fraction.

6 5 Mean-Field Conductivity Approximation

The thermal-conductivity analogue of a mean-field inclusion model can be expressed using a thermal concentration tensor $\mathbf{B}_r$,

$$\mathbf{k}^{eff} = \sum_{r=1}^{N_p} V_r\, \mathbf{k}_r \mathbf{B}_r.$$

For an inclusion phase embedded in a matrix reference medium,

$$\mathbf{B}_r = [\mathbf{I} + \mathbf{P}_r(\mathbf{k}_r - \mathbf{k}_m)]^{-1},$$

where $\mathbf{P}_r$ is a thermal polarization tensor that depends on inclusion geometry and reference conductivity. The current Workbench-safe script does not perform a full tensor integration for $\mathbf{P}_r$; instead, it uses robust engineering approximations based on the parallel, series, filled-matrix, and architecture-corrected expressions.

6 6 Self-Consistent Conductivity Statement

The full self-consistent conductivity problem would embed each phase in the unknown effective medium and solve

$$\sum_{r=1}^{N_p} V_r\,(\mathbf{k}_r - \mathbf{k}^{SC})\mathbf{B}_r = \mathbf{0}.$$

The corresponding fixed-point update is

$$\mathbf{k}^{SC} = \left(\sum_{r=1}^{N_p} V_r\,\mathbf{k}_r\mathbf{B}_r\right)\left(\sum_{r=1}^{N_p} V_r\,\mathbf{B}_r\right)^{-1}.$$

6 7 Textile Architecture Effects

For woven fabrics, conductivity is redistributed by the warp and weft tow architecture. Let w_{warp} and w_{weft} denote the normalized warp and weft fractions. If k_{tow} denotes the tow-axis conductivity and k_t denotes a transverse tow conductivity, the in-plane fabric conductivities are approximated as

$$k_1^{fabric} = f_c\left(w_{warp}k_{tow} + w_{weft}k_t\right),$$

$$k_2^{fabric} = f_c\left(w_{warp}k_t + w_{weft}k_{tow}\right),$$

where f_c is the architecture-adjusted crimp factor. Through-thickness conductivity is reduced by the same architecture penalty in the implemented model,

$$k_3^{fabric} = max(f_c k_3, \epsilon_k),$$

where ϵ_k is a small positive numerical floor. The same architecture framework supports plain weave, twill, satin, basket weave, leno weave, non-crimp stitched fabrics, and triaxial braids.

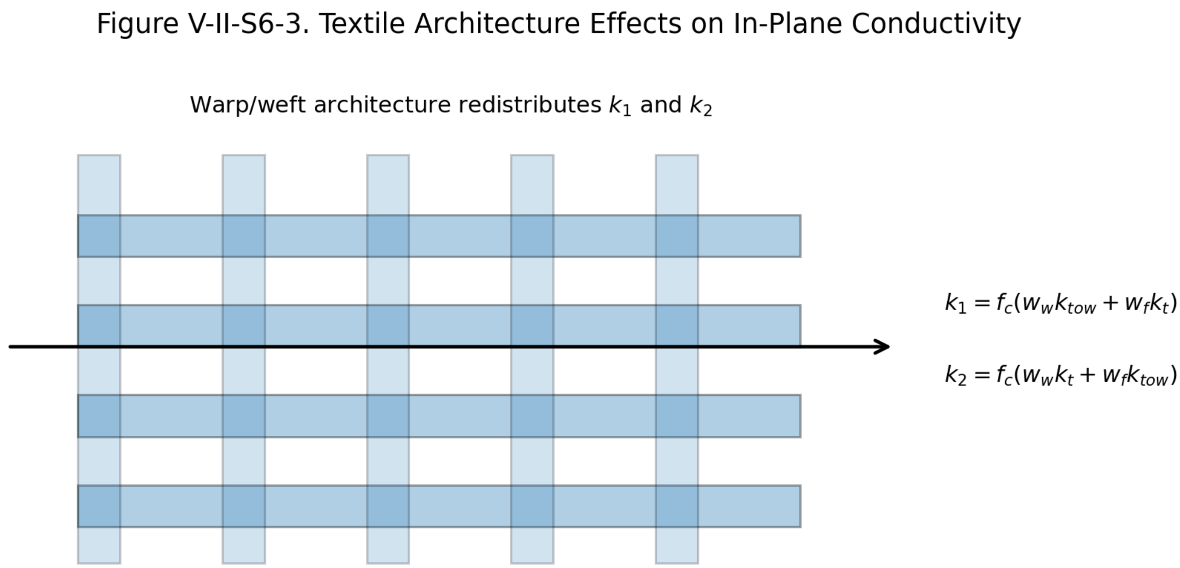

Figure V-II-S6-3. Textile architecture effects on in-plane thermal conductivity.

6 10 Verification Checks

The following checks are recommended for the thermal-conductivity implementation.

- If $V_f = 0$ and no filler is present, the model must recover k_m.
- If $V_f \rightarrow 1$ for aligned continuous fibers, k_1 must approach k_{f1}.
- If the void volume fraction increases, k_2 and k_3 must decrease.
- For a balanced fabric, k_1 and k_2 should approach each other.
- For an unbalanced fabric, k_1/k_2 should track the warp/weft weighting.

6 11 References

Chamis, C. C. (1983). Simplified composite micromechanics equations for hygral, thermal and mechanical properties. *SAMPE Quarterly*, 15, 14-23.

Mura, T. (1987). *Micromechanics of Defects in Solids*. Martinus Nijhoff.

Benveniste, Y. (1987). A new approach to the application of Mori-Tanaka's theory in composite materials. *Mechanics of Materials*, 6, 147-157.

Dvorak, G. J. (2013). *Micromechanics of Composite Materials*. Springer.

Torquato, S. (2002). *Random Heterogeneous Materials: Microstructure and Macroscopic Properties*. Springer.

Jones, R. M. (1999). *Mechanics of Composite Materials*. Taylor & Francis.

34 Section 7 - CTE Micromechanics

Online chapter

Section 7 CTE Micromechanics

Volume II - Section 7 Effective Thermal Expansion and Thermoelastic Micromechanics

7 1 Purpose and Scope

This section documents the coefficient of thermal expansion (CTE) models used by the Workbench micromechanics code. The thermal expansion module converts constituent thermal expansion data for fiber, matrix, filler, void, tow, and fabric phases into effective orthotropic engineering properties. The final outputs are the three material-axis thermal expansion coefficients in directions 1, 2 and 3, which are exported to both effective properties and Abaqus material cards.

The implementation is intentionally consistent with the mechanical micromechanics framework. The same volume fractions, fabric architecture flags, crimp factors, warp/weft weighting factors, and filler/void corrections used for stiffness prediction are also used to assemble thermoelastic material properties.

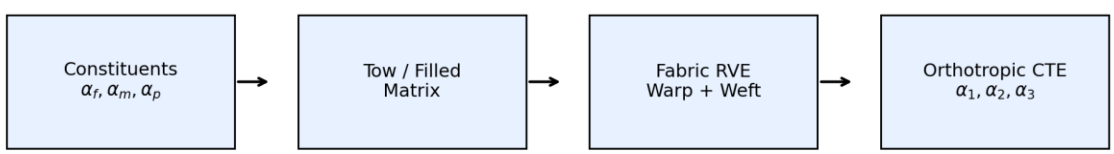

Figure V-II-S7-1. Multiscale CTE prediction workflow.

Figure V-II-S7-1. Multiscale CTE prediction workflow.

7 2 Thermal Strain and Thermoelastic Constitutive Law

For a homogeneous orthotropic material subjected to a temperature increment ΔT, the free thermal strain vector in engineering notation is written as

$$\boldsymbol{\varepsilon}^{th} = \boldsymbol{\alpha} \quad \Delta T$$

where

$$\boldsymbol{\alpha} = [\alpha_1 \quad \alpha_2 \quad \alpha_3 \quad 0 \quad 0 \quad 0]^T.$$

The thermoelastic stress-strain relation is

$$\boldsymbol{\sigma} = \mathbf{C}(\boldsymbol{\varepsilon} - \boldsymbol{\alpha}\Delta T),$$

where C is the effective stiffness matrix. This form is the basis for the Abaqus *EXPANSION, TYPE=ORTHO export generated by the solver script.

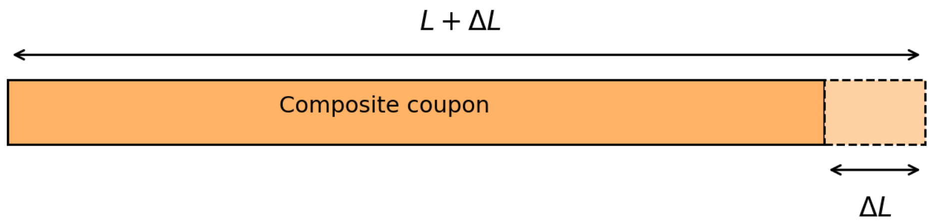

Figure V-II-S7-2. Thermal expansion of an orthotropic composite coupon.

Figure V-II-S7-2. Thermal expansion of an orthotropic composite coupon.

7 3 Phase-Averaged Expansion in Composite Constituents

For a composite with fiber, matrix, filler, and void phases, the unconstrained volumetric expansion estimate is

$$\alpha^{mix} = V_f \alpha_f + V_m \alpha_m + V_p \alpha_p + V_v \alpha_v.$$

The phase-volume constraint is

$$V_f + V_m + V_p + V_v = 1.$$

Because voids do not carry significant thermal stress, the model normally sets the void thermal expansion contribution to zero for the void contribution and accounts for voids primarily through dilution of load-carrying and heat-carrying phases.

7 4 Stiffness-Weighted Longitudinal CTE

For continuous fiber composites, axial expansion is constrained by the stiffness of the phases in the fiber direction. The longitudinal CTE estimate used by the model is therefore stiffness weighted:

$$\alpha_1 = \frac{V_f E_{f1} \alpha_{f1} + V_m E_m \alpha_m + V_p E_p \alpha_p}{V_f E_{f1} + V_m E_m + V_p E_p}.$$

This expression captures the fact that high-modulus fibers dominate axial expansion even when the matrix has a much larger unconstrained thermal expansion coefficient.

7 5 Transverse and Through-Thickness CTE Estimates

The current engineering implementation uses mixture-style transverse and through-thickness expansion estimates:

$$\alpha_2 = V_f \alpha_{f2} + V_m \alpha_m + V_p \alpha_p + V_v \alpha_v,$$

$$\alpha_3 = V_f \alpha_{f3} + V_m \alpha_m + V_p \alpha_p + V_v \alpha_v.$$

7 6 Filled-Matrix CTE

When the filler is treated implicitly as part of the resin-rich phase, the filled matrix CTE is estimated by phase averaging:

$$\alpha_m^* = \left(1 - V_p^{res}\right)\alpha_m + V_p^{res}\alpha_p,$$

where the resin filler fraction is the filler volume fraction inside the resin phase. This filled-matrix value is then used as the matrix phase input for subsequent fiber and fabric homogenization.

7 7 Fabric Architecture Effects on CTE

For textile composites, warp and weft directions exchange the roles of axial and transverse tow properties. The model uses architecture-weighted CTE assembly:

$$\alpha_1^{fab} = w_{warp}\alpha_{tow,1} + w_{weft}\alpha_{tow,2},$$

$$\alpha_2^{fab} = w_{warp}\alpha_{tow,2} + w_{weft}\alpha_{tow,1},$$

where the warp and weft weights are normalized fabric architecture fractions satisfying

$$w_{warp} + w_{weft} = 1.$$

Crimp and architecture effects modify the mechanical constraints and thermal directions indirectly through the same factors used in stiffness assembly.

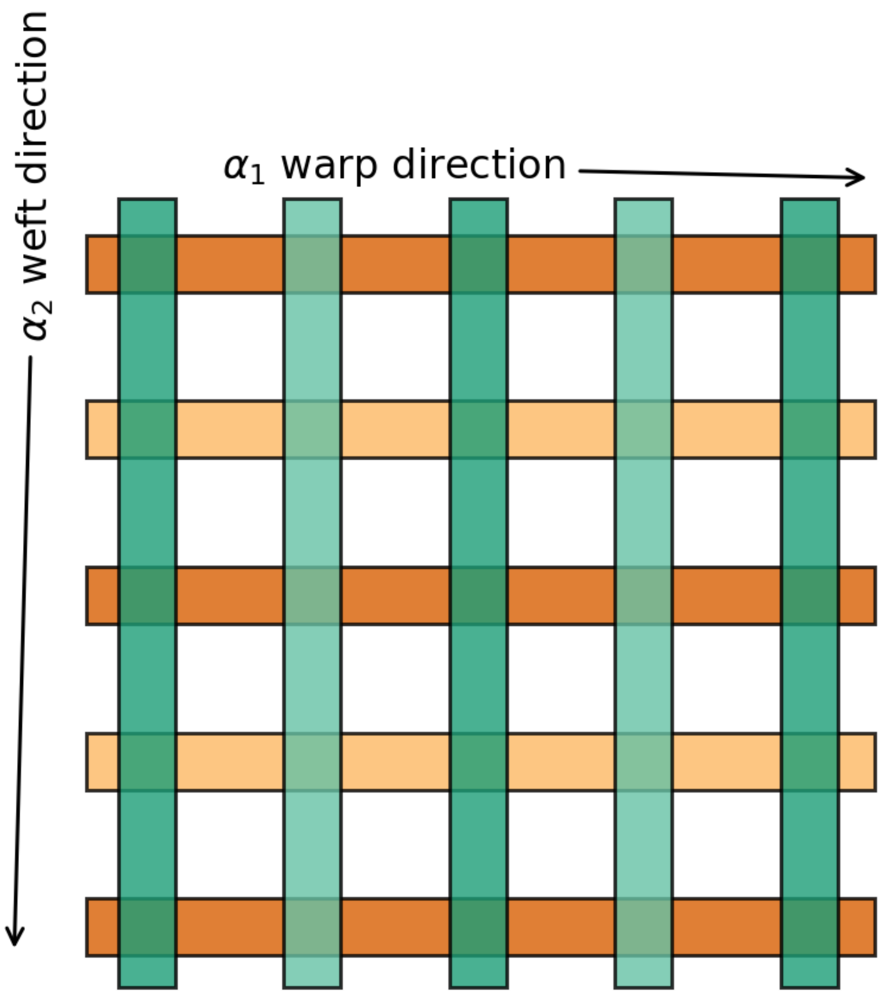

Figure V-II-S7-3. Warp/weft CTE directions in a woven RVE.

Figure V-II-S7-3. Warp/weft CTE directions in a woven RVE.

7 8 Architecture Library and CTE Interpretation

The fabric architecture flag controls the interpretation of the warp/weft CTE assembly. Plain weaves usually exhibit larger crimp and stronger interlacing effects. Satin weaves usually have lower interlacing and reduced tow waviness. Non-crimp fabrics preserve near-straight tow paths and therefore maintain stronger directional anisotropy. Triaxial braids introduce bias-angle effects that couple the two in-plane expansion directions.

The implemented fabric architecture set includes:

- plain weave,
- 2 by 2 twill,

- 4-harness satin,
- 5-harness satin,
- 8-harness satin,
- basket weave,
- leno weave,
- non-crimp biaxial stitched fabric,
- triaxial braid.

7 11 Representative CTE Trend

The stiffness-weighted expression causes the longitudinal CTE of carbon/epoxy composites to decrease rapidly with increasing fiber volume fraction because carbon fibers have low or negative axial CTE and high axial stiffness.

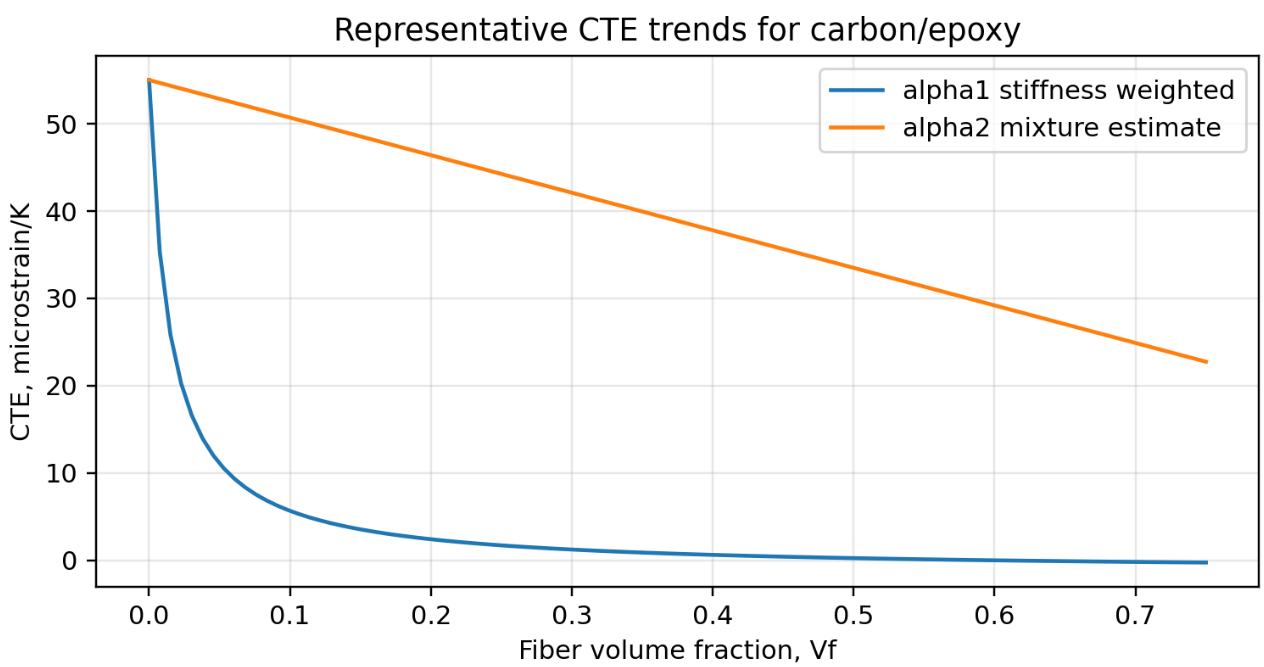

Figure V-II-S7-4. Example CTE trend versus fiber volume fraction.

Figure V-II-S7-4. Example CTE trend versus fiber volume fraction.

7 12 Assumptions and Limitations

The current CTE implementation is an engineering micromechanics approximation. It is appropriate for rapid material-property prediction, Workbench integration, and finite-element preprocessing. It does not solve the full thermoelastic inclusion boundary-value problem for arbitrary ellipsoidal inclusions. For high-fidelity thermoelastic homogenization, the full fourth-order concentration tensors from Mori-Tanaka or self-consistent theory should be coupled directly to the phase eigenstrain tensors.

The implemented model assumes:

- small-strain linear thermoelasticity,
- temperature-independent constituent properties unless externally updated,
- orthotropic effective material axes,

- architecture correction factors shared with the mechanical model,
- voids contribute negligibly to stiffness and thermal expansion constraint.

7 13 References

- Jones, R. M. *Mechanics of Composite Materials*. Taylor & Francis, 1999.
- Chou, T. W. *Microstructural Design of Fiber Composites*. Cambridge University Press, 1992.
- Mura, T. *Micromechanics of Defects in Solids*. Martinus Nijhoff, 1987.
- Dvorak, G. J. *Micromechanics of Composite Materials*. Springer, 2013.
- Schapery, R. A. Thermal expansion coefficients of composite materials based on energy principles. *Journal of Composite Materials*, 1968.
- Rosen, B. W. Thermoelastic behavior of fiber composites. In *Fiber Composite Materials*, ASM, 1965.
- Hashin, Z. Analysis of composite materials - A survey. *Journal of Applied Mechanics*, 1983.
- Ishikawa, T. and Chou, T. W. Stiffness and strength behavior of woven fabric composites. *Journal of Materials Science*, 1982.
- Naik, N. K. *Woven Fabric Composites*. Technomic, 1994.

35 Section 8 - Orthotropic Thermophysical Property Assembly

Online chapter

Section 8 Orthotropic Thermophysical Property Assembly

Volume II - Section 8

Orthotropic Thermophysical Property Assembly and Finite Element Material Definition

8 1 Purpose and Scope

This section describes the final assembly stage used by the Workbench solver micromechanics model to collect the mechanical and thermophysical predictions developed in the preceding sections of Volume II. The goal is to transform the homogenized composite response into a practical engineering material definition suitable for finite element analysis. The assembled output contains orthotropic elastic constants, density, coefficient of thermal expansion, thermal conductivity, and specific heat capacity.

The assembly operation is not a separate micromechanics theory by itself. Rather, it is the final bookkeeping and constitutive closure step that ensures all predicted properties are placed into consistent material directions and exported through the same data structures used by Workbench and Abaqus.

Figure V-II-S8-1. Orthotropic thermophysical property assembly workflow

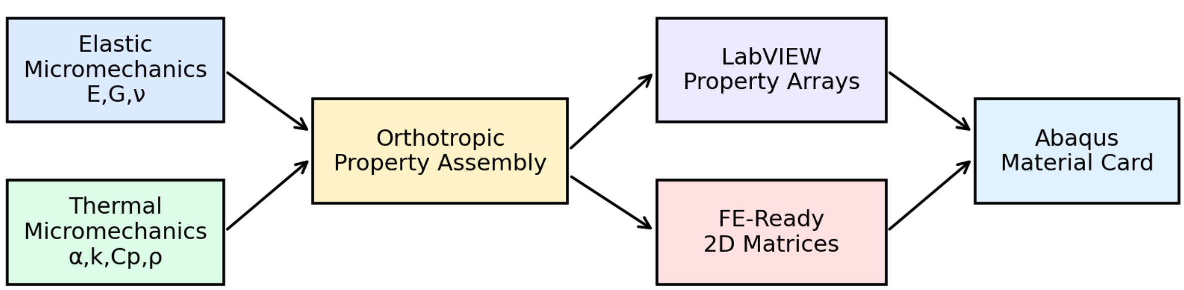

Figure V-II-S8-1. Orthotropic thermophysical property assembly workflow.

8 2 Effective Property Set

The final orthotropic property set is written as

$$\mathbf{P}^{eff} = \{E_1, E_2, E_3, G_{12}, G_{13}, G_{23}, \nu_{12}, \nu_{13}, \nu_{23}, \rho, \alpha_1, \alpha_2, \alpha_3, k_1, k_2, k_3, C_p\}^T.$$

Here, E_i are the orthotropic Young's moduli, G_{ij} are the orthotropic shear moduli, ν_{ij} are the major Poisson ratios, ρ is the effective density, α_i are the coefficients of thermal expansion, k_i are the principal thermal conductivities, and C_p is the effective specific heat capacity.

The model stores the same assembled property set in the effective properties

$$\mathbf{P}_{ortho}^{LV} = \mathbf{P}^{eff}, \qquad \mathbf{P}_{eff}^{LV} = \mathbf{P}^{eff}.$$

This duplication is intentional. The orthotropic vector is used directly for engineering review, while the effective-property vector provides a generic interface for downstream software modules.

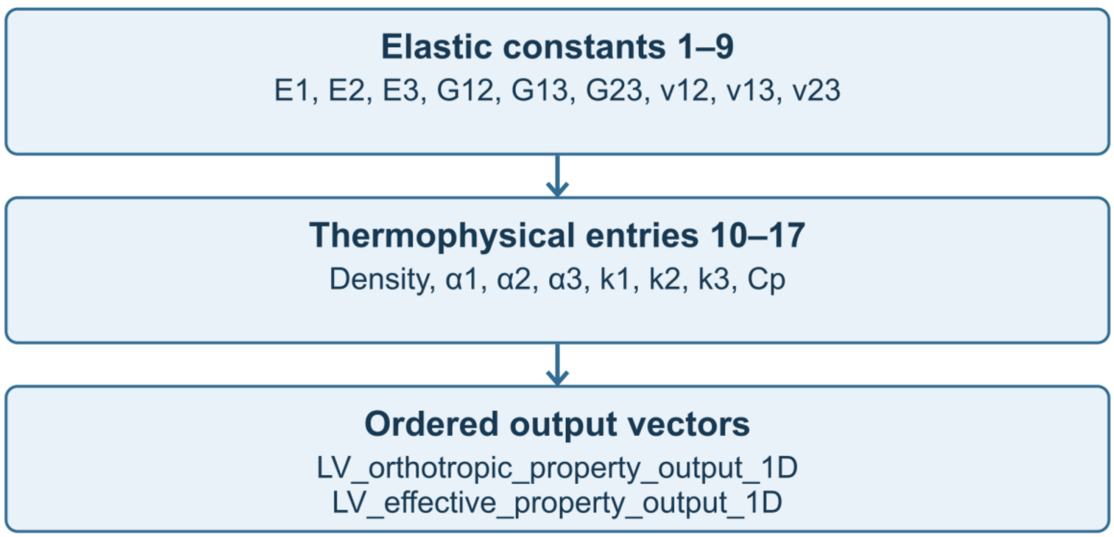

Figure V-II-S8-2. Effective property vector mapping for Workbench export.

8 3 Orthotropic Compliance Matrix

For finite element use, the orthotropic engineering constants are first assembled into the compliance matrix

$$
\mathbf{S} = \begin{bmatrix} \frac{1}{E_1} & -\frac{\nu_{12}}{E_1} & -\frac{\nu_{13}}{E_1} & 0 & 0 & 0 \\ -\frac{\nu_{12}}{E_1} & \frac{1}{E_2} & -\frac{\nu_{23}}{E_2} & 0 & 0 & 0 \\ -\frac{\nu_{13}}{E_1} & -\frac{\nu_{23}}{E_2} & \frac{1}{E_3} & 0 & 0 & 0 \\ 0 & 0 & 0 & \frac{1}{G_{23}} & 0 & 0 \\ 0 & 0 & 0 & 0 & \frac{1}{G_{13}} & 0 \\ 0 & 0 & 0 & 0 & 0 & \frac{1}{G_{12}} \end{bmatrix}.
$$

The stiffness matrix used for anisotropic finite element export is obtained by inversion,

$$
\mathbf{C} = \mathbf{S}^{-1}.
$$

In the solver implementation this matrix is returned as both an orthotropic FE stiffness matrix and an anisotropic FE stiffness matrix. The orthotropic matrix is the symmetric stiffness constructed from engineering constants. The anisotropic matrix is the same matrix in the present model unless additional coupling terms are introduced by future orientation, damage, or transformation modules.

8 4 Thermoelastic Constitutive Form

The coupled orthotropic thermoelastic stress-strain relation is

$$
\boldsymbol{\sigma} = \mathbf{C}(\boldsymbol{\varepsilon} - \boldsymbol{\alpha}\Delta T),
$$

where

$$
\boldsymbol{\alpha} = [\alpha_1 \quad \alpha_2 \quad \alpha_3 \quad 0 \quad 0 \quad 0]^T.
$$

For finite element applications, the thermal strain vector is

$$
\boldsymbol{\varepsilon}^{th} = \boldsymbol{\alpha}\Delta T.
$$

The mechanical strain used in the constitutive update is therefore

$$
\boldsymbol{\varepsilon}^{mech} = \boldsymbol{\varepsilon} - \boldsymbol{\varepsilon}^{th}.
$$

Figure V-II-S8-4. Coupled orthotropic thermoelastic constitutive structure

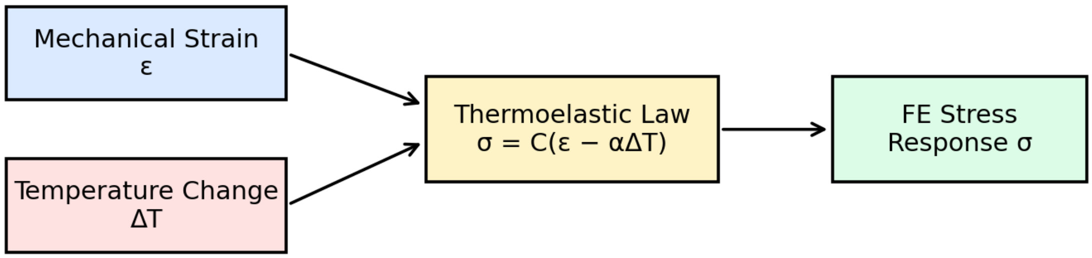

Figure V-II-S8-4. Coupled orthotropic thermoelastic constitutive structure.

8 5 Density and Heat Capacity Closure

The density and specific heat terms are scalar quantities in the finite element material definition. The effective density used in the FE card is

$$\rho^{FE} = \rho^{eff}.$$

The effective specific heat is exported as

$$C_p^{FE} = C_p^{eff}.$$

These values should be interpreted as homogenized continuum properties per unit mass of the equivalent composite material. In coupled thermal analyses, the volumetric heat capacity is

$$\left(\rho C_p\right)^{FE} = \rho^{eff} C_p^{eff}.$$

8 6 Thermal Conductivity Tensor

The orthotropic thermal conductivity matrix is assembled as

$$\mathbf{k} = \begin{bmatrix} k_1 & 0 & 0 \\ 0 & k_2 & 0 \\ 0 & 0 & k_3 \end{bmatrix}.$$

The corresponding heat-flux equation is Fourier's law,

$$\mathbf{q} = -\mathbf{k}\nabla T.$$

For an orthotropic material aligned with the finite element material coordinate system, the conductivity values are exported directly as k_1, k_2, and k_3. If a global material orientation is applied in the structural model, the finite element solver performs the required transformation through the assigned material orientation.

8 8 Abaqus Material Definition

The assembled material properties are written to the single Workbench string variable

$$LV\_abaqus\_material\_card\_string.$$

For an orthotropic engineering-constant definition, the basic Abaqus elastic card is

```
*MATERIAL, NAME=MICROMECHANICS_COMPOSITE
*ELASTIC, TYPE=ENGINEERING CONSTANTS
E1, E2, E3, NU12, NU13, NU23, G12, G13, G23
```

The thermophysical extension appends

```
*DENSITY
rho_eff
*EXPANSION, TYPE=ORTHO
alpha1_eff, alpha2_eff, alpha3_eff
*CONDUCTIVITY, TYPE=ORTHO
k1_eff, k2_eff, k3_eff
*SPECIFIC HEAT
Cp_eff
```

The anisotropic stiffness option exports the independent stiffness coefficients from the 6×6 stiffness matrix rather than engineering constants.

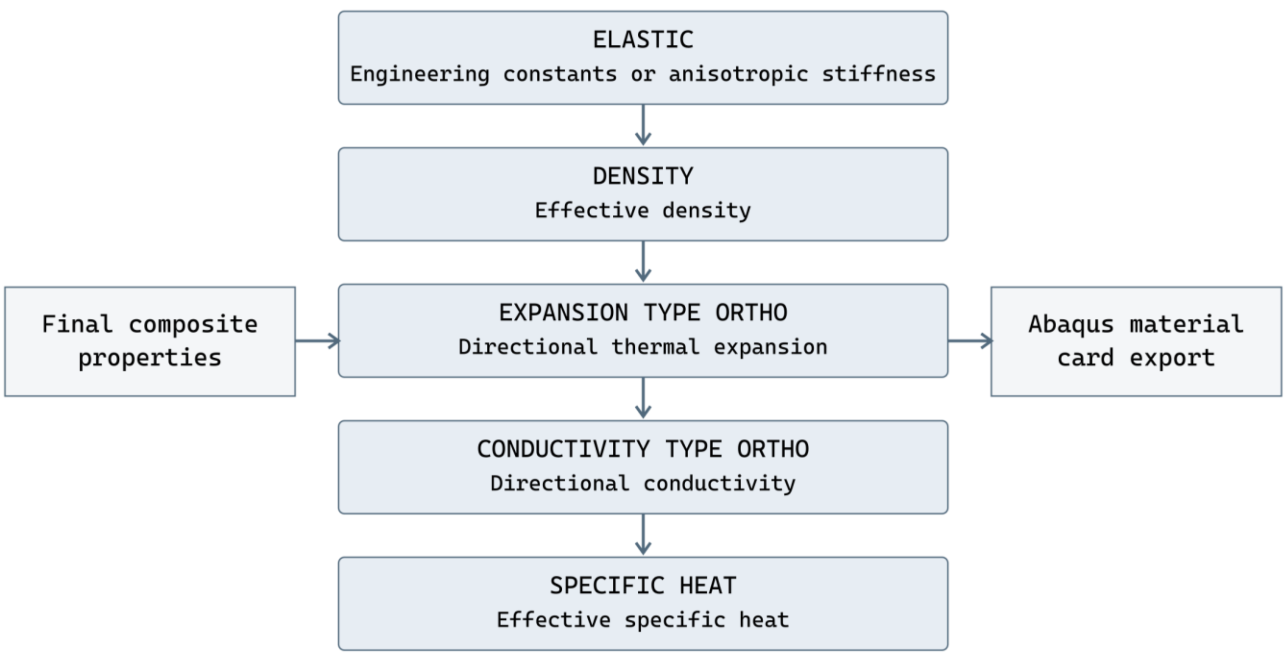

Figure V-II-S8-3. Thermomechanical Abaqus material-card assembly.

8 9 Verification Checks

The final assembly stage should satisfy the following basic consistency checks:

$$E_i > 0, \qquad G_{ij} > 0, \qquad k_i > 0, \qquad \rho > 0, \qquad C_p > 0.$$

The compliance and stiffness matrices should be symmetric,

$$\mathbf{S} = \mathbf{S}^T, \qquad \mathbf{C} = \mathbf{C}^T.$$

The stiffness matrix should be positive definite for a stable linear elastic material,

$$\mathbf{x}^T \mathbf{C} \mathbf{x} > 0 \quad \text{for all nonzero} \quad \mathbf{x}.$$

The thermal properties should also remain within physically reasonable bounds for the selected constituents and architecture.

8 11 Summary

The orthotropic thermophysical assembly step closes the multiscale modeling sequence by collecting all predicted properties into a consistent finite element material description. Mechanical constants are assembled into compliance and stiffness matrices. Density, thermal expansion, thermal conductivity, and specific heat are appended to complete the thermomechanical material definition. This final assembly enables direct use of the micromechanics results in Workbench workflows and Abaqus finite element simulations.

References

- R. M. Jones, *Mechanics of Composite Materials*, Taylor & Francis, 1999.
- G. J. Dvorak, *Micromechanics of Composite Materials*, Springer, 2013.
- T. Mura, *Micromechanics of Defects in Solids*, Martinus Nijhoff, 1987.
- Y. Benveniste, "A new approach to the application of Mori-Tanaka's theory in composite materials," *Mechanics of Materials*, 6, 147-157, 1987.
- T.-W. Chou, *Microstructural Design of Fiber Composites*, Cambridge University Press, 1992.
- Dassault Systemes, *Abaqus Analysis User's Guide*, material definitions for engineering constants, expansion, conductivity, density, and specific heat.

36 Section 9 - Verification Validation and References

Online chapter

Section 9 Verification Validation and References

Volume II - Section 9

Verification Validation and References for Textile and Thermophysical Micromechanics

9 1 Purpose and Scope

This section summarizes the recommended verification and validation methodology for the textile, hybrid, filled-matrix, and thermophysical property models described in Volume II. The purpose is to document how the implemented solver model should be checked against mathematical limits, engineering benchmarks, and published reference data before the output is used for finite-element material definition or Workbench-based design workflows.

The verification process confirms that the implementation obeys expected limiting behavior, conservation laws, tensor symmetry, and material-property bounds. The validation process compares the model predictions with independent data, such as coupon-level textile composite measurements, constituent mixture data, thermophysical test data, and published micromechanics benchmarks.

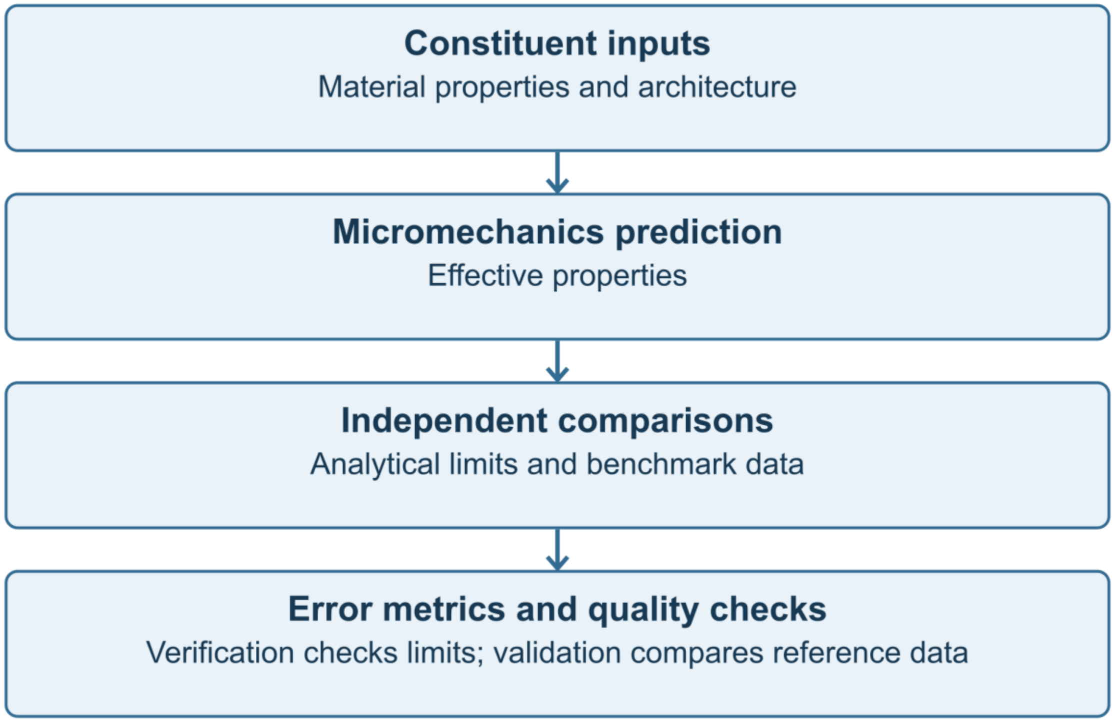

Figure V-II-S9-1. Verification and validation workflow for the textile and thermophysical micromechanics modules.

9 2 Verification Philosophy

Verification asks whether the equations have been implemented correctly. For the present model, verification is performed by exercising the code under controlled limiting cases. The general verification requirement is written as

$$\lim_{\mathbf{x}\to\mathbf{x}_0} \mathbf{P}^{model}(\mathbf{x}) = \mathbf{P}^{expected}(\mathbf{x}_0)$$

where $\mathbf{x}$ is the vector of input variables and $\mathbf{P}$ is the predicted effective property vector. For Volume II, the property vector includes elastic, density, specific heat, thermal conductivity, and thermal expansion terms,

$$\mathbf{P}^{eff} = \left[E_1, E_2, E_3, G_{12}, G_{13}, G_{23}, \nu_{12}, \nu_{13}, \nu_{23}, \rho, \alpha_1, \alpha_2, \alpha_3, k_1, k_2, k_3, C_p\right]^T.$$

The normalized verification error for a scalar property is

$$\epsilon_P = \frac{\left|P^{model} - P^{expected}\right|}{max\left(\left|P^{expected}\right|, P_{floor}\right)}.$$

For a vector of properties, the global relative error is

$$\epsilon_{\mathbf{P}} = \frac{\|\mathbf{P}^{model} - \mathbf{P}^{expected}\|_2}{max\left(\|\mathbf{P}^{expected}\|_2, P_{floor}\right)}.$$

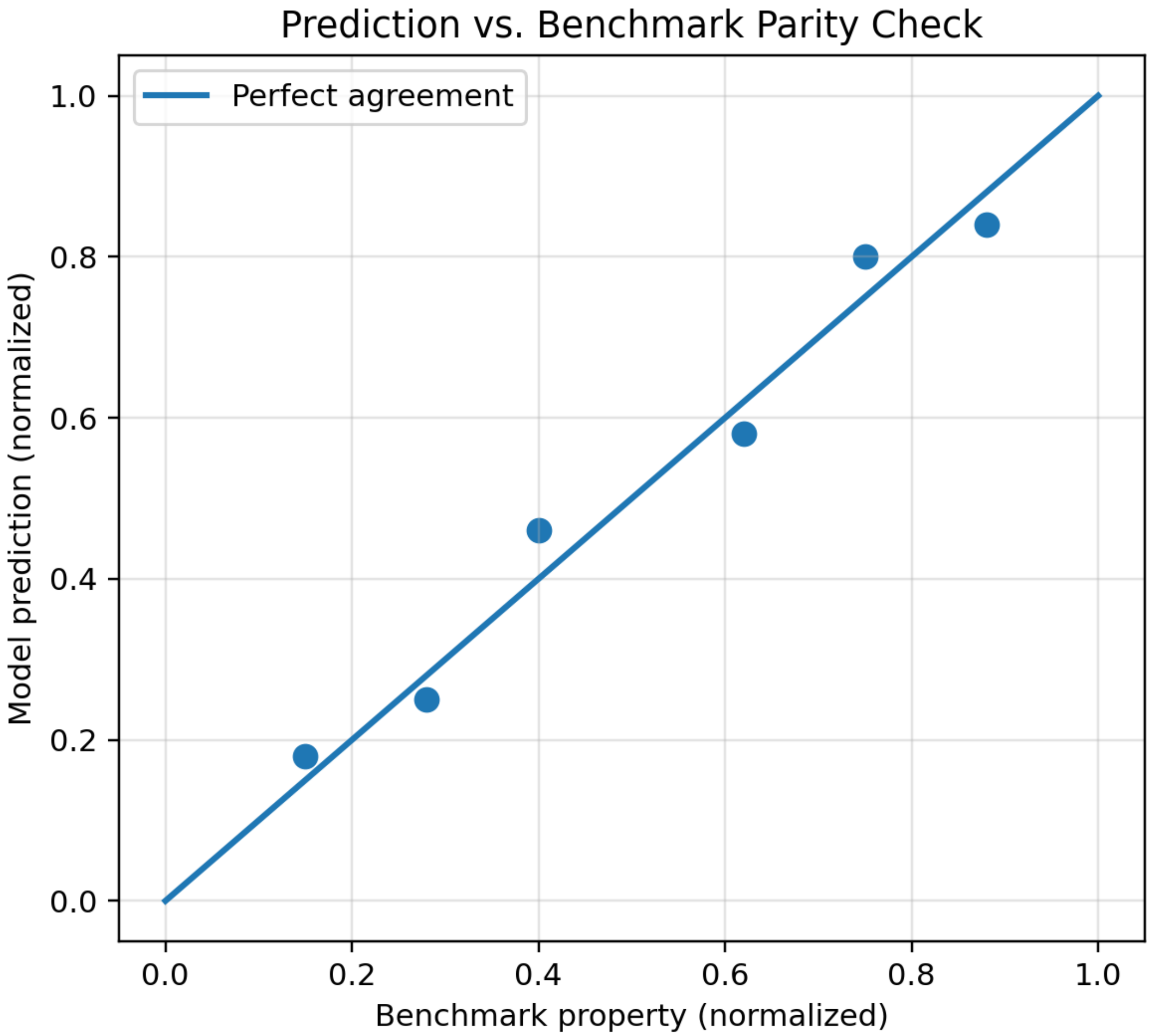

Figure V-II-S9-2. Generic parity plot used to compare model predictions against benchmark data.

9 3 Limiting-Case Checks

The most important verification cases are the limiting conditions that recover known material behavior. When the fiber volume fraction approaches zero, the composite must recover the filled or neat matrix response,

$$\lim_{V_f \to 0} \mathbf{P}^{eff} = \mathbf{P}_m^*.$$

When the filler volume fraction approaches zero, the filled matrix must reduce to the neat resin,

$$\lim_{V_p \to 0} \mathbf{P}_m^* = \mathbf{P}_m.$$

When the void volume fraction approaches zero, the void-corrected property must reduce to the non-voided composite property,

$$\lim_{V_v \to 0} \mathbf{P}^{voided} = \mathbf{P}^{solid}.$$

For a balanced woven composite with equal warp and weft fractions and identical tow properties, the in-plane moduli should approach one another,

$$V_{warp} = V_{weft}, \quad \mathbf{C}_{warp} = \mathbf{C}_{weft} \quad \Rightarrow \quad E_1 \approx E_2.$$

If the crimp amplitude approaches zero, the crimp knockdown should approach unity,

$$\lim_{A/\lambda \to 0} f_{crimp} = 1.$$

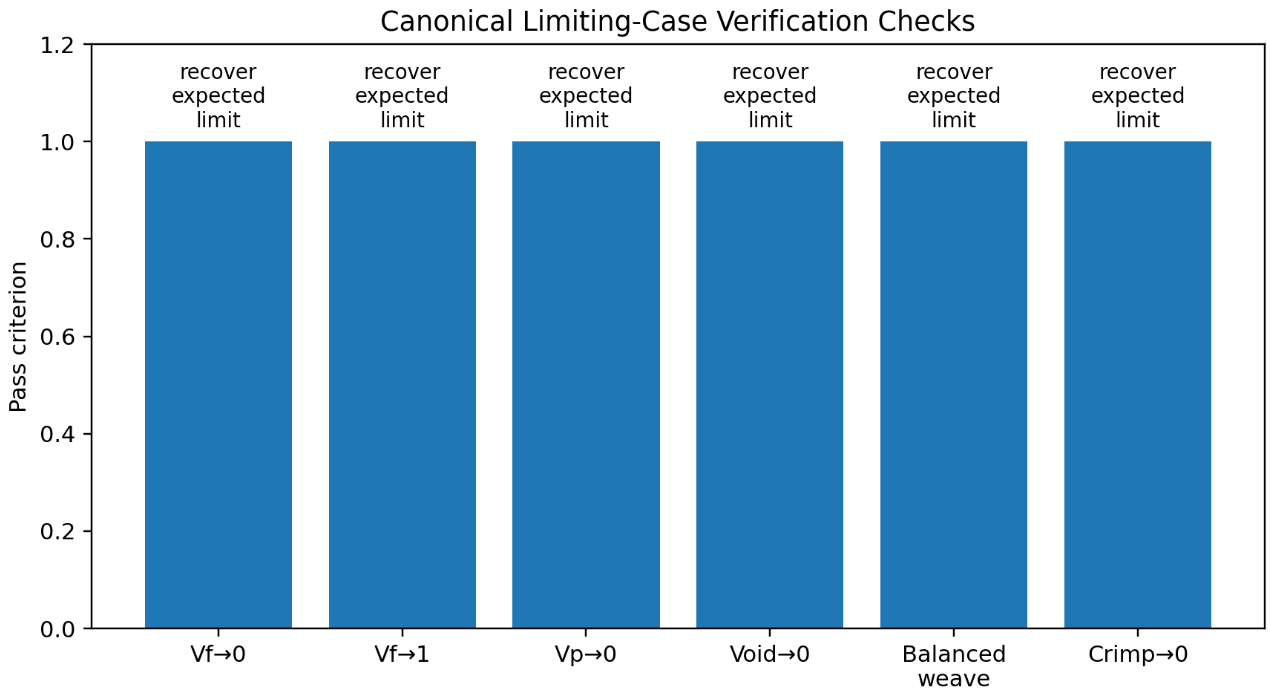

Figure V-II-S9-3. Limiting-case checks used to verify textile and thermophysical model behavior.

9 4 Thermophysical Property Verification

Density is verified using conservation of mass. The implemented effective density must equal the volume-weighted sum of all active phases,

$$\rho^{eff} = \sum_{r=1}^{N_p} V_r \, \rho_r.$$

The specific heat is verified by checking conservation of thermal energy,

$$C_p^{eff} = \frac{\sum_{r=1}^{N_p} V_r \, \rho_r C_{p,r}}{\sum_{r=1}^{N_p} V_r \, \rho_r}.$$

The longitudinal and transverse thermal conductivity predictions should remain bounded by the parallel and series estimates,

$$\left(\sum_{r=1}^{N_p} \frac{V_r}{k_r}\right)^{-1} \leq k_i^{eff} \leq \sum_{r=1}^{N_p} V_r\, k_r.$$

The CTE prediction should approach the matrix expansion coefficient as reinforcement volume fraction approaches zero,

$$\lim_{V_f, V_p \to 0} \alpha_i^{eff} = \alpha_m.$$

For a stiff, low-CTE fiber in a polymer matrix, the axial CTE should typically decrease as fiber volume fraction increases,

$$\frac{\partial \alpha_1^{eff}}{\partial V_f} < 0 \quad for \quad E_f \gg E_m, \quad \alpha_f < \alpha_m.$$

9 5 Textile Architecture Verification

Architecture factors should produce physically meaningful trends. The architecture-corrected fabric stiffness may be expressed schematically as

$$E_1^{fabric} = f_c f_b \left(w_{warp} E_{tow} + w_{weft} E_{trans}\right)$$

and

$$E_2^{fabric} = f_c f_b \left(w_{warp} E_{trans} + w_{weft} E_{tow}\right).$$

For an unbalanced fabric, increasing the warp fraction should increase E_1 and reduce E_2 relative to the balanced case,

$$\frac{\partial E_1}{\partial w_{warp}} > 0, \qquad \frac{\partial E_2}{\partial w_{warp}} < 0.$$

The in-plane shear modulus is penalized by interlacing and crimp corrections,

$$G_{12}^{fabric} = f_c f_s f_i G_{12}^{tow}.$$

For low-interlacing satin architectures, the interlacing penalty should be weaker than for plain weave,

$$f_i^{satin} > f_i^{plain}.$$

For non-crimp fabric, the crimp factor should be close to unity, subject to any stitching knockdown,

$$f_c^{NCF} \approx f_{stitch}.$$

9 6 Validation Against Benchmark Data

Validation compares model predictions against experimental or published benchmark values. For each benchmark property P_j, the percentage error is

$$Error_j = 100 \frac{P_j^{model} - P_j^{data}}{P_j^{data}}.$$

For a set of n properties, the mean absolute percentage error is

$$MAPE = \frac{100}{n} \sum_{j=1}^{n} \left| \frac{P_j^{model} - P_j^{data}}{P_j^{data}} \right|.$$

A root-mean-square normalized error may also be used,

$$RMSE_{norm} = \sqrt{\frac{1}{n} \sum_{j=1}^{n} \left(\frac{P_j^{model} - P_j^{data}}{P_j^{data}} \right)^2}.$$

The recommended benchmark classes are summarized in Figure V-II-S9-4.

Property	Benchmark	Expected Trend
Density	mass/volume	linear volume average
Specific heat	calorimetry	mass-weighted average
Conductivity	guarded hot plate	parallel/series bounds
CTE	dilatometry	stiffness-weighted axial response
Fabric stiffness	coupon tests	crimp/interlacing knockdown

Figure V-II-S9-4. Recommended validation matrix for Volume II textile and thermophysical predictions.

9 7 Recommended Validation Cases

The following validation cases are recommended for the current implementation:

- **Balanced plain-weave carbon/epoxy:** verify $E_1 \approx E_2$, CTE balance, and crimp knockdown.
- **Unbalanced woven glass/epoxy:** verify sensitivity to warp/weft fraction.
- **Satin carbon/epoxy:** verify reduced interlacing penalty relative to plain weave.
- **Non-crimp biaxial fabric:** verify near-straight tow response with stitch knockdown.
- **Particle-filled epoxy:** verify density, conductivity, and stiffness trends with filler volume fraction.
- **Voided composite:** verify monotonic reduction in stiffness and density with increasing void content.
- **Thermal conductivity benchmark:** compare k_1, k_2, and k_3 against parallel/series bounds and measured values.
- **CTE benchmark:** compare α_1, α_2, and α_3 against dilatometry data.

9 8 Numerical Stability Checks

The property extraction and finite-element export require positive stiffness and finite thermophysical outputs. The compliance matrix must be nonsingular,

$$det(\mathbf{S}^{eff}) \neq 0.$$

The stiffness matrix should be symmetric,

$$\mathbf{C}^{eff} = (\mathbf{C}^{eff})^T.$$

The principal elastic moduli and shear moduli must be positive,

$$E_i > 0, \qquad G_{ij} > 0.$$

Thermophysical quantities must remain finite and physically meaningful,

$$\rho > 0, \qquad C_p > 0, \qquad k_i > 0.$$

These checks are particularly important when the model is embedded in Workbench, because inconsistent input data, excessive void fractions, or nonphysical constituent data can otherwise propagate into Abaqus material definitions.

9 10 References

Advani, S. G., and Tucker, C. L. III. 1987. The use of tensors to describe and predict fiber orientation in short fiber composites. *Journal of Rheology*, 31, 751-784.

Chamis, C. C. 1983. Simplified composite micromechanics equations for hygral, thermal and mechanical properties. *SAMPE Quarterly*, 15, 14-23.

Chou, T.-W. 1992. *Microstructural Design of Fiber Composites*. Cambridge University Press.

Daniel, I. M., and Ishai, O. 2006. *Engineering Mechanics of Composite Materials*. Oxford University Press.

Dvorak, G. J. 2013. *Micromechanics of Composite Materials*. Springer.

Ishikawa, T., and Chou, T.-W. 1982. Stiffness and strength behavior of woven fabric composites. *Journal of Materials Science*, 17, 3211-3220.

Jones, R. M. 1999. *Mechanics of Composite Materials*. Taylor & Francis.

Lomov, S. V., Ivanov, D. S., Verpoest, I., Zako, M., Kurashiki, T., Nakai, H., and Hirosawa, S. 2007. Meso-FE modelling of textile composites: Road map, data flow and algorithms. *Composites Science and Technology*, 67, 1870-1891.

Mura, T. 1987. *Micromechanics of Defects in Solids*. Martinus Nijhoff.

Naik, N. K. 1994. Woven fabric composites. *Technomic Publishing*.

Whitcomb, J. D. 1991. Three-dimensional stress analysis of plain weave composites. *Composite Materials: Testing and Design*, ASTM STP.

37 Section 1 - Damage and Failure Framework

Online chapter

Section 1 Damage and Failure Framework

Volume III Damage Failure and Software Implementation

Section 1 Damage and Failure Framework

Executive Summary

This section introduces the damage, failure, and implementation layer of the Workbench micromechanics master model. Volumes I and II define the elastic and thermophysical homogenization framework used to compute effective orthotropic properties for continuous fiber, discontinuous fiber, woven textile, filled matrix, and hybrid composite architectures. Volume III extends the same framework into damage degradation, failure-index evaluation, software data flow, interfaces, and automatic Abaqus material-card export.

The purpose of Section 1 is to define the top-level mathematical and software structure for Volume III. Later sections describe the individual damage models, Tsai-Wu criterion, Hashin criterion, Workbench material properties, and Abaqus export options in greater detail.

1 1 Scope of Volume III

The present volume documents four major capability groups implemented in the solver micromechanics script:

- **Continuum damage mechanics (CDM)** for stiffness degradation.
- **Failure initiation models**, including Tsai-Wu and Hashin failure indices.
- **composite model**, using scalar and vector arrays rather than nested structures or user-defined solver functions.
- **Abaqus material-card generation**, including engineering constants, transversely isotropic, orthotropic, and fully anisotropic material definitions.

The damage and failure layer is applied after the micromechanics homogenization layer. Therefore, the model can be viewed as a sequential operator chain:

$$\boxed{\mathbf{P}^{out} = \mathcal{E}\left[\mathcal{F}\left(D\left(\mathcal{H}\left(\mathbf{P}^{in}\right)\right)\right)\right]}$$

where $\mathcal{H}$ is the homogenization operator, D is the damage operator, $\mathcal{F}$ is the failure-evaluation operator, and $\mathcal{E}$ is the export operator used to assemble Workbench and Abaqus outputs.

1 2 Position of Damage and Failure in the Multiscale Workflow

The model first predicts the undamaged effective composite properties. Damage is then applied to the effective stiffness, not to the constituent stiffnesses. This implementation is computationally efficient and appropriate when damage variables are interpreted as homogenized lamina-level state variables.

The undamaged effective stiffness is obtained from the selected micromechanics model:

$$\mathbf{C}^0 = \mathcal{H}\left(\mathbf{C}_f, \mathbf{C}_m, \mathbf{C}_p, V_f, V_m, V_p, V_v, AR, F_a, F_p\right)$$

where $\mathbf{C}^0$ is the undamaged effective stiffness tensor. The damaged stiffness is then written as

$$\boxed{\mathbf{C}^d = \mathbf{D} \quad \mathbf{C}^0 \quad \mathbf{D}}$$

where $\mathbf{D}$ is the damage degradation operator. This double-sided form preserves major symmetry of the stiffness matrix and is consistent with common engineering implementations of continuum damage mechanics.

A failure model then evaluates whether the current stress state exceeds an initiation criterion:

$$FI = \mathcal{F}(\boldsymbol{\sigma}, \mathbf{X})$$

where FI is the failure index, $\boldsymbol{\sigma}$ is the stress vector, and $\mathbf{X}$ denotes the set of strength allowables.

1 3 Damage Variables Used in the solver Model

The implemented damage model uses three scalar damage variables:

$$\mathbf{d} = [d_f \quad d_m \quad d_s]^T$$

where d_f is the fiber-direction damage variable, d_m is the matrix/transverse damage variable, and d_s is the shear damage variable. Each variable is bounded as

$$0 \leq d_i < 1$$

The corresponding damage operator in Voigt notation is

$$\boxed{\mathbf{D} = \mathrm{diag}\left[1 - d_f, \quad 1 - d_m, \quad 1 - d_m, \quad 1 - d_s, \quad 1 - d_s, \quad 1 - d_s\right]}$$

The use of a single matrix damage variable for both transverse directions is consistent with the engineering assumption that transverse normal damage is matrix dominated. The shear damage variable is applied to all three shear modes in the simplified composite model.

1 4 Engineering-Constant Form of Damage Degradation

$$E_1^d = E_1^0\left(1-d_f\right)^2$$

$$E_2^d = E_2^0(1-d_m)^2$$

$$E_3^d = E_3^0(1-d_m)^2$$

and

$$G_{ij}^d = G_{ij}^0(1-d_s)^2 \qquad ij = 12,13,23$$

where the superscript 0 denotes the undamaged value and d denotes the damaged value. These equations summarize the stiffness-degradation logic implemented in the current Workbench-safe solver script.

1 5 Failure Indices and Failure Initiation Logic

The solver script provides two failure-index options: Tsai-Wu and Hashin. The Tsai-Wu failure model is an interactive polynomial criterion for anisotropic materials. In compact form,

$$FI_{TW} = F_i\sigma_i + F_{ij}\sigma_i\sigma_j$$

Failure initiation is predicted when

$$FI_{TW} \geq 1$$

The Hashin model separates fiber and matrix failure modes. The governing Hashin failure index is evaluated as the maximum of the active mode indices:

$$\boxed{FI_H = max\left(FI_{ft},\quad FI_{fc},\quad FI_{mt},\quad FI_{mc}\right)}$$

where ft, fc, mt, and mc denote fiber tension, fiber compression, matrix tension, and matrix compression, respectively.

The failure module is optional. It can be disabled when strength data are unavailable or when the model is used only for property prediction and Abaqus material-card generation.

1 7 Damage and Failure Settings

Table 1 summarizes the damage, failure and export settings.

Table 1. Damage, failure and export settings.

Setting	Meaning
Fiber damage	Fiber-direction continuum damage variable
Matrix damage	Matrix/transverse continuum damage variable
Shear damage	Shear continuum damage variable
Failure model	Selects no failure, Tsai-Wu, Hashin, or both
Material export	Enables Abaqus material-card string generation
Material definition type	Selects engineering constants, transversely isotropic, orthotropic, or anisotropic card

The damage variables are interpreted as prescribed state variables. The current script does not automatically evolve damage with load history; rather, it provides the constitutive degradation framework into which an external progressive-damage update law can be inserted later.

1 9 Model schematics

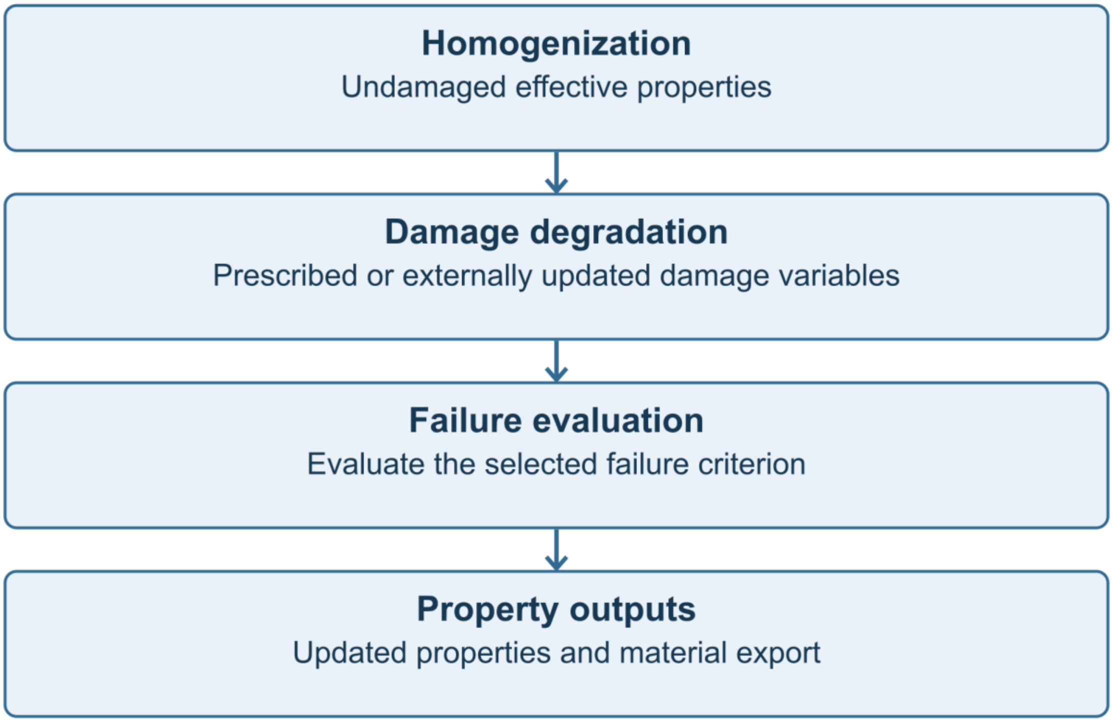

Figure 1. Damage and failure position in the full micromechanics workflow.

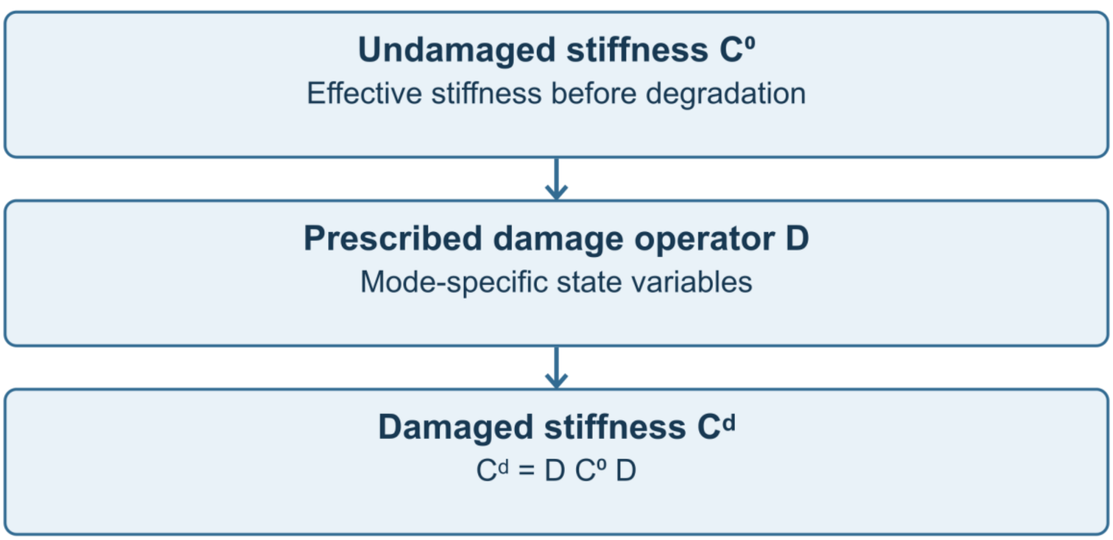

Figure 2. Continuum damage operator acting on the undamaged effective stiffness matrix.

1 10 References

- Lemaitre, J. (1996). *A Course on Damage Mechanics*, 2nd ed. Springer.

- Ladevèze, P. (1983). A damage computational method for composite structures. *Computers & Structures*.
- Tsai, S. W., and Wu, E. M. (1971). A general theory of strength for anisotropic materials. *Journal of Composite Materials*, 5, 58-80.
- Hashin, Z. (1980). Failure criteria for unidirectional fiber composites. *Journal of Applied Mechanics*, 47, 329-334.
- Matzenmiller, A., Lubliner, J., and Taylor, R. L. (1995). A constitutive model for anisotropic damage in fiber-composites. *Mechanics of Materials*, 20, 125-152.
- Abaqus Documentation. Material definitions: engineering constants, orthotropic elasticity, anisotropic elasticity, expansion, conductivity, and specific heat.
- Jones, R. M. (1999). *Mechanics of Composite Materials*, 2nd ed. Taylor & Francis.

1 11 Section Summary

Subsequent sections of Volume III document each damage and failure model and then describe the Workbench and Abaqus implementation details in a software-reference format.

38 Section 2 - Continuum Damage Mechanics

Online chapter

Section 2 Continuum Damage Mechanics

Volume III Section 2

Continuum Damage Mechanics and Stiffness Degradation

2 1 Purpose and Scope

The CDM module is not a full progressive failure solver by itself. Instead, it applies user-supplied damage state variables to the effective engineering constants and exports both undamaged and damaged properties. This structure allows Workbench, Abaqus, test correlation scripts, or a future progressive damage law to update the damage variables externally while keeping the micromechanics model stable and transparent.

In the current implementation, the damage variables are:

Damage variable	solver variable	Physical interpretation
Fiber-direction damage	Fiber damage	Loss of axial fiber-dominated stiffness
Matrix-normal damage	Matrix damage	Loss of transverse matrix-dominated stiffness
Shear damage	Shear damage	Loss of shear-transfer stiffness

2 2 Undamaged Effective Stiffness State

Before damage is applied, the micromechanics branch produces an undamaged orthotropic material state:

$$\mathbf{P}^0 = \{E_1^0, E_2^0, E_3^0, G_{12}^0, G_{13}^0, G_{23}^0, \nu_{12}, \nu_{13}, \nu_{23}\}.$$

The corresponding compliance matrix in engineering Voigt notation is:

$$\mathbf{S}^0 = \begin{bmatrix} 1/E_1^0 & -\nu_{12}/E_1^0 & -\nu_{13}/E_1^0 & 0 & 0 & 0 \\ -\nu_{12}/E_1^0 & 1/E_2^0 & -\nu_{23}/E_2^0 & 0 & 0 & 0 \\ -\nu_{13}/E_1^0 & -\nu_{23}/E_2^0 & 1/E_3^0 & 0 & 0 & 0 \\ 0 & 0 & 0 & 1/G_{23}^0 & 0 & 0 \\ 0 & 0 & 0 & 0 & 1/G_{13}^0 & 0 \\ 0 & 0 & 0 & 0 & 0 & 1/G_{12}^0 \end{bmatrix}.$$

The undamaged stiffness matrix is recovered from:

$$\mathbf{C}^0 = (\mathbf{S}^0)^{-1}.$$

This undamaged state is saved in the solver implementation before degradation so that the output vector can report both pre-damage and post-damage material properties.

2 3 Scalar Damage Variables

The model uses scalar damage variables bounded between zero and unity:

$$0 \le d_f < 1, \qquad 0 \le d_m < 1, \qquad 0 \le d_s < 1.$$

Here, d_f denotes fiber-direction damage, d_m denotes matrix/transverse damage, and d_s denotes shear damage. The limiting values have the following interpretation:

Value	Meaning
$d = 0$	Undamaged response
$0 < d < 1$	Partially degraded stiffness
$d \to 1$	Near-complete loss of the associated stiffness mode

The solver code clips damage values to remain below unity to avoid exactly singular stiffness matrices. This is essential for Workbench and Abaqus workflows, where a zero stiffness can produce ill-conditioned matrices or unstable material cards.

2 4 Damage Operator in Engineering Notation

The implemented damage operator is diagonal in engineering notation:

$$\mathbf{D} = diag\left[1 - d_f, 1 - d_m, 1 - d_m, 1 - d_s, 1 - d_s, 1 - d_s\right].$$

The first component corresponds to the material 1-direction, which is typically the fiber-dominated direction. The second and third components correspond to transverse matrix-dominated normal responses. The final three components correspond to shear responses.

A double-sided damage operation gives the damaged stiffness:

$$\mathbf{C}^d = \mathbf{D} \quad \mathbf{C}^0 \quad \mathbf{D}.$$

The double-sided form preserves the major symmetry of the stiffness matrix:

$$C_{ij}^d = C_{ji}^d.$$

2 5 Engineering-Constant Damage Laws Used in the Code

The implemented stiffness degradation laws are:

$$E_1^d = E_1^0\left(1 - d_f\right)^2,$$

$$E_2^d = E_2^0(1 - d_m)^2,$$

$$E_3^d = E_3^0(1 - d_m)^2,$$

$$G_{12}^d = G_{12}^0(1 - d_s)^2,$$

$$G_{13}^d = G_{13}^0(1 - d_s)^2,$$

$$G_{23}^{d} = G_{23}^{0}(1-d_s)^2.$$

The squared form is intentionally conservative relative to a linear knockdown law and reflects the double-sided degradation operator. It also maintains continuity of stiffness as damage evolves.

The Poisson ratios are not explicitly degraded in the current script:

$$\nu_{12}^{d} = \nu_{12}^{0}, \qquad \nu_{13}^{d} = \nu_{13}^{0}, \qquad \nu_{23}^{d} = \nu_{23}^{0}.$$

This is a practical engineering assumption. In a future extension, Poisson ratios may be recomputed from a fully degraded compliance matrix or linked to damage-mode-specific evolution laws.

2 6 Positive-Definite Stiffness Protection

For numerical robustness, the model applies lower bounds to damaged moduli when the positive-definite projection flag is active. The intent is to ensure:

$$E_i^{d} > 0, \qquad G_{ij}^{d} > 0.$$

At the engineering constant level, the stabilized form may be written as:

$$E_i^{stable} = max\left(E_i^{d}, E_{min}\right),$$

$$G_{ij}^{stable} = max\left(G_{ij}^{d}, G_{min}\right).$$

where E_{min} and G_{min} are small positive stiffness floors. This protection prevents singular compliance matrices during Abaqus export and protects the Workbench execution path from divide-by-zero errors.

2 7 Damage and Thermophysical Properties

The current implementation applies CDM only to mechanical stiffness. Effective density, thermal conductivity, coefficient of thermal expansion, and specific heat are computed independently of the damage variables:

$$\rho^{d} = \rho^{0},$$

$$C_p^{d} = C_p^{0},$$

$$\mathbf{k}^{d} = \mathbf{k}^{0},$$

$$\boldsymbol{\alpha}^{d} = \boldsymbol{\alpha}^{0}.$$

This is appropriate for a first-order engineering material card where damage represents stiffness degradation rather than physical mass loss, crack-surface heat-transfer changes, or evolving thermal expansion. If a coupled thermomechanical damage model is required, thermal conductivity and CTE may be degraded by additional variables or functions of crack density.

2 8 Relationship Between Damage and Failure Criteria

Damage and failure are separate modules in the solver script. Damage modifies the stiffness used to define the exported material response, while failure indices evaluate whether a stress state satisfies a failure criterion. The conceptual workflow is:

Undamaged Micromechanics
↓
Effective Engineering Constants

↓
Apply Damage Variables
↓
Damaged Engineering Constants
↓
Evaluate Failure Indices
↓
Export Workbench and Abaqus Outputs

The current code uses placeholder stress components unless a future Workbench interface extension supplies applied stress or strain states. The damage module therefore provides stiffness degradation capability independent of stress-driven damage evolution.

2 11 Abaqus Material-Card Implications

When Abaqus export is enabled, the engineering constants written to the material card are the damaged values:

$$\{E_i, G_{ij}, \nu_{ij}\}_{Abaqus} = \{E_i^d, G_{ij}^d, \nu_{ij}^d\}.$$

For *ELASTIC, TYPE=ENGINEERING CONSTANTS, this produces:

***ELASTIC, TYPE=ENGINEERING CONSTANTS**
E1d, E2d, E3d, NU12, NU13, NU23, G12d, G13d, G23d

The Abaqus card is therefore consistent with the damaged stiffness state used by the solver model. The original undamaged properties remain available in the scalar output vector for diagnostics.

2 12 Implementation Notes

- Store undamaged effective stiffness values.
- Clip damage variables to admissible bounds.
- Apply squared degradation factors to E_i and G_{ij}.
- Apply stiffness floors if positive-definite protection is active.
- Export damaged properties to subsequent analysis.
- Use damaged constants in the Abaqus material card.

This structure is robust for Workbench because it avoids nested functions, dynamic objects, and nonlinear iterations inside the damage module.

2 13 Model schematics

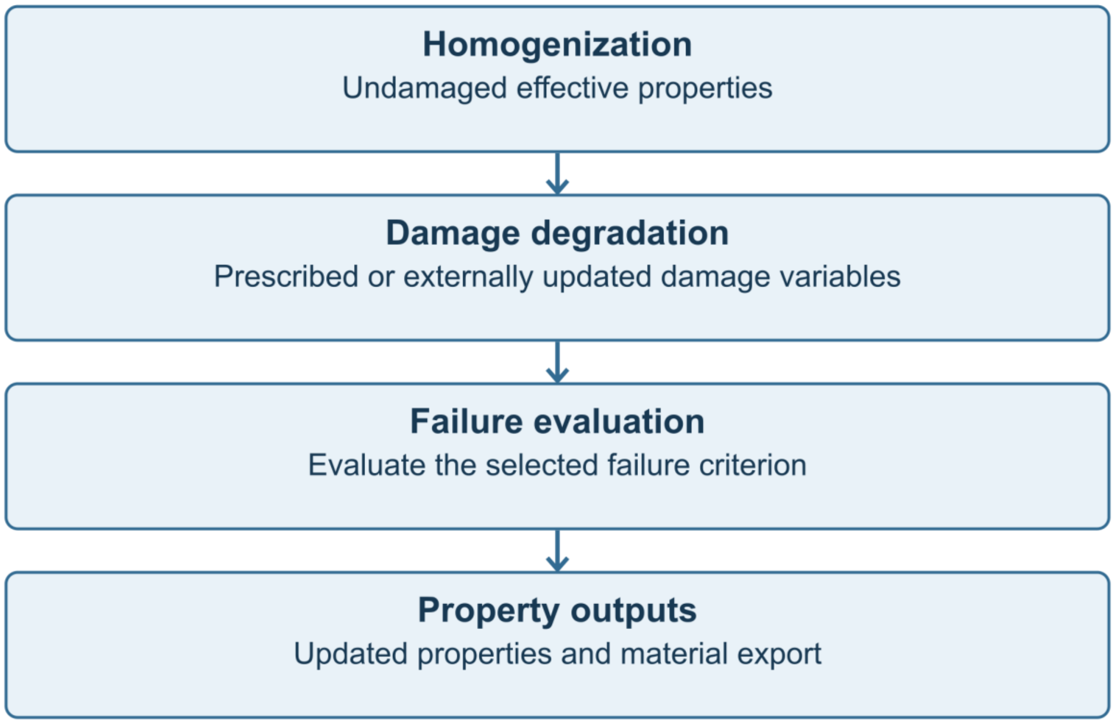

Figure 2.1. CDM workflow in the micromechanics model.

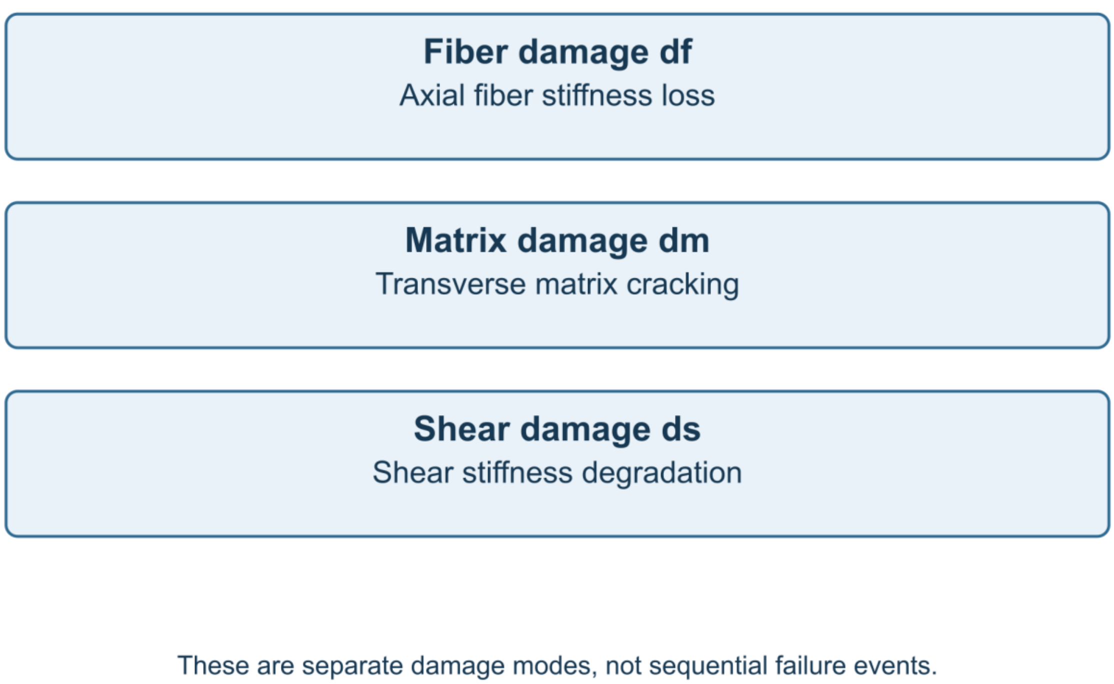

Figure 2.2. Physical interpretation of fiber, matrix and shear damage modes.

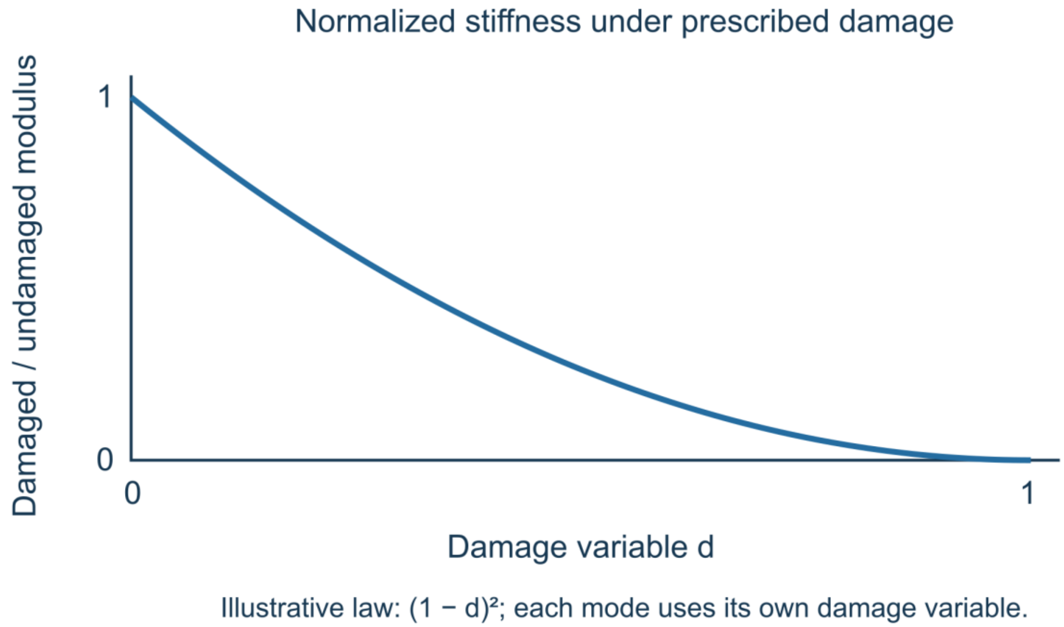

Figure 2.3. Stiffness degradation curves.

2 14 References

- Lemaitre, J. (1996). *A Course on Damage Mechanics*. Springer.
- Kachanov, L. M. (1958). Time of the rupture process under creep conditions. *Izvestiya Akademii Nauk SSSR, Otdelenie Tekhnicheskikh Nauk*.
- Ladevèze, P. (1983). A damage computational method for composite structures. *Computers & Structures*.
- Matzenmiller, A., Lubliner, J., and Taylor, R. L. (1995). A constitutive model for anisotropic damage in fiber-composites. *Mechanics of Materials*.
- Hashin, Z. (1980). Failure criteria for unidirectional fiber composites. *Journal of Applied Mechanics*.
- Tsai, S. W., and Wu, E. M. (1971). A general theory of strength for anisotropic materials. *Journal of Composite Materials*.
- Talreja, R. (1985). Transverse cracking and stiffness reduction in composite laminates. *Journal of Composite Materials*.
- Barbero, E. J. (2018). *Finite Element Analysis of Composite Materials Using Abaqus*. CRC Press.

39 Section 3 - Composite Failure Criteria

Online chapter

Section 3 Composite Failure Criteria

Volume III - Section 3

Composite Failure Criteria

3 1 Purpose of the Failure Module

The current implementation supports two classical composite failure formulations:

- Tsai-Wu interactive failure criterion.
- Hashin mode-separated failure criterion.

The purpose of the failure module is not to replace a full progressive damage analysis, but to provide a consistent first-ply or material-point-level failure indicator using the same material property properties carried into the analysis.

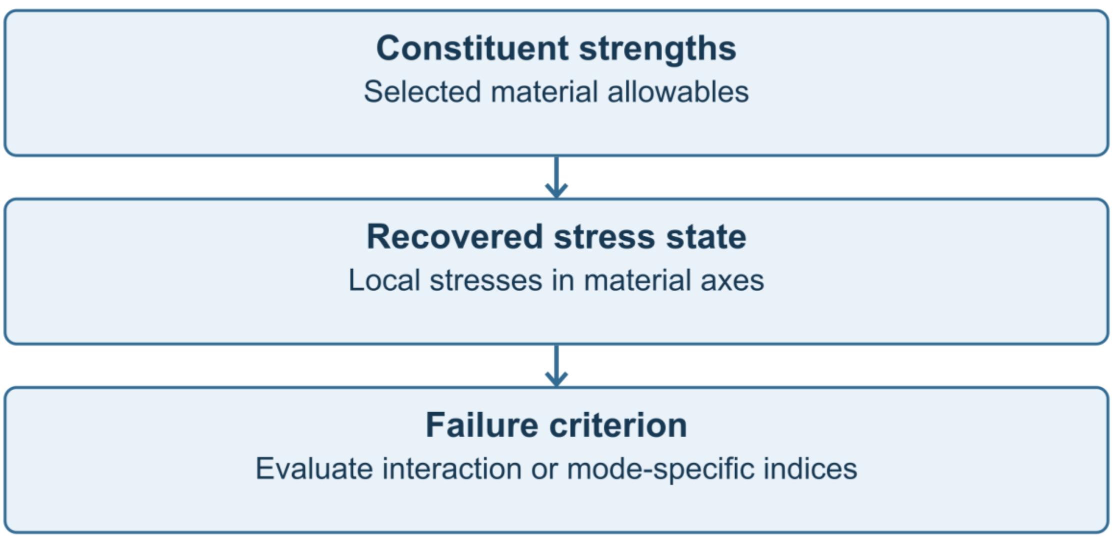

Figure 3.1. Failure evaluation workflow from constituent strengths and material stresses to scalar failure indices.

3 2 Stress Components Used by the Failure Model

The failure model is evaluated in the local material coordinate system. The local stress vector is written as

$$\boldsymbol{\sigma} = [\sigma_1 \quad \sigma_2 \quad \sigma_3 \quad \tau_{23} \quad \tau_{13} \quad \tau_{12}]^T$$

where the subscripts 1, 2, and 3 denote the principal orthotropic material directions. Direction 1 is normally associated with the dominant fiber or tow direction, while directions 2 and 3 are matrix-dominated transverse directions.

In the present solver script, the failure stress state is retained as a placeholder stress vector unless external stress inputs are added through Workbench. This design permits the same code framework to be coupled later to structural analysis outputs, coupon-level stress states, or ply-level laminate analysis.

3 3 Strength Inputs

The fiber material property input vector carries the primary tensile, compressive, and shear allowables used by both Tsai-Wu and Hashin models. The strength set is

$$\mathbf{X} = \{X_t, X_c, Y_t, Y_c, Z_t, Z_c, S_{12}, S_{13}, S_{23}\}$$

where

- X_t and X_c are longitudinal tensile and compressive strengths,
- Y_t and Y_c are transverse tensile and compressive strengths,
- Z_t and Z_c are third-direction tensile and compressive strengths,
- S_{12}, S_{13}, and S_{23} are shear strengths.

The solver input mapping is summarized in Table 3.1.

Table 3.1. Strength input mapping used by the current solver implementation.

Input vector index	**Symbol**	**Units**	**Description**
11	X_t	Pa	Longitudinal tensile strength
12	X_c	Pa	Longitudinal compressive strength
13	Y_t	Pa	Transverse tensile strength
14	Y_c	Pa	Transverse compressive strength
15	Z_t	Pa	Third-direction tensile strength
16	Z_c	Pa	Third-direction compressive strength
17	S_{12}	Pa	1-2 shear strength
18	S_{13}	Pa	1-3 shear strength
19	S_{23}	Pa	2-3 shear strength

3 4 Tsai-Wu Failure Criterion

The Tsai-Wu criterion is an interactive polynomial failure theory for anisotropic composite materials. It combines linear stress terms, quadratic stress terms, and interaction terms into a scalar failure index. Failure is predicted when the index reaches unity.

The general form is

$$FI_{TW} = F_i\sigma_i + F_{ij}\sigma_i\sigma_j$$

with failure initiation defined by

$$FI_{TW} \geq 1$$

For the three-dimensional orthotropic stress state used in the solver model, the expanded form is

$$FI_{TW} = F_1\sigma_1 + F_2\sigma_2 + F_3\sigma_3 + F_{11}\sigma_1^2 + F_{22}\sigma_2^2 + F_{33}\sigma_3^2 + F_{44}\tau_{23}^2 + F_{55}\tau_{13}^2 + F_{66}\tau_{12}^2 + 2F_{12}\sigma_1\sigma_2 + 2F_{13}\sigma_1\sigma_3 + 2F_{23}\sigma_2\sigma_3.$$

The linear coefficients distinguish tensile and compressive strengths:

$$F_1 = \frac{1}{X_t} - \frac{1}{X_c}, \qquad F_2 = \frac{1}{Y_t} - \frac{1}{Y_c}, \qquad F_3 = \frac{1}{Z_t} - \frac{1}{Z_c}$$

The direct quadratic coefficients are

$$F_{11} = \frac{1}{X_t X_c}, \qquad F_{22} = \frac{1}{Y_t Y_c}, \qquad F_{33} = \frac{1}{Z_t Z_c}$$

and the shear coefficients are

$$F_{44} = \frac{1}{S_{23}^2}, \qquad F_{55} = \frac{1}{S_{13}^2}, \qquad F_{66} = \frac{1}{S_{12}^2}.$$

When biaxial interaction data are unavailable, the implementation uses the common engineering approximation

$$F_{12} = -\frac{1}{2}\sqrt{F_{11}F_{22}}, \qquad F_{13} = -\frac{1}{2}\sqrt{F_{11}F_{33}}, \qquad F_{23} = -\frac{1}{2}\sqrt{F_{22}F_{33}}.$$

The Tsai-Wu index is useful when a smooth scalar interaction surface is desired. It is especially convenient for optimization, design-space exploration, and quick screening of material systems.

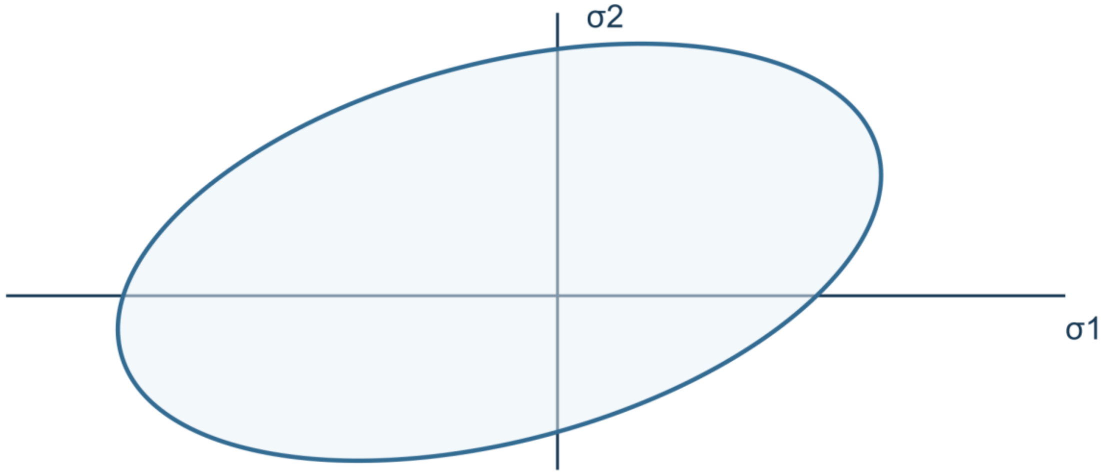

Figure 3.2. Schematic Tsai-Wu interaction surface in normal stress space.

3 5 Hashin Failure Criterion

Hashin failure theory separates failure into physically interpretable fiber and matrix modes. This is useful for composite materials because fiber-dominated and matrix-dominated failures have different consequences for stiffness degradation, residual strength, and progressive damage modeling.

The solver model evaluates four Hashin-type mode indices:

- Fiber tension.
- Fiber compression.
- Matrix tension.
- Matrix compression.

The governing Hashin failure index is the maximum of the active mode indices:

$$FI_H = max\left(FI_{ft}, FI_{fc}, FI_{mt}, FI_{mc}\right)$$

Failure initiation is predicted when

$$FI_H \geq 1.$$

3 6 Fiber Tension Mode

For positive longitudinal stress, the fiber tension index is

$$FI_{ft} = \left(\frac{\sigma_1}{X_t}\right)^2 + \left(\frac{\tau_{12}}{S_{12}}\right)^2 + \left(\frac{\tau_{13}}{S_{13}}\right)^2, \qquad \sigma_1 \geq 0.$$

This mode represents tensile rupture or tensile-driven degradation of the fiber-dominated direction. In a progressive model, this index would normally be associated with the fiber damage variable d_f.

3 7 Fiber Compression Mode

For negative longitudinal stress, the fiber compression index is implemented as

$$FI_{fc} = \frac{|\sigma_1|}{X_c}, \qquad \sigma_1 < 0.$$

3 8 Matrix Tension Mode

The matrix tension mode is evaluated when the transverse normal stress sum is tensile:

$$\sigma_T = \sigma_2 + \sigma_3$$

For $\sigma_T \geq 0$, the matrix tension failure index is

$$FI_{mt} = \left(\frac{\sigma_2 + \sigma_3}{Y_t}\right)^2 + \left(\frac{\tau_{23}}{S_{23}}\right)^2 + \left(\frac{\tau_{12}}{S_{12}}\right)^2 + \left(\frac{\tau_{13}}{S_{13}}\right)^2.$$

Matrix tension is associated with transverse cracking, microcrack initiation, and matrix-dominated stiffness loss.

3 9 Matrix Compression Mode

For $\sigma_T < 0$, the matrix compression index is implemented as

$$FI_{mc} = \left(\frac{\sigma_2 + \sigma_3}{2S_{23}}\right)^2 + \left[\left(\frac{Y_c}{2S_{23}}\right)^2 - 1\right]\frac{\sigma_2 + \sigma_3}{Y_c} + \left(\frac{\tau_{23}}{S_{23}}\right)^2 + \left(\frac{\tau_{12}}{S_{12}}\right)^2 + \left(\frac{\tau_{13}}{S_{13}}\right)^2.$$

This form accounts for the interaction between transverse compression and shear loading, which is often critical in matrix-dominated composite failure.

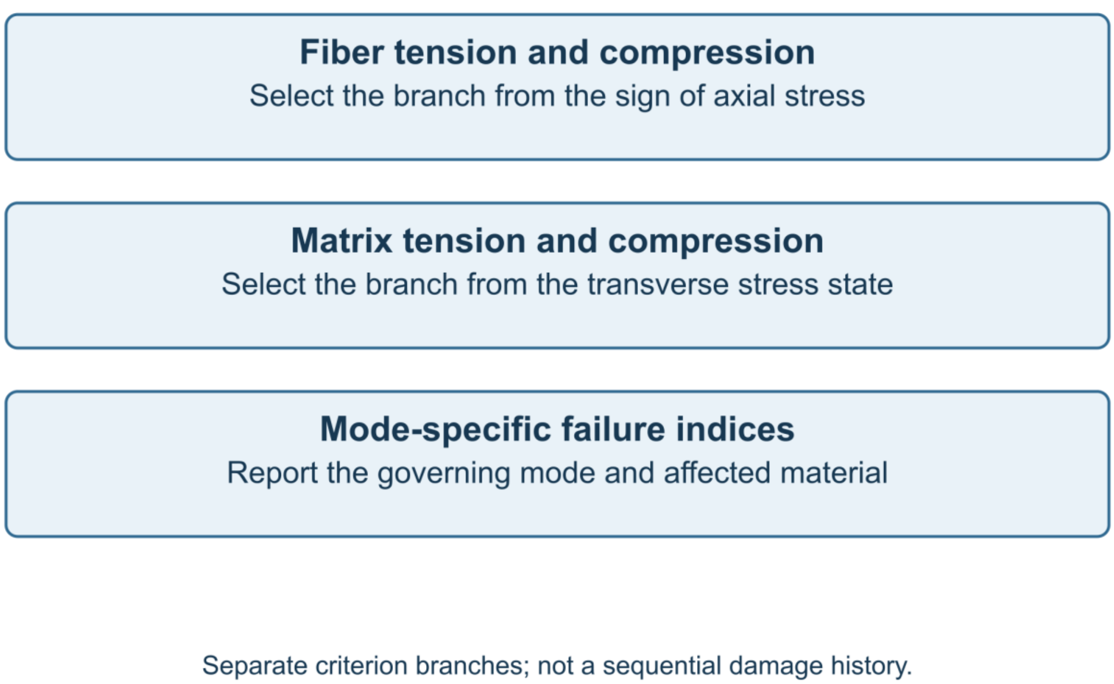

Figure 3.3. Hashin failure mode map showing fiber tension, fiber compression, matrix tension, and matrix compression regions.

3 10 Failure Model Selection

Choose the failure criterion appropriate to the material and the available strength data.

Table 3.2. Failure model selection logic.

Active model
No failure calculation
Tsai-Wu only
Hashin only
Tsai-Wu and Hashin

This flag allows Workbench to activate or deactivate failure calculations without changing the solver script.

3 11 Failure Outputs

The primary scalar outputs from this section are the Tsai-Wu and Hashin failure indices.

Table 3.3. Failure scalar outputs.

Output index	Variable	Units	Description
35	failure_index_tsai_wu	-	Tsai-Wu failure index
36	failure_index_hashin	-	Maximum Hashin failure index

Model outputs use a consistent metadata convention for downstream reporting.

3 12 Relationship to Damage Variables

The failure criteria compute initiation indices. The continuum damage variables described in Section 2 degrade stiffness:

$$\mathbf{C}^d = \mathbf{DCD}$$

A future progressive failure extension may connect the failure indices to damage update laws of the form

$$d_f = d_f\left(FI_{ft}, FI_{fc}, N, T, \Delta t\right)$$

$$d_m = d_m(FI_{mt}, FI_{mc}, N, T, \Delta t)$$

where N may represent cycle count for fatigue extensions, T may represent temperature, and Δt is the analysis increment.

The present solver implementation does not automatically evolve damage variables from the failure indices. Instead, damage variables are prescribed through Workbench scalar inputs, while the failure indices provide diagnostic measures.

3 13 Implementation Workflow

The failure calculation sequence is summarized as follows:

Read strength allowables
|
v
Read or define local stress state
|
v
Compute Tsai-Wu coefficients
|
v
Evaluate Tsai-Wu failure index
|
v
Evaluate Hashin mode indices
|
v
Return scalar failure outputs

This workflow is intentionally simple and deterministic for Workbench execution.

3 14 Applicability and Limitations

The Tsai-Wu model provides a smooth scalar interaction criterion but does not distinguish physical failure modes. Hashin theory provides physically interpretable failure modes but remains an initiation criterion unless coupled to damage evolution laws. Neither criterion alone determines post-failure stiffness evolution. In the current model, stiffness degradation is controlled separately through continuum damage variables.

The failure indices should therefore be interpreted as material-point-level initiation measures and design screening metrics rather than complete progressive failure simulations.

References

- Tsai, S. W., and Wu, E. M. (1971). A general theory of strength for anisotropic materials. *Journal of Composite Materials*, 5, 58-80.
- Hashin, Z. (1980). Failure criteria for unidirectional fiber composites. *Journal of Applied Mechanics*, 47, 329-334.
- Hashin, Z., and Rotem, A. (1973). A fatigue failure criterion for fiber reinforced materials. *Journal of Composite Materials*, 7, 448-464.
- Daniel, I. M., and Ishai, O. (2006). *Engineering Mechanics of Composite Materials*, 2nd ed. Oxford University Press.
- Jones, R. M. (1999). *Mechanics of Composite Materials*, 2nd ed. Taylor & Francis.
- Puck, A., and Schurmann, H. (1998). Failure analysis of FRP laminates by means of physically based phenomenological models. *Composites Science and Technology*, 58, 1045-1067.
- Camanho, P. P., and Matthews, F. L. (1999). A progressive damage model for mechanically fastened joints in composite laminates. *Journal of Composite Materials*, 33, 2248-2280.

40 Section 4 - Damage and Failure Workflow

Online chapter

Section 4 Damage and Failure Workflow

Volume III Section 4

Damage and Failure Evaluation Workflow

4 1 Purpose and Scope

The damage and failure workflow is intentionally modular. The effective elastic and thermophysical property predictions can be executed without activating damage or failure. When damage variables are prescribed, the stiffness tensor or engineering constants are degraded before output. When strength allowables and a stress state are available, failure indices are evaluated using the selected criterion. The solver implementation currently supports a prescribed-damage workflow and a failure-index workflow; it does not automatically evolve damage in time unless an external Workbench or solver-level update law supplies new damage variables.

The key workflow outputs are:

- damaged orthotropic engineering constants,
- undamaged reference properties,
- prescribed damage variables,
- Tsai-Wu failure index,
- Hashin modal failure indices,
- maximum governing failure index,
- Abaqus material card data derived from the damaged properties.

4 2 Position of the Damage/Failure Module in the Full Model

The damage and failure module acts after micromechanical homogenization and architecture correction. The full material-property workflow may be summarized as:

Constituent inputs
-> phase properties
-> filled matrix / hybrid phase assembly
-> micromechanics model selection
-> architecture correction
-> effective undamaged properties
-> CDM stiffness degradation
-> failure index evaluation
-> effective properties
-> Abaqus material card string

The model first computes undamaged engineering constants

$$\mathbf{p}^0 = [E_1^0, E_2^0, E_3^0, G_{12}^0, G_{13}^0, G_{23}^0, \nu_{12}, \nu_{13}, \nu_{23}]^T.$$

After damage degradation, the final output property vector becomes

$$\mathbf{p}^d = \left[E_1^d, E_2^d, E_3^d, G_{12}^d, G_{13}^d, G_{23}^d, \nu_{12}^d, \nu_{13}^d, \nu_{23}^d\right]^T.$$

In the current engineering implementation, the Poisson ratios are retained from the effective undamaged material state unless a later extension explicitly evolves damage-dependent coupling terms.

4 3 Damage State Vector

The prescribed damage state is represented by three scalar variables:

$$\mathbf{d} = \left[d_f, d_m, d_s\right]^T,$$

where d_f is the fiber-direction damage variable, d_m is the matrix-normal damage variable, and d_s is the shear damage variable. Each variable is constrained to the physically meaningful interval

$$0 \le d_i < 1, \qquad i \in \{f, m, s\}.$$

In the solver script, numerical clipping is applied to avoid exactly singular stiffness values:

$$d_i \leftarrow min[max(d_i, 0), 0.999].$$

This rule is not a constitutive law; it is a numerical protection used to maintain finite output properties for Workbench and Abaqus export.

4 4 Engineering-Constant Degradation Workflow

$$E_1^d = E_1^0\left(1-d_f\right)^2.$$

The transverse moduli are degraded by the matrix-normal damage variable:

$$E_2^d = E_2^0(1-d_m)^2,$$

$$E_3^d = E_3^0(1-d_m)^2.$$

The shear moduli are degraded by the shear damage variable:

$$G_{12}^d = G_{12}^0(1-d_s)^2,$$

$$G_{13}^d = G_{13}^0(1-d_s)^2,$$

$$G_{23}^d = G_{23}^0(1-d_s)^2.$$

The quadratic degradation form is numerically smooth and ensures monotonic stiffness reduction. It also mirrors the double-sided tensor degradation form introduced in Section 2:

$$\mathbf{C}^d = \mathbf{D} \quad \mathbf{C}^0 \quad \mathbf{D}.$$

The direct engineering-constant workflow is preferred in the Workbench script because it avoids user-defined solver functions and avoids repeated tensor assembly for simple engineering studies.

4 5 Positive-Definite Stiffness Protection

After degradation, each modulus is bounded below by a positive floor value:

$$E_i^d \leftarrow max\left(E_i^d, E_{min}\right), \qquad i = 1,2,3,$$

$$G_{ij}^d \leftarrow max\left(G_{ij}^d, G_{min}\right), \qquad ij \in \{12,13,23\}.$$

The floor is not intended to represent real residual material stiffness. It prevents singular compliance matrices when the output is converted into a full stiffness matrix for anisotropic Abaqus export.

The compliance matrix used for orthotropic reconstruction is

$$\mathbf{S}^d = \begin{bmatrix} 1/E_1^d & -\nu_{12}/E_1^d & -\nu_{13}/E_1^d & 0 & 0 & 0 \\ -\nu_{12}/E_1^d & 1/E_2^d & -\nu_{23}/E_2^d & 0 & 0 & 0 \\ -\nu_{13}/E_1^d & -\nu_{23}/E_2^d & 1/E_3^d & 0 & 0 & 0 \\ 0 & 0 & 0 & 1/G_{23}^d & 0 & 0 \\ 0 & 0 & 0 & 0 & 1/G_{13}^d & 0 \\ 0 & 0 & 0 & 0 & 0 & 1/G_{12}^d \end{bmatrix}.$$

The corresponding stiffness matrix is obtained by inversion:

$$\mathbf{C}^d = \left(\mathbf{S}^d\right)^{-1}.$$

4 6 Failure-Model Selection

Choose the active failure model:

Failure model
No failure calculation
Tsai-Wu only
Hashin only
Tsai-Wu and Hashin

The selected failure model is evaluated after the damaged properties have been assembled. The failure model does not modify the stiffness by itself. Instead, it reports failure indices that may be used by Workbench, Abaqus, or an external design loop.

4 7 Stress State for Failure Evaluation

The general three-dimensional stress vector is

$$\boldsymbol{\sigma} = [\sigma_1, \sigma_2, \sigma_3, \tau_{23}, \tau_{13}, \tau_{12}]^T.$$

In the current solver implementation, the stress variables are initialized as placeholders unless supplied by a future extension. This design keeps the material-property calculator independent of a structural stress solver. In a coupled workflow, the stress state would be supplied by:

- a laminate analysis tool,
- a finite-element postprocessor,
- a Workbench stress module,
- a load-envelope evaluation routine,
- or a progressive damage loop.

The failure index function can therefore be interpreted as a local material-point assessment operating on the stress vector of Eq. (4.17).

4 8 Tsai-Wu Workflow

When Tsai-Wu is active, the solver computes the scalar failure index

$$FI_{TW} = F_i\sigma_i + F_{ij}\sigma_i\sigma_j.$$

Failure initiation is indicated when

$$FI_{TW} \geq 1.$$

The workflow is:

Read strengths
-> compute Tsai-Wu coefficients
-> read stress vector
-> evaluate quadratic interaction index
-> report FI_TsaiWu

A design margin may be calculated as

$$MS_{TW} = \frac{1}{FI_{TW}} - 1.$$

A positive margin indicates that the evaluated stress state is below the Tsai-Wu failure surface.

4 9 Hashin Workflow

When Hashin is active, the model evaluates separate modal indices:

$$FI_H = max\left(FI_{ft}, FI_{fc}, FI_{mt}, FI_{mc}\right),$$

where ft denotes fiber tension, fc denotes fiber compression, mt denotes matrix tension, and mc denotes matrix compression. Failure initiation is indicated when

$$FI_H \geq 1.$$

The workflow is:

Read strengths
-> identify stress sign
-> evaluate fiber mode
-> evaluate matrix mode
-> select maximum modal index
-> report FI_Hashin

Unlike Tsai-Wu, Hashin provides a failure-mode classification. This makes it useful for diagnostic interpretation and progressive damage modeling.

4 10 Governing Failure Status Logic

The implemented failure-status logic is summarized by a governing index:

$$FI_{gov} = max(FI_{TW}, FI_H),$$

when both criteria are active. A binary failure flag can be defined as

$$\chi_f = \begin{cases} 0, & FI_{gov} < 1, \\ 1, & FI_{gov} \geq 1. \end{cases}$$

The current solver file outputs the indices directly. Workbench can apply Eq. (4.24) externally if a binary pass/fail output is desired.

4 11 Recommended Progressive-Damage Extension

Although the current model uses prescribed damage variables, the same framework can be extended to progressive damage by updating damage as a function of failure index. A simple rate-independent update form is

$$d_i^{n+1} = min\left[d_{i,max}, \quad d_i^n + \Delta d_i\right],$$

where

$$\Delta d_i = \gamma_i \langle FI_i - 1 \rangle,$$

and the Macaulay bracket is

$$\langle x \rangle = max(x, 0).$$

This extension is not required for the present Workbench material-property model, but it provides a clear path for coupling the micromechanics module to nonlinear laminate or finite-element analyses.

4 13 Model schematics

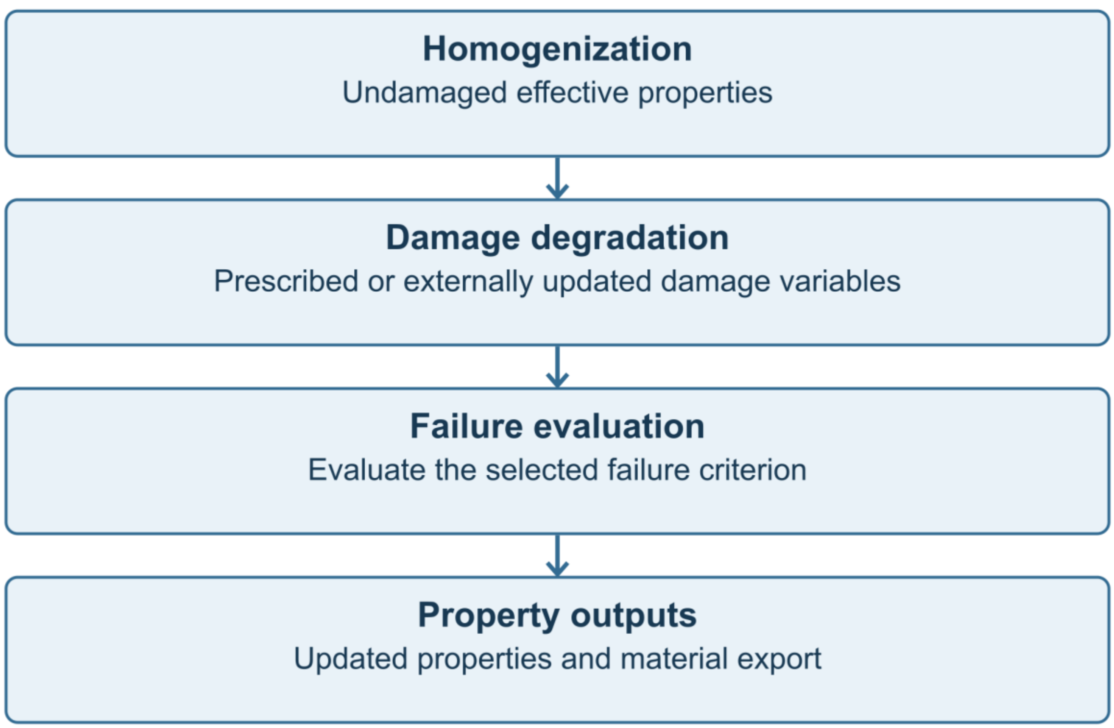

Figure 4.1. Damage and failure workflow.

Failure-model selection. Compare Tsai-Wu and Hashin predictions using the same stress state and strength data.

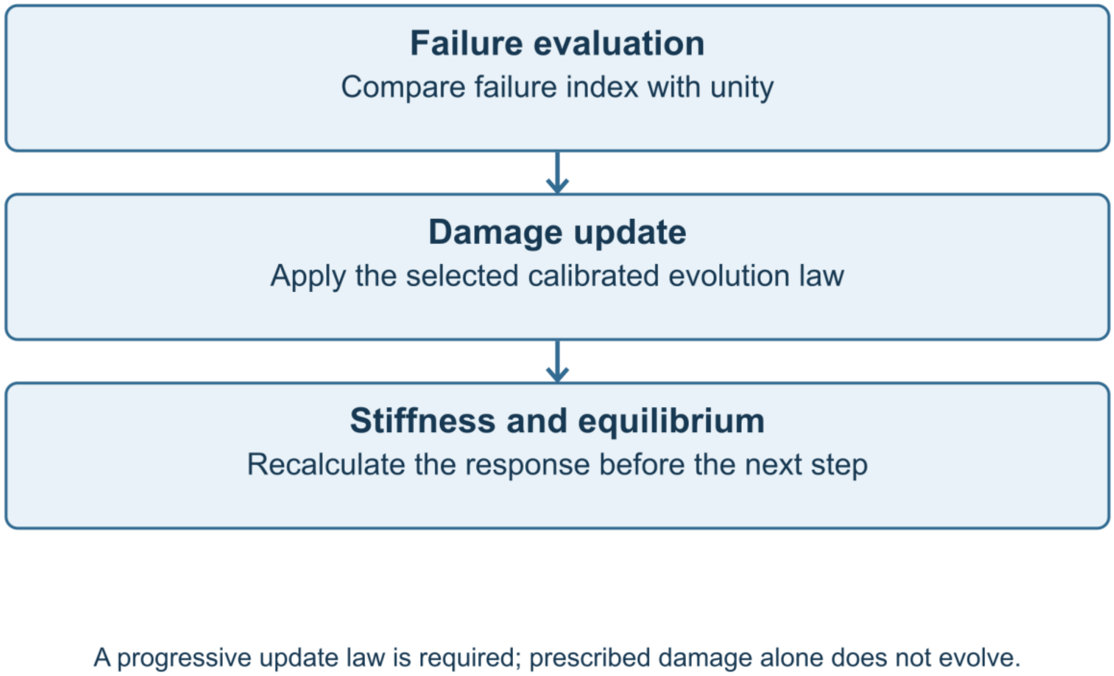

Figure 4.3. Progressive damage extension.

4 14 Implementation Notes

The damage and failure workflow is intentionally kept separate from the homogenization model. This allows the same effective property solver to be used for purely elastic material characterization, damaged-property estimation, or failure-index screening. This separation is also important for Workbench deployment because it avoids state-dependent solver memory unless the user intentionally implements a progressive damage loop outside the script.

- Damage variables are scalar inputs, not hidden internal state variables.
- Failure criteria report indices but do not automatically degrade stiffness.
- Abaqus export uses the final degraded engineering constants.

These rules make the material model deterministic, repeatable, and suitable for automated design studies.

4 15 References

Hashin, Z. (1980). Failure criteria for unidirectional fiber composites. *Journal of Applied Mechanics*, 47, 329–334.

Ladevèze, P. (1983). A damage mechanics approach for composite materials. *Journal of Engineering Materials and Technology*, 105, 280–286.

Lemaitre, J. (1996). *A Course on Damage Mechanics*. Springer.

Matzenmiller, A., Lubliner, J., and Taylor, R. L. (1995). A constitutive model for anisotropic damage in fiber-composites. *Mechanics of Materials*, 20, 125–152.

Tsai, S. W., and Wu, E. M. (1971). A general theory of strength for anisotropic materials. *Journal of Composite Materials*, 5, 58–80.

41 1 Framework and Scope

Online chapter

1 Framework and Scope

CDS release r15 is a unified constituent-to-process-to-structure framework. Every physical ply may independently use automatic property resolution, embedded micromechanics, or direct measured properties; supply its own polymer process data; and enter the common damaged laminate and selectable plate, cylinder, or beam solution. Classical Lamination Theory supplies the membrane-bending foundation while mapped temperature, moisture, cure shrinkage, crystallization shrinkage, cohesive interfaces, and per-ply failure routing remain integrated without treating the stochastic short-fiber branch as the whole formulation.

One connected property chain
Fiber, matrix, filler, void, architecture, and measured overrides resolve into the complete 3D elastic, strength, expansion, density, and transport definition for each ply.

Independent source routing
Each ply can use a linked micromechanics recipe or measured material properties. Different plies may use different sources.

Retained laminate foundation
Thin-laminate CLT, transformed orthotropic ply stiffness, full A–B–D coupling, and three-node-per-ply recovery remain the section-analysis foundation.

Updated failure model
Each ply selects a compatible failure theory. New failures degrade only the activated fiber, matrix, or shear family before equilibrium is solved again at the same load.

Environmental coupling
Temperature and moisture fields generate damaged force and moment resultants. They are recomputed after every stiffness change.

Process-first solution
A heterogeneous 1D heat/moisture model uses independent top and bottom schedules, cure or crystallization kinetics, and per-ply transport properties before structural loading.

Optional interface model
A mixed-mode cohesive law can represent delamination only when local interface separation history is supplied externally.

Uniform 3D traction extension
Prescribed σz, τxz, and τyz are recovered in global and local axes, contribute to failure, and add independent E3, G13, and G23 damage families.

Multi-material laminate
Every active ply can use a different material, orientation, environmental state, strength set, and eligible failure criterion during the same progressive analysis.

Optional Double-Double recommendation
Compatible equal-thickness master-ply stacks can be mapped to a stiffness-matched Tsai Double-Double family. The user chooses whether downstream analysis retains the supplied angles or uses the recommendation.

Tsai Double-Double stiffness matching

For a compatible stack, CDS searches the staggered family $[+\Phi/-\Psi/-\Phi/+\Psi]_{rT}$ on a 0.5° grid. The objective minimizes the normalized mismatch between the supplied laminate extensional stiffness and the candidate Double-Double stiffness while also reporting coupling and homogenization measures.

$$e_A(\Phi,\Psi) = \|A_{\mathrm{DD}}(\Phi,\Psi) - A_{\mathrm{original}}\|_F / \max\left(\|A_{\mathrm{original}}\|_F, \varepsilon\right)$$

Laminate flag 17 equals 0 to retain the supplied angles or 1 to use the compatible recommendation before all downstream laminate and progressive-failure calculations. Every ply row, material, thickness, property, and interface is preserved; only eligible ply angles are replaced. The Double-Double recommendation summarizes compatibility, recommended angles, coupling, homogenization, and stiffness error, while the ply-angle table reports original, recommended, and selected angles.

Connected analysis sequence

- **1. Read one schema** Resolve eight scalar groups, constituent and ply tables, optional matrix shear laws, two surface histories, kinetics, loads, geometry, interfaces, and outputs.
- **2. Generate or accept each ply** Use the established resolver, embedded micromechanics, or direct measured properties independently. Preserve measured overrides.
- **3. Solve discontinuous RVEs when selected** Rebuild interaction segments, insert ordered Weibull breaks, couple RVE curves in series, and screen critical clusters.
- **4. Recommend or retain the layup** When compatible, calculate the stiffness-matched Double-Double candidate and use laminate flag 17 to retain or substitute its angles.
- **5. Solve and map process history** Interpolate schedules, solve heat/diffusion/polymer state, and form per-ply process resultants.
- **6. Assemble equilibrium** Integrate damaged A, B, and D and superimpose mechanical, thermal, moisture, process, and σ_z-Poisson actions.
- **7. Solve the structure** Select plate, shell/Hyer cylinder, or beam and recover stiffness, response, buckling, and frequency results.
- **8. Evaluate and redistribute** Check each ply independently, reduce newly failed families, and repeat equilibrium at the same load until stable.
- **9. Export** Return named engineering results with material lineage, process fields, structural results, detailed discontinuous events, properties, and matrices.

Model intent: this framework is a screening and research implementation. Calibration against the actual material system and target environment is required before design use.

42 2 Common Ply Property Definition

Online chapter

2 Common Ply Property Definition

Every ply supplies the same constitutive property definition, allowing different material types and failure theories to share the laminate equilibrium solver.

$$P_k = \{E_1, E_2, E_3, G_{12}, G_{13}, G_{23}, \nu_{12}, \nu_{13}, \nu_{23}, \text{strengths}, \text{strainallowables}, \alpha, \beta, \rho, k, c_p, \Delta T, \Delta C\}_k$$

Family	Required quantities	Purpose
Elastic	E1, E2, E3; G12, G13, G23; ν12, ν13, ν23	Damaged ABD response and layerwise transverse recovery
Strength	Xt, Xc, Yt, Yc, Zt, Zc; S12, S13, S23	Sign-dependent in-plane and transverse failure evaluation
Strain allowables	ε1t/c, ε2t/c, ε3t/c; γ12, γ13, γ23	Maximum Strain and supplemental transverse failure
Expansion	α1, α2, α3; β1, β2, β3; ply ΔT and ΔC	Thermal and moisture contributions at each ply
Physical	ρ, k1, k2, k3, cp	Laminate density, conductivity, heat capacity, and diffusivity

Plane-stress reduced stiffness

$$Q = \big[[Q_{11}, Q_{12}, 0], [Q_{12}, Q_{22}, 0], [0, 0, Q_{66}]\big]$$

$$\nu_{21} = \nu_{12} E_2 / E_1$$

$$Q_{11} = E_1 / (1 - \nu_{12}\nu_{21})$$

$$Q_{22} = E_2 / (1 - \nu_{12}\nu_{21})$$

$$Q_{12} = \nu_{12} E_2 / (1 - \nu_{12}\nu_{21})$$

$$Q_{66} = G_{12}$$

Strengths and strain allowables must be positive magnitudes. The solver chooses the tensile or compressive value from the sign of the recovered local component.

43 3 Micromechanics and Material Routing

Online chapter

3 Micromechanics and Material Routing

Release r15 adds a source router before the established material/failure router. Each ply first resolves where its pristine properties come from, then resolves which progressive criterion is physically eligible.

Three property sources per ply

Choose a property source for each ply. Use a linked micromechanics recipe to calculate lamina properties, or select measured material properties. Keep the source, units and test conditions traceable.

Four architectures and failure eligibility

ID	Architecture	Resolved family	Failure selection
1	Continuous UD	Deterministic/continuous	Criteria 1–5
2	Aligned discontinuous/short fiber	Aligned discontinuous	Criterion 6 forced
3	Woven, NCF, braid	Deterministic/continuous	Criteria 1–5
4	General multiphase	Deterministic/continuous	Criteria 1–5

A hybrid laminate may combine generated UD, fabric, short-fiber, multiphase, and direct measured plies. Every ply retains its own environment, criterion, and irreversible damage state during the common damaged-ABD solution.

Phase fractions and reduced-order homogenization

$$V_f + V_m + V_p + V_v = 1$$

$$E_1^{\mathrm{ROM}} = V_f E_{f1} + V_m E_m + V_p E_p$$

$$1/E_i^{\mathrm{Reuss}} = \Sigma_j V_j / E_{\mathrm{ji}}$$

$$\eta = (R-1)/(R+\xi)$$

$$P_c = P_m\left(1+\xi\eta V_f\right)/\left(1-\eta V_f\right)$$

Model IDs select ROM/Reuss, Halpin–Tsai, approximate Mori–Tanaka, or approximate self-consistent engineering estimates. Fabric controls modify warp, weft, bias, crimp, stitch, binder, and interlacing contributions. All generated branches return the same 3D ply definition and positive-definite 6×6 stiffness/compliance pair.

Expansion density and transport

$$\rho_c = \Sigma_j V_j \rho_j$$

$$c_{p,c} = \Sigma_j V_j \rho_j c_{p,j} / \rho_c$$

$$\alpha_1 = \Sigma_j V_j E_{j1} \alpha_{j1} / \Sigma_j V_j E_{j1}$$

$$k_{\parallel} = \Sigma_j V_j k_j$$

$$k_{\perp} = (\Sigma_j V_j / k_j)^{-1}$$

Aligned-discontinuous transfer and strength

$$\lambda_s = \sqrt{}[2G_m d_f / (4t_m E_{f1})]$$

$$\eta_L = 1 - \tanh(\lambda_s L_o)/(\lambda_s L_o)$$

$$\sigma_{f,p} = \sigma_0 \{-\ln(1-U)_p L_f c_s / (4L_0)\}^{1/m_w}$$

Only the aligned-discontinuous architecture enters the stochastic break-neighborhood and critical-cluster solver. The embedded micromechanics engine generates pristine properties; progressive damage remains solely in the laminate solver, preventing double degradation.

44 4 Failure Criteria

Online chapter

4 Failure Criteria

Failure is evaluated in local ply axes using mechanical—not total—strain. An intact damage family activates when its applicable index reaches or exceeds one.

ID	Criterion	Eligible ply	Primary use
1	Maximum Stress	Continuous	Transparent component-by-component allowable check
2	Maximum Strain	Continuous	Sign-specific mechanical-strain allowables
3	Tsai–Hill	Continuous	Quadratic in-plane stress interaction
4	Tsai–Wu	Continuous	Tension/compression asymmetry and calibrated interaction
5	2D Hashin	Continuous	Fiber and matrix tensile/compressive modes
6	Discontinuous Fiber	Aligned-discontinuous	Stochastic overlap transfer, Weibull breaks, and cluster instability

Maximum Stress and Maximum Strain

$$\mathrm{FI}_1 = \sigma_1/X$$

$$\mathrm{FI}_2 = \sigma_2/Y$$

$$\mathrm{FI}_6 = |\tau_{12}|/S_{12}$$

X and Y are chosen from tensile or compressive allowables by sign. Maximum Strain uses the same logic with $\varepsilon_{1,mech}$, $\varepsilon_{2,mech}$, and $\gamma_{12,mech}$.

Tsai Hill and Tsai Wu

$$\mathrm{FI}_{\mathrm{TH}} = (\sigma_1/X)^2 - \sigma_1\sigma_2/X^2 + (\sigma_2/Y)^2 + (\tau_{12}/S_{12})^2$$

$$\mathrm{FI}_{\mathrm{TW}} = F_1\sigma_1 + F_2\sigma_2 + F_{11}\sigma_1{}^2 + F_{22}\sigma_2{}^2 + 2F_{12}\sigma_1\sigma_2 + F_{66}\tau_{12}{}^2$$

$F_1=1/X_t-1/X_c$, $F_2=1/Y_t-1/Y_c$, $F_{11}=1/(X_tX_c)$, $F_{22}=1/(Y_tY_c)$, $F_{66}=1/S_{12}^2$, and $F_{12}=F_{12}*\sqrt{(F_{11}F_{22})}$. For combined criteria, CDS attributes the event to the largest normalized intact stress family.

Plane-stress Hashin

$$\mathrm{FI}_{\mathrm{ft}} = (\sigma_1/X_t)^2 + (\tau_{12}/S_{12})^2$$

$$\mathrm{FI}_{\mathrm{fc}} = (\sigma_1/X_c)^2$$

$$\mathrm{FI}_{\mathrm{mt}} = (\sigma_2/Y_t)^2 + (\tau_{12}/S_{12})^2$$

$$\mathrm{FI}_{\mathrm{mc}} = (\sigma_2/2S_{12})^2 + [(Y_c/2S_{12})^2 - 1](\sigma_2/Y_c) + (\tau_{12}/S_{12})^2$$

Mode attribution matters: a shear-dominated state reduces the shear family; it must not automatically reduce E1 or E2.

Supplemental transverse modes

Every criterion is supplemented by independent through-thickness checks. Criterion 2 uses ε3,mech, γ13,mech, and γ23,mech with sign-appropriate strain allowables. All other criteria use a Maximum Stress envelope based on Zt, Zc, S13, and S23. These checks create progressive mode IDs 7–12 and do not replace the ply-selected in-plane criterion.

45 5 Hygro-Thermo-Mechanical CLT and ABD

Online chapter

5 Hygro-Thermo-Mechanical CLT and ABD

The framework retains Classical Lamination Theory and extends its generalized equilibrium to include per-ply temperature and moisture fields and the in-plane Poisson response induced by prescribed σz, all evaluated with current damaged stiffness.

$$A = \Sigma\overline{Q}_k^d(z_k - z_{k-1})$$

$$B = ½\Sigma\overline{Q}_k^d({z_k}^2 - {z_{k-1}}^2)$$

$$D = ⅓\Sigma\overline{Q}_k^d({z_k}^3 - {z_{k-1}}^3)$$

Environmental fields and free strain

$$\Delta T_k = T_k - T_{\mathrm{ref},k}$$

$$\Delta C_k = C_k - C_{\mathrm{ref},k}$$

$$\varepsilon_k^f = \alpha_k \Delta T_k + \beta_k \Delta C_k$$

$$N^{\mathrm{HT}} = \Sigma\int \overline{Q}_k^d \varepsilon_k^f \mathrm{dz}$$

$$M^{\mathrm{HT}} = \Sigma\int \overline{\mathrm{zQ}}_k^d \varepsilon_k^f \mathrm{dz}$$

Damaged generalized equilibrium

$$\left[[A^d, B^d], [B^d, D^d]\right]\{\varepsilon^0, \kappa\} = \{N^m + N^T + N^C + N^{\sigma z}, M^m + M^T + M^C + M^{\sigma z}\}$$

At each ply surface, $\varepsilon(z)=\varepsilon^0+z\kappa$ and $\sigma_k(z)=\bar{Q}^d_k[\varepsilon(z)-\varepsilon^f_k(z)]$. Both total and mechanical strain are retained. Failure criteria use mechanical strain and the solver checks the top and bottom of every ply.

Required coupling: environmental resultants depend on $\bar{Q}^d$. They must be recomputed after damage; retaining pristine resultants after stiffness degradation is inconsistent.

Online chapter

6 Uniform Transverse Traction and z-Response

Release r11 adds a reduced-order layerwise section solution for spatially uniform σz, τxz, and τyz. These directions may be static or progressive, contribute to ply failure, and are reported at three nodes per active ply.

Nine-direction load matrix

Rows	Directions	Column 1	Column 2	Column 3
1–3	x, y, xy membrane	Static stress or resultant	Progressive flag	+ tension / − compression
4–6	x, y, xy bending/twisting	Static surface stress or moment resultant	Progressive flag	Signed ramp direction
7–9	σz, τxz, τyz	Static traction in Pa	Progressive flag	Signed ramp direction

When a row is progressive, its static value is ignored and the shared final progressive magnitude is applied with the sign in column 3. Multiple flagged directions ramp together. Static directions remain superposed throughout the ramp. Rows 7–9 are always entered in Pa, independent of whether rows 1–6 use stress-based or N/M resultant-based loading.

Local traction transformation

$$\{\tau_{13}, \tau_{23}\}^T = \big[[m, n], [-n, m]\big]\{\tau_{xz}, \tau_{yz}\}^T$$

$$\sigma_3 = \sigma_z$$

Transverse strain superposition

$$\varepsilon_3 = -\nu_{13}\sigma_1/E_1 - \nu_{23}\sigma_2/E_2 + \sigma_3/E_3 + \alpha_3 \Delta T_k + \beta_3 \Delta C_k$$

$$\gamma_{13} = \tau_{13}/G_{13}$$

$$\gamma_{23} = \tau_{23}/G_{23}$$

For each ply, σz also creates in-plane Poisson eigenstrains −ν13σz/E1 and −ν23σz/E2. Their transformed equivalent N and M resultants are included before the damaged ABD solve, so membrane, bending, transverse traction, thermal, and moisture effects remain mechanically coupled.

Compatible displacement recovery

$$w(z_j) = w(z_{j-1}) + \int_{\mathrm{zj-1}}^{\mathrm{zj}} \varepsilon_z\,(z)\mathrm{dz}$$

Integrating εz from the laminate bottom produces a continuous through-thickness displacement. The output stores compatible u, v, and w at three recovery nodes per active ply.

Scope boundary: this is a uniform-traction section model, not a 3D finite-element solution. It does not resolve a spatial pressure distribution, transverse-shear equilibrium of a plate, free-edge boundary layers, indentation, impact, holes, crack-tip fields, or 3D stress concentrations.

47 7 Progressive Failure Algorithm

Online chapter

7 Progressive Failure Algorithm

Progressive failure is event-driven. A load step is accepted only after all new failure events at that same load have been resolved.

- Apply the current mechanical and environmental load factor.
- Build each damaged Q matrix and the current ABD matrix.
- Recompute N^{HT} and M^{HT} using damaged stiffness.
- Solve for mid-plane strains and curvatures.
- Recover top/bottom local total strain, mechanical strain, and stress for every ply.
- Evaluate the ply-selected criterion against only intact fiber, matrix, and shear families.
- Degrade each newly activated family and write an event record.
- Return to step 2 without increasing load. Advance only when no additional event occurs.

while new event at λ: rebuild $\bar{Q}^d$ → rebuild ABD^d → rebuild $\{N,M\}^{HT}$ → solve → recover → evaluate → degrade

Termination

The default global stop condition is a loaded-direction retained-stiffness ratio of 0.05. Analyses may also stop at the requested terminal load, a user-defined event condition, or loss of numerical conditioning.

Interpretation: very large load-controlled strains after severe degradation indicate numerical stiffness collapse. They are not a physical ultimate-strain prediction.

48 8 Damage Degradation and Redistribution

Online chapter

8 Damage Degradation and Redistribution

Each ply carries six irreversible stiffness families so the framework can reduce longitudinal, in-plane transverse, through-thickness normal, and three shear responses independently.

$$E_1^d = r_f E_1$$

$$E_2^d = r_m E_2$$

$$E_3^d = r_m E_3$$

$$G_{\mathrm{ij}}^d = r_s G_{\mathrm{ij}}$$

Failure modes	Primary stiffness	Residual family
1–2, fiber tension/compression	E1	rf
3–4, matrix tension/compression	E2	rm
5–6, ± in-plane shear	G12	rs
7–8, through-thickness tension/compression	E3	rm
9–10, ± local 1–3 shear	G13	rs
11–12, ± local 2–3 shear	G23	rs

Only a newly activated intact family is degraded. Previously failed families do not trigger repeatedly. After each update the reduced stiffness, transformed stiffness, ABD matrix, environmental resultants, generalized strains, and all ply stresses are rebuilt, allowing load redistribution to expose secondary failures.

Event identity

Every event stores load step, pseudo-time/load factor, ply number, top or bottom surface, signed failure mode, index value, material type, selected criterion, local stress vector, and through-thickness coordinate.

Defaults are not universal: residual factors are numerical model parameters. Replace them with calibrated values and verify stability and retained-stiffness behavior for the intended laminate.

49 9 Effective Laminate and Transport Properties

Online chapter

9 Effective Laminate and Transport Properties

The full inverse ABD matrix is used so apparent membrane properties preserve extension–bending coupling in unsymmetric laminates.

$$\mathrm{abd} = [[A, B], [B, D]]^{-1}$$

$$E_x = 1/(\mathrm{ha}_{11})$$

$$E_y = 1/(\mathrm{ha}_{22})$$

$$G_{\mathrm{xy}} = 1/(\mathrm{ha}_{66})$$

$$\nu_{\mathrm{xy}} = -a_{12}/a_{11}$$

$$\nu_{\mathrm{yx}} = -a_{12}/a_{22}$$

Effective z-direction elastic and expansion properties

$$E_z = \sigma_z/[(1/h)\int \varepsilon_z \mathrm{dz}]$$

The expression uses a unit axial virtual load in the z direction.

$$\overline{S}_{\mathrm{sh}} = (1/h)\Sigma t_k R_k^T \mathrm{diag}\left(1/G_{13,k}, 1/G_{23,k}\right) R_k$$

$$\overline{K}_{\mathrm{sh}} = \overline{S}_{\mathrm{sh}}^{-1}$$

The diagonal terms of K̄sh provide Gxz and Gyz; its off-diagonal term is the xz–yz shear-coupling stiffness. Unit temperature and moisture load cases produce αz, βz, in-plane CTE/CME values, and free-warpage curvatures while retaining Poisson coupling.

Density heat capacity conductivity and diffusivity

$$\rho_L = (1/h)\Sigma \rho_k t_k$$

$$c_{p,L} = \Sigma \rho_k c_{p,k} t_k/(\rho_L h)$$

$$k_{\mathrm{xy},L} = (1/h)\Sigma k_{\mathrm{xy},k} t_k$$

$$k_{z,L} = h/\Sigma\left(t_k/k_{3,k}\right)$$

$$a_i = k_i/\left(\rho_L c_{p,L}\right)$$

In-plane conductivity uses a thickness average; through-thickness conductivity uses a series model. These are pristine homogenized properties: the current model does not degrade conductivity or heat capacity with cracking and does not solve transient transport.

50 10 Mixed-Mode Cohesive Delamination

Online chapter

10 Mixed-Mode Cohesive Delamination

The optional interface branch uses a bilinear irreversible cohesive law with quadratic initiation and Benzeggagh–Kenane mixed-mode propagation.

$$\{t_n, t_s, t_t\}^{\mathrm{trial}} = \mathrm{diag}(K_n, K_s, K_t)\{\langle\delta_n\rangle, \delta_s, \delta_t\}$$

$$(\langle t_n\rangle/T_{n0})^2 + (t_s/T_{s0})^2 + (t_t/T_{t0})^2 = 1$$

$$G_c = G_{\mathrm{Ic}} + (G_{\mathrm{sc}} - G_{\mathrm{Ic}})B_s^{\eta}$$

$$B_s = (G_{\mathrm{II}} + G_{\mathrm{III}})/(G_I + G_{\mathrm{II}} + G_{\mathrm{III}})$$

$$d = \delta_f(\delta_{\max} - \delta_0)/\left[\delta_{\max}\left(\delta_f - \delta_0\right)\right]$$

The damage variable d is bounded between zero and one.

Tensile and shear tractions are multiplied by (1−d); compression remains elastic. A reduced-order laminate feedback may use $D_{eff}=(1-d_{max})D_{intact}+d_{max}D_{split}$, while $A_{eff}=A_{intact}$.

Required local input: r11 can prescribe uniform σz, τxz, and τyz, but those tractions do not create a displacement discontinuity between bonded ply surfaces. Cohesive interface separation history must still come from a test, detailed submodel, or structural analysis.

51 11 Inputs and Model Selection

Online chapter

11 Inputs and Model Selection

Input data define both the laminate mechanics and the theory used by each ply. Values must describe the same material state, units, conditioning, and temperature range.

Input group	Required content
Fiber database	3D elastic, strength/Weibull, expansion, conductivity, heat capacity, and moisture data
Matrix database	elastic, strength, density, thermal, moisture, toughness, and friction data
Filler database	elastic, density, aspect ratio, expansion, conductivity, heat capacity, and moisture data
Per-ply source routing	Material or solved-lamina selection, fiber architecture, model choice, volume fractions and void content
Laminate	Ply count, thicknesses, orientations, stacking order, reference plane, three recovery nodes per active ply
Loading	six membrane/bending directions plus uniform σz, τxz, τyz; static/progressive flag and signed ramp direction
Ply routing	Material family and compatible failure model
Mechanical	Elastic constants, strengths, and strain allowables
Environmental	Per-ply ΔT and ΔC with α1–α3 and β1–β3, ready for later gradient generation
Physical	Density, k1, k2, k3, and specific heat
Process boundaries	Independent top and bottom boundary schedules with time, temperature, moisture, boundary types, and coefficient/custom-flux values
Ply kinetics	Ply definitions for inert, thermoset, or semicrystalline thermoplastic state, diffusion, heat, and shrinkage
Short fiber	Vf, fiber length/diameter, overlap geometry, interface shear, Weibull parameters, RVE controls
Cohesive	Penalty stiffnesses, strengths, fracture energies, BK exponent, and interface separation history

For each ply, choose its material or solved lamina, thickness and angle. Supply the elastic properties, strength allowables and environmental properties needed by the selected analysis. Missing data must not be interpreted as a pass.

52 12 Outputs and Event Histories

Online chapter

12 Outputs and Event Histories

Outputs separate global laminate response, ply-surface state, damage history, effective properties, and optional interface response so the progressive sequence can be audited.

Output family	Contents
Laminate state	Pristine/current A, B, D and ABD; mid-plane strains; curvatures; mechanical and environmental resultants
Layerwise fields	Three nodes per ply; global/local/principal in-plane fields and global/local transverse fields
Contributions	Total, mechanical, thermal, and moisture stress and strain histories reported independently and by superposition
Progressive events	Step, load factor, ply, surface, mode, FI, stress vector, z-coordinate
Retention	Directional stiffness ratios, terminal condition, and collapse/conditioning flags
Effective properties	Ex, Ey, Gxy, Ez, Gxz, Gyz, transverse Poisson ratios, CTE/CME, density, cp, conductivities, diffusivities, and transverse shear coupling
Delamination	Interface separations, tractions, mode mix, cohesive damage, effective bending feedback

Read stress, strain, deformation, damage and retained stiffness together. Total strain describes deformation; mechanical strain drives strain-based failure.

Progressive visualization

The optional progressive-damage MP4 synchronizes ply damage, stress redistribution, retained stiffness, the load–strain path, full-text failure callouts, and Figure 6 principal stress/strain histories. A second optional MP4 progressively reveals the six Figure 4 global through-thickness stress and strain panels. Every failure-event increment is forced into the frame list so same-load redistribution events are not skipped.

Report context: every result set should identify material routing, selected criteria, residual factors, environmental fields, load control, step count, stochastic seed/RVE settings, and any cohesive input source.

53 13 Verification and Validation

Online chapter

13 Verification and Validation

Verification checks implementation consistency; validation establishes whether the calibrated model predicts the intended material and structure.

Core verification checks

- Source routing: linked and measured property sources must remain traceable independently for every ply.
- Symmetric quasi-isotropic laminates produce B≈0 and expected in-plane symmetry.
- Compatible Double-Double candidates preserve the stiffness objective within the reported error and substitute only ply angles when selected.
- Uniform free temperature/moisture expansion produces near-zero stress when unconstrained.
- Inert adiabatic transport conserves heat and insulated diffusion conserves moisture within numerical tolerance.
- Five-row top/bottom schedules interpolate to the requested transport grid while boundary types remain piecewise constant.
- Damaged thermal, moisture, process, and σz-Poisson resultants are rebuilt in every equilibrium pass.
- Failure uses mechanical strain; exports retain total, mechanical, thermal, moisture, and process-only contributions.
- Three nodes per active ply preserve linear in-plane gradients and compatible integrated w(z).
- Plate, shell/Hyer cylinder, and five beam-section routes return finite structural metadata and schema.
- Generated 6×6 compliance and stiffness matrices remain positive definite and reciprocal within tolerance.

Validation ladder

- Constituent and UD elastic, thermal, moisture, and transport tests.
- Tensile/compressive/shear strengths and strain allowables at relevant conditions.
- Multiaxial tests for interaction calibration, including F_{12}*.
- DCB, ENF, and MMB data for cohesive parameters.
- Short-fiber RVE convergence and statistical repeatability.
- Laminate membrane and bending coupons, including conditioned hot/wet specimens.
- Representative structural details for final assessment.

Verification is not validation. Numerical consistency checks do not replace comparison with relevant physical tests. See the validation evidence attached to individual exercises.

54 14 Assumptions and Limitations

Online chapter

14 Assumptions and Limitations

- The in-plane foundation is thin-laminate CLT with small strains and rotations. The r11 transverse extension prescribes uniform tractions and performs layerwise constitutive recovery; it is not a general 3D equilibrium solution.
- Hashin is the retained 2D plane-stress form; the model does not resolve 3D fiber kinking, fracture-plane rotation, or nonlinear matrix plasticity.
- Transport is one-dimensional through thickness. Lateral heat flow, edge drying, tool-contact geometry, damage-assisted diffusion, and spatial hot spots require a higher-fidelity model.
- Cure, crystallization, diffusion, saturation, reaction heat, and process shrinkage require material-grade and process-specific calibration; default kinetics rows are inert.
- Moduli, strengths, and fracture energies are not currently functions of temperature or moisture concentration.
- The cohesive branch requires externally supplied local kinematics and does not predict crack-front shape, migration, multiple finite-area delaminations, or contact.
- Conductivity and heat capacity are reported as pristine homogenized properties and are not degraded by cracks.
- Residual stiffness factors and stochastic short-fiber parameters require calibration and convergence studies.
- ROM/Reuss, Halpin–Tsai, approximate Mori–Tanaka, approximate self-consistent, fabric, filler, and directional-void branches are reduced-order engineering property generators; critical architecture-specific use requires calibration or a higher-fidelity RVE.
- Micromechanics generates pristine properties. Progressive damage is applied only in the laminate solver.
- Loss of numerical stiffness under load control is a collapse indicator, not a physical post-failure strain trajectory.

Use boundary: outputs support comparison, screening, calibration, and research. They are not material design allowables and do not replace test evidence or structural certification requirements.

55 15 Theory References

Online chapter

15 Theory References

This section incorporates the unified r15 constituent-to-laminate master, the retained r11 progressive-failure and uniform-transverse-traction formulation, and their cited foundations.

- *CDS Unified Composite Solver — Web r17* (29 August 2026), release 2026082901, master CDS_USolve_Web_v2026_08_29_r17.m.
- *A General-Purpose Hygro-Thermo-Mechanical Progressive-Failure Framework for Continuous and Aligned-Discontinuous Composite Laminates* (20 August 2026), source paper supplied for this theory update.
- *ADC General-Purpose Progressive-Failure Model — r11: Uniform 3D Traction and z-Property Extension* (22 August 2026), release 2026082201.
- Hill, R. (1950), *The Mathematical Theory of Plasticity*.
- Tsai, S. W., and Wu, E. M. (1971), "A General Theory of Strength for Anisotropic Materials," *Journal of Composite Materials*, 5(1), 58–80.
- Hashin, Z. (1980), "Failure Criteria for Unidirectional Fiber Composites," *Journal of Applied Mechanics*, 47(2), 329–334.
- Nettles, A. T. (1994), *Basic Mechanics of Laminated Composite Plates*, NASA RP-1351.
- Soden, P. D., Hinton, M. J., and Kaddour, A. S. (1998), comparison of composite failure theories.
- Camanho, P. P., and Dávila, C. G. (2002), mixed-mode decohesion finite-element formulation.
- Benzeggagh, M. L., and Kenane, M. (1996), mixed-mode delamination fracture criterion.
- Turon, A., Camanho, P. P., Costa, J., and Dávila, C. G. (2006), cohesive-zone methodology for delamination.
- Cox, H. L. (1952), shear-lag theory; Halpin, J. C., and Tsai, S. W. (1976), composite property relations; Weibull, W. (1951), statistical strength distribution.
- Pimenta, S., Robinson, P., and collaborators (2014–2018), failure and strength modeling of discontinuous and hybrid composites.
- Tsai, S. W. (2021), "Double-Double: New Family of Composite Laminates," *AIAA Journal*, 59(11), 4293–4305. DOI 10.2514/1.J060659.

Use the Theory Manual for equations and assumptions, the User Guide for controls, and the Training Manual for shared exercises.

56 Models you can use Connections you can follow

Online chapter

The released Workbench model set, grouped by engineering purpose. Open a family for its tree location, inputs, outputs, theory and guided exercise. Availability also depends on your license.

42 model families in the released Workbench

Choose a formulation in Models, edit its linked source record, connect required inputs in Simulation, then watch a quick workflow update or press Run. Tree nesting shows related methods—not permission to combine every method in one solve. A completed calculation is not a validated design pass.

Live updates or Run?

Small compatible workflows refresh after editing pauses, using the current connected materials, Micro, laminate and case inputs. Larger sampling, mode searches, mesh calculations and process histories require Run after upstream changes. Workbench also switches a workload to Run when measured solver time exceeds its live budget; it never reduces numerical accuracy to stay live.

The Solver control shows Live updates or Run required and can pause automatic updates. Hidden tabs do not start background refreshes. Superseded results are discarded, and all automatic runs retain the same model and license checks. Fast reference-state studies remain separate studies: live scheduling does not create new physical coupling.

Materials micromechanics

Design a ply or reinforced feedstock

- Constituents & architecture
- Homogenization
- Ply properties

Explore 1 family · 9 model choices

Micromechanics · 9

Models browser → Micromechanics · source: Micro

Inputs Constituents, architecture, fractions and calibrated modifiers Results / handoff Reference ply properties for each linked laminate ply

- Halpin–Tsai
- Rule of mixtures
- Modified rule of mixtures
- Chamis
- Mori–Tanaka
- Hashin–Rosen
- Self-consistent scheme
- Woven fabric bridging
- Cox shear-lag elastic

One compatible homogenization model per Micro recipe. Use separate recipes for comparisons; they are not combined in a single ply.

Theory & limits

Guided exercise

Heat moisture manufacturing

Cure, pultrusion, conditioning and tool release

- Material laws & boundary cycles
- Transport & reaction
- History & compatible process fields

Explore 4 families · 14 model choices

Cure, crystallization & material transport · 8

Models → material-model folders · assigned through Materials

Inputs Calibrated kinetics, modulus or transport laws and material assignment Results / handoff Material laws consumed by compatible Micro or transport calculations

- Kamal–Sourour autocatalytic
- Kamal–Sourour with diffusion control
- Nth-order Arrhenius
- CHILE (degree of cure)
- UV intensity-dependent cure
- Nakamura–Avrami
- Temperature-dependent tabular
- 1D Fickian diffusion

Independent model records can be linked together through material inputs. A saved model must be assigned to a material before it contributes to a simulation.

Theory & limits

Guided exercise

· Cure kinetics

· Crystallization kinetics

Thermal transport · 3

Models browser → Thermal transport · source: CASES / Thermal

Inputs Laminate transport properties, initial state and the thermal case's own surface cycle Results / handoff Temperature and supported polymer-state histories; mapped fields only when coupling is enabled

- 1D transient heat transfer
- 1D steady-state heat transfer
- 1D pultrusion thermal cure

One transport formulation per thermal case. Select its laminate and configure its own initial conditions and surface cycle; pultrusion additionally requires a distance-based die schedule and pulling velocity.

Theory & limits

Guided exercise

· Pultrusion exercise

· UV cure exercise

Moisture transport · 2

Models browser → Moisture transport · source: CASES / Moisture

Inputs Laminate diffusion properties, initial moisture and its own boundary schedule Results / handoff Moisture history and enabled swelling contribution

- 1D transient moisture diffusion
- 1D steady-state moisture diffusion

One formulation per moisture analysis. Thermal and moisture analyses can both be linked in Simulation; each needs its own boundary conditions.

Theory & limits

Guided exercise

Tool-release shape · 1

Structural models → Tool-release shape

Inputs Laminate and prescribed temperatures, CTE and effective post-gel shrinkage Results / handoff Free-release CLT curvature and separate corner spring-in estimate; not an automatic process-history handoff

- Free-release eigenstrain & spring-in

Free CLT release from prescribed ply-local shrinkage/thermal eigenstrains. Corner spring-in is a separate uniform-strain estimate. Stress-free temperature and effective post-gel shrinkage need calibration. No tool friction, cure kinetics or viscoelastic restraint history.

Theory & limits

Guided exercise

Structural mechanics

Size plates, beams, shells, sandwich panels and joints

- Laminate & geometry
- Load response / stability
- Displacements, stresses & modes

Explore 7 families · 17 model choices

Plate · CLT & FSDT · 6

Structural models → Laminate mechanics · CLT / FSDT

Inputs Laminate stiffness, finite plate dimensions, supported edges and study choice Results / handoff FSDT static bending or selected buckling / modal results; not progressive damage

- CLT
- FSDT
- Static bending
- Modal
- Buckling
- Buckling and modal

Choose a formulation and study. Buckling and modal can be requested together; static bending requires FSDT. These are reference-elastic studies, separate from coupled process or progressive failure.

Theory & limits

Guided exercise

Cylinder · 2

Structural models → Cylinder models

Inputs Laminate, cylinder dimensions and formulation-compatible pressure / axial loading Results / handoff Thin-wall membrane response or layerwise radial fields, with distinct assumptions

- Linear thin-wall membrane
- Layerwise thick-wall elasticity

Choose one cylinder formulation per case record. Geometry and plies remain shared; thick-wall radial results exclude torsion and process strains.

Theory & limits

Guided exercise

· Layerwise thick-wall theory

Membrane, bending & beam buckling · 3

Structural models → Laminate mechanics → Membrane, bending & beam

Inputs Laminate, compatible section and static or Euler load case Results / handoff Membrane / bending response or separate Euler buckling result

- Linear static
- Linear static with failure indices
- Beam Euler buckling

Geometry and the case determine the membrane or beam-test interpretation. Euler buckling requires a compatible beam section and a separate reference-elastic study; it is not a strength or local-buckling pass.

Theory & limits

Guided exercise

Layerwise sections, joints & delamination · 3

Structural models → Layerwise sections & joints

Inputs Section or lap geometry, laminate, loads and calibrated interface properties Results / handoff x–z fields; coupled ply damage and delamination only for the supported layerwise plate path

- Layerwise x-z plane strain
- Single-lap x-z plane strain
- Coupled delamination growth

Coupled delamination is available only for the layerwise Plate section and needs calibrated interface and ply properties. Lap-shear uses its separate joint geometry and perfectly bonded elastic formulation.

Theory & limits

Guided exercise

· Cohesive interface theory

Sandwich bending · 1

Structural models → Sandwich bending

Inputs Faces, core, dimensions and three-point-bend load Results / handoff Deflection and separate face, core and nominal bond-shear screening

- Sandwich three-point bend

Dedicated sandwich screening. Check core, faces and nominal bond shear separately; peel, mixed-mode debonding and crack growth are not assessed.

Theory & limits

Guided exercise

Analytical bonded joint · 1

Structural models → Layerwise sections & joints → Analytical bonded joint

Inputs Identical equivalent-elastic adherends, adhesive, overlap, width and tensile force Results / handoff Volkersen shear and Goland–Reissner shear / peel; no debond growth

- Volkersen & Goland–Reissner joint

Identical equivalent-elastic adherends, long free arms and a thin elastic adhesive. Compare shear-only Volkersen with eccentric single-lap shear and peel. Not a debonding, plasticity or strength calculation.

Theory & limits

Guided exercise

Cylinder buckling · 1

Structural models → Cylinder models → Cylinder buckling

Inputs Thin specially orthotropic shell, radius, length, axial compression and prescribed knockdown Results / handoff Ideal / knocked-down Donnell axial buckling and governing mode; no pressure or postbuckling

- Donnell cylinder · axial buckling

Simply supported, thin, specially orthotropic cylinder under uniform axial compression. Discrete Donnell modes; prescribed knockdown factor explores imperfection sensitivity, not a prediction from measured imperfection amplitude. No pressure, torsion, postbuckling or strength pass.

Theory & limits

Guided exercise

Failure durability variability

Assess strength, service life and sensitivity

- Ply response & calibration
- Selected assessment
- Indices, envelopes & life estimates

Explore 7 families · 15 model choices

Failure & envelope comparison · 5

Structural models → Laminate mechanics → Failure criteria

Inputs Eligible CLT load case, strengths / strain limits and selected criterion Results / handoff First-ply envelopes or supported progressive ply-damage histories; criteria are not blended

- Maximum stress
- Maximum strain
- Tsai–Hill
- Tsai–Wu
- Hashin

One primary failure criterion per load. In Response → Failure, compare all eligible theories or a custom selection in the envelope controls. Each theory runs independently; criteria are not blended.

Theory & limits

Guided exercise

· Failure equations

· Implemented Workbench methods

Fatigue S–N · 5

Structural models → Laminate mechanics → Fatigue

Inputs Intact ply stresses, cyclic loads and measured S–N calibration Results / handoff Separate life assessment; no automatic laminate degradation

- Kim–Zhang
- Sendeckyj
- Weibull S–N
- Kohout–Vechet
- Basquin

Select calibrated S–N curves for each material, direction and stress sign in Fatigue. Different sources can use different models. S–N life does not define residual stiffness or strength.

Theory & limits

Starter load case · add calibrated fatigue

Open-hole strength · 1

Structural models → Laminate mechanics → Failure criteria → Open-hole strength

Inputs Specially orthotropic laminate, hole radius, unnotched strength and calibrated distances Results / handoff Point / average stress strength screening and radial stress profile

- Whitney–Nuismer open-hole tension

Infinite-width, specially orthotropic tension screening. Point and average stress distances must be calibrated independently for this laminate. Not compression, bearing or a joint allowable.

Theory & limits

Guided exercise

Creep & stress relaxation · 1

Structural models → Laminate mechanics → Creep & stress relaxation

Inputs Laminate Ex, Prony fractions / times and held stress or strain at calibration temperature Results / handoff Separate axial creep and relaxation curves with time-refinement safeguards

- Generalized Maxwell · axial Prony

Linear uniaxial response at the calibration temperature. Reference Ex is the instantaneous modulus. Three Maxwell branches; creep is solved from stress equilibrium, not the reciprocal relaxation modulus. No thermal shifting or nonlinear creep.

Theory & limits

Guided exercise

LaRC04 failure initiation · 1

Structural models → Laminate mechanics → Failure criteria → LaRC04

Inputs Laminate, membrane / bending resultants and calibrated effective ply strengths Results / handoff Linear-shear LaRC04 initiation indices at ply faces; no progressive degradation

- LaRC04 · linear shear

NASA LaRC04 linear-shear specialization, evaluated at both faces of every ply under membrane and bending loads. Supplied ply strengths are effective/in-situ values; no automatic thin-ply enhancement. Initiation only, not degradation or nonlinear-shear instability.

Theory & limits

Guided exercise

Fatigue residual properties · 1

Structural models → Laminate mechanics → Fatigue → Residual properties

Inputs Modulus, independently fitted stiffness / strength retention laws, life and elapsed cycles Results / handoff Residual-property curves for the specified constant-amplitude calibration; saved laminate is unchanged

- Calibrated residual-property fatigue

Prescribed power-law retention fitted to constant-amplitude tests at a fixed stress ratio, amplitude and temperature. Stiffness and strength have independent coefficients. S–N life alone cannot calibrate either. Does not modify the saved laminate.

Theory & limits

Guided exercise

Uncertainty & sensitivity · 1

Structural models → Uncertainty & sensitivity

Inputs Laminate, bounded modulus / thickness / angle variations, seed and axial load Results / handoff ABD axial-strain percentiles and signed correlations; not certified reliability

- Seeded laminate uncertainty

Seeded independent uniform sampling of shared modulus, ply-thickness and angle offsets. Recomputes laminate ABD for each sample. Bounds are assumptions, not measured distributions. Percentiles and sensitivity are exploratory, not reliability certification.

Theory & limits

Guided exercise

Virtual test lab

Explore specimen behavior and calibration

- Specimen & material inputs
- Virtual test
- Response & comparison

Explore 10 families · 10 model choices

D6641 · Compression coupon · 1

Models → Structural models → ASTM · Virtual Test Lab

Inputs Linked laminate and explicit specimen, load or measured calibration inputs Results / handoff Uniform small-strain compression using linked laminate Ex and thickness. Measured compressive strength supplies a screening ratio; fixture, tabs, buckling and failure evolution are not simulated.

- Virtual test · compression coupon

Uniform small-strain compression using linked laminate Ex and thickness. Measured compressive strength supplies a screening ratio; fixture, tabs, buckling and failure evolution are not simulated.

Theory & limits

Guided exercise

D5379 / D7078 · Shear coupon · 1

Models → Structural models → ASTM · Virtual Test Lab

Inputs Linked laminate and explicit specimen, load or measured calibration inputs Results / handoff Uniform nominal shear between notches using linked laminate Gxy and thickness. Not a notch/fixture stress field or nonlinear shear solution. Gauge length is the effective shear deformation length, not crosshead travel.

- Virtual test · nominal shear coupon

Uniform nominal shear between notches using linked laminate Gxy and thickness. Not a notch/fixture stress field or nonlinear shear solution. Gauge length is the effective shear deformation length, not crosshead travel.

Theory & limits

Guided exercise

D5528 · DCB opening · 1

Models → Structural models → ASTM · Virtual Test Lab

Inputs Linked laminate and explicit specimen, load or measured calibration inputs Results / handoff Ideal Euler–Bernoulli DCB with equal homogeneous 0° arms, each half the linked laminate thickness. No root rotation, shear, large displacement or cohesive growth. Critical load is an initiation estimate from supplied GIc.

- Virtual test · DCB beam compliance

Ideal Euler–Bernoulli DCB with equal homogeneous 0° arms, each half the linked laminate thickness. No root rotation, shear, large displacement or cohesive growth. Critical load is an initiation estimate from supplied GIc.

Theory & limits

Guided exercise

D7905 · ENF sliding · 1

Models → Structural models → ASTM · Virtual Test Lab

Inputs Linked laminate and explicit specimen, load or measured calibration inputs Results / handoff Ideal equal-arm, homogeneous 0° ENF beam; support span is twice the half-span. Crack must be shorter than the half-span. No shear/root correction or unstable crack growth. GIIc is supplied, not fitted automatically.

- Virtual test · ENF beam compliance

Ideal equal-arm, homogeneous 0° ENF beam; support span is twice the half-span. Crack must be shorter than the half-span. No shear/root correction or unstable crack growth. GIIc is supplied, not fitted automatically.

Theory & limits

Guided exercise

D6671 · Mixed-mode fracture envelope · 1

Models → Structural models → ASTM · Virtual Test Lab

Inputs Linked laminate and explicit specimen, load or measured calibration inputs Results / handoff Benzeggagh–Kenane envelope from calibrated GIc, GIIc and exponent. Supplied GI/GII are energy-release rates from a separate test reduction or analysis. This does not resolve the MMB lever fixture or propagate a crack.

- Virtual test · BK mixed-mode envelope

Benzeggagh–Kenane envelope from calibrated GIc, GIIc and exponent. Supplied GI/GII are energy-release rates from a separate test reduction or analysis. This does not resolve the MMB lever fixture or propagate a crack.

Theory & limits

Guided exercise

D5229 · Moisture uptake calibration · 1

Models → Structural models → ASTM · Virtual Test Lab

Inputs Linked laminate and explicit specimen, load or measured calibration inputs Results / handoff Homogeneous slab, initially dry, both faces held at equilibrium moisture. Fits diffusivity from two early uptake measurements (both ≤50% saturation) using the square-root-time approximation. Edge ingress and temperature dependence are excluded. Does not overwrite material properties.

- Virtual test · Fickian uptake calibration

Homogeneous slab, initially dry, both faces held at equilibrium moisture. Fits diffusivity from two early uptake measurements (both ≤50% saturation) using the square-root-time approximation. Edge ingress and temperature dependence are excluded. Does not overwrite material properties.

Theory & limits

Guided exercise

D5961 · Bearing / bypass screening · 1

Models → Structural models → ASTM · Virtual Test Lab

Inputs Linked laminate and explicit specimen, load or measured calibration inputs Results / handoff Single-pin nominal bearing, net-section and shear-out checks with independent measured allowables. Bypass tension is added to net-section load only. No contact, bolt preload, load redistribution or validated bearing–bypass interaction envelope.

- Virtual test · bearing bypass screening

Single-pin nominal bearing, net-section and shear-out checks with independent measured allowables. Bypass tension is added to net-section load only. No contact, bolt preload, load redistribution or validated bearing–bypass interaction envelope.

Theory & limits

Guided exercise

D6484 · Open-hole compression · 1

Models → Structural models → ASTM · Virtual Test Lab

Inputs Linked laminate and explicit specimen, load or measured calibration inputs Results / handoff Nominal gross/net stress and demand relative to measured open-hole compressive strength for this geometry and layup. This is test-data screening, not an uncalibrated notch-strength prediction. No local buckling or kink-band simulation.

- Virtual test · measured open-hole compression

Nominal gross/net stress and demand relative to measured open-hole compressive strength for this geometry and layup. This is test-data screening, not an uncalibrated notch-strength prediction. No local buckling or kink-band simulation.

Theory & limits

Guided exercise

D6742 · Filled-hole comparison · 1

Models → Structural models → ASTM · Virtual Test Lab

Inputs Linked laminate and explicit specimen, load or measured calibration inputs Results / handoff Compares user-measured open- and filled-hole compressive strengths using gross-section stress. Use matched layup, hole, environment and fastener condition. Filling a hole does not automatically recover strength; no fastener contact/preload model is applied.

- Virtual test · measured filled-hole comparison

Compares user-measured open- and filled-hole compressive strengths using gross-section stress. Use matched layup, hole, environment and fastener condition. Filling a hole does not automatically recover strength; no fastener contact/preload model is applied.

Theory & limits

Guided exercise

D7136 / D7137 · Impact & CAI assessment · 1

Models → Structural models → ASTM · Virtual Test Lab

Inputs Linked laminate and explicit specimen, load or measured calibration inputs Results / handoff Incident energy from measured impact velocity; residual compressive strength from measured peak CAI force. Rebound energy estimates energy not returned to the striker, NOT damage energy. No impact/contact solver, damage-area prediction or energy-to-strength extrapolation.

- Virtual test · measured impact and CAI

Incident energy from measured impact velocity; residual compressive strength from measured peak CAI force. Rebound energy estimates energy not returned to the striker, NOT damage energy. No impact/contact solver, damage-area prediction or energy-to-strength extrapolation.

Theory & limits

Guided exercise

Electromagnetics RF

Design dielectric mixtures, shielding and periodic layers

- Electrical properties & layers
- Effective medium / wave propagation
- Permittivity & RF response

Explore 13 families · 13 model choices

Wiener series and parallel · 1

Models → Electromagnetics · RF → Wiener series and parallel

Inputs Explicit host/inclusion electrical properties and fractions Results / handoff Effective permittivity; manual handoff to an RF layer, not an automatic mechanical-property update

- EM · Wiener series and parallel

Positive lossless dielectric bounds; complex directional estimates.

Theory & limits

Guided exercise

Looyenga / Landau–Lifshitz–Looyenga · 1

Models → Electromagnetics · RF → Looyenga / Landau–Lifshitz–Looyenga

Inputs Explicit host/inclusion electrical properties and fractions Results / handoff Effective permittivity; manual handoff to an RF layer, not an automatic mechanical-property update

- EM · Looyenga / Landau–Lifshitz–Looyenga

One cube-root mixing law, not two independent models.

Theory & limits

Guided exercise

Maxwell–Garnett · 1

Models → Electromagnetics · RF → Maxwell–Garnett

Inputs Explicit host/inclusion electrical properties and fractions Results / handoff Effective permittivity; manual handoff to an RF layer, not an automatic mechanical-property update

- EM · Maxwell–Garnett

Dilute subwavelength spherical inclusions in a host.

Theory & limits

Guided exercise

Normal-incidence laminate TMM · 1

Models → Electromagnetics · RF → Normal-incidence laminate TMM

Inputs Explicit dielectric A/B layers, thicknesses, repetition, frequency and supported polarization Results / handoff Reflection, transmission, absorption and shielding spectra; no mechanical coupling

- EM · Normal-incidence laminate TMM

Coherent isotropic nonmagnetic layers between air half-spaces.

Theory & limits

Guided exercise

Bruggeman symmetric EMT · 1

Models → Electromagnetics · RF → Bruggeman symmetric EMT

Inputs Explicit host/inclusion electrical properties and fractions Results / handoff Effective permittivity; manual handoff to an RF layer, not an automatic mechanical-property update

- EM · Bruggeman symmetric EMT

Two positive-permittivity phases; no explicit contact network.

Theory & limits

Guided exercise

EM Mori–Tanaka · 1

Models → Electromagnetics · RF → EM Mori–Tanaka

Inputs Explicit host/inclusion electrical properties and fractions Results / handoff Effective permittivity; manual handoff to an RF layer, not an automatic mechanical-property update

- EM · EM Mori–Tanaka

Scalar principal-axis ellipsoidal field approximation.

Theory & limits

Guided exercise

EM self-consistent · 1

Models → Electromagnetics · RF → EM self-consistent

Inputs Explicit host/inclusion electrical properties and fractions Results / handoff Effective permittivity; manual handoff to an RF layer, not an automatic mechanical-property update

- EM · EM self-consistent

Scalar principal-axis self-consistency; spherical case equals Bruggeman.

Theory & limits

Guided exercise

Differential effective medium · 1

Models → Electromagnetics · RF → Differential effective medium

Inputs Explicit host/inclusion electrical properties and fractions Results / handoff Effective permittivity; manual handoff to an RF layer, not an automatic mechanical-property update

- EM · Differential effective medium

Incremental mixing with time-step refinement check.

Theory & limits

Guided exercise

Coated sphere and interphase · 1

Models → Electromagnetics · RF → Coated sphere and interphase

Inputs Explicit host/inclusion electrical properties and fractions Results / handoff Effective permittivity; manual handoff to an RF layer, not an automatic mechanical-property update

- EM · Coated sphere and interphase

Concentric subwavelength coated spheres; no dynamic Mie scattering.

Theory & limits

Guided exercise

Generalized multiphase EMT · 1

Models → Electromagnetics · RF → Generalized multiphase EMT

Inputs Explicit host/inclusion electrical properties and fractions Results / handoff Effective permittivity; manual handoff to an RF layer, not an automatic mechanical-property update

- EM · Generalized multiphase EMT

Spherical multiphase Bruggeman with convergence checks.

Theory & limits

Guided exercise

Oblique polarized laminate TMM · 1

Models → Electromagnetics · RF → Oblique polarized laminate TMM

Inputs Explicit dielectric A/B layers, thicknesses, repetition, frequency and supported polarization Results / handoff Reflection, transmission, absorption and shielding spectra; no mechanical coupling

- EM · Oblique polarized laminate TMM

TE or TM waves; scalar isotropic layers, no polarization conversion.

Theory & limits

Guided exercise

1D transmission line matrix · 1

Models → Electromagnetics · RF → 1D transmission line matrix

Inputs Explicit dielectric A/B layers, thicknesses, repetition, frequency and supported polarization Results / handoff Reflected and transmitted pulse histories and spectra; mesh and energy checks

- EM · 1D transmission line matrix

Normal-incidence lossless delay-line mesh with pulse decay, energy and mesh-refinement safeguards. Explicit Run required; not a 3D solver.

Theory & limits

Guided exercise

1D Floquet–Bloch periodic layers · 1

Models → Electromagnetics · RF → 1D Floquet–Bloch periodic layers

Inputs Explicit dielectric A/B layers, thicknesses, repetition, frequency and supported polarization
Results / handoff Periodic-cell eigenvalues, folded Bloch phase and stop-band decay

- EM · 1D Floquet–Bloch periodic layers

Lossless isotropic A/B unit-cell eigenvalues, folded Bloch phase and stop-band attenuation at normal incidence. Not arbitrary-cell homogenization.

Theory & limits

Guided exercise

Reference theory versus released functionality

The wider theory library also describes research and compiled-solver formulations. Event-driven Henry–Pimenta RVE, stochastic discontinuous-fiber failure, Puck, nonlinear-shear LaRC04, impact and general 3D finite-element analysis are not selectable hosted Workbench models. Cox elastic short-fiber homogenization and the separate linear-shear LaRC04 study are available within their stated limits.

Reference-state studies run separately from coupled process or progressive analyses. Residual-fatigue results do not automatically update optimization properties. Tool release uses prescribed eigenstrains rather than importing a cure history.